# Interaction entre le carbone organique dissous et l'hydropédologie dans les bassins afromontagnards (Afrique du Sud)

Rowena Harrison

**THESE DE DOCTORAT DE L'ETABLISSEMENT UNIVERSITE BOURGOGNE FRANCHE-COMTE**
**PREPAREE A University of the Free State/University of Burgundy**

Ecole doctorale n° 9920A41922J

Ecole doctorale - Environnements-Santé

Doctorat de Géodynamique des enveloppes supérieures

par

Rowena Louise Harrison

# INTERACTIONS BETWEEN DISSOLVED ORGANIC CARBON AND HYDROPEDOLOGY IN AFROMONTANE CATCHMENTS (SOUTH AFRICA)

Thèse présentée et soutenue à University of the Free State, South Africa, le 21 June 2023

Composition du Jury :

| | | |
|---|---|---|
| Mr, Ludwig, Wolfgang | Professor University of Perpignan | Président |
| Mr van der Laan, Michael | Directeur de recherche | Rapporteur |
| Mme, Jaffrezic, Anne | Associate Professor, Rennes Agrocampus-ouest | Rapporteur |
| Mr, Barnard Johan | Maître de conférences, University of the Free State | Examinateur |
| Mr, van Tol Johan | Professor University of the Free State | Codirecteur de thèse |
| Mr, Amiotte-Suchet Philippe | Maître de conférences, University of Burgundy | Codirecteur de thèse |
| Mr. Mathieu Olivier | Maître de conférences, University of Burgundy | Invité |

**Titre :** Interaction entre le carbone organique dissous et l'hydropédologie dans les bassins afromontagnards (Afrique du Sud)

**Mots clés :** carbone, hydrologie, hydropédologie, la science du sol

**Resume:** L'objectif principal de cette thèse était de déterminer comment les caractéristiques hydropédologiques interagissent avec la dynamique DOC de ces écosystèmes de bassin versant. Nous avons acquis une compréhension générale des caractéristiques hydropédologiques des bassins versants grâce à l'utilisation d'un exercice de cartographie numérique des sols pour créer des cartes hydropédologiques des bassins versants. Les cartes fournissent une compréhension générale des voies d'écoulement et des zones de stockage de ces bassins versants. Nous avons ensuite utilisé ces cartes et des données spécifiques au site pour étudier les caractéristiques hydropédologiques de chaque bassin versant. Dans identifié les voies d'écoulement dominantes de chaque groupe de sol hydropédologique suite à un événement pluvieux. Un certain nombre de facteurs se sont avérés interdépendants et déterminent les voies d'écoulement et la connexion entre les voies d'écoulement. Ces facteurs sont dominés par l'humidité antérieure du sol, l'intensité des précipitations, la durée des périodes sèches et humides ainsi que la profondeur des profils pédologiques. L'étude a ensuite utilisé une approche de modélisation SWAT pour mieux comprendre les voies d'écoulement hydropédologiques des bassins versants. Deux séries de simulations ont été exécutées, l'une utilisant les entrées de temps latérales par défaut et l'autre les entrées de temps latérales spécifiques et celles-ci ont été comparées au débit observé. Les entrées temporelles latérales spécifiques ont amélioré la précision de la modélisation dans tous les paramètres statistiques utilisés, soulignant que des informations pertinentes sur le sol, basées sur des données fiables spécifiques au site, sont essentielles dans la modélisation hydrologique.

La connaissance du caractère hydropédologique des bassins versants a ensuite été utilisée pour étudier l'effet de différents facteurs environnementaux sur la dynamique du COD. Les principaux facteurs environnementaux qui influencent les concentrations de COD dans 2 des bassins versants sélectionnés ont été étudiés. Des échantillons d'eau ont été analysés pour le COD et cette information couplée avec des mesures prises de la hauteur de l'eau dans les piézomètres. Les piézomètres étaient situés dans diverses classes environnementales, y compris différentes couvertures terrestres, différents groupes de sols, différentes zones topographiques, ainsi que différents profils de courbure des pentes. Les concentrations de COD ont été identifiées pour suivre les tendances saisonnières des précipitations et de la température. Une différence statistique a été enregistrée entre les zones terrestres et les zones humides ainsi qu'entre les sols intercalés et les sols réactifs saturés, ce dernier groupe enregistrant les concentrations de COD les plus élevées. L'étude a mis en évidence l'importance des systèmes de zones humides en tant que principaux moteurs des concentrations de COD.

Des capteurs optiques à haute fréquence ont également été placés dans les déversoirs de deux bassins versants et utilisés pour comprendre l'importance de l'influence de la connectivité hydropédologique des bassins versants sur l'exportation de COD. Les données ont été recueillies sur une période d'étude de trois ans et la concentration moyenne de COD par jour a été calculée. Ces données ont été utilisées pour comparer les concentrations de COD aux précipitations, à la température de l'eau, à la turbidité, à la conductivité, au carbone organique total quotidien et au débit quotidien du débit. De plus, le débit journalier a été calculé. L'étude a identifié qu'il existe une dynamique variable d'exportation de COD dans les bassins versants. La connectivité des voies d'écoulement et la manière dont celles-ci influencent les flux de COD sont importantes.

**Title :** Interaction between dissolved organic carbon and hydropedology in Afromontane catchments (South Africa)

**Keywords :** hydrology, hydropedology, carbon, soil science

**Abstract :** Little work has been conducted on the influence of the hydrological connectivity of catchment flow paths and how these impact the storage and export of DOC in mountain catchments. We therefore utilized 3 research catchments within the uKhahlamba-Drakensberg Mountain range of South Africa to conduct this study to enhance our knowledge of these important headwater catchment areas and how they influence downstream locations. The main aim of this thesis was to determine how the hydropedological characteristics interact with the DOC dynamics of these catchment ecosystems. We gained a general understanding of the hydropedological characteristics of the catchments through the use of a digital soil mapping exercise to create hydropedological maps of the catchments. The maps provide a general understanding of the flow paths and storage areas of these watersheds. We then used these maps and site-specific data to investigate the hydropedological characteristics of each catchment. In identified the dominant flow paths of each hydropedological soil group following a rainfall event. A number of factors were found to be interrelated and determine the flow paths and the connection between flow paths. These factors are dominated by antecedent soil moisture, rainfall intensity, the duration of dry and wet periods as well as the depth of soil profiles. The study then utilised a SWAT modelling approach to gain a deeper understanding of the hydropedological flow paths of the catchments. Two sets of simulations were run, one utilising the default lateral time inputs and one the specific lateral time inputs and these were compared against observed streamflow. The specific lateral time inputs improved modelling accuracy in all statistical parameters used, highlighting that relevant soil information, based on reliable site-specific data, is essential in hydrological modelling. The knowledge of the hydropedological character of the catchments was then used to study the effect of different environmental factors on the dynamics of DOC. The main environmental factors that influence DOC concentrations in 2 of the selected catchments were investigated. Water samples were analysed for DOC and this information coupled with measurements taken of the height of the water within piezometers. Piezometers were located within various environmental classes including different land covers, different soil groups, different topographical areas, as well as different slope curvature profiles. DOC concentrations were identified to follow seasonal trends of rainfall and temperature. A statistical difference was recorded between terrestrial and wetland areas as well as between interflow soils and saturated responsive soils, with the latter group recording the higher DOC concentrations. The study highlighted the importance of wetland systems as major drivers in DOC concentrations. High frequency optical sensors were also placed in the weirs of two catchments and used to gain an understanding of the importance of the influence of the hydropedological connectivity of catchment areas on DOC export. Data was collected for a three-year study period and the average DOC concentration per day was calculated. This data was used to compare DOC concentrations against the rainfall, water temperature, turbidity, conductivity, daily total organic carbon and daily streamflow discharge. Furthermore, the daily flux rate was calculated. The study identified that there are variable DOC export dynamics within the catchment areas. Of importance is the connectivity of flow paths and how these influence the fluxes of DOC. This thesis identified a variety of factors that influence DOC storage and export on a catchment scale. It highlights the importance of understanding the hydropedological characteristics of a watershed for both improving our knowledge on the streamflow aspects as well as understanding the DOC dynamics and how these affect the overall carbon budget of a system.

# INTERACTIONS BETWEEN DISSOLVED ORGANIC CARBON AND HYDROPEDOLOGY IN AFROMONTANE CATCHMENTS (SOUTH AFRICA)

**Rowena Louise Harrison**

submitted in fulfilment of the requirements for the degree of

Doctor of Philosophy

(PhD)

under international joint supervision in the

Department of Soil- and Crop- and Climate Sciences
Faculty of Natural and Agricultural Sciences
University of the Free State
Bloemfontein
South Africa

Biogeosciences, UMR 6282 CNRS
Ecole Doctorale Environnements-Santé (ES)
Université Bourgogne Franche-Comté (UBFC)
Dijon
France

**NOVEMBER 2022**

Promotor: Professor J. van Tol

Co – Promotor: Professor, P. Amiotte Suchet

# ABSTRACT

Mountain catchments are vital sources of freshwater for both national and local economies as well as for ecosystems and ecosystem services. They provide several ecohydrological services to downstream locations, including the ecological and physical processes that control the partitioning and routing of rainfall into evaporation, infiltration, transpiration, recharge, and runoff. The characteristics of the soils of these catchments form the basis of these services.

One of the important components of addressing challenges related to water resource management within these mountain areas is understanding the interaction between carbon dynamics, water resources and the soil profile. The understanding of the movement of soil carbon into water resources has gained considerable interest in recent years. However, despite the numerous research on the dynamics of dissolved organic carbon (DOC) from watersheds, particularly within the northern hemisphere, little work has been conducted on the influence of the hydrological connectivity of catchment flow paths and how these impact the storage and export of DOC. In particular montane grassland dominated catchments, and those in South Africa, have often been overlooked within research associated with the sources and dynamics of DOC. We therefore utilised three research catchments within the uKhahlamba-Drakensberg Mountain range of South Africa to conduct this study in order to enhance our knowledge of these important headwater catchment areas and how they influence downstream locations.

The main aim of this thesis was to determine how the hydropedological characteristics interact with the DOC dynamics of these catchment ecosystems. The first aim of the thesis was to gain a general understanding of the hydropedological characteristics of the catchments through the use of a digital soil mapping exercise. Both a rules-based approach as well as a validation exercise were utilised within the ArcSIE (Soil Inference Engine) software to create hydropedological maps of the catchments. The hydropedological soil maps, classified the three catchment areas into four different hydropedological soil groups based on the South African hydropedology classifications. These included the shallow recharge soils, deep recharge soils, interflow soils, and saturated responsive soils. The maps produced from the digital soil mapping exercise show the optimal relationship between the soils and the landform. However, through the use of the Kappa coefficient, it was identified that there are some discrepancies between the hydropedological soil maps created and the site-specific soils identified within the

catchment areas. The maps, however, provide a general understanding of the flow paths and storage areas of these watersheds. Of importance is that the accuracies and inaccuracies within the maps can be quantified, allowing for a confidence rating in their use.

Utilising the hydropedological soil maps coupled with catchment specific climate and streamflow data, water table depth measurements as well as an understanding of how historic and current land management practices have influenced the soil properties, this study investigated the hydropedological characteristics of each catchment. In particular the research identified the dominant flow paths of each hydropedological soil group following a rainfall event. A number of factors were found to be interrelated and these play a key role in determining the flow paths and the connection between flow paths in these areas. These factors are dominated by antecedent soil moisture, rainfall intensity, the duration of dry and wet periods as well as the depth of soil profiles. Furthermore, the dominant role of wetland systems and how these have drying, and wetting cycles are the key focus in understanding the connectivity between the hydropedological flow paths, and the contribution of soil water to the stream networks of the three catchments.

The study was then expanded to gain a deeper understanding of the hydropedological flow paths of the catchments through the use of a SWAT modelling approach. Two sets of SWAT+ models were set up for each catchment. The default lateral time, which is the measure of the time required for water to flow through the catchment before being discharged into the stream, was used in the first set up. Specific lateral time inputs were utilised in the second model set up and the results compared against observed streamflow. The specific lateral time inputs were based on measured hydraulic properties of the soils and the formation of a hydrograph for CP-VI, coupled with the location of hydrological response units within hydropedological soil maps created for each catchment. The specific lateral time inputs improved modelling accuracy in all statistical parameters used, $R^2$, PBIAS, ST DEV, NSE and KGE. This study highlighted that relevant soil information, based on reliable site-specific data, is essential in hydrological modelling. Soil information should therefore be coupled with ecological information such as the effects of fire, vegetation as well as rates of evapotranspiration on hydrological modelling accuracy. These aspects have been shown to all be interrelated.

Through these studies we gained a deeper understanding of the hydropedological characteristics and how this has an impact on the flow dynamics of the catchments. This

knowledge was then transferred to studying the effect of different environmental factors on the dynamics of DOC. The principle environmental factors that influence DOC concentrations in two of the selected catchments (CP-VI and CP-IX) were investigated. Water samples taken every month between September 2019 and June 2021 from the piezometers installed in the two catchments were analysed for DOC. This information was coupled with measurements taken of the height of the water within the piezometer. This height measurement was calculated from the surface of the soil to the depth of the water table. Piezometers were located within various environmental classes including different land covers (wetland and terrestrial), different soil groups (saturated responsive soils and interflow soils), different topographical areas of the catchments (upper, mid, and lower positions), as well as different slope curvature profiles (convex and concave slopes). DOC concentrations were identified to follow seasonal trends of rainfall as well as temperature variations in the catchment areas. A statistical difference (using the Kruskal Wallis method) was recorded between terrestrial and wetland areas as well as between interflow soils and saturated responsive soils, with the latter group recording the higher DOC concentrations in both catchment areas. The research identified that the position of piezometers within different topographical positions of the catchment areas as well as different slope curvatures did not produce significant results. The study did however highlight the importance of wetland systems as major drivers in DOC concentrations. The connectivity of the wetlands to the streams within both catchments plays a role in the attenuation and export of DOC within these watersheds.

DOC concentration variability is closely linked to distinct DOC source zones in catchments and their hydrologic connectivity to the stream network. High frequency optical sensors placed in the weirs of CP-VI and CP-IX were used to gain a deeper understanding of the importance of the influence of the hydropedological connectivity of catchment areas, and in particular the wetland systems, on DOC export. Data was collected every 15 minutes for a three-year study period from the 1$^{st}$ of July 2019 to the 28$^{th}$ of June 2022. The average DOC concentration per day was calculated from this data set. This data was used to compare DOC concentrations against the daily rainfall, daily average water temperature, daily average turbidity, daily average conductivity, daily average total organic carbon and daily streamflow discharge for the study period. Furthermore, the daily flux rate was calculated utilising the average daily DOC concentration and the daily streamflow measurements recorded at each catchment's individual weir. The study identified that there are variable DOC export dynamics within the catchment areas. There is a seasonal variability of DOC concentrations and flux rates with these being

generally lower in dryer seasons (autumn and winter) and higher in wetter seasons (spring and summer). The study furthermore identified the importance of the connectivity of flow paths and how these influence the fluxes of DOC. Connected flow paths between upslope wetland areas and the stream network increase DOC export from the catchment areas. The hydropedological influence of the soil groups and how these interact with each other at various timescales including seasonal flow paths as well as event flow paths affects the flow of DOC within the stream networks. The impact of rainfall events on the export of DOC was furthermore investigated. Storm events move large quantities of DOC however, this is dependent on the antecedent soil moisture conditions before the event and the connection of soil water flow paths. Rainfall events which occur once the wetlands are saturated, following a dry period flow more as overland flow or shallow subsurface flow and can therefore access available DOC and export this to the stream network. Longer rainfall events, as well as events which take place in very wet conditions, however, have a decrease in DOC concentration with time, following the initial increase, and this may be attributed to a dilution effect of DOC in the soil water that is exported from the catchments.

Given the importance of these mountainous watersheds to the ecohydrological services of downstream ecosystems, long term data gathered within the catchments on the hydrologic pathways and DOC concentrations has the potential to allow for future studies to determine the impact of the ever-changing climatic influence on the dynamics within these catchment areas. These climatic changes will affect flow paths as well as the DOC export, and this has implications of downstream ecosystems. This thesis provides valuable insight into the interactions of DOC and hydropedology in these Afromontane areas. It identifies a variety of factors that influence DOC storage and export on a catchment scale. The results highlight the importance of understanding the hydropedological characteristics of a watershed for both improving our knowledge on the streamflow aspects as well as understanding the DOC dynamics and how these affect the overall carbon budget of a system.

# DECLARATION

I, Rowena Louise Harrison, declare that the thesis that I herewith submit under international joint supervision (Convention de Cotutelle Internationale de these) for the Doctoral Degree at the University of the Free State, and the Université Bourgogne Franche-Comté (UBFC) is my independent work, and that I have not previously submitted it for a qualification at another institution of higher education.

# DECLARATION: PUBLICATIONS

**Publication 1 – Chapter 4 of this thesis**

Harrison, R., van Tol, J. (2022). Digital Soil Mapping for hydropedological purposes of the Cathedral Peak research catchments, South Africa. In: Adelabu, S., Ramoelo, A., Olusola, A., Adagbasa, E. (eds) Remote Sensing of African Mountains. Springer, Cham. https://doi.org/10.1007/978-3-031-04855-5_10

Author Contributions**:** R Harrison: Conceptualization, Methodology, Formal analysis, Validation, Investigation, Data formalisation, writing of the original draft, Editing and Finalisation. J van Tol: Conceptualization, Methodology, Data formalisation, Review. Supervision.

**Publication 2 – Chapter 5 of this thesis**

Harrison, R., van Tol, J., and Amiotte Suchet, P. (2022). Hydropedological characteristics of the Cathedral Peak research catchments. *Hydrology*. 9. 11. 189. https://doi.org/10.3390/hydrology9110189.

Author Contributions: R Harrison: Conceptualization, Methodology, Formal analysis, Writing of the original draft, Writing—review and editing, Visualisation, J van Tol: Conceptualization, Methodology, Formal Analysis, Funding Acquisition, Resources, Supervision, Writing—review and editing. P Amiotte Suchet: Resources, Supervision, Writing-review and editing, Visualisation, Validation.

**Publication 3 – Chapter 6 of this thesis**

Harrison, R.L., van Tol, J. and Toucher, M.L. (2022). Using hydropedological characteristics to improve modelling accuracy in Afromontane catchments. Journal of Hydrology: Regional Studies. 39. https://doi.org/10.1016/j.ejrh.2021.100986.

Author Contributions**:** R Harrison: Conceptualization, Methodology, Formal analysis, Validation, Investigation, Data formalisation, writing of the original draft, Editing and Finalisation. J van Tol: Conceptualization, Methodology, Data formalisation, Review. Supervision. M Toucher: Methodology, Data formalisation, Review.

**Publication 4 – Combined version of Chapter 7 and Chapter 8 of this thesis**

Harrison, R., van Tol, J. Amiotte-Suchet, P., Thevenot, M. and Mathieu, O. (2022). Environmental factors influencing dissolved organic carbon concentrations in Afromontane catchments. *Submitted to Biogeochemistry*

Author Contributions: R Harrison: Conceptualization, Methodology, Formal analysis, Validation, Investigation, Data formalisation, Writing of the original draft, Editing and Finalisation. J van Tol: Conceptualization, Methodology, Data formalisation, Review. Supervision. P. Amiotte-Suchet: Methodology, Data formalisation, Review. Supervision. M. Thevenot: Methodology, Data formalisation, Review, O Mathieu: Methodology, Data formalisation, Review.

# ACKNOWLEDGEMENTS

I would like to firstly thank Professor Johan van Tol for his support, patience, and guidance during my PhD. His humour and encouragement were invaluable during this experience, and I am very grateful to have had him as a Promotor.

I would like to thank my Co-promotor, Professor Philippe Amiotte Suchet as well as Dr. Olivier Mathieu, and Dr. Mathieu Thevenot for all their guidance and encouragement, for allowing me to have this opportunity to work under the Université Bourgogne Franche-Comté (UBFC), and for sharing so much knowledge on carbon dynamics. The French teams invaluable assistance during field work, the provision of equipment, the laboratory analysis, and data management is much appreciated.

Thanks, must also go to Ms. Sue van Rensburg at the South African Environmental Observation Network (SAEON): Grasslands-Forest-Wetlands Node in Pietermaritzburg for giving me the opportunity to pursue my PhD and for all the encouragement along the way.

Thank you to the staff and students of SAEON who have always encouraged me to finish my PhD, including Dr. Michelle Toucher for her assistance with SWAT modelling and data, Mr Kent Lawrence, and Mr Siphiwe Mfeka for their assistance with all the logistical support during the field work and the data management, as well as Busii Mdunge for her help with administrative matters. Thank you to Lindokuhle Dlamini for all his assistance both during field work, as well as being a co-PhD student willing to share ideas during this journey.

Thank you to the Iphakade Earth Stewardship Science Bursary Programme for providing funding during the period of this project.

Thank you to Ezemvelo KZN Wildlife for supporting this research within the Maloti-Drakensberg Park.

Thank you finally to my family and friends, who have always encouraged me to pursue anything I have chosen to do. Your support, understanding and encouragement are forever appreciated.

# TABLE OF CONTENTS

# LIST OF FIGURES

# LIST OF TABLES

# CHAPTER 1 – GENERAL INTRODUCTION

## 1.1. BACKGROUND AND RATIONALE FOR THE STUDY

Mountain catchments are vital sources of freshwater for both national and local economies as well as for ecosystems and ecosystem services. They provide several ecohydrological services to downstream locations, including the ecological and physical processes that control the partitioning and routing of precipitation into evaporation, infiltration, transpiration, recharge, and runoff. The characteristics of the soils of these catchments form the basis of these services. This is because soil and water are the fundamental elements in understanding the hydrological response of the catchments within these mountains (Brooks and Vivoni, 2015, Taylor et al. 2016).

In order to improve management of the ecohydrological services of mountain catchments it is vital that we gain a deeper understanding of the interactions between soil and water in these areas. One of the aspects of addressing challenges related to water resource management is understanding the interaction between carbon dynamics, water resources and the soil profile. A number of studies have highlighted the importance of small mountain streams in the global carbon cycle and the effect these streams have on downgradient locations ((Milliman and Syvitski, 1992, Turowski et al. 2016).

Despite the numerous studies conducted, there is a paucity of research focusing on the relationship between the hydrology of hillslopes, wetlands and headwater streams located in montane areas in general. Controls on carbon losses at the catchment scale are furthermore poorly understood, and yet carbon fluxes may have important consequences for both terrestrial and aquatic ecosystem functions. This is pertinent as managing ecosystems and habitats that act as critical natural carbon sinks, ensure that they retain as much of the carbon trapped in the system as possible. This is becoming an important mitigation against the effects of climate change (Read et al., 2001). Resolving carbon budgets from the small watershed scale to the global scale is essential to obtain better estimates of the amount of organic carbon exported from terrestrial sources to streams and rivers (Hope et al., 1997).

The variations in hydrologic flow paths within catchment areas have often been overlooked as a variable that could influence carbon cycling. Hydropedological pathways are a major source of carbon in the receiving environment, with these pathways being dependent on the connection of flow paths within catchment areas.

DOC influence on stream chemistry is dependent on flow paths, and it has been shown that stream DOC is similar to concentrations found in soil- water from deeper soil horizons despite high concentrations observed in leachate from surface soil (McDowell and Wood, 1984). However, organic-rich surface soils and wetlands have been shown to contribute substantially to stream DOC when hydrologic conditions ensure connectivity of these important DOC sources to their receiving waterways (Morel et al., 2009; Pacific et al., 2010). Changes in the quantity and composition of DOC exported from soils can strongly affect the receiving aquatic ecosystems, by changing their metabolism, light regime, and by modulating the activity of other chemicals and biological processes (Stanley et al., 2012). This necessitates prudent management options to mitigate the undesirable effects of DOC on aquatic life.

In South Africa, the majority of soil organic carbon studies (SOC) are limited to the impact of erosion on the transport and release of SOC in catchments (Chaplot and Poesen., 2012). The available literature suggests that the release of SOC is mostly influenced by biochemical, hydrological processes and properties of the landscape. Various laboratory experiments on the influence of biochemical processes on SOC have revealed that the C:N ratio, high microbial activity, the increase in phosphorus contents and pH all increase the SOC concentrations and fluxes. However, increases in the clay content, Fe-Al oxides/hydroxides and divalent cations have the opposite effect. These results suggest that landscape scale environmental controls may be more important than biochemical factors in the release of SOC from terrestrial to aquatic environments as DOC (Lin, 2012). Land-use and land-use change may therefore be critical factors influencing carbon concentrations and fluxes.

It is therefore important to understand how, when and where DOC concentrations and fluxes are amplified at the catchment scale. The factors influencing the solubility of organic carbon as well as its sources and pathways need to be identified, characterised, and quantified. This is particularly so in montane ecosystems, so that we can understand how these headwater catchments will influence downgradient environments. The understanding of these soil, water,

carbon dynamics can be utilised to predict the impact of land-use and climate change on organic carbon dynamics.

## 1.2. AIMS AND OBJECTIVES

The main aim of this study was to investigate how the hydropedological characteristics of soils interact with and move DOC within and out of a catchment area. To achieve this main aim, the first part of the thesis focuses on gaining an understanding of how the hydropedological characteristics of a catchment area influence the water dynamics and flow paths. This is fundamental to understanding how DOC is stored and moved in the catchment areas. The storage and movement of DOC is then studied in the latter part of the thesis. The following objectives are therefore investigated within this thesis:

1. Identify the hydropedological characteristics of the three catchments, subjected to different land-use, in the Cathedral Peak experimental research site (Chapter 4).
2. Characterise the hydropedological behaviour of the soils and hillslopes in these catchments (Chapter 5).
3. Determine the importance of the hydropedological behaviour of the soils on the streamflow dynamics of the catchment areas (Chapter 6).
4. Establish the principle environmental factors that influence DOC concentrations in the catchment areas (Chapter 7).
5. Determine the influence of the hydropedological characteristics on DOC movement at a catchment scale. (Is carbon storage and export in a catchment dependent on flow paths from wetland systems?) (Chapter 8).

## 1.3. ARRANGEMENT OF THESIS

This thesis consists of nine chapters, of which five chapters (Chapters 4 – 8) are prepared for publication in peer-reviewed journals. Each research paper consists of a literature review related to the aim, a methodology, results, discussion, conclusions, and references of that paper. These papers have been reformatted to ensure continuity in this thesis. As a result of the inclusion of 5 research papers, some repetition was unavoidable. A study site description is however included in Chapter 3, so that this information is not repeated throughout the thesis. The first three experimental chapters (Chapters 4, 5, and 6) focus on understanding the hydropedological characteristics of the catchment areas, while the subsequent two

experimental chapters (Chapters 7 and 8) focus on DOC and how environmental factors and the hydropedological characteristics of the catchments interact with this element. Finally, the thesis has a concluding chapter (Chapter 9) that summarizes the various components of this study.

## 1.4.REFERENCES

Brooks, P.D., and Vivoni, E.R. (2015). Editorial. Mountain ecohydrology: quantifying the role of vegetation in the water balance of montane catchments. Ecohydrology. 1. 187-192. DOI: 10.1002/eco.27.

Chaplot, V., and Poesen, J. (2012). Sediment, soil organic carbon and runoff delivery at various spatial scales. Catena.88.1. 46-56. https://doi.org/10.1016/j.catena.2011.09.004.

Hope, D., Billett, M.F., and Cresser, M.S. (1997). Exports of organic carbon in two river systems in NE Scotland. Journal of Hydrology. 193. 61-82.

Lin, H. (2012). Hydropedology Synergistic Integration of Soil Science and Hydrology. Academic Press. USA.

McDowell, W. H., and Wood, T. (1984). Podzolization: Soil Processes Control Dissolved Organic Carbon Concentrations in Stream Water. Soil Science. 137.1. 23-32.

Milliman, J.D., and Syvitski, J.P.M. (1992). Geomorphic/Tectonic Control of Sediment Discharge to the Ocean: The Importance of Small Mountainous Rivers. The Journal of Geology, 100. 525-544. http://dx.doi.org/10.1086/629606.

Morel, B., Durand, P., Jaffezic, A., Gruau, G. and Molénat, J. (2009). Sources of dissolved organic carbon during stormflow in a head-water agricultural catchment, Hydrological Processes. 23: 2888–2901.

Pacific, V. J., Jensco, K. G., and McGlynn, B. L. (2010). Variable flushing mechanisms and landscape structure control stream DOC export during snowmelt in a set of nested catchments. Biogeochemistry. 99: 193–211. DOI. 10.1007/s10533-009-9401-1.

Read, D., Beerling, D., Cannell, M., Cox, P., Curran, P., Grace, J., Ineson, P., Jarvis, P., Malhi, Y., Powlson, D., Shepherd, J., and Woodward, I. (2001). The role of land carbon sinks in mitigating global climate change London, UK. Royal Society. Policy document, 10/01.

Stanley, E.H., Powers, S.M., Lottig, N.R., Buffam, I., and Crawford, J.T. (2012). Contemporary changes in dissolved organic carbon (DOC) in human-dominated rivers: is there a role for DOC management? Freshwater Biology. 57. 26–42. https://doi.org/10.1111/j.1365-2427.2011.02613.x.

Taylor, S.J., Ferguson, J.W.H., Engelbrecht, F.A., Clark, V.R., van Rensburg, S., and Barker, N. (2016). The Drakensberg Escarpment as the Great Supplier of Water to South Africa. In. G.B. Greenwood. and J.F. Shroder Jr. (eds). Mountain Ice and Water. Investigations of the hydrologic cycle in Alpine Environments. Developments in Earth Surface Processes 21. Elsevier. Netherlands.

Turowski, J.M., Hilton, R.G., and Sparkes, R. (2016). Decadal carbon discharge by a mountain stream is dominated by coarse organic matter. Geology. 44. 27-30. DOI:10.1130/G37192.1.

# CHAPTER 2 – LITERATURE REVIEW

## 2.1. INTRODUCTION

The provision of hydrologic ecosystem services is critical for both human well-being and environmental sustainability (Feger and Hawtree, 2013). Water resources are under growing pressure as the global population rises, and the natural supply, in the form of rainfall, is becoming increasingly variable and uncertain with climate change (Trenberth et al. 2003, Giorgi et al. 2004). Improving and protecting water quality, both for human needs and to sustain aquatic ecosystems is a major challenge (Stanley et al. 2012). Subsequently it is essential that water resources are managed sustainably in terms of both their quantity and quality (Bilotta et al. 2012). A key component in addressing current and future challenges in water resource management is the development of a comprehensive understanding of the complex relationships between soil properties, land use and management, and the hydrological cycle (Feger and Hawtree, 2013).

One of the important components of addressing challenges related to water resource management is understanding the interaction between carbon dynamics, water resources and the soil profile. The understanding of the movement of soil carbon into water resources has gained considerable interest in recent years. This is particularly so in understanding the major routes for the transport of soil organic carbon (SOC) as well as identifying the sources and flow mechanisms responsible for SOC to become organic carbon, and in particular dissolved organic carbon (DOC) in watercourses (Kahmen et al. 2005, Smith, 2014, Zhang et al. 2015, Wei et al. 2016).

In montane ecosystems this is of particular relevance as the headwater stream networks that make up montane catchments are a notable component of the global carbon cycle (Tranvik et al. 2009, Jaffé et al. 2012,) Small mountainous streams are of importance in the export of carbon as, although individually they transport relatively small amounts of sediment, together, their combined loads can contribute to over half the global river sediment flux (Milliman and Syvitski, 1992). They therefore represent a crucial linkage between land and oceans in the global carbon cycle (Aufdendkampe et al. 2011). Despite the significant importance of the movement of organic carbon in aquatic ecosystems, the processes controlling DOC delivery to

stream waters at the catchment scale are still poorly understood and warrant further investigation (Laudon et al. 2011).

## 2.2. SOILS AS SOURCES OR SINKS OF CARBON

Soil carbon is recognised as the largest store of terrestrial carbon (Batjes, 1996, Ontl and Schulte, 2012). There is substantially more carbon stored in the world's soils than is present in the atmosphere. The global soil carbon pool to one-meter depth, was estimated at 2500 Pg C in 2017, of which about 1500 Pg C is SOC. This is about 3.2 times the size of the atmospheric pool and 4 times that of the biotic pool (Lal, 2010, Zomer et al. 2017) (Figure 1).

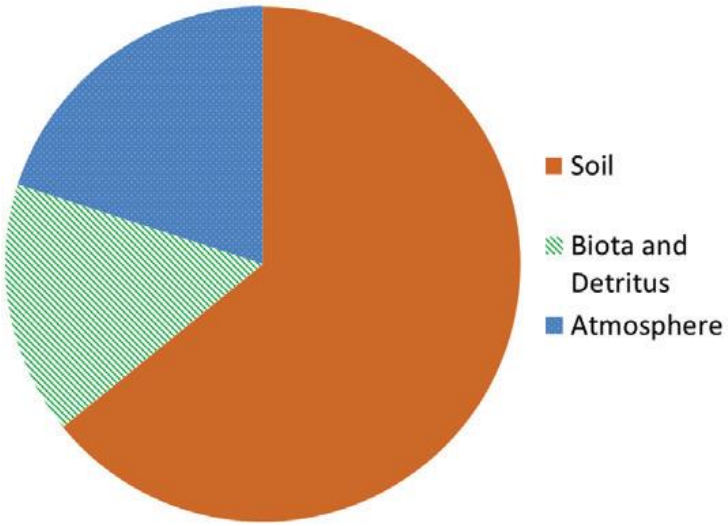


Figure 2.1: Relative size of the active terrestrial carbon pools. Note the size of the soil carbon pool relative to the biological and atmospheric pools, demonstrating the importance of soils in the carbon cycle (Lal, 2010).

Soil carbon storage is a vital ecosystem service, resulting from interactions of ecological processes. SOC levels are directly related to the amount of organic matter contained in soil. Soil organic matter (SOM) is a key component of soil that affects its physical, chemical, and biological properties, contributing meaningfully to its proper functioning. Physically, SOM improves aggregation of soil particles resulting in soil structure that allows for improved air and water movement. Chemically, SOM increases the cation exchange capacity, thus improving retention of nutrients. Additionally, organic-bound nitrogen, phosphorus and sulphur are associated with organic carbon, and upon their decomposition, provide a slow release of nutrients for plant production. SOC, furthermore, provides binding sites for

chemicals and other trace elements, often anthropogenically introduced, thus lowering leaching of hazardous chemicals through the soil profile. Biologically, SOM is the source of carbon and energy for most microorganisms and fauna. Increased SOM increases the biomass and diversity of the soil biota (Rice, 2005; Ontl and Schulte, 2012).

Depending upon management, biomass input levels, micro-climatic conditions, and bioclimatic change soils can act as both sources and sinks of carbon (Zomer et al. 2017). Soil carbon sequestration is a process in which carbon is removed from the atmosphere and stored in the soil carbon pool. This process is primarily mediated by plants through photosynthesis, with carbon stored in the form of SOC (Ontl and Schulte, 2012). Soils act as carbon and greenhouse gas (methane ($CH_4$) and nitrogen dioxide ($N_20$) sinks. This is affected by climate, land use, soil properties as well as nitrogen inputs (Lal, 2019). Examples of this are shown by Mureva et al. (2018) in which soil bulk density and clay content mediate the magnitude and direction of change in SOC. In some grasslands encroached by woody species, SOC was shown to decrease as the soil bulk density increased, while SOC accumulated with increasing clay content. Furthermore soils with greater clay and silt fractions usually have higher carbon concentrations and stocks than those with greater sand fractions (Follett et al. 2012, Cao et al. 2013). This is thought to be as a result of organic materials being preferentially decayed from soils with coarse particles, while carbon decomposition products tend to accumulate in finer clay and silt particles (Amelung et al., 1998). Moreover, it has been suggested that clay and silt physically protect organic materials from decomposition and promote the accumulation of recalcitrant material in the fine particle-size fractions of soils (Hassink, 1997, Zhao et al., 2006).

Soils can also act as sources of carbon in the form of greenhouse gases. Various processes lead to greenhouse gas emissions from soil and litter to the atmosphere. Raich and Tufekcioglu (2000) concluded that the flux of carbon from soils to the atmosphere occurs primarily in the form of carbon dioxide ($CO_2$), which is the result of soil respiration and constitutes the largest terrestrial source of $CO_2$ to the atmosphere. The production of $CO_2$ in non-calcareous soils originates almost entirely from autotrophic (respiration from root, mycorrhizal fungi and microbes living on exudates) and heterotrophic respiration (the respiration of heterotrophic microorganisms decomposing SOM) (Högberg et al. 2001), with the relative contribution from each respiration component largely varying from 10 to 90% of the total soil respiration (Hanson et al. 2000).

A number of factors lead to the contribution of soil as either a source or a sink of SOC. A particular emphasis has been placed on the influence of climate on particular soil properties such as soil and air temperature, rate and type of erosion, weathering rates, desertification of soils as well as changes to salinity levels. More indirect impacts of climate include changes to soil health and soil formation as well as changes to the effects of net primary productivity, hydrological cycles, and energy balance. These impacts have an effect on the soil-gas fluxes of greenhouse gases such as $CO_2$ and $CH_4$ (Lal and Stewart, 2018).

In studies conducted by Lal (2003 and 2010), the vice versa was also found to be the case, with soils having an impact on climate. This was due to the soils effect on the moderation of the atmospheric chemistry by cycling of water, carbon, nitrogen, phosphorus and sulphur and changes in vapour pressure of water through a soil moisture regime. Soil was found to moderate climates at the micro, meso, and macro scales, and over short and long time periods and this has important consequences on the rising atmospheric $CO_2$ levels.

The principal soil properties that affect climate, are the same as those that also affect soil health. These are physical (clay content and mineralogy, structure, plant available water, infiltration rate, colour, albedo, bulk density), chemical (acidity, charge properties, nutrient reserves and dynamics, elemental balance), biological (SOC concentration and attributes, microbial biomass carbon, respiration quotient, enzyme activity, species diversity), and ecological (erosion, decomposition, leaching, compaction, aeration, energy balance, water balance). The relative importance of these properties and processes varies among ecoregions around the globe (Lal and Stewart, 2018).

Studies have shown that the extent of soil quality, SOC and nitrogen stocks varies with vegetation type, climate, soil type, management practice, and land use history (Lemenih and Itanna, 2004) with these all having an impact on the production or sequestration of carbon within a catchment area. Despite its importance for aquatic ecosystem function and watershed carbon budgets, little is known about how land management influences SOC export (Dalzell et al., 2011). Soil carbon sequestration is a critical ecosystem service of grasslands (Stanley et al., 2018).Despite this, land management activities rarely incorporate SOC as a major management criterion (Stanley et al., 2012).

Land management practises can alter both SOC amount and composition via changes in soil organic matter pool, hydrological flow paths and aquatic microbial processing (Dalzell et al., 2011; Stanley et al., 2012). It has been shown that in natural landscapes, $CO_2$ sequestered by plants is partly converted to DOC through leaching and decomposition, then transported into rivers within a few years. In modified landscapes, the uptake of the new carbon can be reduced by deforestation and urbanization, whilst drainage and disturbance of soil exposes carbon that has been stored for hundreds or thousands of years to decomposition and leaching (Evans et al., 2016).

## 2.3. CARBON WITHIN THE STREAM NETWORKS OF CATCHMENT AREAS

The delivery of allochthonous inputs of organic carbon, from carbon pools in headwater watersheds to stream ecosystems is widely accepted as an important process (Mei et al. 2012). Carbon is transported continuously by rivers as organic carbon as well as inorganic carbon that functions in weathering reactions (Maybeck, 1993). Hydrology therefore strongly affects carbon export from terrestrial to aquatic ecosystems by impacting redox biogeochemistry and water flow paths through organic rich soil horizons which are typical carbon sources (Kawasaki et al. 2008).

Carbon can be moved within the stream network of a catchment as either particulate organic carbon (POC), dissolved organic carbon (DOC) or as dissolved inorganic carbon (DIC) that functions in weathering reactions (Maybeck 1993). POC comes from a variety of sources in river ecosystems. It is biologically and chemically active and is part of the labile pool of SOM, as particulate organic matter (POM). POM is one of the most easily decomposable fractions of non-living SOM after microbial biomass. It fulfils many soil functions mediated by organic matter. It is a source of food/energy for microorganisms and soil animals as well as nutrients for plant growth. It furthermore enhances aggregate stability, water infiltration and soil aeration; it increases cation exchange capacity and buffering pH. It also binds environmental pollutants such as heavy metals and pesticides (Dodd and Whiles, 2010; Bauer and Bianchi, 2011). POM is transported to watercourses where it is then considered as POC. POC is organic particles which fall within the size range of >0.45 to <1000 µm that are either suspended in the water column or deposited within lotic habitats. Suspended POC functions as an important food resource for many filter-feeding animals and represents a major pathway of organic matter export downstream (Dodds and Whiles, 2010).

The total inorganic carbon concentration (DIC) in fresh water depends on the pH, which is governed largely by the buffering reactions of carbonic acid and the amount of bicarbonate and carbonate derived from the weathering of rocks. Carbonates exist as a number of polymorphic and hydrated forms. The most important carbonate of aquatic systems is Calcium carbonate (CaCO3), which occurs in natural waters principally as calcite. The solubility of $CO_2$ increases markedly in water that contains carbonate. A definite amount of free $CO_2$ will remain in solution after equilibrium is reached between calcium, bicarbonate, carbonate, and undissociated calcium carbonate (Wetzel, 2001).

The quantity of organic carbon in watercourses is dominated by DOC (Wetzel, 1992) and this constituent is the primary carbon focus of this thesis. DOC is an important component of solutions in terrestrial and aquatic ecosystems through its influence on acidity and mobility of nutrients and contaminants (Hagedorn et al. 2000). This is due to DOC being an important water quality constituent (McGlynn and McDonnell, 2003). One of the most common causes of water quality impairment is the excessive levels of DOC, which can have a range of detrimental effects on water resources, from making a significant contribution to the acidity of natural waters through formation of organic acids and affecting biological activity through light adsorption. DOC can also influence nutrient availability through the formation of organic complexes, and control the solubility, transport, and toxicity of metals. In combination, these alterations to water quality can lead to undesirable effects on human health. For example, DOC has been found to be a major precursor in the formation of carcinogenic and mutagenic disinfection by-products (Chow et al., 2007). It has also been linked to the transport and reactivity of toxic substances such as mercury (Aiken et al., 2011).

Despite the significant importance of DOC in aquatic ecosystems, the processes controlling DOC delivery to stream waters at the catchment scale are still poorly understood (Laudon et al. 2011). Inland water bodies are active, changing, and important regulators of the carbon cycle (Tranvik et al. 2009). In particular the importance of small mountain streams as a major contributor to the spatial distribution patterns of organic carbon is a fundamental factor in the global carbon cycle (Turowski et al. 2016).

One of the most consistent relationships with DOC concentrations in streams has been found with the flow dynamics of catchment areas. Studies have shown correlations between DOC concentrations identified in the headwater catchment areas and the streamflow (Dawson et al.

2002, Billett et al. 2006), thus identifying that both biological and hydrological processes operating within the catchment area affect the DOC concentrations (Roig-Planasdemunt et al. 2017).

To better explore carbon cycling in the freshwater ecosystems of mountainous catchments and understand the fate of the main organic components, it is important to first understand the factors that regulate water flow paths within these catchment areas.

## 2.4. HYDROPEDOLOGY AND SOIL FLOW PATHS

It has long been recognised that the role of soils is critical to how catchments store and release water. This is due to the influence that soil characteristics have on the storage and transfer rates of precipitation through catchment areas, with this store and release capacity attributed to the different physical properties of the various soil types located within these areas (Geris and Tetzlaff, 2015).

Soil forming factors are diverse and include 1) materials (e.g., parent materials, organic matter), 2) climate (e.g., wetting-drying, freezing-thawing), 3) biology (e.g., plant roots, soil fauna), 4) human activities (e.g., tillage, fertilization), and 5) time (e.g., biological timescale, geological timescale). This creates a soil architecture that is highly heterogeneous in different soils and this results in varied soil hydraulic properties (Ma et al., 2017).

Hydropedology combines the study of these different arrangements of soils as well as the interactive processes between the pedologic and hydrologic properties of the vadose zone. It further aims to provide a holistic understanding of the interactions between the pedosphere and the hydrosphere (Ma et al., 2017). The hydropedological characteristics of a catchment play a crucial role in both runoff generation as well as the hydrologic connectivity between hillslopes and streams (Geris and Tetzlaff, 2015).

Jarvis et al (2012) showed that soils and in particular spatial patterns of preferential flow at the landscape scale are far from being completely random. They instead show a clear deterministic component because recognisable diagnostic soil horizons, soil materials, and pedons tend to display characteristic flow and transport patterns. Soil water processes can therefore be described in terms of content (volumetric or gravitational), potential (matric, osmotic, and

gravitational potentials) and movement (subsurface flows in quantity or in speed). All of these descriptions are variable in time and space, yet their range is generally restricted based on location and time (Zhu et al. 2018). They are important controls on the various biological, physical and chemical processes in the earth's critical zone (Ma et al. 2017).

As a result of these clear soil patterns, a landscape can be divided into two broad hydrologic zones: 1) recharge zone and 2) discharge zone (Heath, 1980). The recharge zone is characterized by a downward movement of water from soil surface (unsaturated) to groundwater (saturated). In the discharge zone, water moves from groundwater toward the surface. A flow through zone may also occur on some landscapes where groundwater reaches the surface, but the flow lines are essentially parallel to the ground surface. As water moves it carries with its dissolved constituents such as nutrients, dissolved organic matter, and reduced Fe and Mn (Lindbo and Richardson, 2000, Rhoton et al. 2002).

Further research into the dynamics of hydropedology, particularly within South Africa has shown that the soils and placement of soils within a landscape are not randomly distributed but can be further grouped into hydropedological soil types. These include recharge soils, interflow soils, responsive soils, and stagnating soils. These groups of soils convey water differently and thus have different hydropedological behaviour (van Tol and Le Roux, 2019). This has implications on not only water movement within a catchment but on the soil biogeochemistry of a catchment as well.

## 2.5. HYDROPEDOLOGY AND CARBON DYNAMICS IN SOILS

Soil water dynamics not only affect flow and transport within soils, they also influence the cycling of soil organic matter as well as the export of carbon (Vogel et al. 2013). Hydropedology interacts with soil biogeochemistry in many complex ways, often relating to the spatial and temporal variation in water, nutrients, and carbon (Castellano et al. 2012). In spatial dimensions, soil properties, ranging from the microscopic to the megascopic levels, exert an important control on hydrologic processes and biogeochemical dynamics. In temporal dimensions, both short-term soil functioning processes and long-term soil pedogenic processes are impacted by hydrologic processes, and vice versa (Lin, 2012). Therefore, understanding the role of soils in both the water cycle, as well as the cycles of greenhouse gases requires including not only the surface horizons of soils, but the full depth to the groundwater table,

including the unsaturated (vadose) and the saturated zone (in hydrological terms) (Ma et al. 2017).

Earth's biogeochemistry is largely controlled by cycles of oxidation–reduction (redox) reactions. Organisms use redox reactions to derive energy by transferring electrons from a reduced chemical species (electron donor) to an oxidized chemical species (electron acceptor). In the soil, the rate and chemical pathways of these biogeochemical reactions are indirectly, but tightly linked to the interacting forces of water and soil structure (Dayo-Olagbende et al. 2020).

One of the major soil - water resources that are utilised for their ecosystem services are wetland systems. Wetlands offer many ecosystem services to humankind, including water quality improvement, flood mitigation, coastal protection, and wildlife protection (Mitsch and Gosselink, 2007). Wetlands are the products of the erosional and depositional processes, as well as the presence of geological influences controlled by the variable environment. It is furthermore estimated that 20–30 % of the Earth's soil pool of carbon (Lal, 2003) is stored in wetlands (Roulet 2000, Bridgham et al. 2006), although wetlands comprise only about 5–8 % of the terrestrial land surface (Mitsch and Gosselink 2007).

The various wetland types as well as their respective drying and wetting cycles play different roles in how water flows through a catchment area. For example, hillslope seep wetlands located on gently to steeply sloping terrain and dominated by colluvial, unidirectional movement of water and material down-slope, are fundamental units of the hydrologic landscape in which water inputs are primarily via subsurface flows from an up-slope direction (Ollis et al., 2013). Water movement through seeps is therefore mainly in the form of interflow (Kotze et al., 2007). Valley bottom wetlands on the other hand are located in more of a depositional zone, with water inputs both as surface and subsurface flow. Water movement through these systems can be both as interflow and overland or shallow subsurface flow (Ollis et al., 2013) When hydrological movement through wetlands is generally via interflow, the attenuation of water within the landscape is higher. This attenuation of water allows for the settling out, or filtration of sediment, SOC as well as other minerals. This trapping of carbon within the landscape could allow wetlands to contribute as a carbon sink (Kotze et al., 2007). When wetland systems, in particular valley bottom wetlands, are however saturated these contribute more to hydrological flow as overland flow, limiting their attenuation potential

(Tunaley et al. 2016). The wetland systems can therefore contribute as a carbon source, adding additional variations to the debate on catchment and carbon dynamics.

Overland flow, interflow, and soil erosion, which commonly occur during natural rainfall events, are three major routes for the lateral transport of SOC from soils to aquatic ecosystems (Hua et al, 2016). The contribution of wetlands to the carbon balance can therefore be an important component within catchments. In recent years there has been considerable interest in identifying the sources and flow mechanisms responsible for DOC within watersheds (Inamdar and Mitchell, 2006).

Phillips and Beeri, (2017) conducted research regarding greenhouse gas emissions from wetland landscapes and identified that $CH_4$ and $CO_2$ fluxes were highly variable across spatial patterns associated with hydropedologic zones. Soil moisture and temperature were significant covariates for both $CH_4$ and $CO_2$ fluxes. $CH_4$ emissions were highest in deep wetlands, with a reduction in $CH_4$ emissions with distance from water. Therefore, soils were sources of $CH_4$ in wetland systems but $CH_4$ sinks in the drier upslope environments. Variations in $CO_2$ emissions were likely contributed by variations in plant respiration in the various hydropedologic-vegetation zones.

The influence of hydropedology which affects the flow paths of a catchment provides a conceptual and observational framework for linking soil hydrologic function to landscape carbon cycling (D'Amore et al. 2015). Continued coupling of biogeochemistry and hydropedology is needed to understand ecosystem processes and improve our ability to predict the effects of new management practices and future climate on ecosystem structure and dynamics (Field et al., 2007).

## 2.6. HYDROPEDOLOGY AND CARBON DYNAMICS IN MONTANE GRASSLANDS

Globally, montane grasslands and wetlands deliver a wide array of ecosystem benefits, including flood water retention, sediment stabilisation, maintenance of stream base flows, and habitat for unique vegetation and faunal communities. These grasslands are furthermore important carbon sinks (Norton et al. 2011). Balancing multiple and potentially conflicting economic, social, and conservation goals has become a central focus in the stewardship and conservation of these ecosystems (Roche et al., 2014).

Studies conducted by Wang et al., (2018) in China show that soil-carbon density is greater in high altitude grasslands (6.84 ± 1.23kg C $m^{-2}$) compared to temperate grasslands (5.22 ± 0.47kg C $m^{-2}$) and sub-tropical grasslands (4.02 ± 0.21kg C $m^{-2}$) mainly due to the lower organic matter decomposition rate in the montane grasslands. Grassland soil carbon stocks were found to be a function of the rate of primary production as well as the rate of organic matter mineralisation. A correlation between mean annual precipitation and mean annual temperature was furthermore identified as a factor in determining the carbon stocks. A positive impact of precipitation is driven by evidence that an increase in water availability generally promotes plant growth and thus increases the organic matter input into the soil (Wang et al. 2018). The negative impact of temperature is driven by an increase in microbial activity with increasing temperature thereby reducing the carbon stocks (Miller et al. 2004).

This was also identified by Cao et al. (2013) where a study conducted along an altitudinal gradient examined SOC, total nitrogen (TN), total phosphorus (TP), available nitrogen (AN), available phosphorus (AP), and soil particle size distribution. This study revealed that SOC, TN, TP, AN and AP stocks in the upper 30cm of soil in the higher altitude were significantly higher ($P < 0.05$) when compared to lower altitudes. The study also showed that SOC exhibited the largest spatial variability within the study site. This is due to SOC content being influenced by many factors such as land management, precipitation, air temperature, and grassland type (Jobbágy and Jackson 2000).

Hydropedological conditions and carbon were furthermore studied in high-elevation montane grasslands in California (Roche et al. 2014). Results showed that the driest sites were dominated by mineral horizons with highly decomposed organic horizons present in some cases. Moderately wet patches were dominated by organic horizons of both moderately and highly decomposed organic materials. Surface soil horizons in the wettest patches were dominated by slightly to moderately decomposed organic materials, with highly decomposed residues dominating underlying horizons. SOC, SOM, and TN generally increase with wetness with the greatest differences between the driest and wettest patches. Furthermore, the hydropedological behaviour of the soils which lead to wetter sites with greater SOM, SOC and TN exhibited lower plant diversity and livestock forage quality.

An Italian study conducted in the Andic mountains revealed that these soils have a unique set of morphological, physical, and chemical soil properties. All soils sampled had a high organic

carbon content (mean 3.8%), with deeper soils showing higher carbon contents than shallower soils. This is attributed to the unique properties of the soils associated with this area, i.e., the Andosolization process which is a major soil forming process of Andosol/Andisol soils (Terribile, 2018).

A review of literature revealed that the majority of the studies focusing on SOC fluxes, and particularly those conducted in mountain grasslands have been conducted in temperate regions in the northern hemisphere, and very limited information is available for South Africa. The paucity of information within South Africa and particularly within montane grasslands warrants further investigation on the effects of hydropedology on landscape carbon cycling.

## 2.7. CONCLUSIONS

Interactions between carbon cycling, and in particular DOC, and the hydropedological characteristics of a catchment area are an important component of the global carbon cycle (Brooks and Vivoni, 2015). This study focuses on these interactions within the uKhahlamba-Drakensberg escarpment, an Afromontane area of South Africa. Afromontane areas are important as they are vital sources of freshwater and provide several ecohydrological services to downstream locations. In South Africa they are classified as a strategic water source area (Le Maitre et al., 2018), highlighting their importance within the country's economy.

In order to manage the headwater catchments of these mountains, we first need to gain a deeper understanding of the basic processes which influence both the water dynamics and DOC storage and export within these areas. This knowledge can then be utilised to predict the future impacts of an ever-changing climate as well as land management regimes on these vital services.

## 2.8. REFERENCES

Aiken, G. R., Hsu-Kim, H., and Ryan, J. N. (2011). Influence of Dissolved Organic Matter on the Environmental Fate of Metals, Nanoparticles, and Colloids. Environmental Science and Technology. 45. 8. DOI: 10.1021/es103992s.

Amelung, W., Zech, W., Zhang, X., Follett, R.F., Tiessen, H., Knox, E. and Flach, K.W. (1998). Carbon, nitrogen, and sulfur pools in particle-size fractions as influenced by climate. Soil Science Society of America Journal. 62. 1. 172–181.

Aufdendkampe, A.K., Mayorga, E., Raymond, P.A., Melack, J.M., Doney, S.C., Alin, S.R., Aalto, R.E. and Yoo, K. (2011), Riverine coupling of biogeochemical cycles between land, oceans, and atmosphere. Frontiers in Ecology and the Environment, 9. 53-60. https://doi.org/10.1890/100014.

Bartlett, K. B., Crill, P., Sass, R. C., Harriss, R. C., and Dise, N. B. (1992). Methane emissions from tundra environments in the Yukon-Kuskokwim Delta, Alaska. Journal of Geophysical Research. 97. 16645–16660.

Batjes, N.H. (1996). Total carbon and nitrogen in the soils of the world. European Journal of Soil Science, 47. 151-163.

Bauer, J.E., and Bianchi, T. (2011). Dissolved Organic Carbon Cycling and Transformation. In. Treatise on Estuarine and Coastal Science. Wolanski, E., and McLusky, D, (eds). 5. Waltham. Academic Press. DOI:10.1016/B978-0-12-374711-2.00502-7.

Billett, M. Deacon, C., Palmer, S., Julián, J.M., and Hope, D. (2006). Connecting organic carbon in stream water and soils in a peatland catchment. Journal of Geophysical Research. 111. DOI:10.1029/2005JG000065.

Bilotta, G.S., Burnside, N.G., Cheek, L., Dunbar, M.J., Grove, M.K., Harrison, C., Joyce, C., Peacock C., and Davey-Bowker, J. (2012). Developing environment-specific water quality guidelines for suspended particulate matter. Water Research. 46. 7. 2324-2332. DOI:10.1016/j.watres.2012.01.055.

Bridgham, S. D., Ping, C.L., Richardson, J.L., and Updegraff, K. (2001). Soils of northern peatlands: Histisols and Gelisols. In Richardson, J.L., and Vepraskas, M.J. (eds.). Wetland

Soils: Genesis Hydrology Landscapes and Classification. Lewis Publisher. Boca Raton. Florida.

Brooks, P.D., and Vivoni, E.R. (2015). Editorial. Mountain ecohydrology: quantifying the role of vegetation in the water balance of montane catchments. Ecohydrology. 1. 187-192. DOI: 10.1002/eco.27.

Cao, Y.Z., Lu, X.Y., Yan, Y., and Fan, J.H. (2013). Soil organic carbon and nutrients along an alpine grassland transect across Northern Tibet. Journal of Mountain Science. 10. 4. 564–573. DOI: 10.1007/s11629-012-2431-5.

Castellano, M.J., Lewis, B.D., Andrews, D.M., and McDaniel, M.D. (2012). Coupling Biogeochemistry and Hydropedology to Advance Carbon and Nitrogen Cycling Science. In. Hydropedology. Lin, H. (ed). Academic Press. https://doi.org/10.1016/B978-0-12-386941-8.00022-8.

Chaplot, V., and Ribolzi, O. (2014). Hydrograph separation to improve understanding of Dissolved Organic Carbon Dynamics in Headwater catchments. Hydrological Processes. 28. DOI:10.1002/hyp.10010.

Chow, A.T., Dahlgren, R.A., and Harrison, J.A. (2007). Watershed sources of disinfection byproduct precursors in the Sacramento and San Joaquin Rivers, California. Environmental Science & Technology. 41. 22. 7645–7652. https://doi.org/10.1021/es070621t.

Dalzell, B. J., King, J. Y., Mulla, D. J., Finlay, J. C., and Sands, G. R. (2011). Influence of subsurface drainage on quantity and quality of dissolved organic matter export from agricultural landscapes. Journal of Geophysical Research. 116. doi:10.1029/2010JG001540.

D'Amore, D.V., Edwards, R.T., Herendeen, P.A., Hood, E., and Fellman, J.B. (2015). Dissolved organic carbon fluxes from hydropedologic units in Alaskan coastal temperate rainforest watersheds. Soil Science Society of America Journal. 79. 378–388. https://doi.org/10.2136/sssaj2014.09.0380.

Dawson, J. J. C., Billett, M. F., Neal, C., and Hill, S. (2002), A comparison of particulate, dissolved and gaseous carbon in two contrasting upland streams in the UK, Journal of Hydrology. 257. 226– 246. https://doi.org/10.1016/S0022-1694(01)00545-5.

Dayo-Olagbende, O., Adejoro, S., Ewulo, B. and Awodun, M. (2020). Effects of Oxidation-Reduction Potentials on Soil Microbes. Agricultura. 16. 35-42. DOI:10.18690/agricultura.16.1-2.35-42.2019.

Dodds, W., and Whiles, M. (2010) Freshwater Ecology: Concepts and Environmental Applications of Limnology. 2nd Edition. Elsevier. Amsterdam.

Evans, C.D., Renou-Wilson, F., and Strack, M. (2016). The role of waterborne carbon in the greenhouse gas balance of drained and re-wetted peatlands. Aquatic Sciences. 78 .3. 573–590. doi:10.1007/s00027-015-0447-y.

Follett, R.F., Stewart, C.E., Pruessner, E.G., and Kimble, J.M. (2012). Effects of climate change on soil carbon and nitrogen storage in the US Great Plains. Journal of Soil and Water Conservation. 67. 5. 331–342. https://doi.org/10.2489/jswc.67.5.331.

Feger, K.H. and Hawtree, D. (2013). Soil carbon and water security. In Ecosystem Services and Carbon Sequestration in the Biosphere. Lal, R., Lorenz, K., Hüttl, R.F., Schneider, B.U., and Braun, J. Eds. Springer: Dordrecht, The Netherlands.

Field, C.B., Lobell, D.B., Peters, H.A., and Chiariello, N.R. (2007). Feedbacks of terrestrial ecosystems to climate change. Annual Review of Environment and Resources. 32. 1–29. doi:10.1146/annurev.energy.32.053006.141119.

Geris, J. and Tetzlaff, D. (2015). Resistance and resilience to droughts: Hydropedological controls on catchment storage and run-off response. Hydrological Processes. 29. 4579–4593. DOI:10.1002/hyp.10480.

Giorgi, F., Bi, X., and Pal, J.S. (2004). Mean, interannual variability and trends in a regional climate change experiment over Europe. I: present day climate (1961-1990). Climate Dynamics. 22.7333-756. DOI:10.1007/s00382-004-0467-0.

Hagedorn, F., Schleppi, P., Waldner, P., and Flühler, H. (2000). Export of Dissolved Organic Carbon and Nitrogen from Gleysol Dominated Catchments: The Significance of Water Flow Paths. Biogeochemistry, 50. 2. 137–161. https://doi.org/10.1023/A:1006398105953.

Hanson, P.J., Edwards, N.T., Garten, C.T. and Andrews, J.A. (2000). Separating root and soil microbial contributions to soil respiration: A review of methods and observations. Biogeochemistry. 48. 115–146. https://doi.org/10.1023/A:1006244819642.

Hassink, J. (1997). The capacity of soils to preserve organic C and N by their association with clay and silt particles. Plant Soil. 191. 77 – 87.

Högberg, P., Nordgren, A., Buchmann, N., Taylor, A.F., Ekblad, A., Högberg, M.N., Nyberg, G., Ottosson-Löfvenius, M., and Read, D.J. (2001). Large-scale forest girdling shows that current photosynthesis drives soil respiration. Nature. 411. 789–792. DOI: 10.1038/35081058.

Hua, K., Zhu, B., Wang, X. and Tian, L. (2016). Forms and fluxes of soil organic carbon transport via overland flow, interflow and soil erosion in a hillslope cropland of Regosol China. Soil Science Society of America Journal. 80. 10. 2136-2146. https://doi.org/10.2136/sssaj2015.12.0444.

Inamdar, S.P., and Mitchell, M.J. (2006). Hydrological and topographical controls on storm-event exports of dissolved organic carbon (DOC) and nitrate across catchment scales. Water Resources Research. 42. DOI:10.1029/2005WR004212.

Jaffé, R., Yamashita, Y., Maie, N., Cooper, W., Dittmar, T., Dodds, W., Jones, J. Myoshi, T., Ortiz, J., Podgorski, D., and Watanabe, A. (2012). Dissolved Organic Matter in Headwater Streams: Compositional Variability across Climatic Regions of North America. Geochimica et Cosmochimica Acta. 94. 95–108. DOI:10.1016/j.gca.2012.06.031.

Jarvis, N.J. (2007). A review of non-equilibrium water flow and solute transport in soil macropores: Principles, controlling factors and consequences for water quality, European Journal of Soil Science. 58. 523–546. DOI:10.0111/j.1365-2389.2007.00915.x.

Jobbágy, E.G., and Jackson, R.B. The Vertical Distribution of Soil Organic Carbon and its relation to climate and vegetation. Ecological Applications. 10: 423-436. https://doi.org/10.1890/1051-0761(2000)010[0423:TVDOSO]2.0.CO;2.

Kahmen, A., Perner, J., and Buchmann, N. (2005). Diversity-dependent productivity in semi-natural grasslands following climate perturbations. Functional Ecology. 19. 594–601. https://doi.org/10.1111/j.1365-2435.2005.01001.x.

Kawasaki, M., Ohte, N., Kabeya, N., and Katsuyama, M. (2008). Hydrological control of dissolved organic carbon dynamics in a forested headwater catchment, Kiryu Experimental Watershed, Japan. Hydrological Processes. 22. 3. 429–442. doi:10.1002/hyp.6615.

Kotze, D., Marneweck, G., Batchelor, A., Lindley, D., and Collins, N. (2007). WET-EcoServices: A technique for rapidly assessing ecosystem services supplied by wetlands. WRC Report No TT 339/08. Water Research Commission. Pretoria.

Lal, R. (2003). Soil erosion and the global carbon budget. Environment International. 29. 437–450. https://doi.org/10.1016/S0160-4120(02)00192-7.

Lal, R. (2010). Managing soils and ecosystems for mitigating anthropogenic carbon emissions and advancing global food security. BioScience. 60. 9. 708–721. https://doi.org/10.1525/bio.2010.60.9.8.

Lal, R. and Stewart, B.A. (2018). Soil and Climate. 1st Edition. Advances in Soil Science. CRC Press.

Lal, R. (2019). Carbon Cycling in Global Drylands. Carbon Cycle and Climate: 5 221–232. DOI:10.1007/s40641-019-00132-z.

Laudon, H., Berggren, M., Ågren, A., Buffam, I., Bishop, K., Grabs, T., Jansson, M., and Köhler, S. (2011). Patterns and Dynamics of Dissolved Organic Carbon (DOC) in Boreal Streams: The Role of Processes, Connectivity, and Scaling. Ecosystems. 14. 880-893. DOI:10.1007/s10021-011-9452-8.

Le Maitre, D.C., Walsdorff, A., Cape, L., Seyler, H., Audouin, M, Smith-Adao, L., Nel, J.A., Holland, M., and Witthüser. K. (2018). Strategic Water Source Areas: Management Framework and Implementation Guidelines for Planners and Managers. WRC Report No. TT 754/2/18. Water Research Commission. Pretoria.

Lemenih, M., and Itanna, F. (2004). Soil carbon stocks and turnovers in various vegetation type and arable lands along an elevation gradient in southern Ethiopia. Geoderma. 123. 177–188. https://doi.org/10.1016/j.geoderma.2004.02.004.

Lin, H. (2012). Hydropedology Synergistic Integration of Soil Science and Hydrology. Academic Press. USA.

Lindbo, D.L., and Richardson, J.L. (2000). Hydric soils and wetlands in riverine systems. In:

Richardson, J.L., and Vepraskas, M.J. (Eds.). Wetland Soils: Their Genesis, Morphology, Hydrology, Landscape, and Classification. CRC Press. Boca Raton, Florida. Ch. 12.

Ma, Y., Li, X., and Lin L.H. (2017). Hydropedology: Interactions between pedologic and hydrologic processes across spatiotemporal scales. Earth-Science Reviews. 171. 181-195.

DOI:10.1016/j.earscirev.2017.05.014.

Maybeck, M. (1993). Natural sources of C, N, P, and S. In. Interactions of C, N, P, and S Biogeochemical Cycles and Global Change. R. Wollast (ed.). Springer-Verlag. Berlin.

McGlynn, B.L., and McDonnell, J.J. (2003). Role of discrete landscape units in controlling catchment dissolved organic carbon dynamics. Water Resources Research. 39. 1090, doi:10.1029/2002WR001525.

Mei, Y., Hornberger, G. M., Kaplan, L. A., Newbold, J. D., and Aufdenkampe, A. K. (2012), Estimation of dissolved organic carbon contribution from hillslope soils to a headwater stream. Water Resources Research. 48. DOI:10.1029/2011WR010815.

Milliman, J.D. and Syvitski, J.P.M. (1992). Geomorphic/Tectonic Control of Sediment Discharge to the Ocean: The Importance of Small Mountainous Rivers. The Journal of Geology, 100. 525-544. http://dx.doi.org/10.1086/629606.

Miller, A., Amundson, R., Burke, I.C., and Yonker, C. (2004). The effect of climate and cultivation on soil organic C and N. Biogeochemistry 67. 57-7.

Mitsch, W.J., and Gosselink J.G. (2007). Wetlands. 4th Edition, John Wiley & Sons, Inc. Hoboken.

Mureva, A., Ward, D., Pillay, T., Chivenge, P., and Cramer, M. (2018). Soil Organic Carbon Increases in Semi-Arid Regions while it Decreases in Humid Regions due to Woody-Plant Encroachment of Grasslands in South Africa. Scientific Reports. 8. 15506. https://doi.org/10.1038/s41598-018-33701-7.

Norton, J. B., Jungst, L. J., Norton, U., Olsen, H. R., Tate, K. W., and Horwath. W. R. (2011). Soil carbon and nitrogen storage in upper montane riparian meadows. Ecosystems. 14. 1217–1231. https://doi.org/10.1007/s10021-011-9477-z.

Ollis, D., Snaddon, K., Job, N., and Mbona, N. (2013). Classification Systems for Wetlands and other Aquatic Ecosystems in South Africa. User Manual: Inland Systems. SANBI Biodiversity Series 22. Pretoria: South African National Biodiversity Institute.

Ontl, T. A., and Schulte, L. A. (2012). Soil Carbon Storage. Nature Education Knowledge. 3. 10.

Özbek, F. S., and Leip, A. (2015). Estimating the gross nitrogen budget under soil nitrogen stock changes: A case study for Turkey. Agriculture, Ecosystems and Environment.(205) 48-56. https://doi.org/10.1016/j.agee.2015.03.008.

Phillips, R., and Beeri, O. (2008). The role of hydropedologic vegetation zones in greenhouse gas emissions for agricultural wetland landscapes. Catena. 72. DOI:10.1016/j.catena.2007.07.007.

Raich, J.W. and Tufekcioglu, A. (2000). Vegetation and soil respiration: Correlations and controls. Biogeochemistry 48. 71–90. https://doi.org/10.1023/A:1006112000616.

Rhoton, F.E., Bigham, J.M., and Lindbo, D.L. (2002). Properties of iron oxides in streams draining the loess uplands of Mississippi. Applied Geochemistry. 17. 409-419. https://doi.org/10.1016/S0883-2927(01)00112-3.

Rice, C. W. (2005). Encyclopedia of Soils in the Environment. 1st Edition. Academic Press.

Roig-Planasdemunt, M., Llorens, P., and Latron, J. (2017) Seasonal and storm flow dynamics of dissolved organic carbon in a Mediterranean mountain catchment (Vallcebre, eastern Pyrenees). Hydrological Sciences Journal. 62. 1. 50-63. DOI: 10.1080/02626667.2016.1170942.

Roche, L. M., O'Geen, A. T., Latimer, A. M., and Eastburn. D. J. (2014). Montane meadow hydropedology, plant community, and herbivore dynamics. Ecosphere. 5. 12. 150. http://dx.doi.org/10.1890/ES14-00173.1.

Roulet, N.T. (2000). Peatlands, carbon storage, greenhouse gases, and the Kyoto protocol: prospects and significance for Canada. Wetlands. 20. 605-615.

Smith, P. (2014). Do grasslands act as a perpetual sink for carbon. Global Change Biology. 20. 9. 2708-2711. https://doi.org/10.1111/gcb.12561.

Stanley, E.H., Powers, S.M., Lottig, N.R., Buffam, I., and Crawford, J.T. (2012). Contemporary changes in dissolved organic carbon (DOC) in human-dominated rivers: is there a role for DOC management? Freshwater Biology. 57. 26–42. https://doi.org/10.1111/j.1365-2427.2011.02613.x.

Stanley, P.L., Rowntree, J.E., Beede, D.K., DeLonge, M. S., and Hamm, M.W. (2018). Impacts of soil carbon sequestration on life cycle greenhouse gas emissions in Midwestern USA beef finishing systems. Agricultural Systems. 162. 249-258. https://doi.org/10.1016/j.agsy.2018.02.003.

Terribile, F., Iamarino, M., Langella, G., Manna, P., Mileti, F., Vingiani, S., and Basile, A. (2017). The hidden ecological resource of andic soils in mountain ecosystems: evidences from Italy. Solid Earth Discussions. 1-32. DOI:10.5194/se-2017-57.

Tranvik L. J., Downing J. A., Cotner J. B., Loiselle S. A., Striegl R. G., Ballatore T. J., Dillon P., Finlay K., Fortino K., Knoll L. B., Kortelainen P. L., Kutser T., Larsen S., Laurion I., Leech D. M., McCallister S. L., McKnight D. M., Melack J. M., Overholt E., Porter J. A., Prairie Y., Renwick W. H., Roland F., Sherman B. S., Schindler D. W., Sobek S., Tremblay A., Vanni M. J., Verschoor A. M., von Wachenfeldt E. and Weyhenmeyer G. A. (2009). Lakes and reservoirs as regulators of carbon cycling and climate. Limnology and Oceanography. 54. 2298– 2314. https://doi.org/10.4319/lo.2009.54.6_part_2.2298.

Trenberth, K.E., Dai, A., Rasmussen, R.M. and Parsons, D.B. (2003). The changing character of precipitation. Bulletin of the American Meteorological Society 84.1205–1217.

Tunaley, C., Tetzlaff, D., Lessels, J. (2016). Linking high-frequency DOC dynamics to the age of connected water sources. Water Resources Research. 52. DOI:10.1002/2015WR018419.

Turowski, J.M., Hilton, R.G., and Sparkes, R. (2016). Decadal carbon discharge by a mountain stream is dominated by coarse organic matter. Geology. 44. 27-30. DOI:10.1130/G37192.1.

van Tol, J.J., and Le Roux, P.A.L. (2019). Hydropedological grouping of South African soil forms. South African Journal of Plant and Soil. 36(3). 233-235. DOI: 10.1080/02571862.2018.1537012.

Vogel, H-J., Clothier, B., Li, X-Y., and Lin, H. S., (2013). Hydropedology—A Perspective on Current Research. Vadose Zone Journal. 12. 4. https://doi.org/10.2136/vzj2013.09.0161.

Wang, F-P., Wang, X-C., Yao, B-Q., Zhang, Z-H., Shi, G-X., Ma, Z., Chen, Z., and Zhou, H-K. (2018). Effects of land-use types on soil organic carbon stocks: a case study across an altitudinal gradient within a farm-pastoral area on the eastern Qinghai-Tibetan Plateau, China. Journal of Mountain Science. 15. 2693–2702. https://doi.org/10.1007/s11629-018-4980-8.

Wei, J., Liu, W., Wan, H., Cheng, J. and Li, W. (2016). Differential allocation of carbon in fenced and clipped grasslands: a 13C tracer study in the semiarid Chinese Loess Plateau. Plant and Soil. 406. DOI:10.1007/s11104-016-2879-0.

Wetzel, R.G. (1992). Gradient-dominated ecosystems: sources and regulatory functions of dissolved organic matter in freshwater ecosystems. Hydrobiologia. 229. 181–198.

Wetzel, R.G. (2001). Limnology: Lake and River Ecosystems, 3rd edn. Academic Press. San Diego.

Xie, B., Zhang, H., Yang, D.D., and Wang, Z. (2016). A modeling study of effective radiative forcing and climate response due to increased methane concentration. Advances in Climate Change Research. 7. 241-246. DOI: 10.12006/j.issn.1673-1719.2016.070.

Yashiro, Y., Kadir, W.R., Okuda, T., and Koizumi, H. (2008). The effects of logging on soil greenhouse gas (CO2, CH4, and N2O) flux in a tropical rain forest, Peninsular Malaysia. Agricultural and Forest Meteorology. 148. 799-806.

Zhao, L., Sun, Y., Zhang, X-P., Yang, X., and Drury, C. (2006). Soil organic carbon in clay and silt sized particles in Chinese mollisols: Relationship to the predicted capacity. Geoderma. 132. 315-323. DOI:10.1016/j.geoderma.2005.04.026.

Zhang, M., Huang, X., Chuai, X., Yang, H., Lai, L. and Tan, J. (2015). Impact of land use type conversion on carbon storage in terrestrial ecosystems of China: A spatial-temporal perspective. Scientific Reports. 5. 10233. https://doi.org/10.1038/srep10233.

Zhu, Q., Castellano, M., and Yang, G. (2018). Coupling soil water processes and nitrogen cycle across spatial scales: Potentials, bottlenecks and solutions. Earth-Science Reviews. 187. DOI: 10.1016/j.earscirev.2018.10.005.

Zomer, R.J., Bossio, D.A., Sommer, R., and Verchot, L.V. (2017). Global Sequestration Potential of Increased Organic Carbon in Cropland Soils. Science Report. 7. 15554.

# CHAPTER 3 – STUDY SITE DESCRIPTION

## 3.1. STUDY SITE

This study took place within the Cathedral Peak experimental research catchment site, which is situated in the northern part of the uKhahlamba-Drakensberg escarpment, KwaZulu-Natal, South Africa. The uKhahlamba-Drakensberg escarpment is an erosional mountain range, with the higher ground consisting of basaltic lavas (in areas known as the High Berg) which overlie the Clarens sandstones (in areas known as the Little Berg) (Norman and Whitfield, 2006).

The Little Berg is furthermore made up of the Beaufort Series sandstones, as well as shales, mudstones, and sandstones of the Molteno and Elliot Formations. It is in these geological formations that the research catchments are situated (Nänni, 1956; Norman and Whitfield, 2006; Toucher et al., 2016).

The research catchment site is managed by Ezemvelo KZN Wildlife, while the South African National Environment Observatory Network (SAEON) undertakes the monitoring of the catchments. The catchments, of which there are 15, range in altitude from 1 820 m.a.s.l to 2 463 m.a.s.l. Topography varies from relatively flat to very steep (1–39°) with the aspect ranging from north to south facing (Granger and Schulze, 1977; Gordijn et al. 2018).

These catchments fall within the summer rainfall region of South Africa. The mean annual precipitation (MAP) for the area is approximately 1400 mm, with a gradient from 1300 mm in the southeast to 1700 mm in the west (Schulze,1976). Precipitation events in the catchments are dominated by thunderstorms. which fall during the spring and summer months (September to March), with occasional snowfall received during winter (May to August). The clouds forming these thunderstorms come from the west of the catchment areas. Orographic rainfall, produced from clouds forming in the east of the catchments, also create longer periods of softer rainfall which can fall for several days (Bosch, 1979, Nänni, 1956, Everson et al. 1998, Toucher et al. 2016). The annual average air temperature for the research catchments is 13.8˚C with mean monthly temperatures ranging from 17.1 $^{O}$C to 10 $^{O}$C. Frost is common in autumn and winter (April to August) (Bosch, 1979, Everson et al. 1998, Gordijn et al. 2018; Toucher et al. 2016).

The research catchments are predominantly covered by grasslands of the uKhahlamba Basalt Grassland vegetation type interspersed with Northern Afrotemperate Forest patches and wetlands (Mucina and Rutherford, 2006).

## 3.2. BRIEF HISTORY OF THE STUDY SITE

These catchment areas are long-term research sites established in 1948 by the Union of Forests Department to investigate the influence of land management on water resources. Initially the primary focus was on the impact of commercial plantation forestry on water, with the focus shifting to and including the impacts of different fire regimes as well as grazing influences on hydrological responses (Nänni 1956, Everson et al. 1998, Toucher et al. 2016). Weirs were built and measurements began in an initial ten catchments in 1948, with five more catchment areas added to the monitoring regime in 1975.

In 1988 the management of the catchment areas was handed over to the Natal Parks Board (now Ezemvelo KZN Wildlife), where monitoring continued until 1995, when due to a lack of funding, monitoring in the catchments ceased. In 2011 the SAEON Grasslands-Forests-Wetlands Node began the process of restoring monitoring in the catchments and this monitoring now continues to the present day (Toucher et al. 2016).

In addition to the hydrological monitoring experiments, a number of concentrated experiments were initiated to examine the impacts of controlled burning on grasslands and scrub vegetation. This is due to the vegetation of the Cathedral Peak research catchments being largely controlled by fire (Toucher et al. 2006). Fire regimes which were included as management treatments were established within the catchments by 1957 and included areas burnt frequently (one and three years) and infrequently (five and eight years). These burns were applied during the period winter to early spring. Fire records are kept of the burning regimes, with these specific to a catchment area. Certain burning regimes were in place from 1945 to 1972, with these changing from 1972 to 2000 and then changing again from 2000 onwards. Catchment CP-IX has however been largely protected from fire since 1952, with the exception of some wildfires and accidental burns in some years (Toucher et al. 2006). In this study, a fire management burn took place in CP-VI on the 7$^{th}$ of October 2020 and a wildfire took place in CP-III in July 2019.

## 3.3. CATCHMENTS STUDIED IN THIS THESIS

Three similar catchments were selected for this study and are named CP-III, CP-VI, and CP-IX (Figure 3.1). These catchments have been managed differently both in a historical context as well as currently. Details of each catchment is provided in Table 3.1. CP-III, CP-VI and CP-IX are studied in Chapters 4 – 6, while CP-VI and CP-IX are studied in Chapters 7 and 8. CP-III has been excluded from Chapters 7 and 8 as a result of both drought conditions which made sampling in CP-III difficult as well as a lack of instrumentation in CP-III, but which was present in CP-VI and CP-IX.

Table 3.1: General information on the three selected catchment areas for this study

| **Catchment Name** | **Size (ha)** | **Altitude Range (m.a.s.l.)** | **Description of Catchment** |
|---|---|---|---|
| CP-III | 138.9 | 1847 - 2323 | Mean annual rainfall of 1564 mm. The catchment is degraded as a result of a forestry experiment in which *Pinus patula* was planted throughout the catchment in the 1950s and 1960s as well as accidental fires which led to the removal of these trees in 1981. The catchment was rehabilitated with *Eragrostis curvula*, following the removal of the trees (Toucher et al. 2016). There is however erosion throughout the catchment area, with large portions of the catchment covered by *Pteridium* sp. (Bracken). |
| CP-VI | 67.7 | 1845- 2073 | Mean annual rainfall of 1340 mm. This catchment is covered by mesic grassland of the uKhahlamba Basalt Grassland type which is burned biennially during spring. It is dominated by *Bromus speciosus*, *Pentaschistis tysoniana*, *Cymbopogon nardus* and *Themeda triandra* that are accompanied by numerous herbs and shrubs. CP-VI is considered the core catchment with focused, detailed monitoring ongoing in this catchment. A full array of evaporation, soil moisture and groundwater monitoring are undertaken. |
| CP-IX | 64.5 | 1823 - 1966 | Mean annual rainfall of 1257 mm. This catchment has been completely protected from fire since 1952 but has |

| Catchment Name | Size (ha) | Altitude Range (m.a.s.l.) | Description of Catchment |
|---|---|---|---|
| | | | experienced accidental burns and wildfires in some years. As a result of fire exclusion, this catchment is dominated by woody scrub (*Leucasidea serica* and *Buddleia salvifolia)* |

The collection of rainfall data within the catchments has been undertaken since 1950, with rainfall for this study measured with tipping bucket rain gauges installed in the mid position of each of the catchments. Streamflow monitoring was initiated in the three catchment areas during the late 1940's and 1950's. At the outlet of each catchment a concrete weir and stilling hut, with 90-degree V Notches were installed (Figure 3.2). These V Notches are 45.72 cm (18 inches) deep and are surmounted by 1.82 m (6 feet) wide rectangular notches of varying depth. The stilling ponds were dug to bedrock, and rock walls for the pond were constructed. Details of how early measurements were taken, error checked and processed are given in Toucher et al. (2016). The water stage-height at each weir is currently monitored using an Orpheus Mini (Ott Hydromet GmbH, Germany) at CP-VI weir and a CS451 Stainless steel SDI-12 Pressure Transducers with CR200 loggers at weirs CP-III, CP-VI, and CP-IX. There are two pressure transducers installed at weir CP-VI as this is the core catchment and thus the quality of streamflow records is ensured (Toucher et al. 2016).

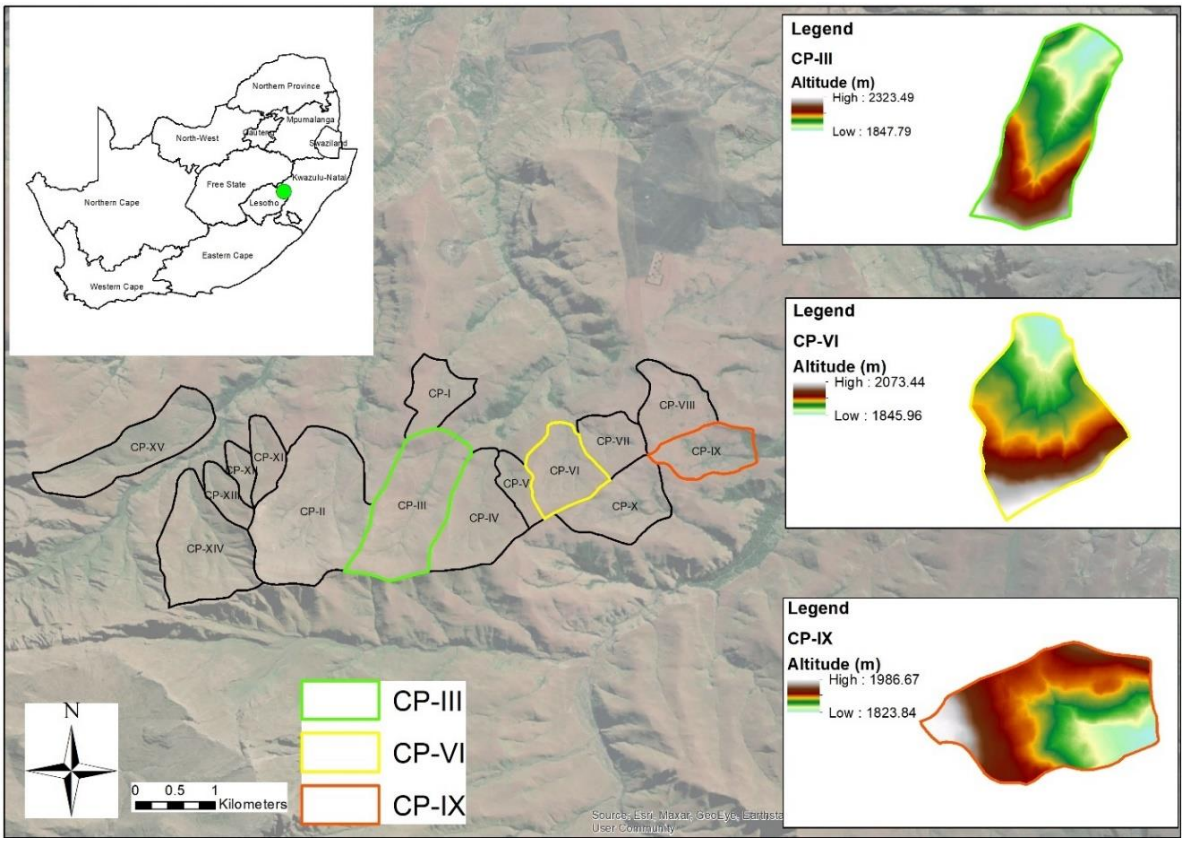


Figure 3.1: Locality of the catchments selected for the study

Figure 3.2: Concrete weir and stilling hut, with 90-degree V Notch installed at CP-VI

## 3.4. FIELD WORK CONDUCTED DURING THIS THESIS

Field work for this thesis was conducted between January 2019 and June 2021. The field work included a number of different aspects. Firstly, piezometers were installed within the three catchments: six piezometers in CP-III, twelve in CP-VI, and nine in CP-IX. The piezometers used were created from PVC piping which was 10 cm in diameter and varied in length depending on the depth of the soil in the area where they were installed. The piezometers were installed in clusters of two or three within a location, with this location chosen to represent the upper, mid, and lower portions of the catchments. Furthermore, the position of the piezometers was chosen within wetland and seepage areas of the catchments. In CP-III, all piezometers were, however, installed in the lower sections of the catchment area as a result of a lack of seepage areas within the upper portions of the catchment. As a result of the drought conditions experienced during the field work time, some of the piezometers had to be discontinued, and thus for this thesis, five piezometers were utilised in CP-III, seven piezometers were utilised in CP-VI, and seven piezometers were utilised in CP-IX. More detail regarding the piezometers is provided in Chapter 5.

Samples from these piezometers were taken during the last week of every month, with the exception of April 2020. This was as a result of the Covid-19 pandemic. Water heights were recorded once a month to the nearest cm. The height of the water within the piezometer was calculated from the surface of the soil to the depth of the water table. Furthermore, water was extracted from the piezometers for DOC analysis between September 2019 and June 2021 and more detail of this procedure is provided in Chapter 7. Water could only be extracted from September 2019 due to the drought conditions experienced for the majority of 2019.

As no soil map of CP-IX existed, a soil mapping exercise was undertaken in October 2020 to both validate the hydropedological soil group maps as discussed in Chapter 4, and to create a soil map for CP-IX. This map details the soil forms of the catchment as per the South African taxonomic classification system (Soil Classification Working Group, 2018).

Lastly two submersible, portable multi-parameter UV–Vis probes (spectro::lyser, s::can Messtechnik GmbH, Austria) were installed in the weirs of CP-VI and CP-IX to aid in gaining a deeper understanding of the DOC dynamics of these catchment areas. Details of these sensors is provided in Chapter 8. The sensors were installed in June 2019 and data for this thesis was

gathered between July 2019 and June 2022 (three years). The data from these optical sensors was downloaded at the site, every month, with the exception of April 2020. Due to the remote nature of the area in which this sensors were installed, some data gaps were unavoidable, as should a power failure occur this could only be checked after the data was downloaded. Details on the data analysis is provided in Chapter 8.

## 3.5. REFERENCES

Bosch, JM. (1979). Treatment effects on annual and dry period streamflow at Cathedral Peak. South African Forestry Journal, 108(1): 29-38.

Everson, C.E., Molefe, G.L., and Everson, T.M. (1998). Monitoring and modelling components of the water balance in a grassland catchment in the summer rainfall area of South Africa. Water Research Commission. RSA. Report 493/1/98.

Gordijn, P.J., Everson, T.M., and O'Connor, T.G. (2018). Resistance of Drakensberg grasslands to compositional change depends on the influence of fire-return interval and grassland structure on richness and spatial turnover. Perspectives in Plant Ecology, Evolution and Systematics. 34. 26-36. https://doi.org/10.1016/j.ppees.2018.07.005.

Granger, J.E., and Schulze, R.E. (1977). Incoming solar radiation patterns and vegetation response: examples from the Natal Drakensberg. Vegetatio. 35. 47–54.

Nänni, U.W. (1956). Forest Hydrological Research at the Cathedral Peak Research Station. Journal of the South African Forestry Association 27(1). 2-35.

Norman, N and Whitfield, G. (2006). Geological Journeys: A Traveller's Guide to South Africa's Rocks and Landforms. Struik Publishers. Cape Town.

Toucher, M.L., Clulow, A., van Rensburg, S., Morris, F., Gray, B., Majozi, S., Everson, C.E., Jewitt, G.P.W., Taylor, M.A., Mfeka, S., and Lawrence, K. (2016). Establishment of a more robust observation network to improve understanding of global change in the sensitive and critical water supply area of the Drakensberg. 2236/1/16. Water Research Commission, Pretoria, South Africa.

Schulze, R.E. (1976). On the application of trend surfaces of precipitation to mountainous areas. WaterSA, 2. 3. 110 – 118.

Soil Classification Working Group. (2018). Soil Classification: A Natural and Anthropogenic System for South Africa. ARC-Institute for Soil, Climate and Water. Pretoria.

# CHAPTER 4 – DIGITAL SOIL MAPPING FOR HYDROPEDOLOGICAL PURPOSES OF THE CATHEDRAL PEAK RESEARCH CATCHMENTS, SOUTH AFRICA

Published as: Harrison, R., and van Tol, J. (2022). Digital Soil Mapping for Hydropedological Purposes of the Cathedral Peak Research Catchments, South Africa. In: Adelabu, S., Ramoelo, A., Olusola, A., Adagbasa, E. (eds) Remote Sensing of African Mountains. Springer, Cham. https://doi.org/10.1007/978-3-031-04855-5_10.

**Abstract**

Conventional soil mapping in montane environments is often a difficult and laborious task given access difficulties, the topography of the environment and the time required to conduct the field investigation. Utilising a remote sensing tool, such as the Arc Soil Inference Engine (ArcSIE) to map soils in these locations can add valuable information for land management. The ArcSIE tool was utilised in the Cathedral Peak research catchments, in KwaZulu-Natal, South Africa with the aim of creating an understanding of the hydropedological behaviour of the soils of three research catchments. A rule-based approach was first undertaken, followed by a case-based validation. A fuzzy membership map of each soil group was produced which integrated all inputs. The overall Kappa coefficient for CP-III is 0.57, for CP-VI is 0.59, and for CP-IX is 0.74. The hydropedological soil group maps achieved an appropriate representation of the complex nature of the soil-landscape relationship, with changes between one soil group and the next being gradual and continuous. Accuracies and inaccuracies within the fuzzy-membership maps can be quantified, allowing for a confidence rating in the use of these maps. These maps can therefore be used in further applications in water and land management for the area.

## 4.1. INTRODUCTION

Conventional soil mapping in montane environments is often a difficult and laborious task given access difficulties, the topography of the environment and the time required to conduct the field investigation (Ismail and Yacoub, 2012; Martín-López, et al., 2019). In recent years thematic mapping has undergone a revolution as the result of advances in geographic information and remote sensing techniques (Ismail and Yacoub, 2012), and this has brought

about the use of Digital Soil Mapping (DSM) as a key tool in reducing the time and financial aspects of conventional soil-based mapping. DSM is the interpretation of spatial and temporal soil property variations using mathematical models based on quantitative relationships between environmental information and soil measurements (Martín-López, et al., 2019).

The use of DSM techniques is supported by the factors of soil formation, coupled with soil-landscape relationships (McBratney et al., 2003, Silva et al., 2019). Jenny (1941) used the well-known and widely accepted model as a mechanistic model for soil development; S = f (c, o, r, p, t) where S (soil) is a function of climate (c), organisms (o), relief (r), parent material (p) and time (t). However, since the late 1960s, there has been an emphasis on more geographic, topographic, and spatial approaches to interpreting the position of soils in relation to the landscape (McBratney et al., 2003). This more recent interest is driven by an increasing recognition of the ecological, economic, and societal benefits of understanding soil properties, their spatial distribution, and the value of this knowledge for use in the management objectives of a variety of industries and land uses (Kimsey, 2020).

The geographic and topographic nature of DSM makes it relevant to pedology and hydrology (Lin et al., 2006, Ma et al., 2019). Soil-water interactions across multiple scales control much of soil development and this results in the spatial variability studied by pedologists. These interactions also control water quantity and quality in surface and groundwater systems, and thus are important to hydrologists (Lin et al., 2006). Combining pedologic and hydrologic expertise can be particularly powerful in addressing complex environmental issues (Bouma, 2006, European Confederation of Soil Science Societies, 2004, Lin et al., 2006, van Tol et al., 2018) and thus the introduction of utilising DSM in hydropedology is an important component in understanding and predicting soil variability within a landscape (Thompson et al., 2012).

A landscape can be divided into two hydrologic zones including the recharge zone and the discharge zone (Heath, 1980). A downward movement of water from the soil surface to the groundwater describes the recharge zone, while the opposite, a movement of water upwards from the groundwater toward the surface portrays the discharge zone. A lateral or flow through zone can also occur in certain landscapes with a shallow water table. Here the groundwater has reached the surface and runs parallel to the ground surface. Dissolved organic matter, sediment, and reduced Iron (Fe) and Manganese (Mn) are carried within this moving water (Lindbo and Richardson, 2000; Rhoton et al., 2002, Vepraskas and Lindbo, 2012).

Research into the dynamics of hydropedology, particularly within South Africa, has shown that the placement of soils within a landscape are not randomly distributed but can be grouped into four hydropedological soil types, namely, recharge soils, interflow soils, responsive soils, and stagnating soils. These groups of soils convey water differently and thus have different hydropedological behaviour (van Tol and Le Roux, 2019).

Previous studies have highlighted the effect of the landscape on the flow dynamics of soils (Diek et al., 2014, Grayson et al., 1997, Mahmood and Vivoni, 2011, Penna et al., 2009, Teuling and Troch, 2005) with soil moisture varying with topography under wet conditions, whereas under drier conditions, soil moisture has been shown to be associated with local soil and vegetation controls. So, although topography, texture and vegetation all influence soil moisture variability, the relative magnitude of these controls can vary strongly (Diek et al., 2014, Grayson et al., 1997, Mahmood and Vivoni, 2011; Penna et al., 2009, Teuling and Troch, 2005). This is due to the complex and varied characteristics of soils which influences their ability to store and transmit water (van Tol et al., 2020).

The spatial distribution of soils within a landscape can also be described utilising the soil catena concept. Described by Milne (1936) as the association of the distribution of soils with the topography of the hillslope, and later by Bushnell (1942) as the identification of the hydrosequence of soils along a hillslope from the ridgetop to the valley bottom or watercourse. The catchment's hydrological response is the sum of the hydrological responses of the individual hillslopes within a catchment (van Zijl et al., 2019). Thus, the importance of grouping soils according to their hydropedological characteristics plays an important part in understanding water fluxes and flow pathways in landscapes (Lin et al., 2006; van Tol, 2020) as well as creating hydrosequences within a catchment. The use of DSM in determining the hydropedological grouping of soils is therefore important in assessing such properties of a catchment including soil water retention, flooding potential, erosion hazard and depth to the seasonal high-water table (Thompson et al., 2012).

One of the baseline inputs in DSM is identifying where the wetlands and watercourses are situated. Wetlands are a transitional ecosystem between terrestrial and open-water or aquatic environments (Mitsch and Gosselink, 2015). They therefore contain either open water bodies, dense vegetation, or a mixture of the two (Kaplan and Avdan, 2017). The use of satellite imagery has been successfully used in the past for open-water delineations, as well as for

vegetation classification and change detection in wetland ecosystems. Several mapping studies have demonstrated the potential of applying remote sensing methods to wetland identification (Berberoglu et al., 2004, Frohn et al., 2009, Klemas 2005, Klemas, 2011, Lunetta and Balogh, 1999, Phillips et al., 2005, Quinn and Epshtein, 2014). Further studies illustrate how vegetation characteristics such as density, vitality, and spatial extent serve as important ecohydrologic indicators (Kokaly et al., 2003, Lin and Liquan, 2006). Applying these indicators, one can use remote sensing techniques such as Normalized Difference Vegetation Index (NDVI) analysis to gain an understanding of where the wetlands are situated within a catchment.

This baseline information can then be utilised with topographical indices to determine the distribution of soils or the properties of soils within a catchment. Several studies have highlighted the use of DSM programmes for these mapping exercises (Behrens et al., 2005, Lagacherie, 2008, McBratney et al., 2003). One such programme is ArcSIE (Soil Inference Engine) which has been utilised in a number of studies across the globe focusing on both soil classification mapping as well as soil properties mapping (Ashtekar et al., 2014, de Menezes et al., 2014, Silva, 2014, Smith et al., 2010). ArcSIE supports a knowledge-based approach to establish relationships between soils and the environment in which the soils are formed (Shi, 2013). It is thus ideally suited to mapping the hydropedological behaviour of soils within a catchment area.

The aims of this chapter are therefore to use remote sensing techniques and DSM for hydropedological purposes on a catchment scale in order to understand the various flow dynamics of these catchments. The information obtained from the mapping of the hydropedological soil groups and the interactions between these groups aims to further enhance land use and water management planning in these areas.

## 4.2. METHODOLOGY

### *4.2.1. Study site*

Details of the study site are given in Chapter 3.

### *4.2.2. Classification of hydropedological soil groups*

The grouping of the hydropedological character of soils (based on the classifications from van Tol and Le Roux, 2019) were utilised in this study. The hydropedological soil groups are defined for this study as (Harrison et al. 2022):

1. Recharge Shallow Soils – these are freely drained and are shallow in nature (<500mm). The freely drained B horizon merges with fractured rock or a lithic horizon. These soils occur on steeper convex slopes in the higher lying parts of the catchments.
2. Recharge Deep Soils – these are freely drained and are deeper than the Recharge Shallow Soils (>500mm). The freely drained B horizon merges into fractured rock or a lithic horizon. These soils where identified throughout the catchments on gentler convex and concave slopes.
3. Interflow soils – these have a freely drained upper horizons which overlie relatively impermeable bedrock. Hydromorphic properties are identified at this interface and signify periodic saturation associated with a water table. These soils occur on gentler concave slopes in areas delineated as wetlands as well as adjacent to watercourses.
4. Responsive Saturated – these display indications of long-term saturation and were identified in permanently saturated wetlands in the valley bottom positions of the catchments as well on gentle concave slopes. As these soils are close to saturation all year round, the respond quickly to rainfall events and generate overland as any additional precipitation will flow overland due to saturation excess.

### *4.2.3. Normalized Difference Vegetation Index Analysis*

The first aim of the DSM study was to broadly identify and map the watercourses and wetlands located within each of the three catchment sites. In order to achieve this, the use of satellite imagery and the analysis of this imagery was undertaken. Imagery from the Sentinel-2 satellite was utilised. Sentinel-2 is an Earth observation satellite operated by the European Space Agency. It was launched on the 23$^{rd}$ of June 2015 as part of the European Copernicus Programme to perform terrestrial observations in support of services such as forest monitoring, land cover changes detection, and natural disaster management. Sentinel-2 records 13 bands in the visible, near infrared, and short-wave infrared part of the spectrum and its images have a resolution of 10 to 60 meters (Drusch et al., 2012, Kaplan and Avdan, 2017). The images can be downloaded free from the Copernicus Open Access Hub (https://scihub.copernicus.eu/).

Sentinel-2 imagery from the 25th of June 2020 was used in this study to map the wetlands and watercourses within each of the catchments. This date was chosen as cloud cover over the selected catchments was 1.2% and thus the area of study was clearly visible. Preprocessing of the data was undertaken utilising the semi-automatic classification plugin for QGIS version 3.10.9. This allowed for the individual bands to be set according to their central wavelengths (Congedo, 2014).

After preprocessing, a Normalized Difference Vegetation Index (NDVI) analysis was conducted. The NDVI processing utilises the following formula, for classifying different land covers within the catchments (Zhao et al., 2017).

$$\text{NDVI} = \text{Index (NIR, RED)} = \frac{\text{NIR - RED}}{\text{NIR + RED}}$$

Where NIR is the near infrared band and RED the red band, so for the Sentinel-2 images the following applies:

$$\text{Sentinel-2 images NDVI} = \text{Index (Band 8, Band 4)} = \frac{\text{Band 8 – Band 4}}{\text{Band 8 + Band 4}}$$

According to the Earth Resources and Observation Science (EROS) Centre, Values of the NDVI analysis range from -1 to 1. Areas of bare soil and/or open water have a very low NDVI value (i.e., 0.1 or less). Sparse vegetation results in moderate NDVI values (approximately 0.2 to 0.5), while high NDVI values (0.6 to 0.9) correspond to dense vegetation.

Based on prior knowledge of the catchments, areas which are known to be wetlands and watercourses are associated with denser vegetation as compared to terrestrial areas. Therefore, initial classification of wetlands and watercourses within the catchments was taken as areas with NDVI values higher than 0.4.

### *4.2.4. Rule-Based Digital Soil Mapping utilising the Arc Soil Inference Engine (ArcSIE)*

The creation of the digital soil maps for the three catchment areas utilised the ArcSIE (Soil Inference Engine) version 10.2.105. ArcSIE is a toolbox that functions as an Extension of ArcMap and generates soil maps based on the soil-environment model:

$$S = f(E)$$

This model states that the information about soil (S) can be derived from the information about the soil formative environment (E), including topography, geology, climate, and vegetation (Zhu et al., 2010).

ArcSIE was designed for creating soil maps using fuzzy logic in which DSM is performed according to existing relationships between soil attributes and landforms (de Menezes et al., 2014). The fuzzy logic model is based on the concept of fuzzy sets (Zadeh, 1965) and the complex nature of soils and landscapes which creates a more gradual and continuous change in soils and their properties. This forms an uncertainty in the allocation of boundaries between one soil group and another and should therefore not be represented by the abrupt lines depicted in polygon-based maps. Fuzzy logic therefore attempts to represent this uncertainty by predicting the soil groups as an alternative that is more adapted to the reality of the environment (Martín-López, et al., 2019). Unlike ordinary sets, fuzzy sets enable their elements to show a partial degree of membership in the range from 0 (no membership) to 1 (full membership). In this way, fuzzy logic models are capable of representing continuous graduations from one class to another class (Hellwig et al., 2016a, Shi et al., 2004).

A 5 m resolution Digital Elevation Model (DEM) (Ezemvelo KZN Wildlife et al., 2016) was utilised to create Digital Terrain Models (DTM) utilising ArcGIS version 10.2 and ArcSIE version 10.2.105 to represent the distribution of the topographical features across the three catchment sites. The slope, elevation and planform curvature were calculated directly from the DEM, while the wetness index was created from the filled DEM and a multipath flow accumulation raster.

A rule-based approach was undertaken. This involved understanding the relationships between the soil and landscape and was based on knowledge of the catchments and previous soil surveys. Furthermore, the aim of this study was to group the identified soil types into hydropedological groups based on the behaviour of the soils in relation to the flow dynamics of the catchment. The hydropedological classes were therefore classified as (i) recharge shallow soils; (ii) recharge deep soils; (iii) interflow soils; and (iv) responsive saturated soils (van Tol and Le Roux, 2019). The relationship between these hydropedology soil groups and the slope, elevation, topographical curvature, and inverse wetness index was identified.

A number of rules were applied to the inference engine within the ArcSIE tool. These rules were based on the outcome of the DTMs as well as knowledge of the catchments, with various parameters overlapping with each other due to the fuzzy logic nature of the rules applied. The following parameters were set for each of the DTMs within CP-III, CP-VI, and CP-IX (Table 4.1). This table represents the information used to produce the optimal curves that describe quantitatively the relationships between soil type and a particular DTM (de Menezes et al., 2014, Zhu et al., 1997). Furthermore, the wetness index was compared against the results of the NDVI analysis and mask polygons created where wetlands are known to occur. These mask polygons formed part of the input rules for the model.

Table 4.1: Environmental control variables of the hydropedological soil groups in CP-III, CP-VI, and CP-IX

| **Catchment** | **Hydropedological Soil Group** | **Wetness Index** | **Elevation (m)** | **Slope (%)** | **Planform Curvature** |
|---|---|---|---|---|---|
| CP-III | Recharge shallow | < 1 | 1900 - 2280 | > 30 | < -5 |
| | Recharge Deep | 1 - 9 | 1848 - 2200 | 22 - 30 | -5 - -0.6 |
| | Interflow | 8 - 15 | 1848 - 2100 | 18 - 30 | -0.6 – 2 |
| | Responsive Saturated | 15 - 21 | 1848 - 1956 | < 18 | 2 – 3.6 |
| CP-IV | Recharge shallow | < 2 | 1860 - 2040 | > 80 | < -2.3 |
| | Recharge Deep | 3 – 5 | 1830 - 2070 | 25 – 79 | -2.3 – 0.4 |
| | Interflow | – 7 | 1830 - 2040 | 15 – 25 | 0.4 – 3.6 |
| | Responsive Saturated | > 8 | 1830 - 2000 | < 15 | > 3.6 |
| CP-IX | Recharge shallow | < 4 | 1838 - 1985 | > 29 | > 0 |

| Catchment | Hydropedological Soil Group | Wetness Index | Elevation (m) | Slope (%) | Planform Curvature |
|---|---|---|---|---|---|
| | Recharge Deep | 3 - 8 | 1820 - 1985 | 1 - 28 | -0.5 – 3.6 |
| | Interflow | 7 - 10 | 1820 - 1930 | 14 - 28 | -3.5 - -0.4 |
| | Responsive Saturated | 9 - 13 | 1820 - 1911 | <15 | -6.9 - -0.5 |

After identifying the environmental control variables for each of the hydrological soil groups in each of the catchments, the continuous function curves set by ArcSIE were utilised to precisely define each parameter. The continuous function is applicable to environmental features with interval or ratio values (e.g., elevation, and slope gradient) and these were utilised for each of the parameters defined in this study. ArcSIE provides three basic function curves, which are used to further fine-tune the curve shape. These are the bell-shape curve, s-shape curve, and z-shape curve. These are described by Shi (2013) as follows.

The bell-shape curve optimality value decreases as the difference between the environmental feature and the central value increases (e.g., in CP-VI, the bell-shape curve defines that for the interflow hydropedological soil group a 15% to 25% slope is optimal i.e., receiving the highest membership and the membership value decreases as the slope increases from 25% or decreases from 15%). The s-shape curve defines the optimality of the environmental variable will always get the maximum value if the environmental feature values are greater than a defined value (e.g., in CP-III, the s-shape curve defines that for the recharge shallow hydropedological group, a slope steeper than 30% is always optimal and thus receiving the highest membership). The z-shape curve defines that the optimality will always receive the maximum value if the environmental feature values are less than a defined value (e.g., in CP-VI, the z-shape curve defines that for the responsive saturated hydropedological group, a slope gentler than 21% are always optimal and thus receiving the highest membership). Examples of these function curves are provided in Figure 4.1.

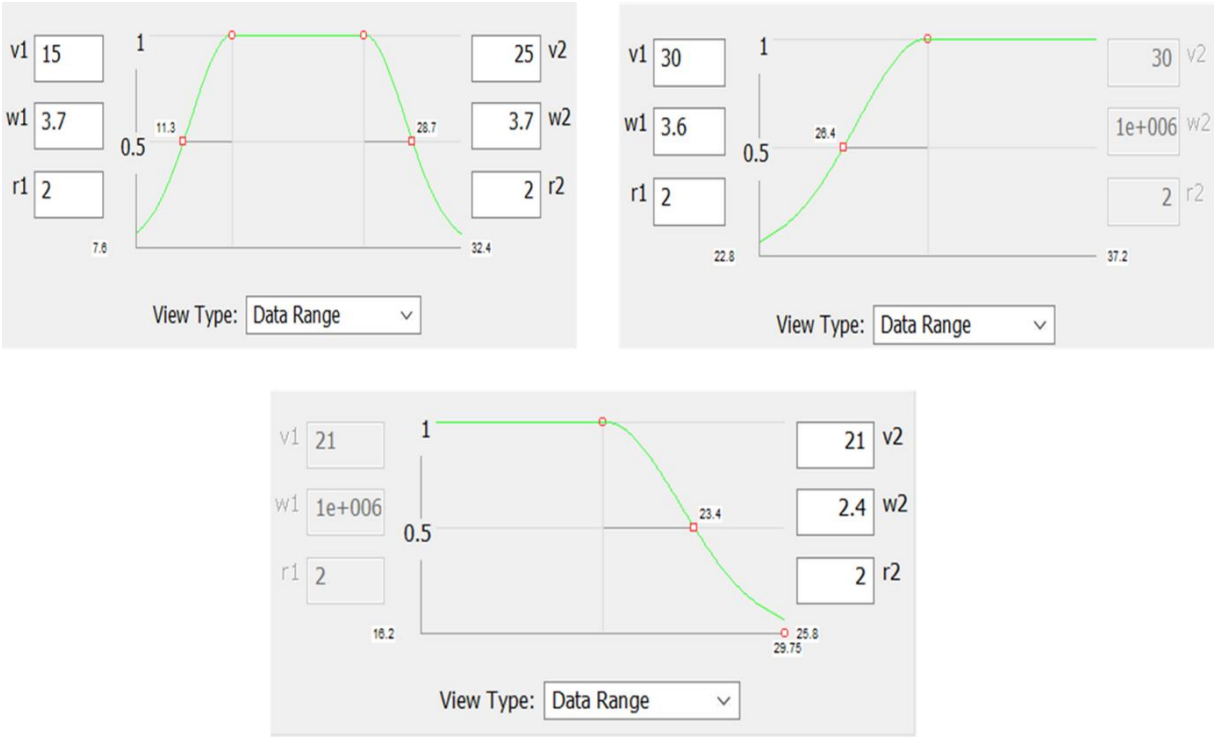


Figure 4.1: Examples of the Bell-Shape, S-Shape and Z-Shape optimality curves utilised in the ArcSIE inference interface

### *4.2.5. Ground truthing and validation*

The ArcSIE interface allows for the input of case-based features with the aim of adjusting the predictive models created within the rule-based phase, to better reflect the knowledge about a particular landscape. Cases are spatial features (points, lines, polygons, or raster cells) pinpointed, delineated, or derived by the soil scientist to express the knowledge of local soils (Shi, 2019). Existing soil maps and soil information gathered at specific points within the catchments were added as individual cases to the ArcSIE interface and this information utilised to refine the mapping rules. Forty-nine validation points were utilised for CP-III, forty-seven for CP-VI and twenty-seven for CP-IX. Soil sampling points were chosen to cover the range in altitude, planform curvature, slope, and topographical wetness of the individual catchment areas. The soils were classified as per the South African soil classification system (Soil Working Group, 2018) and their locations are displayed in Figure 4.2.

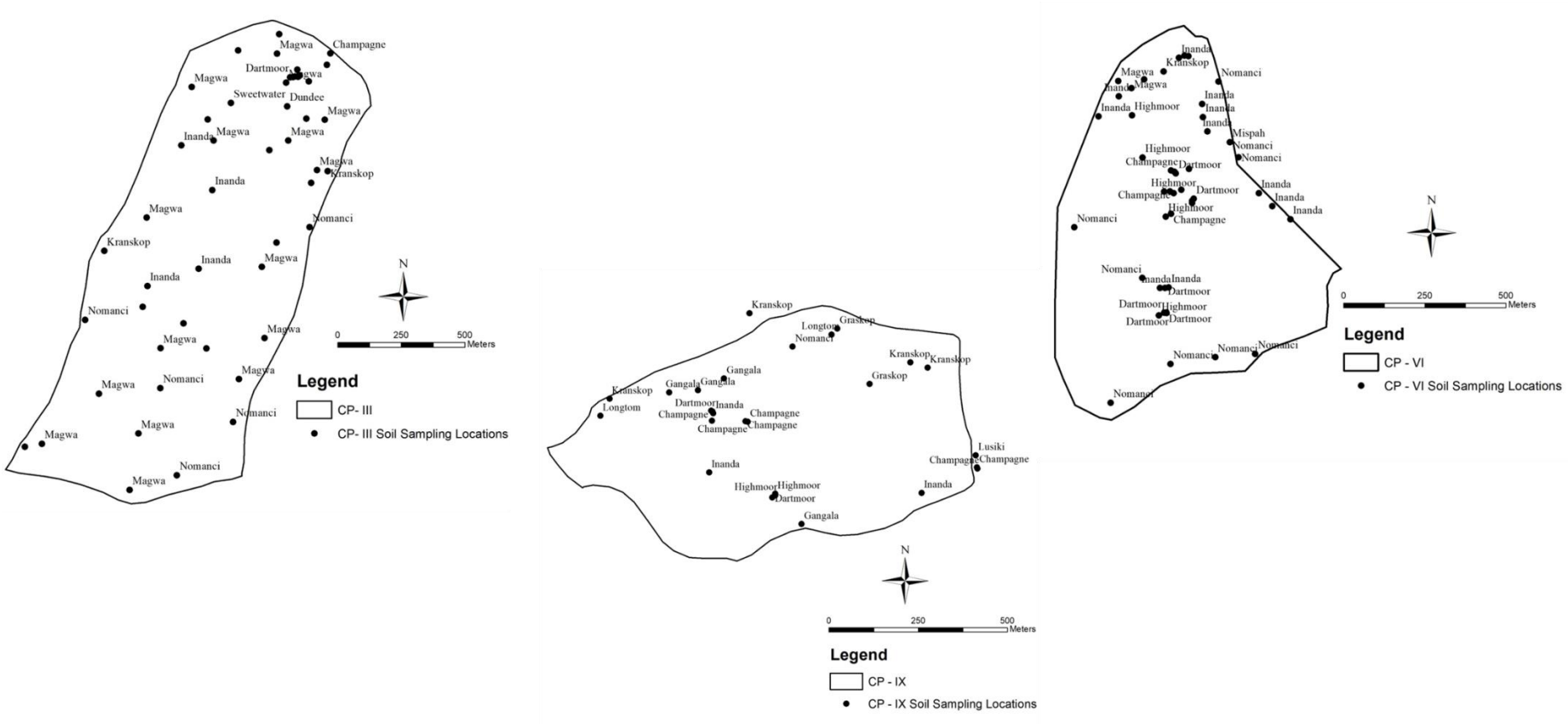


Figure 4.2:Location of the soil sampling points as well as the classification of the soils in (A) CP-III, (B) CP-VI and (C) CP-IX

The weighted average function was furthermore utilised in the validation process. Under the weighted-average method, ArcSIE calculates a linear weighted average of the optimality values of individual environmental features to get the overall optimality value for the instance. It therefore assigns different weights to different environmental features utilising the Analytical Hierarchy Process, which uses a structured process to assign weights consistently (Shi, 2013; Shi, 2019). An example of this is given in CP-III where slope is specified to be more important than elevation. The ArcSIE interface then quantifies this specification by assigning the score of slope against elevation.

### *4.2.6. Statistical Validation*

The performance of the ArcSIE interface to create the combined hydropedological maps for each of the catchments was analysed using the Kappa coefficient of agreement. This was used to measure the accuracy of the classifications utilised in the maps.

This was first undertaken using the classification of the pixel values versus the ground-truthed results that were obtained during previous soil surveys. Following the identification of the accuracies presented for each hydropedological soil group in each catchment, the Kappa coefficient equation (Cohen, 1960) was calculated. For computational purposes, the following formula is presented:

$$K = \frac{P_o - P_e}{1 - P_e}$$

Where $P_o$ = sum of each hydropedological group accuracy/total number of variables

$P_e$ = (sum of probability of a random raster pixel being in the correct hydropedological group) – (sum of probability of a random raster pixel being in the incorrect hydropedological group)

## 4.3. RESULTS AND DISCUSSION

The results section follows the same sub-headings as set out in the methodology section. These sub-sections identify the hydropedological classification of the soils delineated within the three catchments, the results of the NDVI analysis, the ArcSIE rule-based and validation inputs, as

well as the statistical analysis of the results obtained. A discussion of the results then highlights the effectiveness of utilising ArcSIE for the mapping of the hydropedological soil groups.

### *4.3.1. Hydropedological classification of soils*

Soil surveys to map the soils were undertaken within the three catchment areas. These soils were classified as per the South African soil classification system (Soil Working Group, 2018). The soils were then reclassified according to their hydropedological character, based on the classifications from van Tol and Le Roux (2019). The hydropedological soil groups are defined for this study as per Table 4.2.

Table 4.2: Hydropedological soil groups mapped in the catchments

| **Hydropedological Soil Group** | **Soil Forms (Soil Working Group, 2018)** | **Characteristics of soils** |
|---|---|---|
| Recharge Shallow Soils | Nomanci, Mispah, Graskop | These are soils that are freely drained and do not show any indication of saturation. They are typically shallow in nature (<500mm). The freely drained B horizon merges with fractured rock or a lithic horizon. These soils typically occur on steeper convex slopes in the higher lying or steeper parts of the catchments. |
| Recharge Deep Soils | Kranskop, Magwa, Inanda, Longtom, Sweetwater, Gangala | These are soils that are freely drained and do not show any indication of saturation. They are typically deeper than the Recharge Shallow Soils (>500mm). The freely drained B horizon merges into fractured rock or a lithic horizon. These soils where identified throughout the catchments on gentler convex and concave slopes and away from wetlands and watercourses. |
| Interflow soils | Dartmoor, Highmoor | These soils have a freely drained upper solum which overlies relatively |

| Hydropedological Soil Group | Soil Forms (Soil Working Group, 2018) | Characteristics of soils |
|---|---|---|
| | | impermeable bedrock. Hydromorphic properties are identified at this interface and signify periodic saturation associated with a water table. They typically occur on gentler concave slopes in areas delineated as wetlands as well as adjacent to watercourses. |
| Responsive Saturated Soils | Champagne, Katspruit | These soils display morphological indications of long-term saturation. They characteristically respond quickly to rainfall events and generate overland flow as they are typically close to saturation during the wet season and therefore any additional precipitation will flow overland due to saturation excess. These soils were identified in the valley bottom positions of the catchments, in permanently saturated wetlands. They typically occur on gentle concave slopes. |

### *4.3.2. NDVI Analysis*

The results of the NDVI analysis are given in Figure 4.3. The NDVI values vary from 0 to 0.79 for all catchments with lower values indicating bare soil and higher values vegetation. The higher the value the denser the vegetation. The CP-III NDVI values ranged from 0.05 to 0.79, CP-VI results ranged from 0.06 to 0.55 and CP-IX results varied from 0 to 0.64. Firebreaks, which had been burned around the boundary of each of the catchments are clearly visible, with these areas displaying low values (<0.2) due to the exposure of bare soil as a result of the fire. Based on knowledge of the catchments, areas which are known to be wetlands and watercourses displayed values in the mid to high value ranges and are displayed in Figure 4.3 as areas with values higher than 0.4 (blue colouring). As CP-IX consists of denser vegetation as a result of the dominance of the woody scrub, *Leucasidea serica*, wetlands and watercourses

were classified as areas with a higher NDVI value, 0.5, compared to CP-III and CP-IV. As the satellite imagery was taken in June (dry season), no areas of open water were identified.

The use of the NDVI analysis to form a basis for the location of wetlands and watercourses relied on the knowledge of the catchments and the use of previous soil survey work. Watercourses and wetland zones were defined in all three catchments in the NDVI analysis as areas with denser vegetation. Prior knowledge of these areas as well as the use of the topographical wetness index as part of the rule-based processing of the maps confirmed their classification as watercourses and wetland systems. It is therefore difficult to delineate watercourses and wetlands with the use of NDVI analysis alone. This is corroborated in various studies in which it was concluded that rule-based classifiers provide more accurate results if supported by ancillary data such as Digital Elevation Models (Lidzhegu et al., 2019; Ozesmi and Bauer, 2002, Quinn and Epshtein, 2014). The NDVI analysis results combined with the topographical wetness index and knowledge of the catchments, however, provided useful data in the creation of polygon masks which were input into the ArcSIE interface to aid in the correct prediction of areas as wetlands and watercourses.

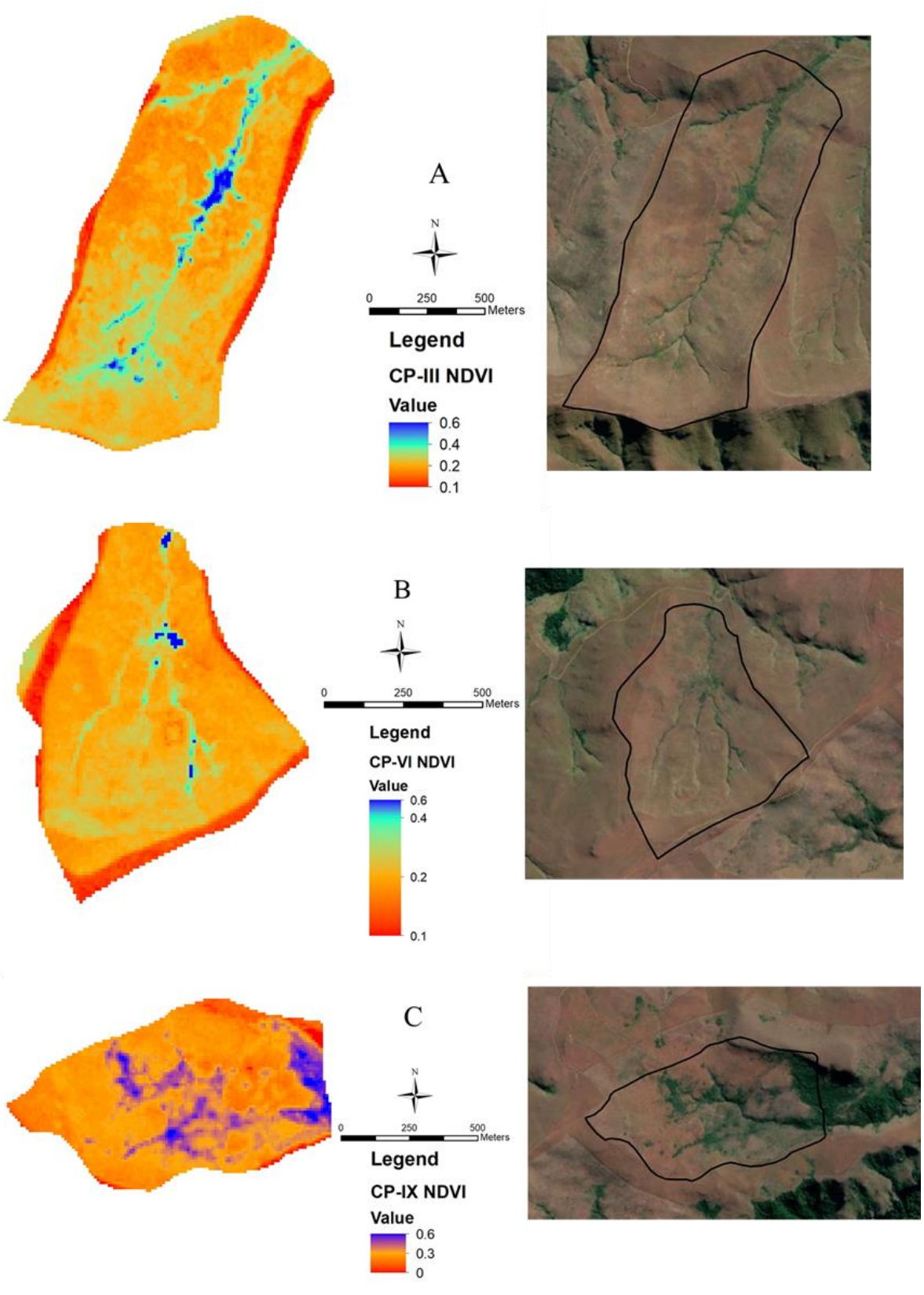


Figure 4.3: NDVI Analysis results for the three catchments A) CP-III; B) CP-VI and C) CP-IX

### *4.3.3. Rule-Based Digital Soil Mapping*

Figure 4.4 shows an example of the fuzzy membership maps produced for the four hydropedological classes in CP-III. These were created according to the instances for each of these classes (Table 4.1) and the input of polygon masks where wetlands and watercourses are known to occur. Similar fuzzy membership maps were created for CP-VI and CP-IX. These maps are the first product generated by the inference engine and are used as the basis for the final map. Every pixel in each of the fuzzy membership maps is assigned a value ranging from 0 to 100 depending on the similarity of that pixel location to the hydropedology classed being mapped.

These maps reveal more details about the hydropedology classes than conventional polygon maps because they are made at pixel size spatial resolution (de Menezes, et al., 2014). The ArcSIE interface then allows for the creation of a combined map in which the individual fuzzy membership maps are integrated and a draft map of the hydropedological classes for the catchments created (Figure 4.4).

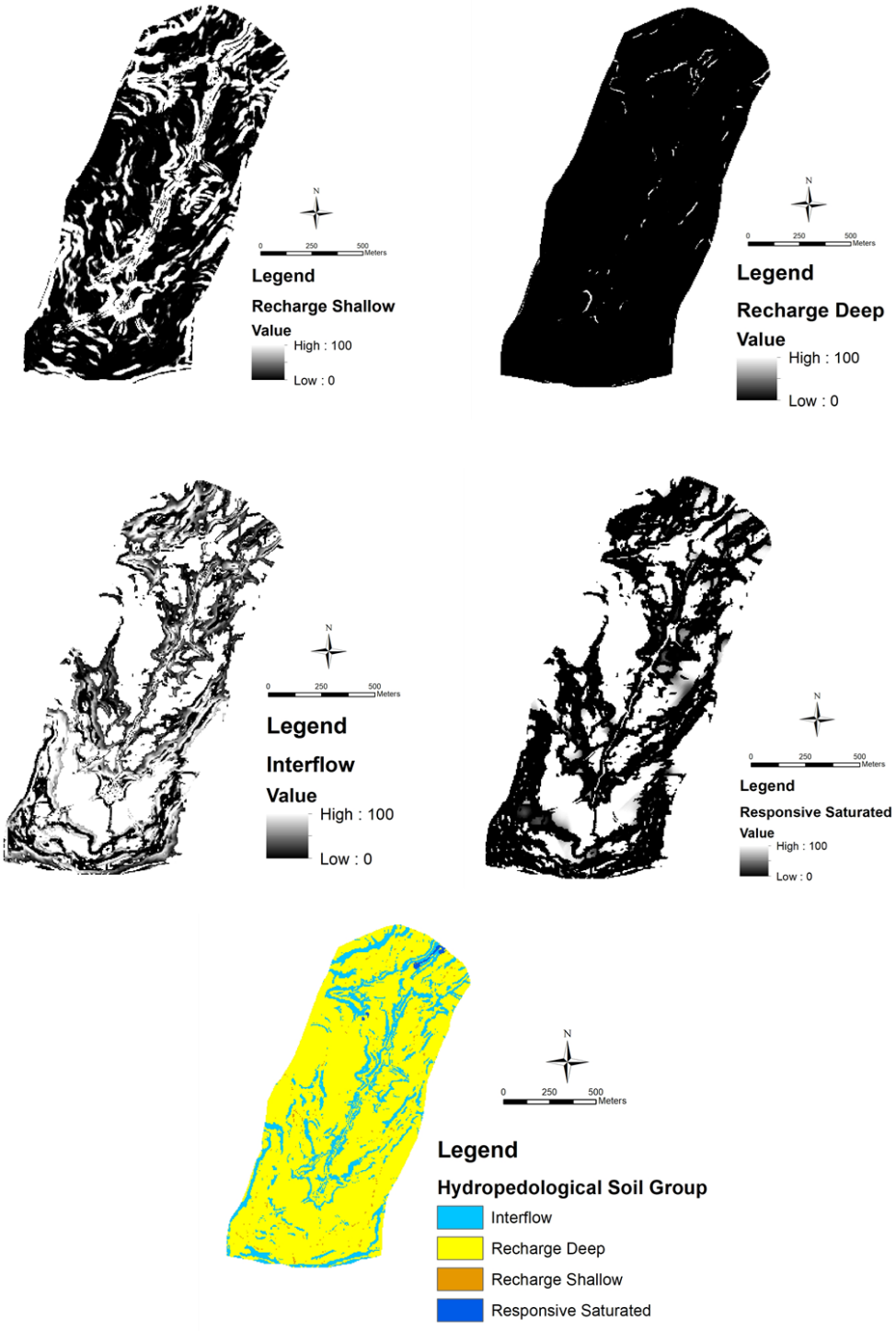


Figure 4.4: Fuzzy membership maps for each hydropedological soil group as well as the draft combined map for CP-III

### *4.3.4. Validation*

Based on the specific locations of the soil points in each of the catchments, the results of the NDVI analysis, as well as the use of the linear weighted average, a finalised refined hydropedological soil group map was created. These are displayed in Figure 4.5.

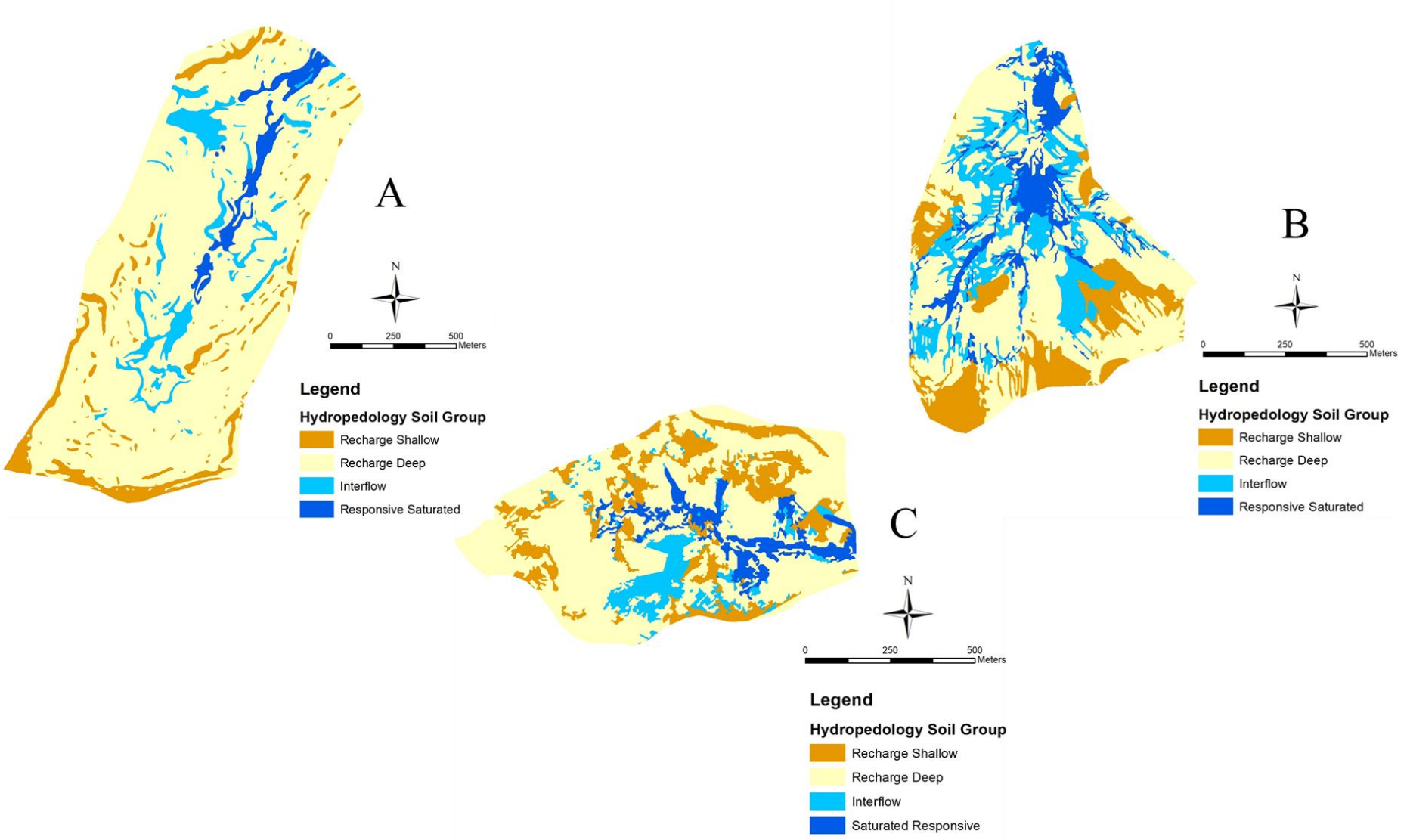


Figure 4.5: Refined Hydropedological Soil Group Maps for the three catchments A) CP-III; B) CP-VI and C) CP-IX

### *4.3.5. Statistical analysis*

The accuracy table displaying the classification of the pixel values versus the ground-truthed results of each catchment is presented in Table 4.3. Accuracy percentage values varied between catchments and between the different hydropedological soil groups.

Table 4.3: Accuracies for modelled hydropedological group versus ground-truthed hydropedological group in CP-III, CP-VI, and CP-IX

| **Catchment** | **Hydropedological Soil Group** | **Ground-truthed Recharge Shallow** | **Ground-truthed Recharge Deep** | **Ground-truthed Interflow** | **Ground-truthed Responsive Saturated** | **Total** | **Accuracy %** |
|---|---|---|---|---|---|---|---|
| CP-III | Recharge Shallow | **4** | 1 | 0 | 0 | 5 | 80 |
| | Recharge Deep | 4 | **21** | 1 | 2 | 28 | 75 |
| | Interflow | 1 | 1 | **8** | 0 | 10 | 80 |
| | Responsive Saturated | 2 | 2 | 0 | **2** | 6 | 34 |
| | Total | 11 | 25 | 9 | 4 | **49** | |
| CP-VI | Responsive Saturated | **8** | 0 | 1 | 4 | 13 | 62 |
| | Recharge Shallow | 0 | **9** | 1 | 0 | 10 | 90 |
| | Recharge Deep | 1 | 0 | **11** | 5 | 17 | 65 |
| | Interflow | 0 | 0 | 2 | **4** | 6 | 67 |
| | Total | 9 | 9 | 15 | 13 | **46** | |
| CP-IX | Recharge Deep | **9** | 0 | 1 | 1 | 11 | 82 |
| | Recharge Shallow | 2 | **5** | 0 | 0 | 7 | 71 |
| | Interflow | 0 | 0 | **3** | 0 | 3 | 100 |

| Catchment | Hydropedological Soil Group | Ground-truthed Recharge Shallow | Ground-truthed Recharge Deep | Ground-truthed Interflow | Ground-truthed Responsive Saturated | Total | Accuracy % |
|---|---|---|---|---|---|---|---|
| | Responsive Saturated | 1 | 0 | 0 | **5** | 6 | 83 |
| | Total | 12 | 5 | 4 | 6 | **27** | |

The overall Kappa coefficient for CP-III is 0.57, for CP-VI is 0.59, and for CP-IX is 0.74. These values range from a weak (CP-III and CP-VI) to a moderate (CP-IX) agreement between the predicted maps and the ground-truthed points (McHugh, 2012). Various studies which utilise DSM for the prediction of both soil types and physical properties of soils within catchments have resulted in similar (weak to moderate) agreements (de Menezes et al., 2014, Hellwig et al., 2016a, Hellwig et al., 2016b, Silva et al., 2019).

The quality of the hydropedological soil group maps produced is determined by the method (rule-based versus case-based) and the environmental covariates used for the model predictions. The accuracy of the DEM utilised in the initial rule-based approach plays a large role in determining the effects of slope, elevation, planform curvature and the wetness index on the modelled predictive maps for each hydropedological soil group. Furthermore, inaccuracies and uncertainties in the input of the value ranges in the function curves as part of the rule-based approach, as well as the use of weighted average function in the case-based approach plays a role in determining the quality of the final maps produced. These inaccuracies and uncertainties were highlighted in various studies which recommended validation procedures to improve inaccuracies in the predictive models (de Menezes et al., 2014, Hellwig et al., 2016b). The accuracy of the location of each individual hydropedological soil group also influences the overall accuracy of the final maps produced. This varied for each catchment and depended on the quantity of observation points made in previous soil surveys.

The determined quality of the final digital soil maps reinforces the need to combine the knowledge of soil experts with soil-landscape relationships. This increases the accuracy of prediction models of soil properties within a landscape (de Menezes et al., 2014).

Readily available soil information is increasingly being sought after as the importance of soil in ecosystem management is more widely recognised. The security of soils including their capability, health, connectivity, and classification forms the basis of all spheres of land management from food and nutrition security, water security, energy security, climate change and human health. With the use of DSM our knowledge and understanding of future soil security can be enhanced for larger areas with the use of competitive budgets and timeframes (Searle et al., 2021, van Zijl, 2019).

## 4.4. CONCLUSION

Results indicate that while the use of ArcSIE is a powerful tool to be used to gain a general idea of the relationship between the soils and the landscape from a hydropedological stance, the knowledge of the soil-landscape relationship, as with the traditional soil mapping exercise, is still necessary to improve the accuracy of the tool. The quality of the digital soil map produced is furthermore dependant on the method employed (rule-based versus case-based) as well as the environmental covariates used for the model predictions. This is true for all inputs to the prediction model. The results of the NDVI analysis, which were utilised as another input to improve the accuracy of the prediction model, identified that it is difficult to delineate the wetlands and watercourses without prior knowledge of the catchments. Therefore, the more knowledge one has of the landscape processes under study, the more accurate the outcome of the digital soil mapping exercise.

However, the hydropedological soil group maps achieved an appropriate representation of the complex nature of the soil-landscape relationship, with changes between one soil group and the next being gradual and continuous. These soil group correlations are not well represented in polygon-based maps and therefore require the fuzzy membership logic utilised by the ArcSIE interface to depict these relationships. The use of the ArcSIE interface to derive the hydropedological soil group maps of the three different catchments provided adequate results with regards to understanding the overall behaviour of the soils in the catchments. Of importance is that the accuracies and inaccuracies within the fuzzy-membership maps can be quantified, allowing for a confidence rating in the use of these maps. These maps can therefore be used in further applications in water and land management for the area.

Numerous studies have utilised ArcSIE to create not only soil classification maps but also more detailed studies of the properties of soils across the globe (Akumu et al., 2015; de Menezes et al., 2014; Moonjun et al., 2020, Pittman et al., 2021), however the use of any DSM programme has rarely been applied in Africa and particularly in Afromontane environments, with the majority of studies coming out of South Africa and Kenya. These studies are furthermore aimed at agricultural studies, the mapping of soil organic carbon, clay percentage and for industrial and commercial developments (Mora-Vallejo et al., 2008, van Zijl, 2019).

Afromontane environments provide several ecohydrological services to downstream locations, including the ecological and physical processes that control the partitioning and routing of precipitation into evaporation, infiltration, transpiration, recharge, and runoff (Brooks and Vivoni, 2015). The characteristics of the soils of these catchments form the basis of these services. However, the remoteness and often inaccessible terrain associated with Afromontane environments often reduces the knowledge and understanding of these areas. The use of DSM which is suited to these types of environments would allow for more integration of soil knowledge into land management policies across the continent. Further training of DSM programmes in Africa would therefore lead to an improved understanding of the basis of ecohydrological processes.

## 4.5. REFERENCES

Akumu, C.E., Johnson, J. A., Etheridge, D., Uhlig, P., Woods, M., Pitt, D.G., and McMurray, S. (2015). GIS-fuzzy logic-based approach in modeling soil texture: Using parts of the Clay Belt and Hornepayne region in Ontario Canada as a case study. Geoderma. 239-240. https://doi.org/10.1016/j.geoderma.2014.09.021.

Ashtekar, J.M., Owens, P.R., Brown, R.A., Winzeler, H.E., Dorantes, M., Libohova, Z., Dasilva, M., and Castro, A. (2014). Digital mapping of soil properties and associated uncertainties in the Llanos Orientales, South America. In Global Soil Map: Basis of the Global Spatial Soil Information System - Proceedings of the 1st Global Soil Map Conference. 367-372. DOI:10.1201/b16500-67.

Behrens, T., Förster, H., Scholten, T., Steinrücken, U., Spies, E-D., and Goldschmitt, M. (2005). Digital soil mapping using artificial neural networks. Journal of Plant Nutrition and Soil Science. 168 (1). 21-33. doi.org/10.1002/jpln.200421414.

Berberoglu, S., Yilmaz, K.T., and Ozkan, C. (2004). Mapping and monitoring of coastal wetlands of Cukurova Delta in the Eastern Mediterranean region. Biodiversity and Conservation. 13. 615-633.

Bouma, J. (2006). Hydropedology as a powerful tool to environmental policy research. Geoderma. 131. 275-286.

Brooks, P.D., and Vivoni, E.R. (2015). Editorial. Mountain ecohydrology: quantifying the role of vegetation in the water balance of montane catchments. Ecohydrology. 1. 187-192. DOI: 10.1002/eco.27.

Bushnell, T.M. (1942). Some aspects of the soil catena concept. Soil Science Society of America, Proceedings. 7. 466-476.

Cohen, J. (1960). A Coefficient of Agreement for Nominal Scales, Educational and Psychological Measurement. Vol. 20. No. 1. 37-46.

Congedo, L. (2014). Semi-Automatic Classification Plugin Documentation. Release 5.0.0.1.

de Menezes, M.D., Silva, S.H.G., Owens, P.R., and Curi, N. (2014). Digital Soil Mapping Approach Based on Fuzzy Logic and Field Expert Knowledge. Ciência e Agrotecnologia. Vol. 37. No. 4. Lavras.

de Menezes, M.D., Silva, S.H.G., Owens, P.R., and Curi, N. (2014). Solum depth spatial prediction comparing conventional with knowledge-based digital soil mapping approaches. Scientia Agricola. Vol. 71. No. 4. http://dx.doi.org/10.1590/0103-9016-2013-0416.

Diek, S., Temme, A.J.A.M., and Teuling, A. (2014). The effect of spatial soil variation on the hydrology of a semi-arid Rocky Mountains catchment. Geoderma. 235-236. 113-126.

Drusch, M., Del Bello, U., Carlier, S., Colin, O., Fernandez, V., Gascon, F., Hoersch, B., Isola, C., Laberinti, P.,Martimort, P., Meygret, A., Spoto, F., Sy, O., Marchese, F., Bargellini, P. (2012). Sentinel-2: ESA's optical high-resolution mission for GMES operational services. Remote Sensing of Environment. 120. 25-36.

European Confederation of Soil Science Societies. (2004). Scientific Basis for the Management of European Soil Resources: Research Agenda, Guthman-Peterson. Vienna.

Ezemvelo KZN Wildlife, National Lottery, University of KwaZulu-Natal, and African Conservation Trust. (2016). Maloti-Drakensberg Transfronteir Aerial Mapping Project Data.

Frohn, R.C., Reif, M., Lane, C., and Autrey, B. (2009). Satellite remote sensing of isolated wetlands using object-oriented classification of Landsat-7 data. Wetlands 29. (3). 931-941.

Grayson, R.B., Western, A.W., Chiew, F.H.S., and Blöschl, G. (1997). Preferred states in spatial soil moisture patterns: local and nonlocal controls. Water Recourses Research. 33 (12). 2897–2908.

Harrison, R.L., van Tol, J. and Toucher, M.L. Using hydropedological characteristics to improve modelling accuracy in Afromontane catchments. Journal of Hydrology: Regional Studies. 39. https://doi.org/10.1016/j.ejrh.2021.100986.

Heath, R.C. (1980). Basic elements of groundwater hydrology with reference to conditions in North Carolina. US. Geological Survey. Water Resources Investigations. Open File Report No. 80-44. Pp.87.

Hellwig, N., Graefe, U., Tatti, D., Sartori, G., Anschlag, K., Beylich, A., Gobat, J., and Broll, G. (2016a). Upscaling the spatial distribution of enchytraeids and humus forms in a high mountain environment on the basis of GIS and fuzzy logic. European Journal of Soil Biology. 79. 1-13.

Hellwig, N., Anschlag, K., and Broll G. (2016b). A Fuzzy Logic Based Method for Modelling the Spatial Distribution of Indicators of Decomposition in a High Mountain Environment, Arctic, Antarctic, and Alpine Research, 48:4, 623-635, DOI: 10.1657/AAAR0015-073.

Ismail, M., and Yacoub, R. K. (2012). Digital soil map using the capability of new technology in Sugar Beet area, Nubariya, Egypt. The Egyptian Journal of Remote Sensing and Space Science, 15(2), 113–124. doi:10.1016/j.ejrs.2012.08.001.

Jenny, H. (1941). Factors of Soil Formation. McGraw-Hill. New-York.

Kaplan, G., and Avdan, U. (2017). Mapping and Monitoring Wetlands Using Sentinel-2 Satellite Imagery. ISPRS Annals of the Photogrammetry, Remote Sensing and Spatial Information Sciences. Vol. IV-4/W4. 4th International GeoAdvances Workshop. 14–15 October 2017, Safranbolu, Karabuk, Turkey.

Kimsey M.J. (2020) Soil Mapping, Monitoring, and Assessment. In: Pouyat R., Page-Dumroese D., Patel-Weynand T., Geiser L. (eds) Forest and Rangeland Soils of the United States Under Changing Conditions. Springer, Cham. https://doi.org/10.1007/978-3-030-45216-2_9.

Klemas, V. (2005). Remote sensing: wetlands classification. *In*: Schwartz, M.L. (Ed.). Encyclopedia of Coastal Science. Springer, Dordrecht, the Netherlands, pp. 804-807.

Klemas, V. (2011). Remote sensing of wetlands: case studies comparing practical techniques. Journal of Coastal Research. 27. (3). 418-427.

Kokaly, R.F., Despain, D.G., Clark, R.N., and Livo, K.E. (2003). Mapping vegetation in Yellowstone National Park using spectral feature analysis of AVIRIS data. Remote Sensing of Environment. 84. 437-456.

Lagacherie P. (2008) Digital Soil Mapping: A State of the Art. In: Hartemink A.E., McBratney A., Mendonça-Santos M. (EDS) Digital Soil Mapping with Limited Data. Springer, Dordrecht. doi.org/10.1007/978-1-4020-8592-5_1.

Lidzhegu, Z., Ellery, W.N., Mantel, S.K., and Hughes, S.K. (2019). Delineating wetland areas from the cut-and-fill method using a Digital Elevation Model (DEM). South African Geographical Journal. DOI: 10.1080/03736245.2019.1638825.

Lin, H. (2003). Hydropedology: bridging disciplines, scales, and data. Vadose Zone Journal. 2. 1–11. http://dx.doi.org/10.2113/2.1.1.

Lin, H. (2012). Hydropedology Synergistic Integration of Soil Science and Hydrology. Academic Press. USA.

Lin, H., Bouma, J., Wildling, L.P., Richardson, J.L., Kutilik, M., and Nielsen, D.R. (2005). Advances in hydropedology. Advances in Agronomy. 85. 307-353.

Lin, H., Bouma, J., Pachepsky, Y., Western, A., Thompson, J., van Genuchten, R., Vogel, H., and Lilly, A. (2006). Hydropedology: Synergistic integration of pedology and hydrology. Water Resources Research. VOL. 42. W05301. doi:10.1029/2005WR004085.

Lin, Y., and Liquan, Z. (2006). Identification of the spectral characteristics of submerged plant Vallisneria spiralis. *Acta* Ecologica *Sinica*. 26. 1005-1011.

Lindbo, D.L., and Richardson, J.L. (2000). Hydric soils and wetlands in riverine systems. In:

Richardson, J.L., and Vepraskas, M.J. (Eds.). Wetland Soils: Their Genesis, Morphology, Hydrology, Landscape, and Classification. CRC Press. Boca Raton, Florida. Ch. 12.

Lunetta, R.S., and Balogh, M.E. (1999). Application of multi-temporal Landsat $5^{TM}$ imagery for wetland identification. Photogrammetric *Engineering* & *Remote Sensing*. 65. 1303-1310.

Ma, Y., Minasny, B., Malone, B.P., and McBratney, A.B. (2019). Pedology and digital soil mapping (DSM). European Journal of Soil Science. 70. 216–235. doi: 10.1111/ejss.12790.

Mahmood, T.H., and Vivoni, E.R. (2011). A climate-induced threshold in hydrologic response in a semiarid ponderosa pine hillslope. Water Recourses Research. 47. (9). W09529.

Martín-López, J.M., Da Silva, M., Valencia, J., Quintero, M., Keough, A., and Casares, F. (2019). A comparative Digital Soil Mapping (DSM) study using a non-supervised clustering analysis and an expert knowledge-based model - A case study from Ahuachapán, El Salvador. Presented at: Joint Workshop for Digital Soil Mapping and Global Soil Map March 12-16 2019.

McBratney, A.B., Mendonca Santos, M.L., Minasny, B. (2003). On Digital Soil Mapping. Geoderma. 117. 3-52.

McHugh, M.L. (2012). Interrater reliability: the kappa statistic. Biochemia Medica. 22(3): 276–282.

Milne, G. (1936). Normal erosion as a factor in soil profile development. Nature. 138(3491). 548-549. doi:10.1038/138548c0.

Mitsch, W. J., and Gosselink, J.G. (2015). Wetlands. Wetlands. 155-204.

Moonjun, R., Shrestha, P. D., and Jetten, V. G. (2020). Fuzzy logic for fine-scale soil mapping: A case study in Thailand. Catena. 190. 104456 https://doi.org/10.1016/j.catena.2020.104456.

Mora-Vallejo, A., Claessens, L., Stoorvogel, J., and Heuvelink, G. (2008). Small scale digital soil mapping in Southeastern Kenya. Catena. 76. 44-53. DOI:10.1016/j.catena.2008.09.008.

Mucina, L., Rutherford, M.C. & Powrie, L.W. (eds). (2006). Vegetation Map of South Africa, Lesotho and Swaziland. Edn. 2. South African National Biodiversity Institute, Pretoria. ISBN 978-1-919976-42-6.

Nanni, U.W. (1956). Forest Hydrological Research at the Cathedral Peak Research Station. Journal of the South African Forestry Association 27(1). 2-35.

Ozesmi, S.L., and Bauer, M.E. (2002). Satellite remote sensing of wetlands. Wetlands Ecology and Management, 10, 381–402.

Penna, D., Borga, M., Norbiato, D., Dalla Fontana, G. (2009). Hillslope scale soil moisture variability in a steep alpine terrain. Journal of Hydrology. 364 (3–4). 311–327.

Phillips, R.L., Beeri, O., and DeKeyser, E.S. (2005). Remote wetland assessment for Missouri Coteau prairie glacial basins. Wetlands. 25. 335-349.

Pittman, R., Hu, B., and Webster, K. (2021). Improvement of soil property mapping in the Great Clay Belt of northern Ontario using multi-source remotely sensed data. Geoderma. 381. 114761. https://doi.org/10.1016/j.geoderma.2020.114761.

Quinn, N.W.T., and Epshtein, O. (2014). Seasonally-managed wetland footprint delineation using Landsat ETMþ satellite imagery. Environmental Modelling & Software. 54. 9-23.

Rhoton, F.E., Bigham, J.M., and Lindbo, D.L. (2002). Properties of iron oxides in streams draining the loess uplands of Mississippi. Applied Geochemistry. 17. 409-419.

Searle, R., McBratney, A., Grundy, M., Kidd, D., Malone, B., Arrouays, D., Stockman, U., Zund, P., Wilson, P., Wilford, J., Van Gool, D., Triantafilis, J., Thomas, M., Stower, L., Slater, B., Robinson, N., Ringrose-Voase, A., Padarian, J., Payne, J., Orton, T., Odgers, N., O'Brien, L., Minasny, B., McLean Bennett J., Liddicoat, C., Jones, E., Holmes, K., Harms, B., Gray, J., Bui, E., and Andrews K. (2021). Digital soil mapping and assessment for Australia and beyond:A propitious future. Geoderma Regional. 24. https://doi.org/10.1016/j.geodrs.2021.e00359.

Shi, X., Zhu, A., Burt, J.E., Qi, F., and Simonson, D. (2004). A Case-based Reasoning Approach to Fuzzy Soil Mapping. Soil Science Society of America Journal. 68. 885–894.

Shi, X. (2013). ArcSIE User Guide. http://www.arcsie.com/Download/htm. Accessed 08 June 2020.

Shi, X. (2019). ArcSIE Tutorial with Geodatabase. http://www.arcsie.com/Download/htm. Accessed 08 June 2020.

Silva, B.P.C., Silva, M.L.N., Avalos, F.A.P., de Menezes, M.D., and Curi, N. (2019). Digital soil mapping including additional point sampling in Posses ecosystem services pilot watershed, southeastern Brazil. Scientific Reports 9, 13763. https://doi.org/10.1038/s41598-019-50376-w.

Soil Classification Working Group. (2018). Soil Classification: A Natural and Anthropogenic System for South Africa. ARC-Institute for Soil, Climate and Water. Pretoria.

Smith, S., Bulmer, C., Flager, E., Frank, G., and Filatow, D. (2010). Digital Soil Mapping at multiple scales in British Columbia, Canada. In Program and Abstracts. 4th Global Workshop on Digital Soil Mapping. 24-26 May 2010. Rome, Italy. pg 17.

Teuling, A.J., and Troch, P.A. (2005). Improved understanding of soil moisture variability dynamics. *Geophysical Research Letters*. 32. (5). L05404.

Thompson, J.A., Roecker, S., Grunwald, S., and Owens, P.R. (2012). Digital Soil Mapping: Interactions with and Applications for Hydropedology. Chapter 21. Hydropedology. Edited by H. Lin. DOI: 10.1016/B978-0-12-386941-8.00021-6.

Toucher, M.L., Clulow, A., van Rensburg, S., Morris, F., Gray, B., Majozi, S., Everson, C.E., Jewitt, G.P.W., Taylor, M.A., Mfeka, S., and Lawrence, K. (2016). Establishment of a more robust observation network to improve understanding of global change in the sensitive and critical water supply area of the Drakensberg. 2236/1/16. Water Research Commission, Pretoria, South Africa.

van Tol, J.J., Lorentz, S.A., van Zijl, G.M., and Le Roux, P.A.L. (2018). The contribution of hydropedological assessments to the availability and sustainable water, for all (SDG#6). *In* Lal, R., Horn, R., and Kosaki, T. (eds). Soil and Sustainable Development Goals. Catena-Schweizerbart, Stuttgart. 102 - 117.

van Tol, J.J., and Le Roux, P.A.L. (2019). Hydropedological grouping of South African soil forms. South African Journal of Plant and Soil. 36(3). 233-235. DOI: 10.1080/02571862.2018.1537012.

van Tol, J.J., van Zijl, G., and Julich, S. (2020). Importance of Detailed Soil Information for Hydrological Modelling in an Urbanized Environment. Hydrology. 7(2). 34. https://doi.org/10.3390/hydrology7020034.

van Zijl, G. (2019). Digital soil mapping approaches to address real world problems in southern Africa. Geoderma. 337. 1301-1308. https://doi.org/10.1016/ j.geoderma.2018.07.052.

van Zijl, G., van Tol, J.J., Tinnefeld, M., and Le Roux, P. (2019). A hillslope based digital soil mapping approach, for hydropedological assessments. Geoderma. 354. 113888.

Vepraskas, M.J., and Lindbo, D.J. (2012). Chapter 5 - Redoximorphic Features as Related to Soil Hydrology and Hydric Soils. *In* Lin, H. (ed). Hydropedology. Academic Press. 143-172. https://doi.org/10.1016/B978-0-12-386941-8.00005-8.

Zadeh, L.A. (1965). Fuzzy sets. Information and Control. 8. 338-353.

Zhao, L., Zhang, P., Ma, X., and Pan, Z. (2017). Land Cover Information Extraction Based on Daily NDVI Time Series and Multiclassifier Combination. Mathematical Problems in Engineering. Vol. 2017. Article ID 6824051. https://doi.org/10.1155/2017/6824051.

Zhu, A.X., Band, L., Vertessy, R., and Dutton, B. (1997). Derivation of soil properties using a soil land inference model (SoLIM). Soil Science Society of American Journal. 61. 523-533.

Zhu, A.X., Qi, F., Moore, A., Burt, J.E. (2010). Prediction of soil properties using fuzzy membership values. Geoderma. 158. 199-206.

# CHAPTER 5 – HYDROPEDOLOGICAL CHARACTERISTICS OF THE CATHEDRAL PEAK RESEARCH CATCHMENTS

Published as: Harrison, R., van Tol, J., and Amiotte Suchet, P. (2022). Hydropedological characteristics of the Cathedral Peak research catchments. *Hydrology*. 9. 11. 189. https://doi.org/10.3390/hydrology9110189.

**Abstract**

It has long been recognised that the role of soils is critical to the understanding of how catchments store and release water. This study aimed to gain an understanding of the hydropedological characteristics and flow dynamics of the soils of three mountain catchment areas. Digital soil maps of the hydropedological characteristics of the catchments were interpreted and a conceptual response of these watersheds to precipitation was formed. This conceptual response was then tested with the use of site-specific precipitation and streamflow data. Furthermore, piezometers were installed in soils classified as the interflow hydropedological soil group as well as the saturated responsive hydropedological soil group and water table depth data for the three catchments were analysed. Climatic data indicated that there is a lag time effect in the quantity of precipitation that falls in the catchment and the corresponding rise in streamflow value. This lag time effect coupled with data obtained from the piezometers show that the various hydropedological soil groups play a pivotal role in the flow dynamics. Of importance is the unique influence of different wetland systems on the streamflow dynamics of the catchments. The drying and wetting cycles of individual wetland systems influenced both the baseflow connectivity as well as the overland flow during wetter periods. They are the key focus in understanding the connectivity between the hydropedological flow paths and the contribution of soil water to the stream networks of the three catchments.

## 5.1. INTRODUCTION

Understanding how catchments store and release water, and the resulting ecosystem services they provide is a crucial element in improving the management of these resources (Lazo et al. 2019). It has long been recognised that the role of soils is critical to these processes. The study of hydropedology, as an intertwined branch of soil science and hydrology, is used at multiple

scales to gain a better understanding of the variability of saturated and unsaturated surface and subsurface environments and how these influence rainfall-runoff processes (Lin et al. 2008). Hydropedology has therefore gained popularity in establishing the role of soils in the storage, flow dynamics and connectivity between hillslopes and streams of watersheds, thereby regulating the water cycle (Geris and Tetzlaff, 2015, Pinto et al. 2018).

Soils are three-dimensional bodies in the landscape, with different arrangements of vertical horizons and lateral variability of soil properties (Lin, 2012). Jarvis et al. (2007) showed that the quantity and type of soil macropores are variable across short distances, but spatial patterns of preferential flow at the landscape scale are far from being completely random. They instead show a clear pattern comprised of recognizable diagnostic soil horizons, soil materials, and pedons which all display characteristic flow and transport arrangements. Soil water processes can therefore be described in terms of content (volumetric or gravitational), potential (matric, osmotic, and gravitational potentials) and movement (subsurface flows in quantity or in speed). All of these descriptions are variable in time and space, creating multiple variations in the temporal structure of how precipitation moves through a landscape and is then discharged (Juez and Nadal-Romero, 2020).

Despite these variations in soil patterns, the range of specific soil types within a catchment is generally restricted based on location (Zhu et al. 2018). This distribution of different soil characteristics over a landscape is the key to connecting the pedon scale to the landscape scale (Lin et al. 2006, Lin et al, 2008). These soil patterns are expressed in the different soil forms identified within a catchment area. The periodicity of water movement through a soil causes distinct processes of oxidation and reduction. For example, the vertical and lateral percolation of water through a soil profile can cause the leaching out of iron and manganese, creating a unique set of characteristics that pertain to a particular soil form. In other areas, where there is excess water, soil forms are expressed by an accumulation of organic matter and/or a reduction process within the soil horizons. These specific morphological features in the soil profile are indicators of landscape processes including percolation, lateral flow, and water storage (Novak, 1986). These different types of flow paths within a catchment area may be isolated or connect the flow paths to a stream network (Zuecco et al. 2019). Thus, the characteristics of a soil profile can be utilised to gain an understanding of hydrological dynamics at landscape scale. A further contributing factor is soil thickness, as this is a key factor in the storage and redistribution of rainfall within the soil profile. It therefore plays an important role in

controlling the types of various runoff processes and is often a decisive factor in the processes that generate baseflow as well as overland flow (Fu et al. 2011).

In mountainous regions, changes within the landscape occur over short distances, and this creates a marked internal (i.e., subsurface) heterogeneity within soils, as well as heterogeneity in the catchment conditions. This makes it difficult to determine the direct measure of how much water is stored within particular areas of the catchment as well as the internal flow dynamics (Lazo et al. 2019). This is particularly so given the added interrelated influence of climate, geology, topography, and vegetation characteristics on the flow dynamics of these watersheds (Geris and Tetzlaff, 2015). The understanding of these processes is important as mountainous headwater catchments provide key water–related services for downstream ecosystems, and the regulation of streamflow by these catchments is highly influenced by their capacity to store and release water (Lazo et al. 2019). Recent studies have shown that the way in which water is stored and transferred within catchment areas is furthermore a crucial link in generating both base flows as well as storm flows during precipitation events as well as influences the sediment yield (Geris and Tetzlaff, 2015, Juez et al. 2021).

In South Africa, the uKhahlamba-Drakensberg Mountain range is one such area in which the spatial heterogeneity of catchments allows for the study of these various processes over a relatively short distance. Utilising this area, one can gain a deeper understanding in the way in which soil landscape functions control the movement of water in these areas and influence streamflow discharge. This is an initial and important component in understanding how streamflow discharge from these areas impacts on downstream ecosystems.

The aims of this chapter are therefore to gain an understanding of the hydropedological characteristics and flow dynamics of the soils of three mountain catchments, within the uKhahlamba-Drakensberg Mountain range. This is achieved through (1) interpreting hydropedological soil maps to conceptualize the hydrological functioning of the catchments in terms of dominant flowpaths and storage mechanisms and how these influence the streamflow dynamics and (2) to test the conceptual understanding of the hydropedological character of the catchment areas through a series of site-specific measurements taken within the catchment areas.

## 5.2. MATERIALS AND METHODS

### *5.2.1. Study Site*

Details of the study site are given in Chapter 3. The study period for this chapter was from September 2019 to June 2021. Table 5.1 displays the rainfall and streamflow dynamics during the study period.

Table 5.1.General details of the three catchment areas during the study period (adapted from Harrison et al. 2022)

| **Catchment Name** | **Rainfall dynamics during study period** | **Streamflow discharge dynamics during study period** |
|---|---|---|
| CP-III | Mean (mm) 4.34<br>Max (mm)<br>65.23<br>Min (mm)<br>0.00<br><br>Annual PCP<br>2019 – 1095 mm<br>2020 – 1572 mm<br>2021 – 1664 mm | Mean (mm): 2.33<br>Max (mm): 13.39<br>Min (mm): 0.22 |
| CP-VI | Mean PCP (mm) 3.62<br>Max PCP (mm)<br>65.28<br>Min (PCP) (mm)<br>0.00<br><br>Annual PCP<br>2019 – 829 mm<br>2020 – 1261 mm<br>2021 – 1472 mm | Mean (mm): 1.84<br>Max (mm): 18.90<br>Min (mm): 0.00 |
| CP-IX | Mean PCP (mm) 3.70<br>Max PCP (mm)<br>68.34<br>Min (PCP) (mm)<br>0.00<br><br>Annual PCP | Mean (mm): 1.28<br>Max (mm): 11.81<br>Min (mm): 0.09 |

| Catchment Name | Rainfall dynamics during study period | Streamflow discharge dynamics during study period |
|---|---|---|
| | 2019 – 884.94 mm<br>2020 – 1274 mm<br>2021 – 1378 mm | |

*5.2.2. Climate and hydrological monitoring*

The Cathedral Peak research catchments fall within the summer rainfall region of South Africa. The mean annual precipitation (MAP) for the area is approximately 1400 mm with a gradient of increasing rain between the south-eastern areas (which receive approximately 1300 mm) to the western areas (receive approximately 1700 mm). CP-III has a MAP of 1564 mm, CP-VI has a MAP of 1340 mm, and CP-IX has a MAP of 1257 mm [Toucher et al. 2016]. Rainfall is measured with tipping bucket rain gauges installed in the mid position of each of the catchments. Half of the rainfall events in the catchments are brought about by localised thunderstorms which fall during the spring and summer months (September to March), with occasional snowfall received during winter (May to August). The clouds forming these thunderstorms come from the west of the catchment areas. Orographic rainfall, produced from clouds forming in the east of the catchments, also create longer periods of softer rainfall which can fall for several days (Bosch, 1979, Nänni, 1956, Everson et al. 1998, Toucher et al. 2016). Mean monthly temperatures range from 17.1$^{O}$C to 10$^{O}$C with frost common in autumn and winter (April to August) (Bosch, 1979, Everson et al. 1998, Gordijn et al. 2018; Toucher et al. 2016).

Streamflow monitoring was initiated in the three catchment areas during the late 1940's and 1950's (Toucher et al., 2016). At the outlet of each catchment a concrete weir and stilling hut, with 90-degree V Notches were installed. These V Notches are 45.72 cm deep and are surmounted by 1.82 m wide rectangular notches of varying depth. Details of how early measurements were taken, error checked and processed are given in (Toucher et al., 2016). The water stage-height at each weir is currently monitored using an Orpheus Mini (Ott Hydromet GmbH, Germany) at CP-VI weir and a CS451 Stainless steel SDI-12 Pressure Transducers with CR200 loggers at weirs CP-III, CP-VI, and CP-IX (Toucher et al., 2016).

Catchment specific rainfall and streamflow data were therefore utilised for this study period (September 2019 to June 2021). However, in CP-III and CP-IX accidental fires, weir silting, and equipment problems have led to periods of missing streamflow discharge data. In CP-III there is no streamflow discharge data between February and November 2020, while in CP-IX there is no streamflow discharge data in October 2019 as well as between August and November 2020. These periods of missing data were removed from the database.

### *5.2.3. Hydropedology and soil mapping*

The development of hydropedology studies in South Africa has led to the classification of hydropedological soil types and how these are distributed down a hillslope catena (van Tol, 2020). A digital soil mapping exercise was undertaken for the three catchment areas utilising these hydropedological soil classifications (van Tol and Le Roux, 2019). The procedure used for the digital soil maps (DSMs), is detailed in Harrison and van Tol (2022) and is briefly described here. The soils of the three catchment areas were mapped and classified as per the South African classification system (Soil Working Group, 2018) and then regrouped into hydropedological soil types, namely, shallow recharge soils, deep recharge soils, interflow soils, and saturated responsive soils. The dominant properties of these soils are provided in Table 5.2.

Table 5.2.Dominant properties of the dominant hydropedological soil groups (Harrison and van Tol, 2022)

| **Hydropedological soil group** | **Characteristics of the soils** |
|---|---|
| Recharge Shallow | These are soils that are freely drained and do not show any indication of saturation. They are typically shallow in nature (<500mm). The freely drained B horizon merges with fractured rock or a lithic horizon. These soils typically occur on steeper convex slopes in the higher lying or steeper parts of the catchments. |
| Recharge Deep | These are soils that are freely drained and do not show any indication of saturation. They are typically deeper than the Recharge Shallow Soils (>500mm). The freely drained B horizon merges into fractured rock or a lithic horizon. These soils where identified throughout the catchments on gentler convex and concave slopes and away from wetlands and watercourses. |

| Hydropedological soil group | Characteristics of the soils |
|---|---|
| Interflow | These soils have a freely drained upper solum which overlies relatively impermeable bedrock. Hydromorphic properties are identified at this interface and signify periodic saturation associated with a water table. They typically occur on gentler concave slopes in areas delineated as wetlands as well as adjacent to watercourses. |
| Responsive Saturated | These soils display morphological indications of long-term saturation. They characteristically respond quickly to rainfall events and generate overland flow as they are typically close to saturation during the wet season and therefore any additional precipitation will flow overland due to saturation excess. These soils were identified in the valley bottom positions of the catchments, in permanently saturated wetlands. They typically occur on gentle concave slopes. |

The ArcSIE (Soil Inference Engine) version 10.2.105 was used to create the DSMs. A rules-based approach was first utilised based on knowledge of the catchments as well as the outcomes of the creation of Digital Terrain Models (DTMs) with the following environmental control variables applied to the rules: wetness index, slope, elevation, and planform curvature. The rules applied were aimed at producing the optimal relationships between soil type and a particular DTM (de Menezes et al. 2014, Zhu et al. 1997). The initial maps created following the rules-based approach were then validated based on the information gained during soil surveys undertaken within each of the catchment areas. The maps were refined according to the validation points taken during these surveys. The final hydropedological soil group maps are displayed in Figure 5.2. The performance of the ArcSIE interface to create the combined hydropedological maps for each of the catchments was analysed using the Kappa coefficient of agreement. The Kappa coefficient for CP-III is 0.57, for CP-VI is 0.59, and for CP-IX is 0.74, showing that there are some discrepancies between the hydropedological soil maps created and the site-specific soils identified within the catchment areas.

### *5.2.4. Dominant hydropedological soil groups of the catchments*

Comparison of the hydropedological soil group maps revealed that each catchment had a different percentage of the various hydropedological soil groups. This is based on the different topographies of the catchments as well as the various soil characteristics of each hydropedological soil group (Harrison and van Tol, 2022). Table 5.3 gives an indication of the dominant hydropedological soil groups in CP-III, CP-VI, and CP-IX.

Table 5.3.Percentage of the catchment area covered by each hydropedological soil group

| | **CP-III** | **CP-VI** | **CP-IX** |
|---|---|---|---|
| Hydropedological soil group | Percentage of catchment covered by each hydropedological soil group | | |
| Recharge Shallow | 18.3 | 17.1 | 27.6 |
| Recharge Deep | 43.3 | 33.8 | 38.4 |
| Interflow | 24.1 | 28.7 | 15.9 |
| Responsive Saturated | 14.3 | 20.4 | 18.1 |

As shown in Table 5.3, CP-III, CP-VI, and CP-IX are dominated by the recharge deep hydropedological soil group (43.3, 38.8 and 38.4 % of the catchment area respectively), followed by the interflow soil group in CP-III (24.1 %) and CP-VI (28.7 %), and the recharge shallow group in CP-IX (27.6 %). CP-VI has a greater area classified as responsive saturated soils (20.4 %) as compared to CP-III (14.3 %) and CP-IX (18.1%).

By utilising the hydropedological soil group maps as well as the dominant groups identified in each catchment, a theoretical interpretation of the various flowpaths for each catchment was identified and described.

### *5.2.5. Piezometer installations*

Piezometers were installed within the three catchments: six piezometers in CP-III, twelve in CP-VI, and nine in CP-IX. The piezometers were installed in clusters of two or three within a location, with this location chosen to represent the upper, mid, and lower portions of the catchments. Furthermore, the position of the piezometers was chosen within wetland and seepage areas of the catchments. In CP-III all piezometers were however installed in the lower sections of the catchment area, as a result of a lack of seepage areas within the upper portions of the catchment. This is due to the shallow nature of soils within the upper reaches of this catchment.

Soil profiles were dug using an extension Dutch auger to refusal, with signs of a gleyic or gley horizon noted within the profiles. These horizons display gleying and are considered indicators of the redox state of the soil. Gley horizons are recognised by low chroma grey matrix colours

which may contain blue or green tints. The gleyic horizon displays low chroma, grey and light-yellow colours, with the morphology of this horizon indicating less reduction and shorter duration of water saturation compared to the gley horizon (Soil Classification Working Group, 2018). A PVC pipe with slits cut around the end of the pipe to a height of 30 cm were then installed into the auger holes. The diameter of the PVC pipe utilised ensured a close fit with the hole. The piezometers were then capped, and measurements taken once a month between January 2019 to June 2021, however due to a drought within the region, the majority of piezometers only received water in September 2019 and thus this was chosen as the start point for comparison of water levels.

As a result of the drought conditions, some of the piezometers had to be discontinued, and thus, water was sampled and water heights were recorded each month in five piezometers in CP-III, seven piezometers in CP-VI, and seven piezometers in CP-IX (Figure 5.1). The height of the water within the piezometer was calculated from the surface of the soil to the depth of the water table.

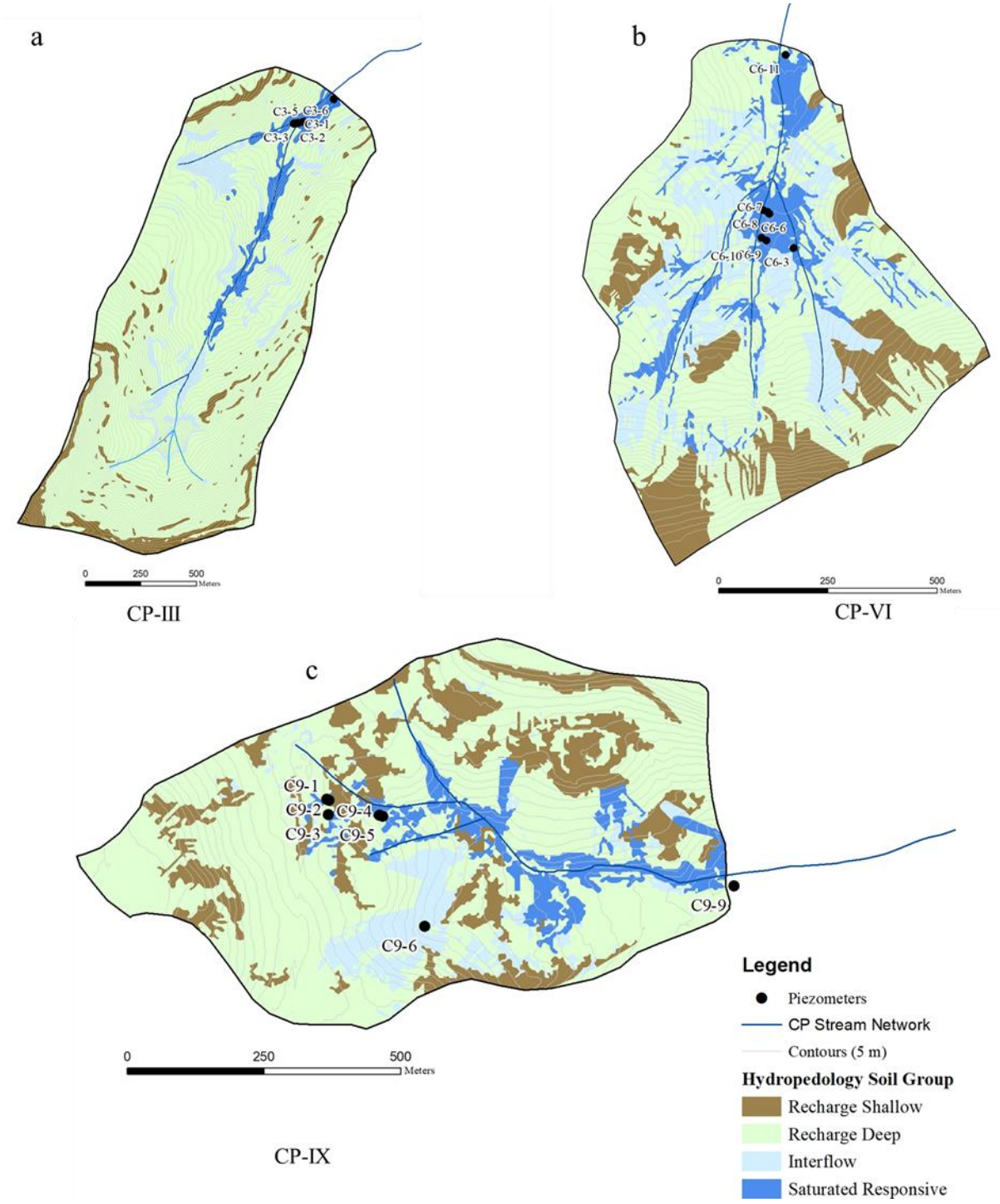


Figure 5.1: Location of the piezometers in relation to the hydropedological soil group in CP-III, CP-VI, and CP-IX

## 5.3. RESULTS AND DISCUSSION

### *5.3.1. Conceptual response based on hydropedological interpretations*

From the hydropedological soil maps created for each catchment, coupled with the descriptions of these dominant soil groups the principal hillslopes and flowpaths could be conceptually described. These conceptual descriptions were used as a working hypothesis of how the catchments' function. The conceptual descriptions are then evaluated against site-specific measurements.

When precipitation falls in the upper reaches of the three catchment areas it will enter the hydropedological recharge soil group. The dominant flow direction in recharge soils is the vertical flow of water through and out of the profile into the underlying bedrock. In the three catchment areas this hydropedological soil group is separated into the recharge shallow soils and the recharge deep soils. Recharge shallow soils occur in the steeper areas of the catchments, and this forms their shallow nature (<500 mm). In this soil group the freely drained B horizon merges with fractured rock or a lithic horizon. The recharge deep soils are similar to the recharge shallow soils, but the thickness of the profile is far greater (>500 mm). This is largely due to their position within gentler topographical areas of the catchments. Water that moves through these soils would recharge the deeper aquifers associated with the catchment areas, or if it encounters less permeable rock such as non-weathered and compacted sandstone or basaltic outcrops, it will flow laterally, and recharge shallow aquifers associated with seasonal hillslope seepage areas.

Interflow soils located downgradient of the recharge soils are associated with two dominant flow paths. Precipitation would first flow vertically through the free-draining upper profile of these soils before it encounters relatively impermeable bedrock. Hydromorphic properties have developed at this point in the soil profile, signifying periodic saturation associated with a water table. At this soil bedrock interface water will move laterally into the stream network or downgradient.

The responsive saturated soils are located in the permanently saturated wetlands of the catchment areas. These soils show morphological evidence of long periods of saturation such as a gleyed matrix as well as mottling. They are close to saturation, particularly during the wet

season and once saturated, and cannot attenuate any further water, will generate overland flow to the stream network.

From the hydropedological soil maps created for each catchment, the dominant hillslopes and flowpaths could be conceptually described. These conceptual descriptions were used as working hypothesis of how the catchments' function and then evaluated against measurements.

### *5.3.2. Precipitation and streamflow dynamics*

Precipitation data for CP-III, CP-VI, and CP-IX during the study period September 2019 to June 2021 showed that precipitation largely falls within the spring-summer months (September to March), with little to no rain within the autumn and winter months (April to August) (Figure 5.2). There is a decline in annual rainfall from CP-III to CP-VI to CP-IX. Furthermore, a greater quantity of precipitation was recorded in all three catchments for the spring-summer season of 2020-2021 (CP-III = 1492 mm, CP-VI = 1307 mm and CP-IX = 1045 mm) as compared to the same season within the preceding year (2019-2020) as a result of the drought conditions experienced in 2019 (CP-III = 1150 mm, CP-VI = 842 mm, and CP-IX = 771 mm).

Streamflow discharge values, like the precipitation values, were highest during the spring-summer months, and lowest during the autumn-winter months. Streamflow discharge for the study period also varied between catchment areas, with the greatest values obtained in CP-VI (ranged from 0.0 mm to 18.89 mm), followed by CP-III (ranged from 0.2 mm to 13.39 mm) and CP-IX (ranged from 0.0 mm to 11.81 mm).

The correlation between rainfall and streamflow values is non-linear, particularly during the drier period associated with the drought conditions in 2019 as well as the seasonal variations in the quantity of rainfall received. This is due to a lag time effect in the quantity of precipitation that falls in the catchment and the corresponding rise in streamflow value that is noticeable when comparing daily precipitation and daily streamflow discharge values within all three catchment areas over the study period. As shown in Figure 3, a lag time effect occurs in all three catchments from when a rainfall event occurs, to when there is a corresponding increase in streamflow discharge. This lag time differs depending on the pre-rainfall event hydrological conditions of the catchment. For example, following the end of the drought conditions experienced in the catchment areas in 2019, the first large rainfall event took place between 06/02/2020 and 11/02/2020 in which 153.67 mm fell into the CP-VI. Given the largely

desiccated conditions of the soils within CP-VI at the time, there is little effect of this rainfall event on the streamflow discharge values during the same time period (streamflow discharge has a combined value of 15.34 mm over the 5 days). No corresponding increase in streamflow discharge takes place during the time of the rainfall event as well as within the following month after the rainfall event. When a similar rainfall event took place in CP-VI but during the wetter season from 01/01/2021 to 06/01/2021, in which 138.94 mm of rain fell, there is a corresponding increase in streamflow discharge approximately 1 month after the event from 29/01/2021 to 04/02/2021 (streamflow discharge has a combined value of 65.34 mm for the time period).

In CP-IX a similar trend was noticed. Just after the drought of 2019, the same larger rainfall event between 06/02/2020 and 11/02/2020 in which 139.45 mm fell, had little effect on the streamflow discharge both at the time of the event as well as within the following month after the event. Again, the desiccated soils were becoming saturated before they could contribute to the streamflow. During the same rainfall event as in CP-VI, which occurred between 01/01/2021 to 06/01/2021, in which 136.91 mm of rain fell, there is a corresponding increase in the streamflow discharge approximately one month after the event, where the streamflow discharge has a combined value of 45.43 mm for the time period 29/01/2021 to 04/02/2021. Given the wetter time in which the storm event occurred, the soils in the catchment were already partially saturated, thus storm events which occurred during this time could lead to over-saturation of the wetlands, and the subsequent creation of overland and shallow subsurface flow, which contributed to the increase in streamflow discharge values.

Given the limited streamflow data available for CP-III, obtaining correlation examples between rainfall and streamflow discharge were not possible. However, a similar trend was noted in comparison to CP-VI and CP-IX, particularly in the time after the drought period. Following the drought period, a rainfall event occurred between 03/12/2019 and 06/12/2019 in which 69.08 mm of rain fell. Little effect on the streamflow discharge is observed during the event as well as within the following month after the event. The wetlands in this catchment were, like in CP-VI and CP-IX, becoming saturated again. However, unlike CP-VI and CP-IX, once the wetlands were saturated the corresponding rise in streamflow discharge values following a rainfall event responded at a much quicker rate. For example, a rainfall event takes place from the 28/12/2020 to the 15/01/2021. There is an immediate increase in streamflow discharge values both during the event and in the following days after the event, with the streamflow

values peaking (13.39 mm) on the 29/01/2021 following a 60.45 mm rainfall event the preceding day.

So, while the hydrological preconditions of the soil groups in all three catchments play a pivotal role in the storage and runoff dynamics of the catchment areas, in CP-III there is a far more immediate response in streamflow discharge following a rainfall event. This could be attributed to the topography of the catchment, the streamflow network or the shallower soils within this catchment, which have largely been created as a result of erosion brought about by the use of the catchment as a *Pinus patula* plantation.

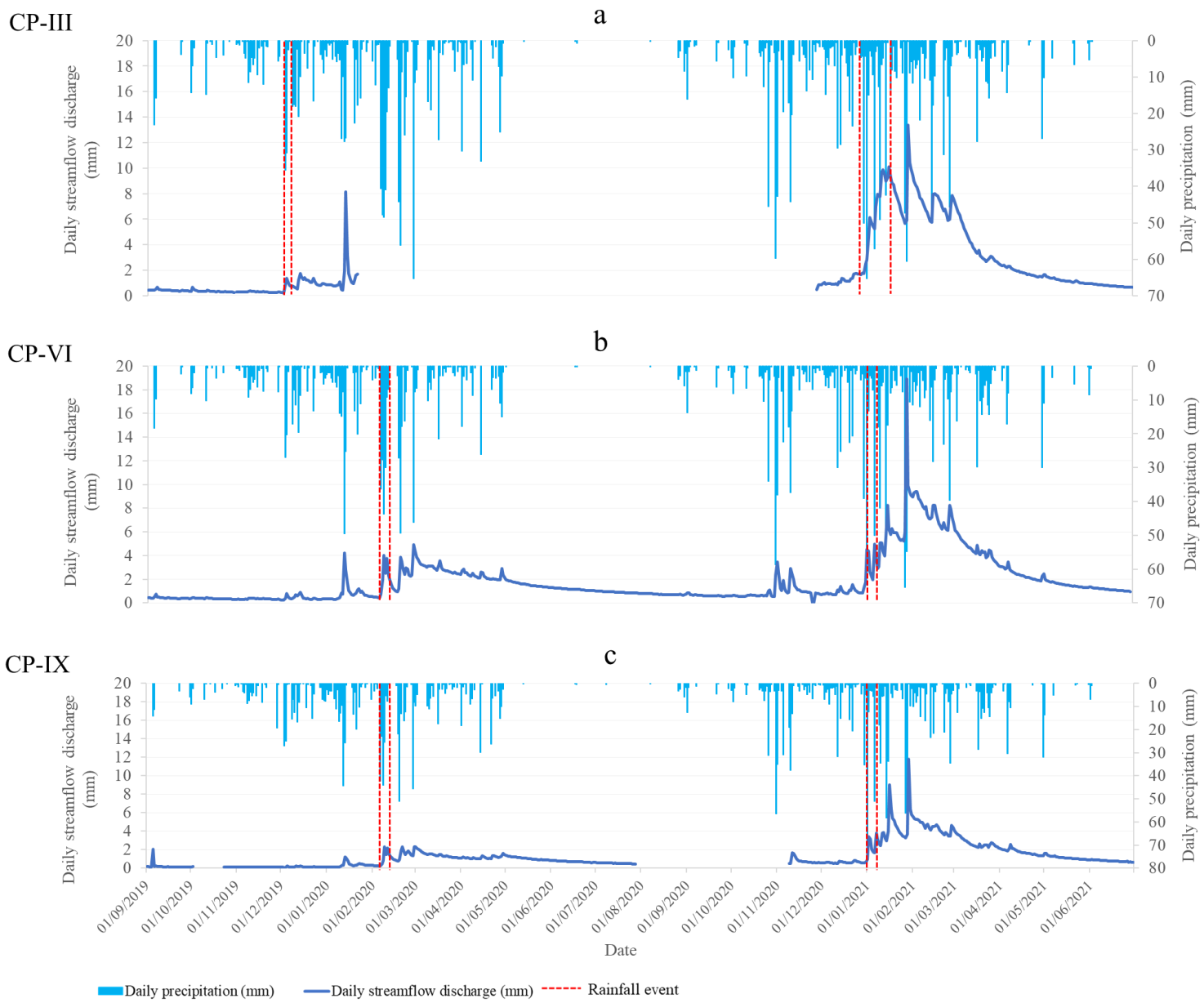


Figure 5.2: Depictions of the relationship between precipitation and streamflow discharge for CP-III, CP-VI, and CP-IX.

### *5.3.3. Piezometer data and flow paths*

The water table height within the areas where piezometers were installed varied throughout the study period and was dependent on the depth of the soil profile, the location of the piezometer within the catchment (i.e., the topographical position) as well as seasonal climatic variations. Average depths to the water table showed that, following the end of the drought conditions, the saturated responsive soils became saturated and remained so throughout the study period, while the depth to the water table within the interflow soil group showed greater variation, in all three catchment areas. The three catchment areas are explained in more detail in the following sections.

### *5.3.4. CP-III*

In CP-III, the average depth to the water table for the saturated responsive soil group, decreased from 530 mm, following the end of the drought in September 2019 to 70 mm in November 2019 and remained between 30 mm and 150 mm for the rest of the study period, depending on the seasonal variations in the rainfall received. In comparison the average depth to the water table for the interflow soil group, remained at a depth of 1200 mm until January 2020, where it decreased to 768 mm and then increased again to over 1000 mm during the dryer period of 2020 (March to September). Following the onset of the spring rains in October 2020, the average depth to the water table decreased to 900 mm where it fluctuated throughout the wetter summer period (between 800 mm and 1100 mm) depending on the rainfall received. With the onset of the drier autumn to winter period from April 2021 the depth to the water table increased again (1100 mm to 1200 mm) (Figure 5.3).

Individual piezometers followed a similar pattern to the average depth to the water table, with the piezometers located in the saturated responsive soil group, becoming saturated in December 2019, and remaining at or near saturation for the entire study period, depending on the seasonal rainfall received. This saturation level showed that when rainfall was received in the catchment, the wetland systems became over saturated and contributed more to overland and shallow subsurface flow toward the stream network (Figure 5.3). With regards to the piezometers installed in the interflow soil group, C3-2 and C3-3 (average water depth is 1051 mm and 985 mm respectively), which were situated higher in the catchment, received more water compared to C3-1 (average water depth of 1241 mm). C3-1 is situated in close proximity to the stream network. All three piezometer locations are associated with deep water table depths, and this could be attributed to this location contributing more to the baseflows of the stream discharge

values and not to overland flow. The more water in C3-2 (average depth of 1051 mm) and C3-3 (average depth of 985 mm) compared to C3-1 (average depth of 1241 mm), shows a down gradient flow path from the upslope recharge soil group, through the interflow soils, where the piezometers are located, and then laterally into the stream network.

Given the quicker rate in which the streamflow discharge values responded to rainfall events, particularly once the wetland systems were saturated, and taking into account the deep-water table depths of the interflow soils as well as the small size of the wetland systems in which the saturated responsive soil piezometers were located, it is apparent that infiltration of rainfall does not occur on the recharge soils during larger rainfall events but that rather overland or shallow subsurface flow occurs and water reaches the streamflow network at a much quicker rate.. This is most likely as a result of erosion, particularly from the upper reaches of the catchment, and the resultant shallow nature of these recharge soils and therefore the reduced recharge properties that these soil profiles. Figure 5.4 shows a diagram of these flow paths during both the drier and wetter seasons.

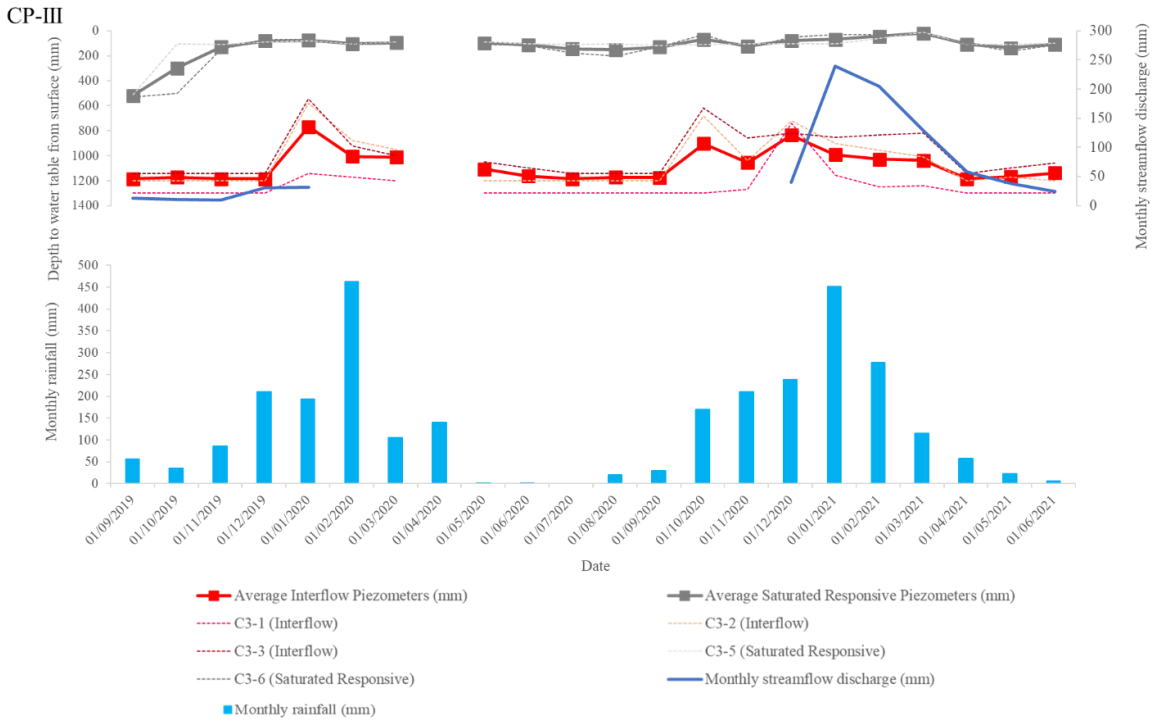


Figure 5.3: Comparisons of piezometer data installed in the interflow and saturated responsive soils in CP-III

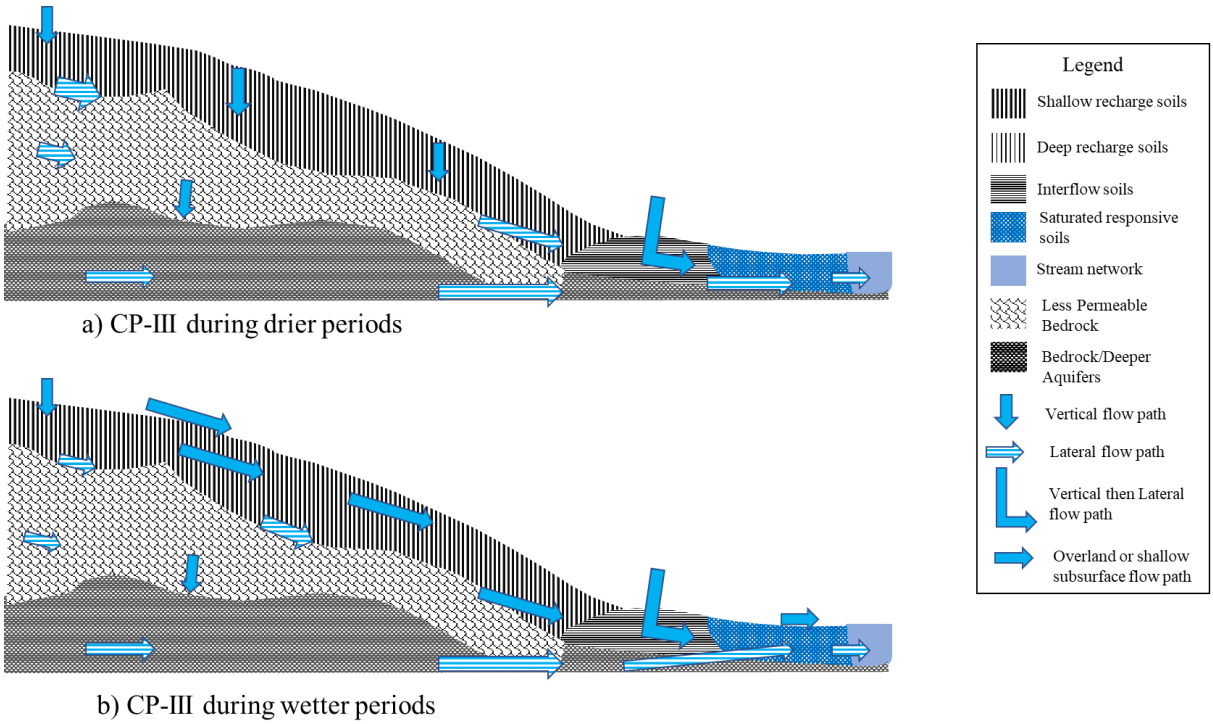


Figure 5.4: Flow path diagrams for a) the drier periods and b) wetter periods for CP-III

### *5.3.5. CP-VI*

In this catchment the average depth to the water table within the piezometers installed in the saturated responsive soils decreased from 720 mm in December 2019, following the onset of rains after the drought period, and fluctuated between 200 mm and 18 mm for the remainder of the study period. The average depth to the water table for the interflow soil group, fluctuated between 700 mm (December 2019) to 287 mm (December 2020). The average depth to the water table for the interflow soil group furthermore fluctuated depending on the rainfall conditions, with an increase in the depth during the drier autumn to winter months and a decrease in depth in the wetter spring to summer months (Figure 5.5).

As can be seen in Figure 5.5, each piezometer had a varied fluctuation in the depth to the water table, with some piezometers remaining more saturated compared to others. In the saturated responsive soil group, the C6-7 piezometer remained more saturated compared to the remaining piezometers in this group, particularly during the drought conditions. The C6-3, C6-9, and C6-10 piezometers which are situated higher in the catchment compared to the C6-7 piezometer, became far drier during the drought conditions. With the onset of rains, and the end of the drought period, these piezometers became saturated and then fluctuated slightly, depending on the seasons and associated rainfall conditions. Once saturated, during rainfall events, the

wetlands in which the piezometers were located would become over saturated and contribute to overland and shallow subsurface flow (Figure 5.6).

Individual piezometers in the interflow soil group also responded differently. Saturation content of the piezometers decreased from C6-8 to C6-6 to C6-11, with the C6-8 piezometer consistently more saturated than the C6-6 and C6-11 piezometers. This piezometer was situated in close proximity but outside of the permanently saturated areas of the C6-7 piezometer. The C6-6 piezometer was furthermore located on the edge of the same wetland system. The C6-11 piezometer was located at the lower end of the catchment, adjacent to the weir and remained drier throughout the study period in comparison to the other interflow piezometers.

These saturation levels of the piezometers show that the interflow soils largely contribute to the baseflow of the streams following a downgradient movement of water from the higher reaches of the catchment, before moving laterally into the stream network (Figure 5.6). During the drought, the wetland system located where the piezometers C6-6, C6-7, and C6-8 (average depth to water table from September 2019 to February 2020 was 436 mm) were installed, attenuated more water compared to other wetland systems (average depth to water table from September 2019 to February 2020 was 682 mm)within the catchment. Water moved downgradient from the upper reaches of the catchment and was attenuated within this wetland before moving further downgradient toward the outlet of the catchment area. This movement of water within the drier phase of the study period contributed to the baseflow of the stream network. Once the rains began, the wetland in which the C6-6, C6-7, and C6-8 piezometers were installed became wetter (average depth to water table increased to between 50 mm and 270 mm in January 2020) at a quicker rate than other wetlands within the catchment and started contributing to overland and shallow subsurface flow. The wetlands in which C6-3, C6-9, and C6-10 piezometers were installed became saturated in January/February 2020 (average depth to the water table increased to between 10 mm and 210 mm in February 2020) and then contributed to overland and shallow subsurface flow (Figure 5.6).

CP-VI

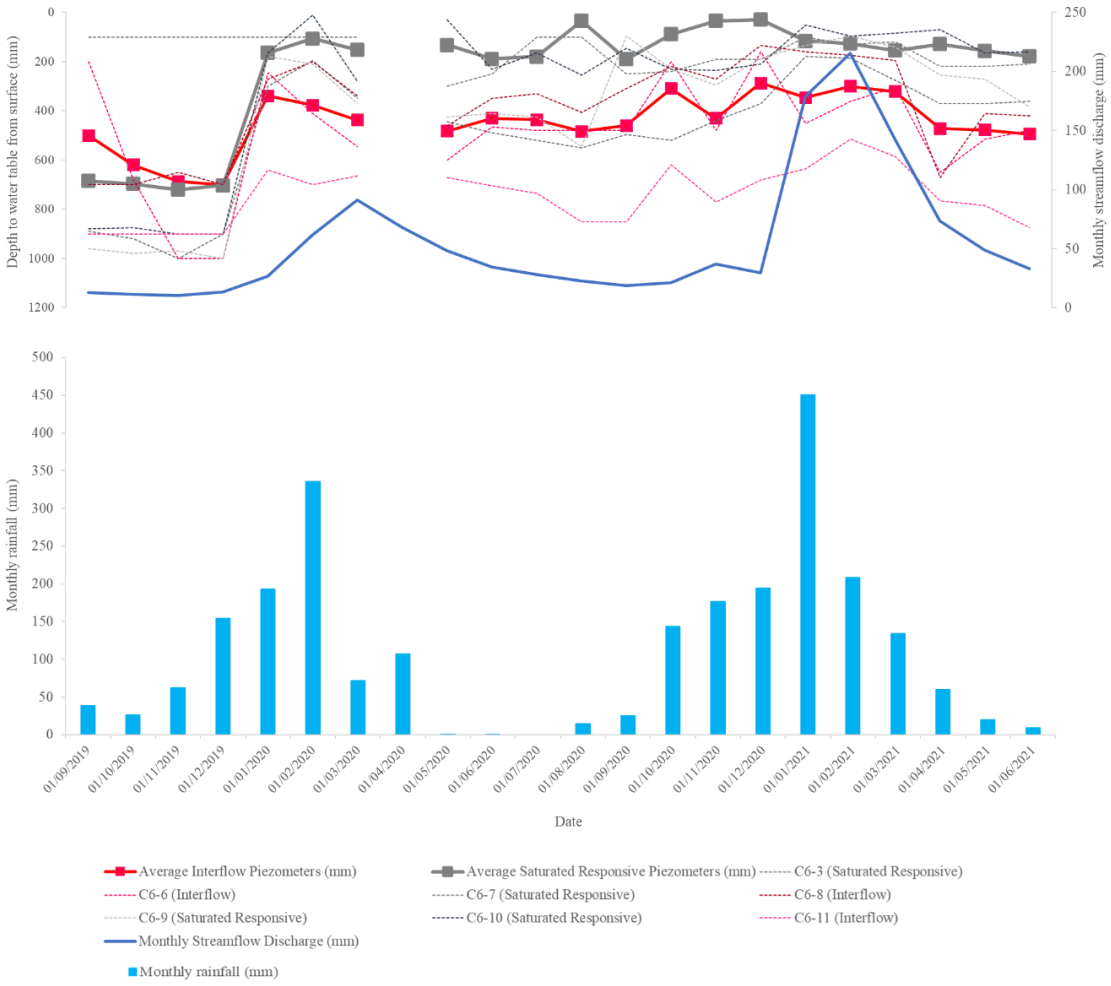


Figure 5.5: Comparisons of the data obtained from the various piezometers installed in both the interflow and saturated responsive soils as well as the monthly rainfall in CP-VI

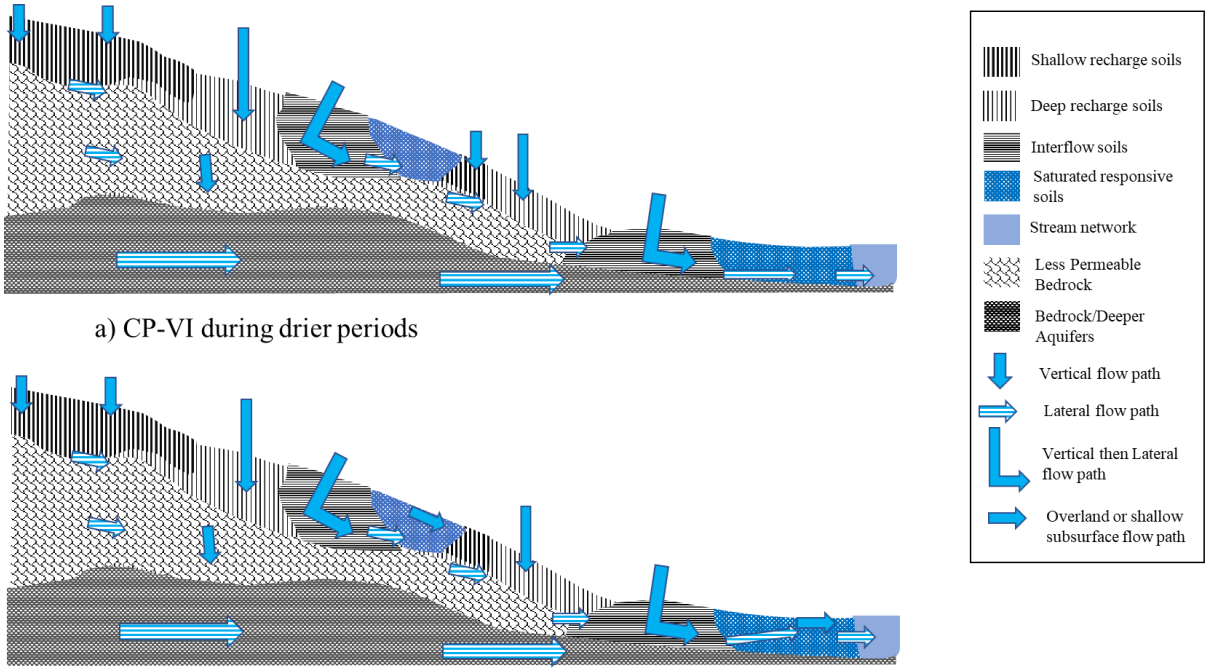


a) CP-VI during drier periods

b) CP-VI during wetter periods

Figure 5.6: Conceptual flow path diagrams for a) the drier periods and b) wetter periods for CP-VI

### *5.3.6. CP-IX*

In CP-IX the average depth to the water table for the saturated responsive soil group decreased from 487 mm to 102 mm following the onset of the rains by January 2020. The average depth to the water table then remained between 200 mm and 75 mm depending on the seasonal variation of rainfall received. The average depth to the water table for the piezometers installed in the interflow soil group also decreased following the onset of rains from 1000 mm in September 2019 to 326 mm in January 2020. The fluctuation of the average depth to the water table then also followed the seasonal variation in the rainfall received, but this variation was more pronounced in comparison to the saturated responsive soil group (depths ranged from 636 mm at the start of spring in October 2020 to 211 mm in February 2021) (Figure 5.7).

The depth to the water table was different in the individual piezometers. In the saturated responsive soil group, C9-3 remained more saturated, even during the drought conditions compared to the other piezometers (water table depth remained at 10 mm until January 2020), followed by C9-4 (water table depth fluctuated between 400 mm and 75 mm until January 2020). C9-5 and C9-9 dried out in comparison and became saturated again in January 2020

with a decrease in water table depth from 750 mm to 140 mm in C9-5 and a decrease from 630 mm to 185 mm in C9-9 (Figure 5.7).

Piezometers located in the interflow soil group had a greater depth to the water table during the drought conditions, with this depth decreasing following the onset of rains until they reached a peak depth in January and February 2020. The C9-1 and C9-2 piezometers (average water table depth of 330 mm and 460 mm respectively) which are situated higher up in the catchment remained more saturated compared to C9-6 (average water table depth of 797 mm) which is situated mid catchment.

As was the case in CP-III and CP-VI, the interflow soils contribute more to the lateral flow of water in the sub-horizons of the soil profile (average water table depth ranges from 1000 mm and the base flow of the streams within the catchment. The saturated responsive soils, which become saturated and remain so, contribute both to the baseflow of the streams as well as storm flow, in the form of overland and shallow subsurface flow once they become saturated. Figure 5.8 shows a diagram of these flow paths during both the drier and wetter seasons.

CP-IX

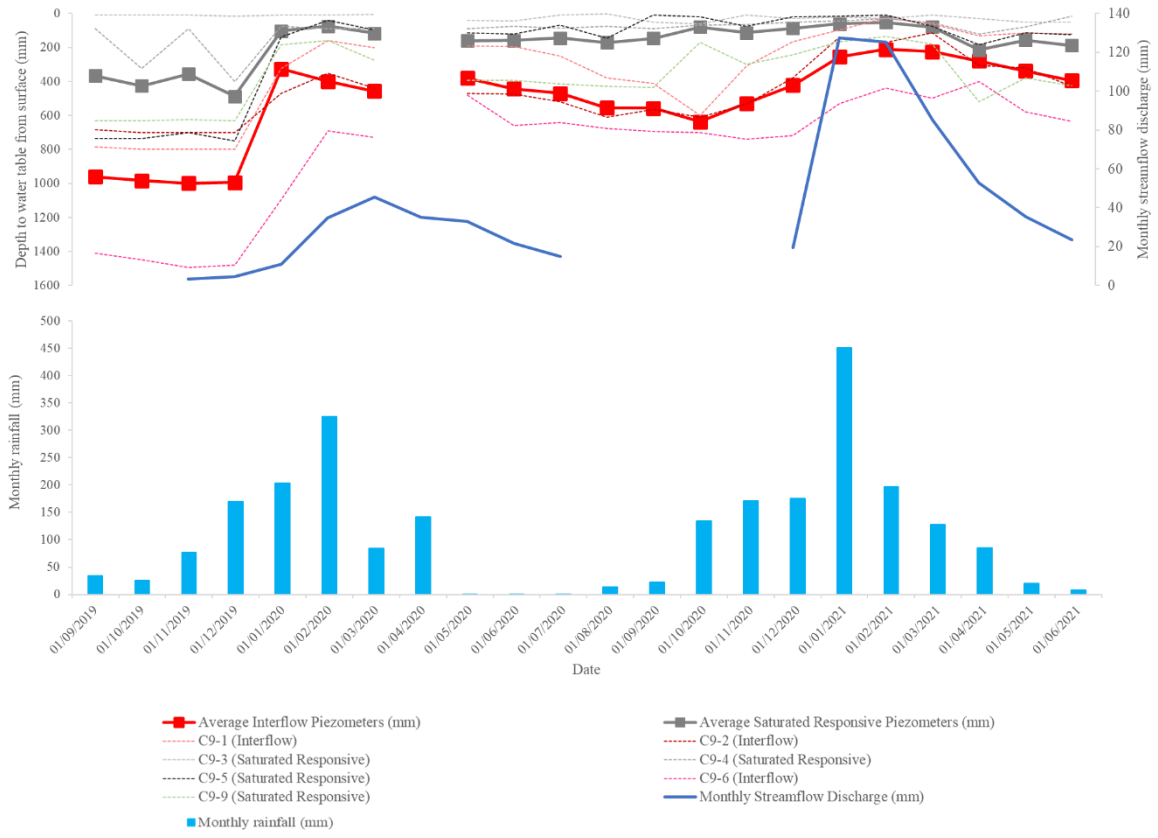

Figure 5.7: Comparisons of piezometer data installed in the interflow and saturated responsive soils in CP-IX

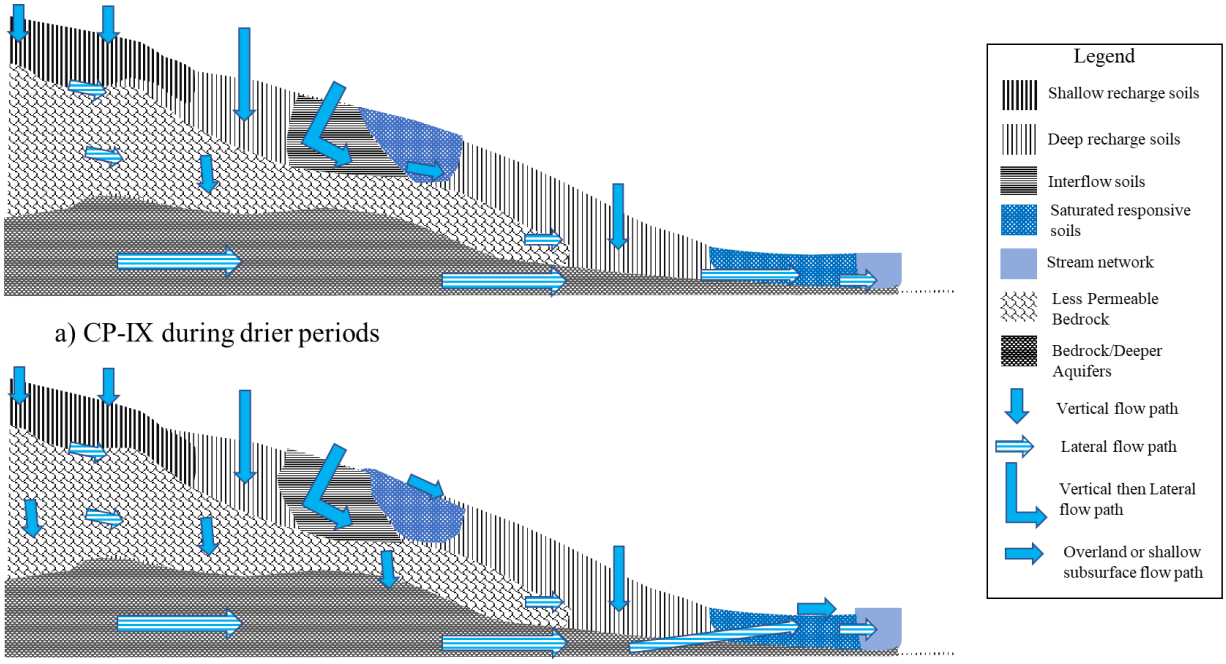


a) CP-IX during drier periods

b) CP-IX during wetter periods

Figure 5.8: Flow path diagrams for a) the drier periods and b) wetter periods for CP-IX

### *5.3.7. Catchment specific attributes affecting the hydropedological flow paths*

Data obtained from the climatic and hydrologic variables (rainfall and streamflow discharge) as well as the piezometers, shows that water moves through the soils of the catchment areas before contributing to the streamflow. The various hydropedological soil groups of the catchment area, which affect the flow rates of water through the catchment before it contributes to streamflow therefore play a pivotal role in the flow dynamics of the catchment areas.

These hydropedological soil groups were mapped following a digital soil mapping process, and while this allowed us to gain a general understanding of the dominant flow paths of these catchment areas, the more detailed investigation of the climatic, hydrologic and water table depth fluctuations have shown that the hydropedological characteristics of the catchment areas are both specific to the catchment and are created as a result of various interrelated factors.

The various interactions between the flow dynamics of the hydropedological soil groups of an area and how they become disconnected and reconnected to each other during drying and wetting cycles is unique to the various landscapes in which the flow paths are situated. A number of studies have been conducted in a variety of landscapes (D'Amore et al. 2012,

MacEwan et al. 2012, Zuecco et al. 2019). However, studies conducted in mountainous landscapes highlight the effect of the lower reaches of catchment areas continuously receiving water from the steeper surrounding hillslopes and these flow dynamics contributing to the baseflow of streams. During the wetter periods, the connectivity between the various hydropedological soil groups becomes more established and this allows for the generation of greater overland and shallow subsurface fluxes of water, particularly during larger rainfall events. These flows contribute to peaks within the streamflow hydrographs during storm events (van Tol et al. 2010, Tetzlaff et al. 2014, Blumstock et al. 2016, Pinto et al. 2018).

The connectivity between the hydropedological soil groups is furthermore influenced by the topography of the mountain catchments. In CP-VI for example, the wetland, in which the C6-6, C6-7, and C6-8 piezometers were installed, and that remained more saturated when compared to other wetland systems in the catchment, is situated in an area with a gentler slope as well as a concave landform. Various studies have shown similar findings, with catchment areas that have gentler terrain resulting in poorer drainage conditions and therefore the storage of higher volumes of water. Areas with steeper terrain increases the hydraulic gradients of the soils thus increasing the flow between the different hydropedological soil groups and reducing the storage capacity of these soils (Tetzlaff et al. 2014, Lazo et al. 2019). This influence of topography on the flow dynamics should be studied further within these research catchments.

A further effect on the hydropedological characteristics of the catchment areas is both the historic and current land management practices. The hydropedological dynamics of a site in a certain time is not the result of present processes and events but is related to and strongly influenced by the land use management history as well as the natural plant succession patterns (Gómez-Tagle, 2009).

In CP-III, the historic use of the area as a *Pinus patula* plantation and the subsequent lack of rehabilitation has led to a decrease in basal cover and erosion, particularly of the upper reaches of this catchment. This erosion has created shallower soils and therefore reduced the storage capacity and infiltration rates of the recharge hydropedological soil group. This reduced infiltration capacity has likely changed the flow dynamics of the catchment, compared to what would have been historically present, and this is evident in the quicker response of the streamflow discharge values following a rainfall event during the wetter periods of this study. The impact of erosion on the hydropedological characteristics of a catchment area has been

highlighted in other studies, with Pinto et al. (2016) identifying that soils with a degraded structure tend to have increased bulk density and consequently a decrease in soil porosity. This impacts on the water movement in the soil profile, having knock-on effects at the landscape scale. Fu et al. (2011) showed that rainfall infiltration into shallower soils, will reach the bedrock interface quickly and flow along this interface as preferential flow. The slope runoff from these areas will therefore appear to occur as subsurface stormflow (i.e., similar to overland flow) but occurring at the shallow soil/bedrock interface. In areas of thicker soil profiles, as is the case in CP-VI and CP-IX rainfall infiltration into the deeper recharge soils will supply the stream network largely as shallow groundwater and contribute more to the baseflow.

The erosion of the upper reaches has also led to deeper deposition areas within the lower reaches of CP-III. It is within these deposition areas that the interflow soil group piezometers were installed. When comparing the depth to the water table in all interflow soil group piezometers from the three catchment areas, CP-III has the deepest water table depths. This is due to the burying of the original soil profile by sediment which has been eroded from the top of the catchment and this has implications for the flow dynamics of this area of the catchment. Dikinya et al. (2006) showed that in areas of deposition, soil particles have been mixed and this causes changes in the pore structure of the soil matrix resulting in pore clogging and the reduction in the soil hydraulic capabilities. Thus, in these areas of CP-III, there is likely to be a slow reconnection of the subsurface flow paths following dry periods and these flow paths reconnecting to the stream network. This is shown in the fact that the interflow soil group piezometers located in the depositional areas did not have a substantial increase in water table depth throughout the study period in comparison to the interflow soil group piezometers in CP-VI and CP-IX and thus are likely to contribute slowly to the baseflow of the stream network and not to the stormflow peaks of the hydrograph of this catchment even following large rainfall events.

CP-VI is managed as a mesic grassland interspersed with wetland systems, while the fire exclusion since 1952 in CP-IX has led to this catchment becoming a woody dominated area. When comparing CP-VI and CP-IX fluctuations in the average water table depths of the saturated responsive soil groups show that in both catchments the wetland areas dried out to an extent during the drought period, and these became re-saturated in January/February 2020 and then remained saturated throughout the study period. The wetlands in both catchments contributed to shallow sub-surface flow and at times overland flow depending on rainfall

conditions. The average water table depth of the interflow soil group also followed similar patterns when comparing the two catchment areas. The effect of plant cover on the hydropedological characteristics of catchment areas has been reported in different environmental settings (Zimmerman et al. 2006, Zou et al. 2007, Gómez-Tagle, 2009, Zuecco et al. 2019), with these studies showing that woody cover areas have greater infiltration rates compared to pasture areas and that tree canopies can reduce the interception of rainfall within catchment areas, influencing infiltration rates within soils (Zou et al. 2007). These studies are conducted in commercial plantations, fallow pastures, and old wood forests. The results of this study, suggest that the flow dynamics of each catchment area not a product of land cover but are a factor of a combination of interrelated components.

The pivotal role that the wetland systems play in the streamflow dynamics of the catchment areas has been highlighted in this study. The drying and wetting cycles of individual wetland systems as well as specific saturation zones of these wetlands influenced both the baseflow connectivity as well as the overland flow during wetter periods. Furlan et al. (2020) identified similar findings utilising remote sensing techniques to show how a wetland system has different internal saturation compartments and how these both differ in saturation content depending on the climatic conditions as well as how they differ in providing lateral flow and overland flow to downgradient environments. Tetzlaff et al. (2014) furthermore utilised isotopes to show that baseflow within the stream network is predominantly from pre-event water (or dryer cycles) with larger rainfall events (particularly during the wetter cycles) displacing this water within the wetland systems and moving it as overland flow to the stream networks. The contribution of wetland systems to the stream network is therefore a heterogeneous and complex interaction of a both the soil physical properties, the climatic conditions, and the land management of an area. This has an impact on areas within the catchments classified as saturated responsive soils as these areas do not always contribute to overland flow, but rather the timing of their contribution to both baseflow and overland flow is specific to the wetland system, its location within the catchment, and climatic variables. Future isotopic studies within the Cathedral Peak research catchments are recommended to help gain a deeper understanding of flow dynamics from the wetland systems to the stream networks.

## 5.4. CONCLUSION

This study has highlighted the effects of climate, hydrologic conditions, land management and soil properties on the hydropedological characteristics of three montane catchment areas. The results suggest that a number of factors which are interrelated play a key role in determining the flow paths and the connection between flow paths in these areas. These factors are dominated by antecedent soil moisture, rainfall intensity, the duration of dry and wet periods as well as the depth of soil profiles.

The conceptual interpretation of the hydropedological flow paths of each catchment area following the creation of the digital soil maps, provided a general understanding of the flow paths and storage areas of these watersheds. However, utilising catchment specific climate and streamflow data, coupled with water table depth measurements as well as an understanding of how historic and current land management practices have influenced the soil properties, we were able to gain a more accurate interpretation of the response of each hydropedological soil group following a rainfall event. The dominant role of wetland systems and how these have drying and wetting cycles (the average water table depth ranged from 520 mm to 20 mm in CP-III, from 720 mm to 28 mm in CP-VI and from 487 mm to 51 mm in CP-IX) are the key focus in understanding the connectivity between the hydropedological flow paths and the contribution of soil water to the stream networks of the three catchments.

Given the importance of small mountain watersheds in maintaining water supplies to downgradient systems, the understanding of how streamflow is generated and maintained in these headwater catchments is of importance. This is particularly so in understanding the importance of the water storage capacity and water flux rate of the wetlands of the catchments in creating a buffering capacity against hydroclimatic variability which is becoming an ever-increasing reality (Blumstock et al. 2016). The health of the wetland systems in storing water during droughts, and their capacity to become saturated quickly and then contribute to the stream network is an important consideration in the ecological services these mountain headwater catchments provide.

## 5.5. REFERENCES

Blumstock, M., Tetzlaff, D., Dick, J. J., Nuetzmann, G., and Soulsby, C. (2016). Spatial organization of groundwater dynamics and streamflow response from different hydropedological units in a montane catchment. *Hydrological Processes.* 30. 3735– 3753. DOI:10.1002/hyp.10848.

Bosch, JM. (1979). Treatment effects on annual and dry period streamflow at Cathedral Peak. South African Forestry Journal, 108(1): 29-38.

Everson, C.E., Molefe, G.L., and Everson, T.M. (1998). Monitoring and modelling components of the water balance in a grassland catchment in the summer rainfall area of South Africa. Water Research Commission. RSA. Report 493/1/98.

D'Amore, D.V., Fellman, J.B. Edwards, R.T., Hood, E.W., and Ping. C.L. (2012). Hydropedology of the North American coastal temperate rainforest. In: H. Lin, editor, Hydropedology: Synergistic integration of soil science and hydrology. Academic Press, Waltham, MA.

de Menezes, M.D., Silva, S.H.G., Owens, P.R., and Curi, N. (2014). Solum depth spatial prediction comparing conventional with knowledge-based digital soil mapping approaches. Scientia Agricola. Vol. 71. No. 4. doi.org/10.1590/0103-9016-2013-0416.

Dikinya, O., Hinz, C., and Aylmore, G. (2006). Dispersion and re-deposition of fine particles and their effects on saturated hydraulic conductivity. Australian Journal of Soil Research. 44. DOI:10.1071/SR05067.

Fu, Z., Li, Z., Cai, C., Shi, Z-H., Xu, Q., and Wang, X. (2011). Soil thickness effect on hydrological and erosion characteristics under sloping lands: A hydropedological perspective. Geoderma. 167. 41-53. DOI:10.1016/j.geoderma.2011.08.013.

Furlan, L.M., Rosolen, V., Salles, J., Moreira, C.A., Ferreira, M.E., Bueno, G.T., de Sousa Coelho, C.V., and Mounier, S. (2020). Natural superficial water storage and aquifer recharge assessment in Brazilian savanna wetland using unmanned aerial vehicle and geophysical survey. Journal of Unmanned Vehicle Systems. 8. 3. 224-244. DOI:10.1139/juvs-2020-0004.

Geris, J. and Tetzlaff, D. (2015). Resistance and resilience to droughts: Hydropedological controls on catchment storage and run-off response. Hydrological Processes. 29. 4579–4593. DOI: 10.1002/hyp.10480.

Gómez-Tagle, A. (2009). Linking hydropedology and ecosystem services: Differential controls of surface field saturated hydraulic conductivity in a volcanic setting in central Mexico. Hydrology and Earth System Sciences Discussions. 6. DOI:10.5194/hessd-6-2499-2009.

Gordijn, P.J., Everson, T.M., and O'Connor, T.G. (2018). Resistance of Drakensberg grasslands to compositional change depends on the influence of fire-return interval and grassland structure on richness and spatial turnover. Perspectives in Plant Ecology, Evolution and Systematics. 34. 26-36. https://doi.org/10.1016/j.ppees.2018.07.005.

Granados, M.E., Vilagrosa, A., Chirino, E., and Vallejo, R. (2016). Reforestation with resprouter species to increase diversity and resilience in Mediterranean pine forests. Forest Ecology and Management. 362. 231-240. 10.1016/j.foreco.2015.12.020.

Harrison, R., and van Tol, J. (2022). Digital Soil Mapping for Hydropedological Purposes of the Cathedral Peak Research Catchments, South Africa. In: Adelabu, S., Ramoelo, A., Olusola, A., Adagbasa, E. (eds) Remote Sensing of African Mountains. Springer, Cham. https://doi.org/10.1007/978-3-031-04855-5_10.

Jarvis, N.J. (2007). A review of non-equilibrium water flow and solute transport in soil macropores: Principles, controlling factors and consequences for water quality, European Journal of Soil Science. 58. 523–546. DOI:10.0111/j.1365-2389.2007.00915.x.

Juez, C., Nadal-Romero, E., Cammeraat, E., and Regüés, D. (2021). Spatial and temporal variability of water table dynamics in an afforested catchment of the Central Spanish Pyrenees. Hydrological Processes. 35. DOI:10.1002/hyp.14311.

Juez, C., and Nadal-Romero E. (2020). Long-term time-scale bonds between discharge regime and catchment specific landscape traits in the Spanish Pyrenees. Environ Res. 191. 110158. doi:10.1016/j.envres.2020.110158.

Lazo, P., Mosquera, G., McDonnell, J., and Crespo, P. (2019). The role of vegetation, soils, and precipitation on water storage and hydrological services in Andean Páramo catchments. Journal of Hydrology. 572. 805-819. DOI:10.1016/j.jhydrol.2019.03.050.

Lin H. (2006) Temporal stability of soil moisture spatial pattern and subsurface preferential flow pathways in the Shale Hills Catchment. Vadose Zone Journal. 5. 317–340.

Lin, H. (2012). Hydropedology Synergistic Integration of Soil Science and Hydrology. Academic Press. USA.

Lin, H., Brooks, E., Mcdaniel, P., and Boll, J. (2008). Hydropedology and Surface/Subsurface Runoff Processes. In: Encyclopedia of Hydrological Sciences. DOI:10.1002/0470848944.hsa306.

MacEwan, R., Dahlhaus, P., and Fawcett, J. (2012). Hydropedology, Geomorphology, and Groundwater Processes in Land Degradation: Case Studies in South West Victoria, Australia. Hydropedology. 449-481. In: H. Lin, editor, Hydropedology: Synergistic integration of soil science and hydrology. Academic Press, Waltham, MA. DOI:10.1016/B978-0-12-386941-8.00014-9.

Mucina, L., Rutherford, M.C. & Powrie, L.W. (eds). (2006). Vegetation Map of South Africa, Lesotho and Swaziland. Edn. 2. South African National Biodiversity Institute, Pretoria. ISBN 978-1-919976-42-6.

Nänni, U.W. (1956). Forest Hydrological Research at the Cathedral Peak Research Station. Journal of the South African Forestry Association 27(1). 2-35.

Novak, P. (1986). Soil Genetics in Hydropedological Survey in Mountain Areas. Soil Science Annual. 37. 215-223.

Pinto, L. C., de Mello, C.R., Owens, P.R., Norton, L.D., and Curi, N. (2016). Role of inceptisols in the hydrology of mountainous catchments in Southeastern Brazil. Journal of Hydrologic Engineering. DOI:/abs/10.1061/(ASCE)HE.1943-5584.0001275.

Pinto, L., de Mello, C., Darrell, N., Poggere, G., Owens, P., and Curi, N. (2018). A hydropedological approach to a mountainous Clayey Humic Dystrudept. *Scientia Agricola*. 75. 60-69. DOI:10.1061/(ASCE)HE.1943-5584.0001275.

Soil Classification Working Group. (2018). Soil Classification: A Natural and Anthropogenic System for South Africa. ARC-Institute for Soil, Climate and Water. Pretoria.

Tetzlaff, D., Birkel, C., Dick, J., Geris, J., and Soulsby, C. (2014), Storage dynamics in hydropedological units control hillslope connectivity, runoff generation, and the evolution of

catchment transit time distributions. *Water Resources Research.* 50. 969– 985, DOI:10.1002/2013WR014147.

Toucher, M.L., Clulow, A., van Rensburg, S., Morris, F., Gray, B., Majozi, S., Everson, C.E., Jewitt, G.P.W., Taylor, M.A., Mfeka, S., and Lawrence, K. (2016). Establishment of a more robust observation network to improve understanding of global change in the sensitive and critical water supply area of the Drakensberg. 2236/1/16. Water Research Commission, Pretoria, South Africa.

van Tol, J. (2020). Hydropedology in South Africa: Advances, applications and research opportunities. South African Journal of Plant and Soil. 37. 1. 23-33. DOI:10.1080/02571862.2019.1640300.

van Tol, J.J., and Le Roux, P.A.L. (2019). Hydropedological grouping of South African soil forms. South African Journal of Plant and Soil. 36.3. 233-235. DOI: 10.1080/02571862.2018.1537012.

van Tol, J.J., Le Roux, P., Hensley, M., Lorentz, S.(2010). Soil as indicator of hillslope hydrological behaviour in the Weatherley Catchment, Eastern Cape, South Africa. Water S.A. 36. DOI:10.4314/wsa.v36i5.61985.

Zhu, A.X., Band, L., Vertessy, R., and Dutton, B. (1997). Derivation of soil properties using a soil land inference model (SoLIM). Soil Science Society of American Journal. 61. 523-533.

Zhu, Q., Castellano, M., and Yang, G. (2018). Coupling soil water processes and nitrogen cycle across spatial scales: Potentials, bottlenecks and solutions. Earth-Science Reviews. 187. DOI: 10.1016/j.earscirev.2018.10.005.

Zuecco, G., Rinderer, M., Penna, D., Borga, M., and van Meerveld, H.J. (2019). Quantification of subsurface hydrologic connectivity in four headwater catchments using graph theory. Science of The Total Environment. 646. 1265-1280. https://doi.org/10.1016/j.scitotenv.2018.07.269.

# CHAPTER 6 –USING HYDROPEDOLOGICAL CHARACTERISTICS TO IMPROVE MODELLING ACCURACY IN AFROMONTANE CATCHMENTS

Published as: Harrison, R.L., van Tol, J., and Toucher, L. (2022). Using hydropedological characteristics to improve modelling accuracy in Afromontane catchments. Journal of Hydrology: Regional Studies. 39. 100986. https://doi.org/10.1016/j.ejrh.2021.100986.

**Abstract**

Study Region

Three Afromontane catchments in the Cathedral Peak experimental research site, within the uKhahlamba-Drakensberg escarpment, KwaZulu-Natal, South Africa.

Study Focus

Gaining insight into the hydropedological behaviour of catchments enables a deeper understanding of the unique lateral flow dynamics of a landscape and how these affect the hydrological cycle. This study aimed to highlight the importance of understanding the hydropedological behaviour of soils to improve modelling accuracy.

New hydrological insights

Two sets of SWAT+ models were set up for each catchment. The default lateral time, which is the measure of the time required for water to flow through the catchment before being discharged into the stream, was used in the first set up. Specific lateral time inputs, derived from hydropedological soil maps, were utilised in the second model set up and the results compared against observed streamflow. The specific lateral time inputs were based on measured hydraulic properties of the soils coupled with the location of hydrological response units within hydropedological soil maps created for each catchment. The specific lateral time inputs improved modelling accuracy in all statistical parameters used, $R^2$ (i.e., 0.550 to 0.903), PBIAS (i.e., 19.742 to 18.239), ST DEV (i.e., 63.42 to 51.81), NSE (i.e., 0.316 to 0.864) and KGE (i.e., 0.630 to 0.807). This study has highlighted that relevant soil information, based on reliable site-specific data, is essential in hydrological modelling.

## 6.1. INTRODUCTION

One of the important components of addressing challenges related to water resource management is understanding the interaction between water resources and the soil profile (Kahmen et al. 2005, Smith, 2014, Wei et al. 2016, Zhang et al. 2015). This is because soil and water are the fundamental elements in understanding the hydrological response of catchments and therefore the way in which a catchment responds to different management regimes (Bouma, 2016).

In a catchment, each soil type is expected to have a unique influence on its hydrology (van Tol, et al. 2013) which also directly regulates soil water flows (Mamera and van Tol, 2018). Soils therefore play a crucial role in rainfall-runoff processes and constituent loading. Soil properties that relate to the rate of infiltration, or ability to store water, significantly affect the water balance in watersheds (Geroy et al. 2011, Krpec et al. 2020). These soil properties include texture, organic matter content, bulk density/porosity, hydraulic conductivity, and water retention characteristics. Some of these properties e.g., texture and organic matter, are easily measured and typically recorded during routine soil surveys. These properties are then used to predict those properties which are laborious and expensive to measure (e.g., water retention and hydraulic conductivity) through pedotransfer functions (Bouma, 1989; Vereecken et al.1992, Vereecken et al. 2016). Poor results in hydrological modelling are however produced when simulation models assume homogeneity in soil properties and particularly pedotransfer functions as these functions are only applicable in areas where they were developed (Bouma et al. 2011, Bouma, 2016). To reduce the uncertainty in model outputs, realistic site-specific input data are needed (Robinson et al. 2012).

Hydropedology is an interdisciplinary science, incorporating the concepts of pedology, soil physics, and hydrology to understand soil–water interactions at various scales (Lin, 2003, Lin et al. 2005, 2006). It can therefore provide a significant contribution to the better understanding of soil-water interactions in a specific landscape. Considering hydropedology in watershed modelling has the potential to improve accuracies as its approach is to partition rainfall into infiltration and runoff, thereby redistributing water in soils and landscapes (Bryant et al. 2006) and highlighting the effects of lateral flow on the streamflow dynamics of a landscape (Me et al. 2015).

Understanding the unique lateral flow dynamics of a landscape and how these strongly alter the flow patterns of water, is an important component in hydrological modelling (Bouma, 2006). This is due to runoff potential being influenced by soil properties such as depth to seasonal water table, saturated hydraulic conductivity, and depth to impermeable barriers. These properties determine the rate of infiltration during both dry periods and after prolonged wetting (Bryant et al. 2006, Neitsch et al. 2002), having an influence on the streamflow dynamics of catchment areas.

The KwaZulu-Natal Drakensberg is a mountain escarpment that forms the watershed between the interior catchments of Lesotho and the rivers in KwaZulu-Natal, thus enabling this province to contribute to a quarter of South Africa's streamflow (Nel, 2009, Whitmore, 1970). This escarpment is therefore crucial for runoff generation, and it is consequently classified as a strategic water source area (Le Maitre et al., 2018). The runoff generation from the montane catchments of the Drakensberg not only supplies KwaZulu-Natal's water needs but is important in maintaining the water requirements of the economic hub, Gauteng (Nel, 2009).

The main aim of this study was therefore to highlight the importance of understanding the hydropedological behaviour of soils within three Afromontane catchments of this escarpment to improve modelling accuracy. The hypothesis for this study tests that hydropedologic information is needed to understand how water moves through a watershed and model the length of time required for water to flow through the catchment as it dictates the partitioning of rainfall between runoff and infiltration. This is achieved through the following objectives: digital soil mapping of the hydropedological behaviour of the three catchments, utilising detailed soil data, particularly of the hydraulic properties of the soils, and using modelling to simulate a more accurate representation of the flow dynamics of the three catchment areas. Our aim was not to calibrate our SWAT+ models. According to Oreskes et al. (1994) the term calibration refers to the process of the manipulation of independent variables of the model to obtain a match between the simulated results and the observed results. It is therefore the process of adjusting model parameters so that the model is forced into particular margins. We did not aim to do this but rather we used the best available data for the catchments to set the models up and then improved the models with the use of detailed soil information in the form of specific lat_time information. We did not perform calibrations on any parameters of the model.

## 6.2. MATERIALS AND METHODS

### *6.2.1. Study area and collection of monitoring data*

Details of the study area as well as collection of monitoring data are given in Chapter 3. It must be noted that between 1987 and 2015, little to no data were collected in any of the three catchment areas due to funding constraints. Thus, this time period was excluded from the model runs. Furthermore, accidental fires, weir silting, and equipment problems has led to periods of missing data from 2016 to 2021 in CP-III and CP- IX.

### *6.2.2. Soil and Water Assessment Tool*

For this study, the Soil and Water Assessment Tool (SWAT) + version 1.2.2 with QSWAT version 3.10.9-A Coruña was utilised to set up the hydrological models. Model inputs include spatial information, terrain, climate, soil, and land-use. SWAT+ is an adjusted and more flexible version of SWAT (Arnold et al. 1998, Bieger et al. 2016), which is one of the most widely used hydrologic models in the world, being applied in many watersheds across the globe (Bieger et al. 2016). SWAT is a physically based semi-distributed hydrologic model operating on a daily time step to calculate runoff. SWAT+ combines land processes and land management with channel processes to create a more spatially represented outcome of the interactions and process within a watershed (Bieger et al. 2016), with improved runoff routing capabilities (Bieger et al. 2019, Kakarndee and Kositsakulchai, 2020). The SWAT+ model divides subbasins into water areas and landscape units (LSUs). The LSUs are then subdivided into Hydrological Response Units (HRUs), which are designated as separate spatial objects, with their hydrologic interaction, defined by the user. For example, an HRU can have an interaction with an aquifer as either overbank flow, lateral flow, or surface flow and this can be set by the user based on site specific details (Bailey et al. 2020).

### *6.2.3. Model inputs*

#### 6.2.3.1. Terrain, land-use, and climate

Data inputs for the SWAT+ model include a Digital Elevation Model (DEM), land cover information, climatic data as well as soil information. A 5 m resolution DEM (Ezemvelo KZN Wildlife et al. 2016) as well as the 2013-2014 SA land cover map information with a 30m resolution (Geoterraimage, 2015) were utilised. Given that the land cover of CP-III was plantations of *Pinus patula* until 1981, historic model runs of this catchment area utilised a separate land cover map, created to represent this more accurately. Weather data were obtained

from SAEON. Rainfall and temperature data have been recorded on a daily basis from 1950, with additional weather data (solar radiation, relative humidity, and wind speed) available from 2012 (Toucher et al. 2016). Rainfall data were obtained for each individual catchment, while the remaining weather data including temperature, relative humidity, wind speed and solar radiation were obtained from the Mikes Pass weather station (GPS Coordinates: 28°58'32.10"S; 29°14'8.83"E) located approximately 2km (CP-III), 4km (CP-VI), and 6km (CP-IX) from the catchments. While more site specific than utilising data from the global SWAT+ database, the use of weather data from the Mikes Pass weather station is seen as a limitation to the study as a result of the distance between catchments and this station.

#### 6.2.3.2. Soil Maps

The soil maps utilised in this study were created following a digital soil mapping exercise for the three catchment areas. The procedure used for the digital soil maps (DSMs), is detailed in Harrison and van Tol (2022) and is briefly described here. Soil maps of the three catchments were classified using the South African classification system (Soil Working Group, 2018) and then regrouped into hydropedological soil types, namely, shallow recharge soils, deep recharge soils, interflow soils, and saturated responsive soils, based on the classifications from van Tol and Le Roux, (2019). These groups of soils convey water differently and thus have different hydropedological behaviour. The ArcSIE (Soil Inference Engine) version 10.2.105 was used to create the DSMs. A rules-based approach was first utilised based on knowledge of the catchments as well as the outcomes of the creation of Digital Terrain Models (DTMs) with the following environmental control variables applied to the rules: wetness index, slope, elevation, and planform curvature. The rules applied were aimed at producing the optimal relationships between soil type and a particular DTM (de Menezes et al. 2014, Zhu et al. 1997). The initial maps created following the rules-based approach were then validated based on the information gained during soil surveys undertaken within each of the catchment areas. The maps were refined according to the validation points taken during these surveys. These final hydropedological soil group maps (Figure 6.1) were then utilised as the input maps for the SWAT+ model.

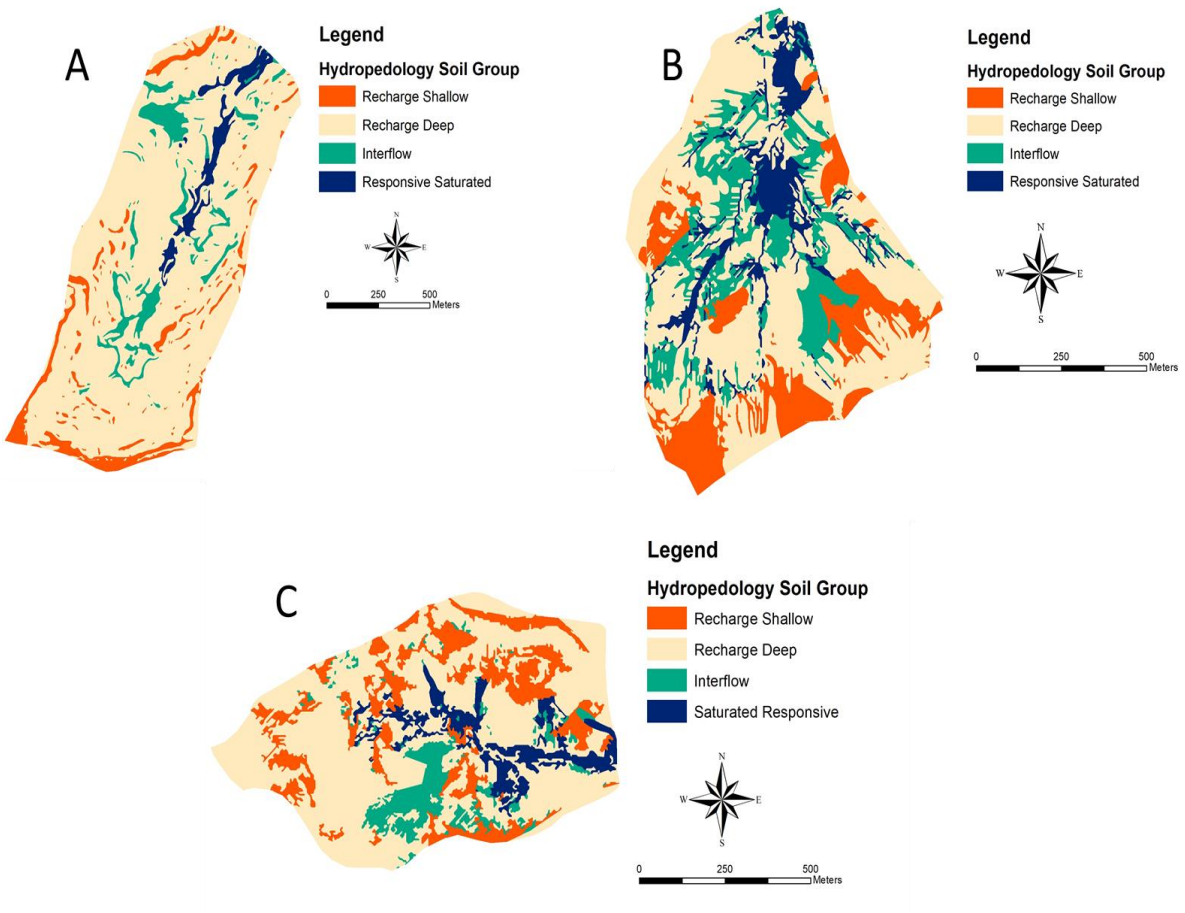


Figure 6.1: Hydropedological soil group maps utilised for the SWAT+ model for (A) CP-III, (B) CP-VI, and (C) CP-IX, adapted from Harrison and van Tol (2022)

6.2.3.3.Soil parameters

Detailed soil information was obtained from a combination of laboratory-based assessments for both particle size analysis utilising the pipette method (Gee and Bauder, 1986) and carbon analysis using the Leco element analyzer, (St. Joseph, Michigan) as well as the work by Kuenene et al. (2007). This work provided details on the bulk density (Bd) and available water capacity (AWC). Saturated hydraulic conductivity (Ks) was calculated was calculated with Rosetta, which is a plugin pedotransfer function available in HYDRUS-1D, version 4.17.0140 (Simunek et al. 2008) from the particle size analysis for the different horizons for each soil group.

Kuenene et al. (2011) utilised a combination of measured hydrograph and soil water content data to create drainage curves for the main soils associated with CP-VI. These drainage curves were created from measuring the soil water content at appropriate time intervals from a

saturated profile until the decrease in soil water content becomes negligible (Hensley et al. 1993). Soil water content was measured using neutron water meter access tubes for a period of four years, between 1991 and 1994, along a 200m transect in CP-VI. Over the four years approximately weekly soil water content measurements were made at 0.25 m depth intervals. Evapotranspiration values were then subtracted from the total change in soil water content to give the actual change in soil water content due to drainage. The volumetric water content versus time data is used to construct a drainage curve for the particular profile. This was undertaken in three separate profiles of the soils associated with CP-VI to represent deep soils (1800 mm), moderately deep soils (1600 mm) and shallow soils (1300 mm). The main components of the streamflow in CP-VI were identified to be attributed to overland flow and subsurface flow from the vadose zone. This information resulted in the formation of a series of time-steps (in days) that shows how water flows through the catchment and contributes to the streamflow. An example of a drainage curve produced by Kunene et al. (2011) is shown in Figure 6.2. Here the different phases, marked P1 to P6 of the hydrograph are displayed in relation to the time taken for water to move through the catchment.

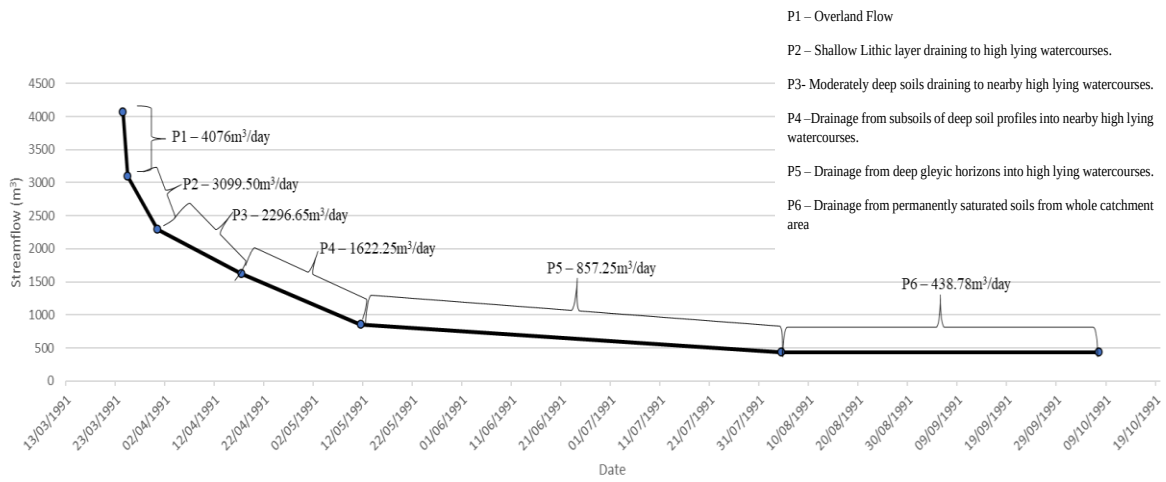


Figure 6.2: Hydrograph for CP-VI for the period 24/03/1991-07/10/91, together with the average flow rates per day during six phases, marked P1 to P6 (Kunene et al. 2011)

Utilising these results, along with the hydropedological soil group maps, it was hypothesized that the data obtained from the drainage curves formed in CP-VI could be transferred to the lateral time (lat_time) it takes for each hydropedological soil group to contribute to the streamflow. The lat_time is the flow time required for water to flow through the catchment before being discharged into the stream. Within SWAT+ the default value is set to 0 by default,

which allows the model to calculate the travel time based on the soil hydraulic properties input into the model (Neitsch et al. 2002).

Based on the information obtained from the drainage curves and subsequent identification of the travel time required for water to move through CP-VI and be discharged within the streamflow (Kunene et al. 2011), the lat_time input data were then manually specified within the model. This was undertaken to test the hypothesis that this information will improve the accuracy of the model simulations.

### *6.2.4. Model setup*

The model was configured individually for each of the three catchments. Once the individual models were created the phenology trigger for the plant communities was set as a moisture trigger for growth. Moisture was chosen as the growth trigger over temperature as a number of studies have highlighted that plant growth dynamics are mainly controlled by rainfall rather than temperature in sub-Saharan Africa (Alemayehu et al. 2017, Lotsch et al. 2003, Nkwasa et al. 2021). Furthermore, studies in CP-VI have identified that soil moisture and particularly subsurface flow are major contributors to the hydrology and overall ecological drivers of the catchment (Everson et al. 1998).

The model was initially configured and run using the default lat_time. Following this, a second run was conducted, where a specific lat_time was used, and all other parameters held constant. The specific lat_time inputs were based on the location of the HRU within the hydropedological soil group map which was used as one of the base maps for delineating the HRUs. Depending on the location of the HRU and the associated hydropedological soil group, a specific lat_time number was manually input into the model. These model runs were undertaken for two time periods as a result of the gap in data between 1987 and 2015. One run was therefore based on historic data and one run on current data. This was to establish whether the inclusion of specific lat_time values within the model improves the accuracy of the model both in the long term (historic period) and well as more short term (current period) data sets. For CP-III the time periods were 1957-1983 (historic) and then 2015-2021 (current), for CP-VI the time periods were 1962-1987 and then 2015-2021 and for CP-IX the time periods were 1957-1987 and then 2016-2021.

### *6.2.5. Model validation*

Observed streamflow data were obtained from SAEON. Both daily streamflow and the sum of the daily streamflow as a monthly timestep was utilised in comparisons with the simulated results. In a review of SWAT papers Gassman et al. (2014) showed that the majority of studies cite Moriasi et al. (2007) with regards to judging the success of their SWAT testing results. The strongest results of these papers are reported for the aggregated annual and monthly timesteps. However, Gassman et al. (2014) also noted that over half of these studies further report relatively strong daily timestep statistics. There is thus an increasing number of SWAT studies reporting successful testing at a daily timestep. The use of monthly and daily timesteps in this study was therefore to highlight the strong statistical results for an improvement in the modelling accuracy.

The performance of the simulated results compared with the observed streamflow was analysed using the Nash-Suttclife Efficiency (Nash and Sutcliffe, 1970), as well as the alternative metric, the Kling–Gupta Efficiency (KGE). The Nash-Suttclife Efficiency (NSE) indicates how well the plot of observed versus simulated data fits the 1:1 line. NSE ranges between -∞ and 1.0, with 1.0 being the optimal value. Values between 0.0 and 1.0 are generally viewed as being acceptable levels of performance (Knoben et al. 2019). The NSE is however sensitive to peak flows at the expense of a better performance during low flow conditions (Krause et al. 2005). The KGE was developed by Gupta et al. (2009) to address shortcomings in NSE and is increasingly utilised in model calibration and evaluation. However unlike in the NSE, there is no specific meaning attached to KGE = 0. The mean flow is therefore used as a KGE benchmark, and model simulations between $-0.41 < KGE < 1$ are considered as reasonable performance (Knoben et al. 2019).

The coefficient of determination ($R^2$), percent bias (PBIAS), and the percent difference in standard deviation (ST DEV) were additional criteria used for the performance evaluation. The PBIAS measures the average tendency of the simulated data to be larger or smaller than the observed data. The optimal value of PBIAS is 0.0, with positive numbers indicating an overestimation, and negative values indicating an underestimation of the model (Gupta et al. 1999).

Equations 1 to 3 were used to calculate the performance indices:

$$NSE = 1 - \left[\frac{\sum_{i=1}^{n}\left[Y_i^{obs} - Y_i^{sim}\right]^2}{\sum_{i=1}^{n}\left(Y_i^{obs} - Y_i^{mean}\right)^2}\right] \quad (1)$$

$$\mathrm{KGE} = 1 - \sqrt{(r-1)^2 + \left(\frac{\delta_{sim}}{\delta_{obs}} - 1\right)^2 + \left(\frac{\mu_{sim}}{\mu_{obs}} - 1\right)^2} \quad (2)$$

$$PBIAS = \left[\frac{\sum_{i=1}^{n}\left(Y_i^{obs} - Y_i^{sim}\right) * 100}{\sum_{i=1}^{\Pi}\left(Y_i^{obs}\right)}\right] \quad (3)$$

where $Y_i^{obs}$ is the ith observation for the evaluated model, $Y_i^{sim}$ is the ith simulation for the evaluated model, $Y_i^{mean}$ is the mean of the observed data for the evaluated model and $n$ is the total number of observations.

r is the linear correlation between observations and simulations, $\delta_{obs}$ is the standard deviation in observations, $\delta_{sim}$ the standard deviation in simulations, $\mu_{sim}$ the simulation mean, and $\mu_{obs}$the observation mean.

Graphical representations showing the comparison between the observed flow, default lat_time and specific lat_time simulations were created. A flow duration curve was created for each model run as an additional performance diagram for the models. The flow-duration curve is a cumulative frequency curve that shows the percent of time during which specified discharges (the observed streamflow of the catchments) were equalled or exceeded in a given period. Flow duration curves set up at a specific site have a key role to play in the knowledge of the streamflow characteristics at that site. This is due to the flow duration curves providing information on the flow variability of the water regime of a specific site during a specific period of interest (Ridolf et al. 2018). The flow duration curves show the improvement in the specific lat_time model runs in this study.

### *6.2.6. Sensitivity analysis*

Sensitivity analysis was conducted on the lat_time parameter in order to determine if this parameter contributes greatly to the model outputs (sensitive parameter) or if it has only minor

relevance (non-sensitive parameter) to the overall performance of the model simulations (Moreira et al. 2018). The model run for CP-VI current time period was chosen for the sensitivity analysis as the specific lat_time parameters were derived from the drainage curves created for this catchment. The value range for lat_time within the SWAT+ model is 0 to 180 days. An initial mean value of 65 days was utilised within the sensitivity analysis as CP-VI is largely dominated by HRUs within the hydropedological soil group with a lat_time of 65 days. Lenhart et al. 2002, calculates a sensitivity index, I, as a ratio between the relative change of the model output and the relative change of the parameter (lat_time input). A change of 25% of the entire lat_time range (0-180 days) was utilised. This method does not account for interactions among different parameters.

Sensitivity was calculated based on the equation by Lenhart et al. 2002:

$$I = \frac{(y_2 - y_1)/y_0}{2\Delta x/x_0}$$

in which I is the sensitivity index, $y_0$ is the model output calculated from the initial value ($x_0$), which in this case is 65 days. This initial parameter is varied by $\pm\Delta x$ (25%) yielding $x_1$ and $x_2$ with corresponding $y_1$ and $y_2$ values. The calculated sensitivity indices were ranked into four classes (Table 6.1) as per (Lenhart et al. 2002).

Table 6.1: Sensitivity classes (Lenhart et al. 2002)

| Class | Value Range | Sensitivity |
|---|---|---|
| I | 0.00-0.05 | Small to negligible |
| II | 0.05-0.20 | Medium sensitivity |
| III | 0.20-1.00 | High sensitivity |
| IV | >1.00 | Very High sensitivity |

## 6.3. RESULTS

### *6.3.1. Lateral time used in the model hypothesis*

The lateral times taken for each hydropedological soil group to contribute to the streamflow within CP-VI is displayed in Table 6.2. The same lateral times were applied to CP-III and CP-

IX as the soil forms and associated characteristics are similar in all three catchments studied. These times were input into each of the models set up for each of the three catchments based on the location of the HRU within the hydropedological soil group map.

Table 6.2: Lateral time required for water to move through each hydropedological soil group before it contributes to streamflow (adapted from Kunene et al. 2011)

| **Hydropedological Soil Group** | **Lateral Time (days) required for water to move through the hydropedological soil group as per the drainage curves from Kunene et al. (2011)** | **Dominant drainage processes and sources of water** |
|---|---|---|
| Recharge Shallow Soils | 6 | These are soils that are freely drained and do not show any indication of saturation. They are typically shallow in nature (<500mm). The freely drained B horizon merges with fractured rock or a lithic horizon. These soils typically occur on steeper convex slopes in the higher lying or steeper parts of the catchments. The recharge shallow soils drain rapidly into nearby drainage channels and wetlands. |
| Recharge Deep Soils | 24 | These are soils that are freely drained and do not show any indication of saturation. They are typically deeper than the Recharge Shallow Soils (>500mm). The freely drained B horizon merges into fractured rock or a lithic horizon. These soils where identified throughout the catchments on gentler convex and concave slopes and away from wetlands and watercourses. |

| **Hydropedological Soil Group** | **Lateral Time (days) required for water to move through the hydropedological soil group as per the drainage curves from Kunene et al. (2011)** | **Dominant drainage processes and sources of water** |
|---|---|---|
| | | Drainage from the vadose zone of the deep recharge soils flows into nearby drainage channels and wetlands |
| Interflow soils | 65 | These soils have a freely drained upper solum which overlies relatively impermeable bedrock. Hydromorphic properties are identified at this interface and signify periodic saturation associated with a water table. They typically occur on gentler concave slopes in areas delineated as wetlands as well as adjacent to watercourses. Drainage from the deep phreatic zone of the interflow soils flows into drainage channels and wetlands. The wetlands in all three catchment areas remain saturated throughout the year and are thus continuously fed through this drainage process. |
| Responsive Saturated | 85 | These soils display morphological indications of long-term saturation. These soils were identified in the valley bottom positions of the catchments, in permanently saturated wetlands. They typically occur on gentle concave slopes. Drainage from the responsive saturated soils flows through the wetlands and drainage channels. The wetlands in all three catchment areas remain saturated throughout the year and are thus |

| **Hydropedological Soil Group** | **Lateral Time (days) required for water to move through the hydropedological soil group as per the drainage curves from Kunene et al. (2011)** | **Dominant drainage processes and sources of water** |
|---|---|---|
| | | continuously fed through this drainage process as well as the interflow process. |

### *6.3.2. HRU and hydropedological soil group outputs*

Both model outputs in all three catchments had the same HRUs as the same input data were used in both model simulations with the exception of specific inputs in the lat_time. For CP-III the HRUs were 800, for CP-VI there were 717 HRUs and for CP-IX there were 712 HRUs created. Comparison of the HRUs with the hydropedological soil group maps revealed that each catchment had different number of HRUs in the four different hydropedological soil groups and this is based on the different topographies of the catchments as well as the various soil inputs and land covers. CP-III is dominated by the deep well drained soils of the Recharge Deep group, which take 24 days to convey water through the catchment before they contribute to streamflow. In CP-VI the specific lat_time taken for the soils to contribute to streamflow is dominated again by soils of the Recharge Deep hydropedological soil group followed closely by the Interflow soil group. In CP-IX, the Recharge Deep hydropedological soil group again dominates, but in this catchment Recharge Shallow soils follow a close second. The different flow dynamics of each soil type as well as the dominating hydropedological soil group therefore affects the streamflow dynamics of the individual catchment.

### *6.3.3. Model Outputs*

The SWAT+ model was first run in CP-VI as this catchment was utilised to create the drainage curves used to input the specific lat_time values for each hydropedological soil group. The models were run again with the same hypothesis used in CP-VI as similar soils and similar hydropedological recharge groups were identified in both CP-III and CP-IX. The model was run twice, with the integration of (1) the ‘default lat_time and (2) the specific lat_time (hydropedological data) incorporated into the model parameters. As stated previously data collection from the three catchments is patchy in some years and these have reduced the number

of observed and simulated data inputs in the statistical equations utilised. It has also led to gaps in the graphical representations of the simulated and observed flows.

### *6.3.4. CP-VI*

In CP-VI climatic and streamflow data from 01/01/1961 to 31/12/1987 (termed historic time period) and then from 01/01/2014 to 31/03/2021 (termed current time period) were utilised in separate runs of the model. Printed data from 1961 as well as 2014 were not utilised as this was regarded as a warm-up period for the models. Daggupati et al. (2015) explains why a comprehensive guideline for warm-up periods cannot be given due to the complexity of watershed-scale processes. They however recommend a warm-up period of one to four years with this being related to the temporal and spatial scale of the governing processes. Shorter warm-up periods are required when input values are measured as compared to estimated, the watershed is smaller in size, and the model is set-up to evaluate soil moisture processes as compared to groundwater processes. As this study is set in three small watersheds, is studying soil moisture processes and detailed information on the catchments has been input into the models, 1 year warm-up period was regarded as being sufficient.

Statistical results are presented in Table 6.3 for both daily and monthly time steps, with graphical representations of a 5-year period for the monthly comparisons as well as the flow duration curves displayed in Figure 6.3.

Table 6.3: SWAT+ model simulations for CP-VI for monthly data

| Time step of data | Dates of model run | Model simulation type | $R^2$ | PBIAS | NSE | KGE | ST DEV |
|---|---|---|---|---|---|---|---|
| Monthly | 01/01/1962 – 31/12/1987 | Default Simulation | 0.550 | 19.742 | 0.316 | 0.630 | 63.42 |
| | | Simulation with specific lat_time | 0.903 | 18.239 | 0.864 | 0.807 | 51.81 |
| | 01/01/2015-31/03/2021 | Default Simulation | 0.491 | 25.812 | -0.023 | 0.463 | 66.86 |
| | | Simulation with specific lat_time | 0.931 | 14.305 | 0.903 | 0.849 | 50.56 |
| Daily | 01/01/1962 – 31/12/1987 | Default Simulation | 0.418 | 19.743 | -0.541 | 0.283 | 3.16 |
| | | Simulation with specific lat_time | 0.836 | 19.542 | 0.802 | 0.835 | 1.73 |
| | 01/01/2015-31/03/2021 | Default Simulation | 0.428 | 25.912 | -0.630 | 0.216 | 3.04 |
| | | Simulation with specific lat_time | 0.744 | -21.485 | 0.597 | 0.681 | 2.19 |

In the historical 1962 to 1987 data, both the default simulation as well as the specific lat_time simulations show an overestimation of streamflow compared to the observed flow in all runs of the model with the exception of an underestimated flow in the specific lat_time simulated run for the daily time step 2015 to 2021. The overestimated runs however show an underestimation of the baseflows and overestimation of the peak flows in the original simulations, with these variations from the observed flows being less pronounced in the specific lat_time simulations (Figure 6.3). There was an improvement in the $R^2$, ST DEV, and NSE values in all specific lat_time simulations compared to the default simulations. The NSE values for the specific lat_time simulated runs are all categorised as ‘very good’ (>0.65) with the exception of the specific lat_time simulated run for the current time period which is

categorised as ‘adequate’ (0.54 to 0.65) as per the classifications by Moriasi et al. (2007). According to Knoben et al. (2019), KGE values between -0.41 and 1.0 are considered reasonable, and thus all simulated runs (original and lat_time runs) are classified as reasonable.

The flow duration curves created for the monthly time step for both the historical and current time period shows a marked improvement in the simulated lat_time model run versus the observed streamflow as compared to the default model run and the observed streamflow. This is particularly so in the current time period (Figure 6.3) and highlights the improvement in the accuracy of the model runs with the input of the specific lat_time.

### *6.3.5. CP-III*

In CP-III climatic data as well as streamflow data from 01/01/1957 to 31/12/1987 (termed historic time period) and then from 01/01/2015 to 31/03/2021 (termed current time period) were utilised in separate runs. Printed data from 1958 as well as 2015 were not utilised as these were regarded as warm-up periods for the model. Statistical results are presented for both daily and monthly time steps in Table 6.4, along with graphical representations of a 5-year period for the monthly comparisons as well as the flow duration curves displayed in Figure 6.4.

Table 6.4: Statistical results for the SWAT+ model simulations for CP-III

| Time step of data | Dates of model run | Model simulation type | $R^2$ | PBIAS | NSE | KGE | ST DEV |
|---|---|---|---|---|---|---|---|
| Monthly | 01/01/1958 - 31/12/1983 | Default Simulation | 0.529 | 3.300 | 0.474 | 0.723 | 49.99 |
| | | Simulation with specific lat_time | 0.785 | -1.381 | 0.767 | 0.730 | 39.32 |
| | 01/09/2016 - 31/03/2021 | Default Simulation | 0.681 | -4.994 | 0.569 | 0.760 | 64.29 |
| | | Simulation with specific lat_time | 0.867 | 1.251 | 0.866 | 0.891 | 50.96 |
| Daily | 01/01/1958 - 31/12/1983 | Default Simulation | 0.300 | 2.370 | -0.591 | 0.332 | 2.80 |
| | | Simulation with specific lat_time | 0.686 | 2.412 | 0.634 | 0.567 | 1.13 |
| | 10/09/2016 - 31/03/2021 | Default Simulation | 0.270 | 6.311 | -1.033 | 0.181 | 3.21 |
| | | Simulation with specific lat_time | 0.863 | 7.652 | 0.858 | 0.863 | 1.76 |

The historical time period for both the daily and monthly time step showed an underestimation of the simulated flows compared to the observed flows in both the default simulated and specific lat_time simulated runs. The current time period showed an overestimation of the default simulated and specific lat_time simulated model runs. In both time periods the graphical representation of the model runs shows an improvement in the simulation of baseflows as well as peak flows in the specific lat_time runs of the model, with the simulated data following the curves of the observed data more closely (Figure 6.4).

As with CP-VI there was an improvement in the $R^2$, ST DEV, and NSE values in all specific lat_time simulations compared to the default simulations for both time periods (historic and current) as well as for both time steps used. The NSE values for the specific lat_time simulated runs improved in all models from classifications of 'unsatisfactory' and 'satisfactory' (>0.5) to adequate (0.54 to 0.65) and 'very good' (0.65) in the specific lat_time simulations. The 'very good' classifications were obtained in the current time period for both the daily and monthly time step. However, the consideration of the disjointed input data for this current time period must be taken into consideration when comparing the historical and current time periods. All KGE values for all model runs are between -0.41 and 1.0 and are considered reasonable.

As with CP-VI the flow duration curves created for the monthly time step for both the historical and current time periods in CP-III show the improvement in the accuracy of the model with the input of the specific lat_time. Again, this is especially apparent in the current time period (Figure 6.4).

### *6.3.6. CP-IX*

In CP-IX climatic data as well as streamflow data from 01/02/1957 to 31/12/1987 and then from 01/01/2015 to 31/03/2021 were utilised in separate runs. Printed data from 1957 as well as 2015 was not utilised as these were regarded as warm-up periods for the models. Statistical results are presented for both daily and monthly time steps in Table 6.5, along with graphical representations of a 5-year period for the monthly comparisons as well as the flow duration curves displayed in Figure 6.5.

Table 6.5: Statistical results for the SWAT+ model simulations for CP-IX

| **Time step of data** | **Dates of model run** | **Model simulation type** | **$R^2$** | **PBIAS** | **NSE** | **KGE** | **ST DEV** |
|---|---|---|---|---|---|---|---|
| Monthly | 01/01/1958-31/12/1987 | Default Simulation | 0.611 | 4.801 | 0.123 | 0.598 | 57.83 |
| | | Simulation with specific lat_time | 0.888 | 7.809 | 0.843 | 0.844 | 44.29 |

| Time step of data | Dates of model run | Model simulation type | $R^2$ | PBIAS | NSE | KGE | ST DEV |
|---|---|---|---|---|---|---|---|
| | 01/09/2016 - 31/03/2021 | Default Simulation | 0.678 | -11.344 | -0.063 | 0.291 | 50.07 |
| | | Simulation with specific lat_time | 0.904 | -7.173 | 0.803 | 0.723 | 37.69 |
| Daily | 01/01/1958- 31/12/1987 | Default Simulation | 0.344 | 5.216 | -1.373 | 0.012 | 2.89 |
| | | Simulation with specific lat_time | 0.725 | -51.023 | 0.327 | 0.416 | 1.89 |
| | 02/09/2016 - 31/03/2021 | Default Simulation | 0.424 | -8.421 | -1.826 | -0.205 | 2.42 |
| | | Simulation with specific lat_time | 0.840 | -5.564 | 0.753 | 0.770 | 1.36 |

The historical time period for the monthly time step showed an overestimation of the simulated flows compared to the observed flows in both the default simulated and specific lat_time simulated runs. The remaining model runs (monthly current time period as well as daily historical and current time periods) showed an underestimation of the default simulated and specific lat_time simulated model runs. As is the case in CP-III, the graphical representation of the model runs shows an improvement in both time periods in the specific lat_time simulation of baseflows as well as peak flows, with the simulated data following the curves of the observed data more closely when compared to the default simulated flow (Figure 6.5).

As with CP-VI and CP-III there was an improvement in the $R^2$, ST DEV, and NSE values in all specific lat_time simulations compared to the default simulations for both time periods as well as for both time steps used. The NSE values for the specific lat_time simulated runs are categorised as ‘very good’ (>0.65) for both monthly time step periods as well as the current time period daily time step model run. The historical time period daily time step run is categorised as ‘satisfactory’ (>0.5). All KGE values for all model runs are between -0.41 and

1.0 and are considered reasonable, with the exception of the default simulated run (-0.205) for the current time period daily time step. The KGE values improve with the specific lat_time run for the same time period (0.770) and are classified as reasonable.

As with CP-VI, and CP-III the flow duration curves created for the monthly time step for both the historical and current time periods in CP-IX show the improvement in the accuracy of the model with a comparison of the default lat_time versus the specific lat_time compared to the observed streamflow. This is apparent in both the historic and current time periods (Figure 6.5).

A

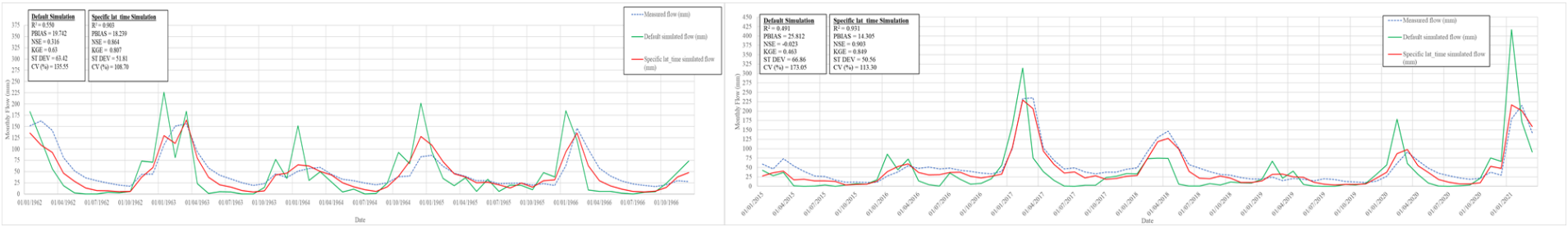


B

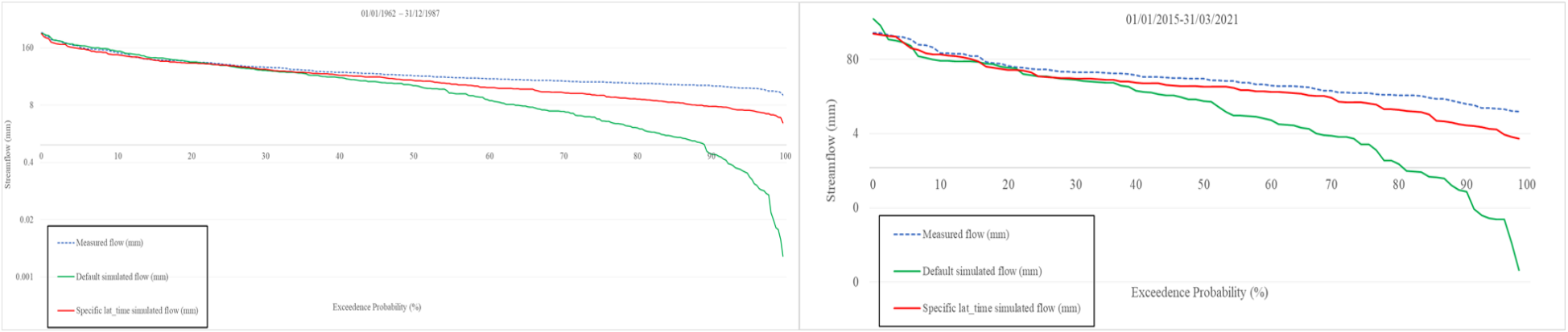


Figure 6.3: (A) Graphical representations of the monthly comparisons between the default simulated flow as well as the specific lat_time simulated flow and the observed flow for a 5-year period within the two time periods for CP-IV, and (B) Flow duration curves for the monthly data for the two time periods for CP-VI

A

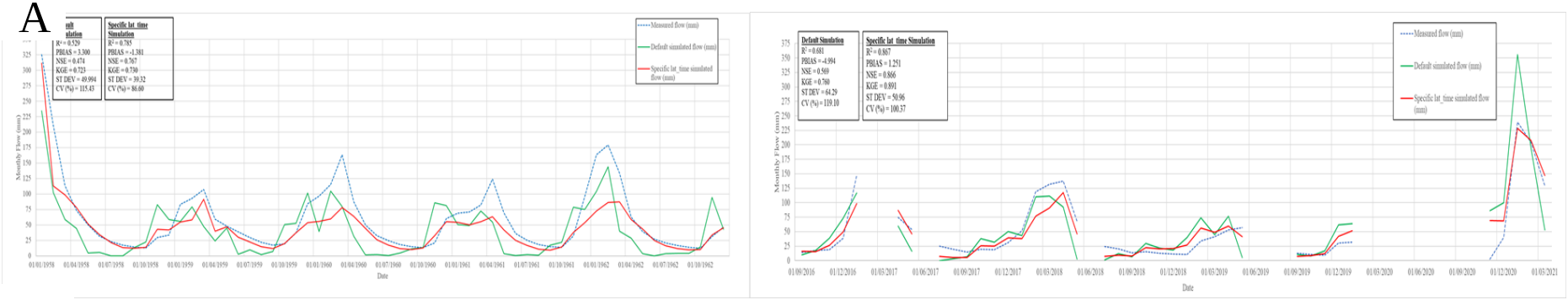


B

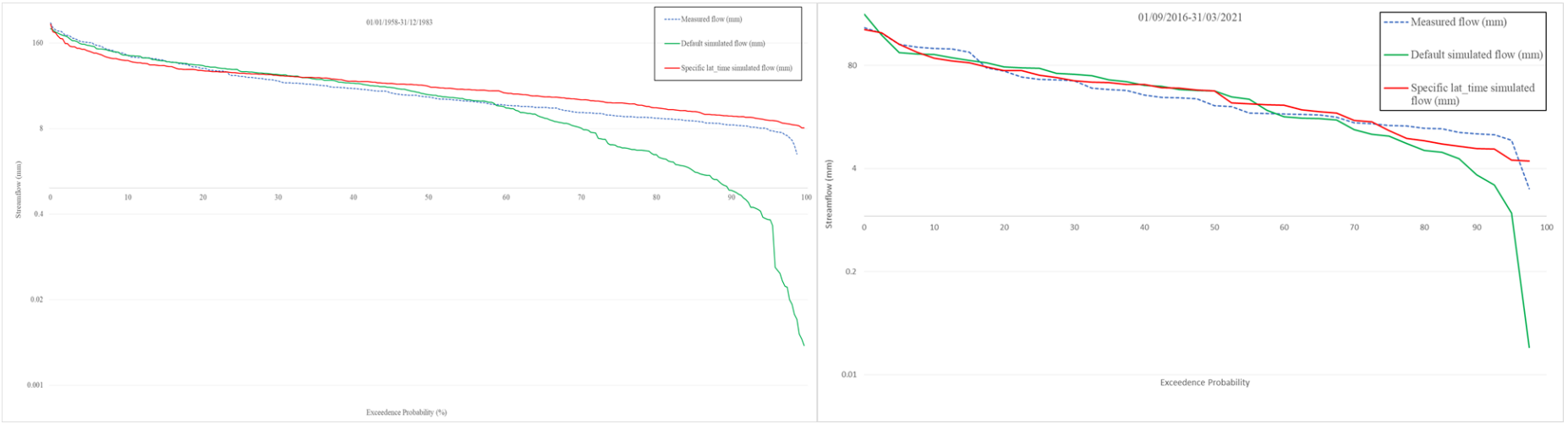


Figure 6.4: (A) Graphical representations of the monthly comparisons between the default simulated flow as well as the specific lat_time simulated flow and the observed flow for a 5-year period within the two time periods for CP-III, and (B) Flow duration curves for the monthly data for the two time periods for CP-III

A

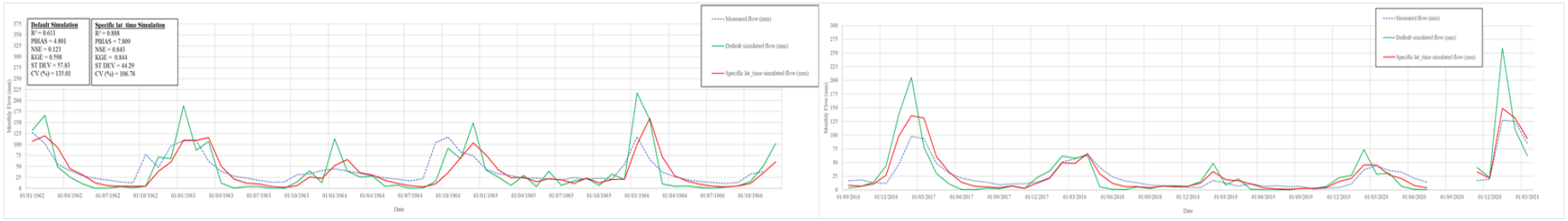


B

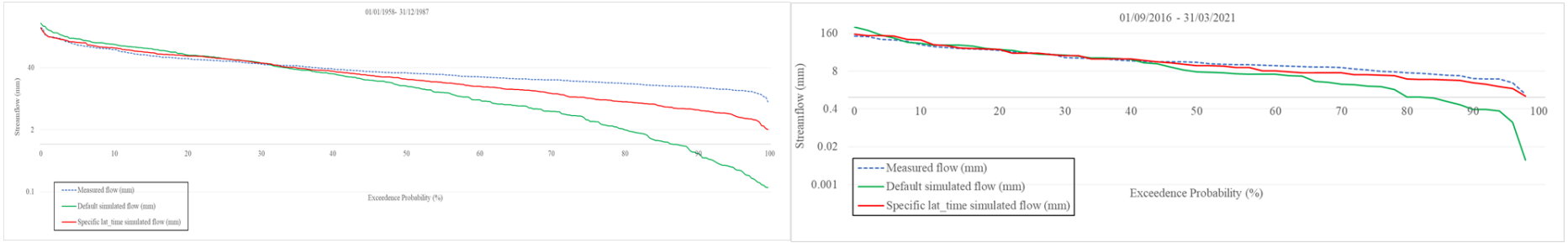


Figure 6.5: (A) Graphical representations of the monthly comparisons between the default simulated flow as well as the specific lat_time simulated flow and the observed flow for a 5-year period within the two time periods for CP-IX, and (B) Flow duration curves for the monthly data for the two time periods for CP-IX

### *6.3.7. Sensitivity analysis*

The sensitivity index calculated for the CP-VI monthly timestep, and current time period is -0.092. This is categorised as Class II and medium sensitivity (Lenhart et al. 2002).

## 6.4. DISCUSSION AND CONCLUSIONS

In this study the distribution of the hydropedological soil groups within each of the catchments played a role in how rainfall flows through the catchment, either through overland flow or infiltration through the soil profile, how it moved through the various areas of the catchment and how it influenced the streamflow. For example, CP-IX had a greater distribution of soils in the Recharge Shallow group as compared to CP-III and CP-VI and thus there is quicker distribution of water flow from the top of this catchment to the streamflow outlet in this catchment. CP-VI had a greater combined percentage of soils in the Interflow and Responsive Saturated groups compared to soils in the Recharge Deep and Recharge Shallow groups and thus there is a longer lateral time taken for water to move through these soils before it contributes to streamflow. The importance of understanding and incorporating specific lateral time periods, taken for water to move through a catchment before it contributes to streamflow was identified in other studies (Jiao et al. 2020, Johnson et al. 2003, Ma et al. 2017, Me et al. 2015). The ability to define the specific lateral time for each HRU in this study was seen as a beneficial input of the SWAT+ model which helped to improve the understanding of the catchments' dynamics.

The statistical parameters used in this study ($R^2$, PBIAS, ST DEV, NSE and KGE) show a definitive improvement in modelling accuracy with the input of the specific lat_time measurements per HRU. These improvements are apparent in all three catchments, with CP-VI obtaining the largest increase in $R^2$ values, particularly for the monthly time step when comparing the default simulations with the specific lat_time simulations. Improvements in the other statistical parameters are clear in all three catchments with none of the catchments improving the most in a particular statistical validation. This is despite the specific lat_time inputs being derived from drainage curves created for the conditions of CP-VI. It is therefore postulated that the specific lat_time inputs associated with CP-III and CP-IX are due to the similar soil properties identified in these catchments as well as the detailed soil information input into the model which is particular to each catchment.

The sensitivity analysis conducted for this study showed that the sensitivity of the lat_time parameter is classified as medium. Leng et al. (2020) detailed the use of sensitive versus insensitive parameters in improving modelling accuracy and found that the use of an apparent insensitive parameter, such as soil Bd, enhanced their model significantly, with the $R^2$, NSE and RSR parameters improving. This suggested complex hydrological processes occurring in the watershed and a wider variety of sensitive and insensitive parameters that need to be applied to the hydrologic model. The same principles can be applied to this study with a number of parameters being sensitive to modelling accuracy including the detailed soil information, the corresponding and detailed digital soil maps which highlight the hydropedological behaviour of the catchments as well as the detailed information obtained from Kuenene et al. (2011) on the soil drainage curves and how these translate into the time taken for lateral water movement to contribute to streamflow.

Numerous research studies have highlighted the importance of detailed soil information on improving SWAT model accuracy (Adem et al. 2020; Chen et al. 2016, Krepec et al. 2020, Peschel et al. 2006). Soil information should be coupled with ecological information of the catchments such as the effects of fire, vegetation as well as rates of evapotranspiration on hydrological modelling accuracy. These aspects have been shown to be all interrelated. In a study by Manson et al. (2007), within the Cathedral Peak area, frequent burning was shown to result in nitrogen limited soils, which in turn affects the vegetation type as well as vegetation condition which affects the soil condition and therefore the flow dynamics of the catchment. A further study in the Cathedral Peak research catchments by Gordijn and O'Connor, (2021) shows that species diversity increased with heterogenous fire regimes over the long term. Improved species diversity has an impact on soil fertility and flow dynamics (Bai et al, 2001; Mason and Zanner, 2005) having an impact on the hydrological flow of the catchment. Evapotranspiration is another important input into hydrological models as it is a vital component of the water cycle (Aouissi et al. 2016; Zhao et al. 2013).

Several studies furthermore emphasise the importance of understanding the hydropedological character of a catchment or study area and translating this knowledge into input variables within hydrologic models (Bouma et al. 2011, Bryant et al. 2006, Sierra et al. 2018, van Tol et al. 2020, and van Tol et al. 2021). In all these studies there is an improvement in the overall accuracy of the models following the input of soil and hydropedological information or an improved accuracy in a certain section of the model. For example, in van Tol et al. (2021),

internal catchment processes were reflected more accurately with rerouting of water fluxes between specific HRUs within the SWAT+ model.

In response to mounting environmental challenges, integrative studies are needed, requiring both specialists within a field as well collaborative efforts across disciplines (Hopmans, 2020, Pachepsky, 2010). The use of soil hydraulic properties within a hydrology model can help one to understand the physical processes that control the partitioning and routing of rainfall into evaporation, infiltration, transpiration, recharge, and runoff (Brooks and Vivoni, 2015), thus improving the model runs for specific catchments.

This study contributed to the understanding of the hydropedological character of three Afromontane catchments and how the characteristics of the soils as well as the flow dynamics of the catchments improves modelling accuracy. It has highlighted that relevant information, based on reliable data, is essential to assess not only the current condition of water resources in a given catchment but also past trends and future possibilities (Droogersa and Bouma, 2014).

## 6.5. REFERENCES

Adem, A.A., Dile, Y.T., Worqlul, A.W., Ayana, E.K., Tilahun, S.A., and Steenhuis, T.S. (2020). Assessing digital soil inventories for predicting streamflow in the headwaters of the Blue Nile. Hydrology. 7.1. doi.org/10.3390/hydrology7010008.

Alemayehu, T., van Griensven, A., Woldegiorgis, T.B., and Bauwens, W. (2017). An improved SWAT vegetation growth module and its evaluation for four tropical ecosystems. Hydrological Earth System Science. 21. 4449–4467. doi.org/10.5194/hess-21-4449-2017.

Aouissi, J., Benabdallah, S., Chabaâne, Z.L., and Cudennec, C. (2016). Evaluation of potential evapotranspiration assessment methods for hydrological modelling with SWAT—Application in data-scarce rural Tunisia. Agricultural Water Management. 174. 39-51. https://doi.org/10.1016/j.agwat.2016.03.004.

Arnold, J.G.; Srinivasan, R.; Muttiah, R.S., and Williams, J.R. (1998) Large area hydrologic modelling and assessment, part I: Model development. Journal of the American Water Resources Association. 34, 73–89.

Bai, Y., Abouguendia, Z., and Redmann, R. (2001). Relationship between Plant Species Diversity and Grassland Condition. Journal of Range Management. 54. 177-183. DOI:10.2307/4003180.

Bailey, R.T., Park, S., Bieger, K., Arnold, J.G., Allen, P.M. (2020). Enhancing SWATþ simulation of groundwater flow and groundwater-surface water interactions using MODFLOW routines. Environmental Modelling and Software 126. 104660. doi.org/10.1016/j.envsoft.2020.104660.

Bieger, K., Arnold, J.G., Rathiens, H., White, M.J., Bosch, D.D., Allen, P.M., Srinivasan, R. (2016). Introduction to SWAT+, a completely restructured version of the soil and water assessment tool. Journal of the American Water Resources Association. 1-16. DOI:10.1111/1752-1688.12482.

Bieger, K., Arnold, J.G., Rathjens, H., White, M.J., Bosch, D.D., and Allen, P.M. (2019). Representing the Connectivity of Upland Areas to Floodplains and Streams in SWAT+. Journal of the American Water Resources Association. 55.3. doi.org/10.1111/1752-1688.12728.

Bosch, JM. (1979). Treatment effects on annual and dry period streamflow at Cathedral Peak. South African Forestry Journal, 108(1): 29-38.

Bouma, J. (1989). Using Using Soil Survey Data for Quantitative Land Evaluation Advances in Soil Science 9. 177- 213.

Bouma, J. (2006). Hydropedology as a powerful tool for environmental policy research. Geoderma. 131. 275-286.

Bouma, J. (2016). Hydropedology and the societal challenge of realizing the 2015 United Nations Sustainable Development Goals. Vadose Zone Journal. DOI:10.2136/vzj2016.09.0080.

Bouma, J., Droogers, P., Sonneveld, M.P.W., Ritsema, C.J., Hunink, J.E., Immerzeel, W.W., and Kauffman. S. (2011). Hydropedological insights when considering catchment classification. Hydrological Earth System Science. 15:1909–1919. DOI:10.5194/hess-15-1909-2011.

Brooks, P.D., and Vivoni, E.R. (2015). Editorial. Mountain ecohydrology: quantifying the role of vegetation in the water balance of montane catchments. Ecohydrology. 1. 187-192. DOI: 10.1002/eco.27.

Bryant, R.B., Gburek, W.J., Veith, T.L., and Hively, W.D. (2006). Perspectives on the potential for hydropedology to improve watershed modeling of phosphorus loss. Geoderma. 131. 299-307.

Chen, L., Wang, G., Zhong, Y., Zhao, X., and Shen, Z. (2016). Using site-specific soil samples as a substitution for improved hydrological and nonpoint source predictions. Environmental Science and Pollution Research. 23. 16037–16046. DOI:10.1007/s11356-016-6789-8.

Daggupati, P., Pai, N., Ale, S., Mankin, K., Zeckoski, R., Jeong, J., Parajuli, P., Saraswat, D., and Youssef, M. (2015). A Recommended Calibration and Validation Strategy for Hydrologic and Water Quality Models. Transactions of the ASABE (American Society of Agricultural and Biological Engineers). 58. 1705-1719. 10.13031/trans.58.10712.

de Menezes, M.D., Silva, S.H.G., Owens, P.R., and Curi, N. (2014). Solum depth spatial prediction comparing conventional with knowledge-based digital soil mapping approaches. Scientia Agricola. Vol. 71. No. 4. doi.org/10.1590/0103-9016-2013-0416.

Droogersa, P., and Bouma, J. (2014). Simulation modelling for water governance in basins. International Journal of Water Resources Development. 30. 3. doi.org/10.1080/07900627.2014.903771.

Everson, C.E., Molefe, G.L., and Everson, T.M. (1998). Monitoring and modelling components of the water balance in a grassland catchment in the summer rainfall area of South Africa. Water Research Commission. RSA. Report 493/1/98.

Ezemvelo KZN Wildlife, National Lottery, University of KwaZulu-Natal, and African Conservation Trust. (2016). Maloti-Drakensberg Transfronteir Aerial Mapping Project Data.

Gassman, P., Sadeghi, A., and Srinivasan, R. (2014). Applications of the SWAT Model Special Section: Overview and Insights. Journal of Environmental Quality. 43. 1-8. 10.2134/jeq2013.11.0466.

Gee and Bauder, J.W. (1986). Particle-size analysis. 312-383. In Klute, A. (ed.) Methods of soil analysis: Part 1. Physical and mineralogical methods. ASA, CSSA and SSSA. Madison, WI.

Geoterraimage. (2015). 2013–2014 South African National Land-Cover Dataset; Report Created for Department of Environmental Sciences; DEA/CARDNO SCPF002: Implementation of Land Use Maps for South Africa; Department of Environmental Affairs: Pretoria, South Africa.

Geroy, I.J., Gribb, M.M., Marshall, H.P., Chandler, D.G., Benner, S.G., and McNamara, J.P. (2011). Aspect influences on soil water retention and storage. Hydrological Processes. 25. 3836–3842. doi.org/10.1002/hyp.8281.

Gordijn, P.J., and O'Connor, T.G. (2021). Multidecadal effects of fire in a grassland biodiversity hotspot: Does pyrodiversity enhance plant diversity? Ecological Applications. 00(00): e02391. 10.1002/eap.2391.

Gordijn, P.J., Everson, T.M., and O'Connor, T.G. (2018). Resistance of Drakensberg grasslands to compositional change depends on the influence of fire-return interval and grassland structure on richness and spatial turnover. Perspectives in Plant Ecology, Evolution and Systematics. 34. 26-36. https://doi.org/10.1016/j.ppees.2018.07.005.

Gupta, H.V., Kling, H., Yilmaz, K.K., and Martinez, G.F. (2009). Decomposition of the mean squared error and NSE performance criteria: Implications for improving hydrological modelling. Journal of Hydrology. 377. 80–91. DOI:10.1016/j.jhydrol.2009.08.003.

Gupta, H.V., Sorooshian, S., and Yapo, P.O. (1999). Status of Automatic Calibration for Hydrologic Models: Comparison with Multilevel Expert Calibration. Journal of Hydrologic Engineering. 4.2. doi.org/10.1061/(ASCE)1084-0699(1999)4:2(135).

Harrison, R., van Tol, J. (2022). Digital Soil Mapping for Hydropedological Purposes of the Cathedral Peak Research Catchments, South Africa. In: Adelabu, S., Ramoelo, A., Olusola, A., Adagbasa, E. (eds) Remote Sensing of African Mountains. Springer, Cham. https://doi.org/10.1007/978-3-031-04855-5_10.

Hellwig, N., Graefe, U., Tatti, D., Sartori, G., Anschlag, K., Beylich, A., Gobat, J., and Broll, G. (2016). Upscaling the spatial distribution of enchytraeids and humus forms in a high mountain environment on the basis of GIS and fuzzy logic. European Journal of Soil Biology. 79. 1-13.

Hensley, M., Hattingh, H.W., and Bennie, A.T.P. (1993). A water balance modelling problem and a proposed solution. In: M. Kronen (Editor). Proceedings of the 4th Annual Scientific Conference. Windhoek. Namibia. 11-14 October 1993. 479-482.

Hopmans, J. (2020). Transdisciplinary soil hydrology. Vadose Zone Journal. Special Section: Transdisciplinary Contributions and Opportunities in Soil Physical Hydrology I. DOI: 10.1002/vzj2.20085.

Jiao, Y., Zhao, D., Xu, Q., Liu, Z., Ding, Z., Ding, Y., Liu, C., and Zha, Z. (2020). Mapping lateral and longitudinal hydrological connectivity to identify conservation priority areas in the water-holding forest in Honghe Hani Rice Terraces World Heritage Site. Landscape Ecology. doi.org/10.1007/s10980-020-00975.

Johnson, M.S., Coon, W.F., Mehta, V.K., Steenhuis, T.S., Brooks, E.S., and Boll, J. (2003). Application of two hydrologic models with different runoff mechanisms to a hillslope dominated watershed in the northeastern US: a comparison of HSPF and SMR. Journal of Hydrology. 284. 57-76.

Kahmen, A., Perner, J. and Buchmann, N. (2005). Diversity- dependent productivity in semi-natural grasslands following climate perturbations. Functional Ecology. 19. 594–601.

Kakarndee, I., and Kositsakulchai, E. (2020). Comparison between SWAT and SWAT+ for simulating streamflow in a paddy-field-dominated basin, northeast Thailand. E3S Web of Conferences 187. 06002. doi.org/10.1051/e3sconf /202018706002.

Knoben, W.J.M., Freer, J.E., and Woods, R.A. (2019). Technical note: Inherent benchmark or not? Comparing Nash–Sutcliffe and Kling–Gupta efficiency scores. Hydrology and Earth System Sciences. Discuss. 23. 4323-4331. doi.org/10.5194/hess-23-4323-2019.

Krause, P., Boyle, D.P., and Bäse, F. (2005). Comparison of different efficiency criteria for hydrological model assessment. Advances in Geosciences. 5. 89-97.

Krpec, P., Horáček, M., and Šarapatka, B. (2020). A comparison of the use of local legacy soil data and global datasets for hydrological modelling a small-scale watersheds: Implications for nitrate loading estimation. Geoderma. 377. 114575. doi.org/10.1016/j.geoderma.2020.114575.

Kuenene, B.T., van Huyssteen, C.W., Le Roux, P.A.L., Hensley, M., and Everson, C.S. (2011). Facilitating interpretation of the Cathedral Peak VI catchment hydrograph using soil drainage curves. South African Journal of Geology. 114. 3-4. 525-534. DOI:10.2113/gssajg.114.3-4.525.

Kuenene, B.T., van Tol, J.J., Bezuidenhoudt, J.C., Van der Merwe, J.H., and Le Roux, P.A.L. (2007). Soil Survey Report of the Cathedral Peak VI Catchment. Unpublished.

Le Maitre, D.C., Walsdorff, A., Cape, L., Seyler, H., Audouin, M, Smith-Adao, L., Nel, J.A., Holland, M. and Witthüser. K. (2018) Strategic Water Source Areas: Management Framework and Implementation Guidelines for Planners and Managers. WRC Report No. TT 754/2/18, Water Research Commission. Pretoria.

Leng, M., Yu, Y., Wang, S., and Zhang, Z. (2020). Simulating the Hydrological Processes of a Meso-ScaleWatershed on the Loess Plateau, China. Water. 12. 878. doi:10.3390/w12030878.

Lin, H. (2003). Hydropedology: bridging disciplines, scales, and data. Vadose Zone Journal. 2. 1–11. doi.org/10.2113/2.1.1.

Lenhart, T, Eckhardt, K., Fohrer, N., and Frede, H.G. (2002). Comparison of two different approaches of sensitivity analysis. Physics and Chemistry of the Earth. 27. 645-654.

Lin, H., Bouma, J., Pachepsky, Y., Western, A., Thompson, J., van Genuchten, R., Vogel, H., and Lilly, A. (2006). Hydropedology: Synergistic integration of pedology and hydrology. Water Resources Research. VOL. 42. W05301. DOI:10.1029/2005WR004085.

Lin, H., Bouma, J., Wildling, L.P., Richardson, J.L., Kutilik, M., and Nielsen, D.R. (2005). Advances in hydropedology. Advances in Agronomy. 85. 307-353.

Lotsch, A., Friedl, M.A., and Anderson, B.T. (2003). Coupled vegetation-precipitation variability observed from satellite and climate records. Geophysical Research Letters. 30. 14.1774. DOI:10.1029/2003GL017506.

Ma, Y., Li, X., and Lin L.H. (2017). Hydropedology: Interactions between pedologic and hydrologic processes across spatiotemporal scales. Earth-Science Reviews. Vol. 171. 181-195.

Mamera, M., and van Tol, J.J. (2018). Application of Hydropedological Information to Conceptualize Pollution Migration from Dry Sanitation Systems in the Ntabelanga Catchment Area, South Africa. Air, Soil and Water Research. doi.org/10.1177/1178622118795485.

Manson, A.D., Jewitt, D., and Short, A.D. (2007). Effects of season and frequency of burning on soils and landscape functioning in a moist montane grassland. African Journal of Range & Forage Science. 24(1). 9–18.

Martín-López, J.M., Da Silva, M., Valencia, J., Quintero, M., Keough, A., and Casares, F. (2019). A comparative Digital Soil Mapping (DSM) study using a non-supervised clustering analysis and an expert knowledge-based model - A case study from Ahuachapán, El Salvador. Presented at: Joint Workshop for Digital Soil Mapping and Global Soil Map March 12-16 2019.

Mason, S.J., and Jury, M.R. (1997). Climatic variability and change over southern Africa: a reflection on underlying processes. Progress in Physical Geography 21: 23–50.

Mason, J. A. and Zanner, C.W. (2005). Grassland Soils. In. Hillel, D. (Ed). Encyclopedia of Soils in the Environment. Elsevier. Oxford. 138-145. https://doi.org/10.1016/ B0-12-348530-4/00028-X.

Me, W., Abell, J.M., and Hamilton, D.P. (2015). Effects of hydrologic conditions on SWAT model performance and parameter sensitivity for a small, mixed land use catchment in New Zealand. Hydrology and Earth System Sciences. 19. 4127-4147. DOI:10.5194/hess-19-4127-2015.

Moriasi, D.N., Arnold, J.G., Van Liew, M.W., Bingner, R.L., Harmel, R.D., and Veith, T.L. (2007). Model Evaluation Guidelines for Systematic Quantification of Accuracy in Watershed Simulations. Transactions of the ASABE. American Society of Agricultural and Biological Engineers. 50. 3. 885−900. DOI:10.13031/2013.23153.

Mucina, L., Rutherford, M.C. & Powrie, L.W. (eds). (2006). Vegetation Map of South Africa, Lesotho and Swaziland. Edn. 2. South African National Biodiversity Institute, Pretoria. ISBN 978-1-919976-42-6.

Nanni, U.W. (1956). Forest Hydrological Research at the Cathedral Peak Research Station. Journal of the South African Forestry Association 27(1). 2-35.

Nash, J.E., and Sutcliffe, J.V. (1970). River Flow Forecasting through Conceptual Model. Part 1—A Discussion of Principles. Journal of Hydrology. 10. 282-290. doi.org/10.1016/0022-1694(70)90255-6.

Neitsch, S.L., Arnold, J.G., Kiniry, T.R., Williams, J.R., and King, K.W. (2002). Soil and Water Assessment Tool. Theoretical Documentation. Report #TR-191. Texas Water Resources Institute College Station. Texas.

Nel, W. (2009). Rainfall trends in the KwaZulu-Natal Drakensberg region of South Africa during the twentieth century. International Journal of Climatology 29. 1634–1641. DOI: 10.1002/joc.1814.

Nel, J., Colvin, C., Le Maitre, D., Snith, J., and Haines, I. (2013). Defining South Africa's Water Source Areas. WWF South Africa. Cape Town. 32pp.

Nkwasa, A., Chawanda, C.J., Jägermeyr, J., and van Griensven, A. (2021). Improved Representation of Agricultural Land Use and Crop Management for Large Scale Hydrological Impact Simulation in Africa using SWAT+. Hydrological Earth System Science Discuss [preprint]. doi.org/10.5194/hess-2021-247, in review.

Oreskes, N., Shrader-Frechette, K., and Belitz, K. (1994). Verification, Validation, and Confirmation of Numerical Models in the Earth Sciences. Science. 263. 5147. 641-646. DOI: 10.1126/science.263.5147.641.

Pachepsky, Y. (2010). Promises of Hydropedology. CAB Reviews Perspectives in Agriculture Veterinary Science Nutrition and Natural Resources. 3. 040. DOI:10.1079/PAVSNNR20083040.

Peschel, J.M., Haan, P.K., and Lacy, R.E. (2006). Influences of soil dataset resolution on hydrologic modelling. Journal of the American Water Resources Association. 42.5. doi.org/10.1111/j.1752-1688.2006.tb05307.

Ridolf, E., Kumar, H., and Bárdossy, A. (2018). A methodology to estimate flow duration curves at partially ungauged basins. Hydrological Earth System Science Discuss, in review.

Robinson, D.A., Hockley, N., Dominati, E., Lebron, I., Scow, K.M., and Reynolds, B. (2012). Why soil science has to embrace an ecosystem approach. Vadose Zone Journal. 11.1. DOI:10.2136/vzj2011.0051.

Shi, X., Zhu, A., Burt, J.E., Qi, F., and Simonson, D. (2004). A Case-based Reasoning Approach to Fuzzy Soil Mapping. Soil Science Society of America Journal. 68. 885–894.

Sierra, A.L.M., Roqueñí-Gutiérrez, N., and Loredo-Pérez, J. (2018). Methodology for the Generation of Hydropedological Parameters Associated with Edaphic GIS Coverage and Databases for Hydrological Modeling. Proceedings. 2. 1411. DOI:10.3390/proceedings2231411.

Smith, P. (2014). Do grasslands act as a perpetual sink for carbon? Global Change Biology. 20. (9). 2708-2011.

Soil Classification Working Group. (2018). Soil Classification: A Natural and Anthropogenic System for South Africa. ARC-Institute for Soil, Climate and Water. Pretoria.

Taylor, S.J., Ferguson, J.W.H., Engelbrecht, F.A., Clark, V.R., Van Rensburg, S. and Barker, N. (2016). The Drakensberg Escarpment as the Great Supplier of Water to South Africa. In. G.B. Greenwood. and J.F. Shroder Jr. eds. Mountain Ice and Water. Investigations of the hydrologic cycle in Alpine Environments. Developments in Earth Surface Processes 21. Elsevier. Netherlands.

Toucher, M.L., Clulow, A., van Rensburg, S., Morris, F., Gray, B., Majozi, S., Everson, C.E., Jewitt, G.P.W., Taylor, M.A., Mfeka, S., and Lawrence, K. (2016). Establishment of a more robust observation network to improve understanding of global change in the sensitive and critical water supply area of the Drakensberg. 2236/1/16. Water Research Commission, Pretoria, South Africa.

van Tol, J.J., and Le Roux, P.A.L. (2019). Hydropedological grouping of South African soil forms. South African Journal of Plant and Soil. 36(3). 233-235. DOI:10.1080/02571862.2018.1537012.

van Tol, J., Bieger, K., and Arnold, J.G. (2021). A hydropedological approach to simulate streamflow and soil water contents with SWAT+. Hydrological Processes. 35. e14242. doi.org/10.1002/hyp.14242.

van Tol, J.J., Le Roux, P.A.L., Lorentz, S.A., and Hensley, M. (2013). Hydropedological Classification of South African Hillslopes. Vadose Zone Journal. DOI:10.2136/vzj2013.01.0007.

van Tol, J., van Zijl, G., and Julich, S. (2020) Importance of Detailed Soil Information for Hydrological Modelling in an Urbanized Environment. Hydrology. 7. 34. DOI:10.3390/hydrology7020034.

Vereecken, H. 1992. Derivation and vaUdation of pedotransfer functions for soil hydraulic properties. Pages 473-488 in M.Th. van Genuchten. F.J. Leij. and L.J. Lund. eds. Indirect methods for estimating the hydraulic properties of unsaturated soils. Proc. of the International Workshop on Indirect Methods for Estimating the Hydraulic Properties of Unsaturated Soils. 11-13 October 1989, Riverside, Cal., U.S.A.

Vereecken, H., Schnepf, A., Hopmans, J.W., Javaux, M., Or, D., Roose, T., Vanderborght, J., Young, M.H., Amelung, W., Aitkenhead, M., Allison, S.D., Assouline, S., Baveye, P., Berli, M., Brüggemann, N., Finke, P., Flury, M., Gaiser, T., Govers, G., Ghezzehei, T., Hallett, P, Hendricks Franssen, H.J., Heppell, J., Horn, R., Huisman, J.A., Jacques, D., Jonard, F., Kollet, S., Lafolie, F., Lamorski, K., Leitner, D., McBratney, A., Minasny, B., Montzka, S., Nowak, W., Pachepsky, Y., Padarian, J., Romano, N., Roth, K., Rothfuss, Y., Rowe, E.C., Schwen, A., Šimůnek, J., Tiktak, A., Van Dam, J., van der Zee, S.E.A.T.M., Vogel, H.J., Vrugt, J.A., Wöhling, T., and Young, I.M. (2016). Modeling Soil Processes: Review, Key Challenges, and New Perspectives. Vadose Zone Journal. 15.5. DOI: 10.2136/vzj2015.09.0131.

Whitmore, J.S. (1970). The Hydrology of Natal. Symposium Water Natal: Durban.

Wei, J., Liu, W., Wan, H., Cheng, J. and Li, W. (2016). Differential allocation of carbon in fenced and clipped grasslands: a 13C tracer study in the semiarid Chinese Loess Plateau. Plant and Soil. 406. (10). 1007.

Zadeh, L.A. (1965). Fuzzy sets. Information and Control. 8. 338-353.

Zhang, M., Huang, X., Chuai, X., Yang, H., Lai, L. and Tan, J. (2015). Impact of land-use type conversion on carbon storage in terrestrial ecosystems of China: A spatial-temporal perspective. Scientific Reports. 5. 10233.

Zhao, L., Xia, Jun., Xu, C., Wang, Z., Sobkowiak, L., and Long, C. (2013). Evapotranspiration estimation methods in hydrological models. Journal of Geographical Sciences. 23. 359-369. DOI:10.1007/s11442-013-1015-9.

Zhu, A.X., Band, L., Vertessy, R., and Dutton, B. (1997). Derivation of soil properties using a soil land inference model (SoLIM). Soil Science Society of American Journal. 61. 523-533.

Zhu, A.X., Qi, F., Moore, A., Burt, J.E. (2010). Prediction of soil properties using fuzzy membership values. Geoderma. 158. 199-206.

# CHAPTER 7 – ENVIRONMENTAL FACTORS INFLUENCING DISSOLVED ORGANIC CARBON CONCENTRATIONS IN AFROMONTANE CATCHMENTS

**Abstract**

Concentrations of DOC can be attributed to several environmental factors, including climate, hydrology, land cover, land management, soil type, and topography. Montane grassland environments are highly variable due to the spatial heterogeneity, and this has an influence on DOC export, making it often site and land-use dependent Despite the importance of small mountain streams in the global flux of sediment and associated DOC, little is known about the environmental factors controlling DOC in Afromontane areas. This study aimed to gain an understanding of the various environmental factors driving the temporal patterns of DOC export in Afromontane catchments. Piezometers were installed within two Afromontane catchments and water samples were analysed for DOC between September 2019 and June 2021. Furthermore, the height of the water within the piezometer was calculated from the surface of the soil to the depth of the water table. Piezometers were located within various environmental classes including different land covers (wetland and terrestrial), different soil groups (saturated responsive soils and interflow soils), different topographical areas of the catchments (upper, mid, and lower positions), as well as different slope curvature profiles (convex and concave slopes). DOC concentrations followed seasonal trends of precipitation as well as temperature variations in the catchment areas. A statistical difference (using the Kruskal Wallis method) was recorded between terrestrial and wetland areas (CP-VI: $p=0.043$ and CP-IX: $p= <0.0001$) as well as between interflow soils and saturated responsive soils (CP-VI: $p=0.001$ and CP-IX: $p= 0.041$), with the latter group recording the higher DOC concentrations in both catchment areas. DOC concentrations between piezometers installed within different topographical positions and different slope curvatures were not statistically different. The importance of wetland systems as major drivers in DOC concentrations was highlighted in this study. The connectivity of the wetlands to the streams within both catchments plays a role in the attenuation and export of DOC within these watersheds.

## 7.1. INTRODUCTION

Soil organic carbon (SOC) is a key component of the global carbon cycle. It is the largest terrestrial carbon pool (Ciais et al. 2013, Tao et al. 2020, Liu et al. 2021) as it is estimated that

the carbon contained in soil constitutes 75% of the total organic carbon stock stored in terrestrial ecosystems (Dixon et al. 1994, Six et al. 2002, Reyna-Bowen et al. 2019). Therefore, studying the spatial distribution patterns of soil organic carbon and its influencing factors is essential for understanding the carbon cycle in terrestrial ecosystems (Wan et al. 2014).

Organic carbon within the soil can be divided into the labile and stabile fractions depending on its density, with the stabile fraction accounting for 90% of the soil's total organic carbon (TOC) (Six et al. 2002; Sainepo et al. 2018). The stabile fraction is not easily affected by land use or management practices (Sainepo et al. 2018). This is due to a number of factors which control the stabilization of this organic carbon including the soil type, the clay mineralogy, the soil aggregation, the availability of metal oxides, soil fauna and microorganism activity, as well as landscape controls in the form of topography, vegetation cover, parent materials and climate (Wiesmeier et al. 2019)

The labile fraction includes dissolved organic carbon (DOC). It has a high turnover rate and is easily affected by management systems as well as erosion. It is therefore an easily available source of carbon for microorganisms, as well as a source of organic carbon and nutrients in the deeper soil horizons (Jinbo et al. 2007; Zhang et al. 2011). DOC is therefore one of the most active and mobile carbon pools and has an important role in global carbon cycling (Kalbitz et al**.** 2000) and is the focus of this study.

DOC production is governed by the abiotic and biotic biogeochemical processes. The DOC concentration in soil solution is controlled by its production, leaching, stabilisation, and degradation (Kalbitz et al., 2000). The importance of DOC for the functioning of terrestrial and aquatic ecosystems is widely known (Mann and Wetzel, 1995; Schindler and Curtis, 1997; Lennon et al. 2013). It serves as the major energy source for aquatic microbial communities, it links different carbon pools, attenuates UV radiation, and plays a role in the acid-base chemistry of soils and surface waters. It furthermore influences nutrient cycling and affects the mobility and availability of metals and contaminants (Kalbitz et al., 2000, Bolan et al. 2011, Strohmeier et al. 2013). The transport of DOC along streams and rivers therefore represents a crucial linkage between land and oceans in the global carbon cycle (Cole et al. 2001, Battin et al. 2009, Aufdendkampe et al. 2011).

Many land surface models represent soils in a simplistic way and often neglect the production and export of DOC from soils to rivers. This leads to an overestimation of the potential carbon sequestration of a particular area, leading to uncertainties in the predictions of the soil carbon response to land management changes as well as climate change (Camino-Serrano et al. 2018). Understanding the dynamics that control how DOC is exported from soils to aquatic systems is thus important for accurate estimations of C budgets. This is because DOC corresponds to a fraction of the carbon taken up from the atmosphere that is not sequestered in soils (Regnier et al. 2013, Le Quéré et al. 2015, Camino-Serrano et al. 2018).

DOC export from ecosystems depends on its production and its consumption. Therefore, its transport within soils and watersheds is dependent on soil characteristics, biological constraints and the contact time with the microbial communities that decompose soil organic matter (SOM) (Don and Schulze 2008, Tranvik et al. 2009, Laudon et al. 2011, Kaiser and Kalbitz 2012, Hagedorn and Joos, 2013, Ran et al. 2013). Concentrations of DOC can therefore be attributed to several environmental factors, including climate, hydrology, land cover, land management, soil type, and topography (Pagano et al. 2014, Ryder et al. 2014, Wei et al. 2021), as well as disturbances such as fire (Wei et al. 2021).

In montane grassland environments fire is often used as a management tool. This is particularly the case in Afromontane grasslands such as those found in the KwaZulu-Natal Drakensberg Mountain range (Findlay et al. 2022). Studies have both highlighted that fires in these systems can be regarded as causes of soil degradation as well as agents that mobilise nutrients and restore soil fertility (Snyman, 2003, Novara et al. 2013). Fires are furthermore known to cause the alteration of SOM, with several studies recording a decrease in SOC after fires, while others showed no significant change or even an increase in SOC content (Fernández et al., 1997, Novara et al. 2013, Findlay et al. 2022). These differences in the results of the various studies are likely due to the variations in the controlling factors of SOC and the fact that these environmental factors often change over temporal and spatial scales (Clark et al. 2010).

Furthermore, concentrations of DOC in montane environments are highly variable due to the spatial heterogeneity of these areas. Mountain ecosystems have variations in their microclimate, such as high quantity and high intensity of rainfall, greater sunshine incidence on certain slopes, depending on their aspect, as well as variations in the soils of these areas (Garcia-Pausas, 2007, Garcia-Pausas, 2017). Mountain soils are often located on steep

topography and are generally shallow and have a high erosion rate but can also be deep in deposition areas (Garcia-Pausas, 2017). Thus, the physiography of a catchment area, which is linked to the percentage of wetlands within the catchment, are important controls on DOC concentrations and fluxes (Eckhardt and Moore,1990, Clair et al. 1994, Billett et al. 2006). Furthermore, altitude greatly affects the accumulation and decomposition of SOC. In particular, changes in climate with altitude influence the composition and productivity of vegetation and affect the quantity and turnover of SOC by controlling soil water balance, soil erosion and deposition processes. Due to the complex interaction of climate, soil, vegetation and management conditions, ecosystem DOC export is often site and land-use dependent (Sheikh et al. 2009, Garcia-Pausas, 2017).

As a result of the high erosion and deposition rates of mountainous areas, several studies have highlighted the importance of small mountain streams in the global flux of sediment and associated DOC (Hilton et al. 2012, Galy et al. 2015, Turowski et al. 2016). One of the most consistent relationships with DOC concentrations in streams has been found with the flow dynamics of catchment areas. Studies have shown correlations between DOC concentrations identified in the headwater catchment areas and the streamflow (Rutherford and Hynes, 1987, Grieve, 1990, Hinton et al. 1998, Dawson et al. 2002, Billett et al. 2006), thus identifying that both biological and hydrological processes operating within the catchment area affect the DOC concentrations (Roig-Planasdemunt et al. 2016). This is particularly prevalent during storm events, with several studies reporting increases in DOC concentration in streamflow during rainfall (Knorr, 2013, Roig-Planasdemunt et al. 2016, Warner et al. 2020). In small mountainous streams, Lee et al. (2019a) identified that DOC is flushed into streams during storm events, particularly when hillslope flow paths are connected to the streams, when for example wetlands are saturated. Here wetlands and riparian areas play an important role in transporting DOC to the stream network.

Further to this, DOC concentrations within soil solution have been shown to be enhanced with wetting and drying cycles associated with a fluctuating water table, as well as temperature variations (Boyer et al. 1997, Billett et al. 2006). DOC within soil solution is associated with the temporal biological and hydrological processes, acting in soils. Higher concentrations are observed during the growing season, while lower concentrations follow DOC losses due to water fluxes during the wet period (Roig-Planasdemunt et al. 2016).

There is thus a need to improve our understanding of how and by how much various environmental factors are driving the temporal patterns of DOC export in order to accurately model and evaluate terrestrial carbon storage and fluxes (Wei et al. 2021) as well as predict the effect of land use and climate changes on these dynamics. The variabilities in the environmental attributes of mountain ecosystems often within small catchment areas, make montane ecosystems ideal locations to study how different landscape aspects affect the concentration of DOC. This study aims to identify the principle environmental factors that influence DOC concentrations within two Afromontane catchments, that are similar in shape and size but have different land management regimes. With the understanding of the landscape controls on the dynamics of the DOC concentrations within these two headwater catchments, one can begin to gain an understanding of the concentrations in DOC found in downstream watercourses.

## 7.2. MATERIALS AND METHODS

### *7.2.1. Study Site*

Details of the study area are given in Chapter 3. Two of the research catchments were selected for this study, namely, CP-VI and CP-IX.

### *7.2.2. Piezometer installations*

Piezometers were installed within both catchment sites. Twelve piezometers were installed in CP-VI and nine were installed in CP-IX. The piezometers were installed in clusters of two or three within a location, with this location chosen to represent the upper, mid, and lower portions of the catchments. Furthermore, the position of the piezometers was chosen within wetland and seepage areas of the catchments. Soil profiles were dug using an extension Dutch auger to the first signs of a gleyic or gley horizon. These horizons display gleying and are considered indicators of the redox state of the soil. Gley horizons are recognised by low chroma grey matrix colours which may contain blue or green tints. The gleyic horizon displays low chroma, grey and light-yellow colours, with the morphology of this horizon indicating less reduction and shorter duration of water saturation compared to the gley horizon (Soil Classification Working Group, 2018). A PVC pipe with slits cut around the end of the pipe to a height of 30 cm were then installed into the auger holes (Figure 7.1). The PVC pipe utilised ensured a close fit with the hole. The piezometers were then capped, and measurements taken once a month between January 2019 to June 2021, however due to a drought within the region, the majority

of piezometers only received water in September 2019 and thus this was chosen as the start point for the piezometer records.

As a result of the drought conditions, some of the piezometers had to be discontinued, and thus seven piezometers were sampled every month in CP-VI, and seven were sampled every month in CP-IX (Figure 7.1). Water heights were recorded once a month to the nearest cm. The height of the water within the piezometer was calculated from the surface of the soil to the depth of the water table.

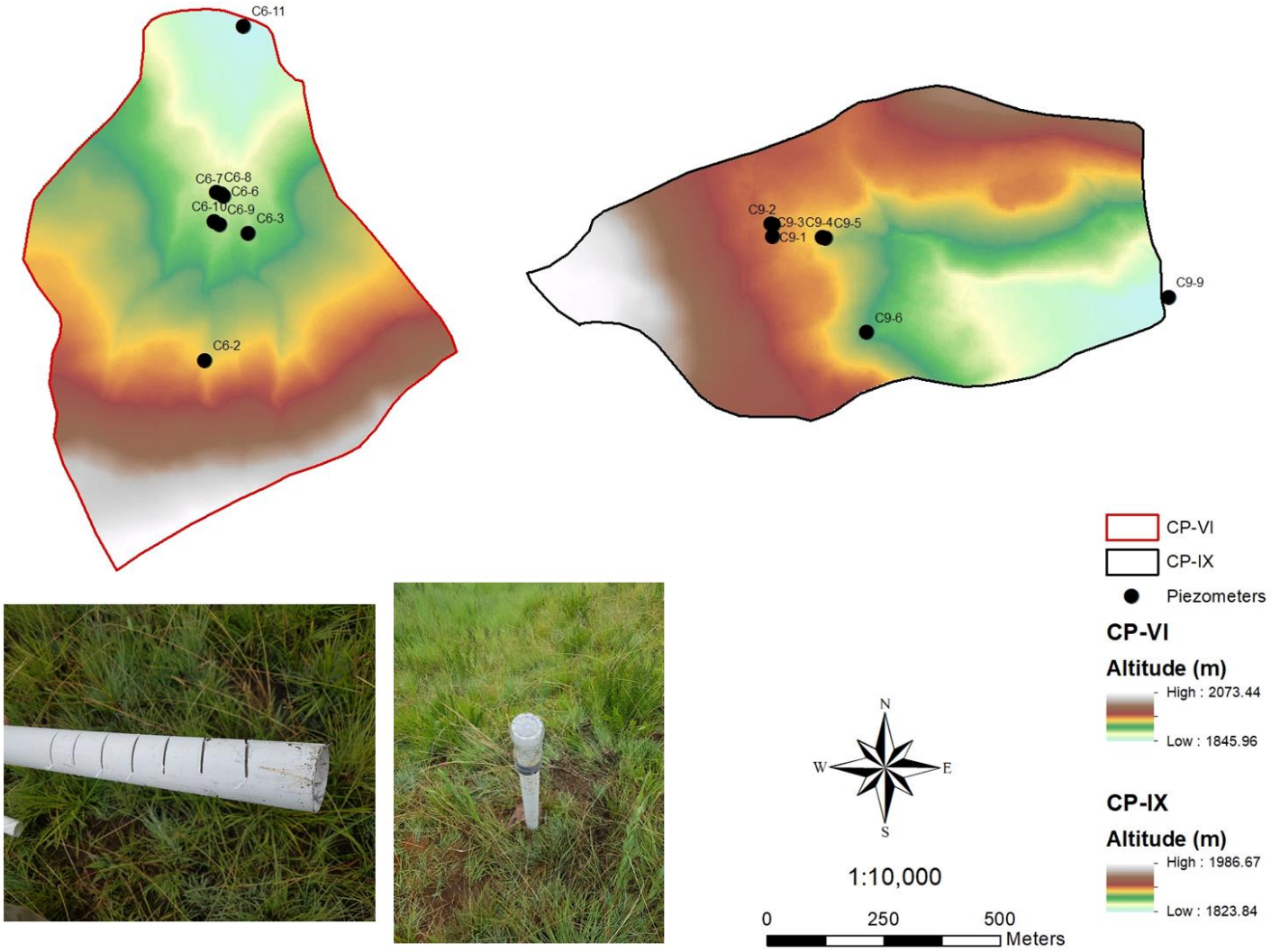


Figure 7.1: Locality of the piezometers within CP-VI and CP-IX. Photograph showing the slits cut around the end of the pipe to a height of 30 cm to ensure water enters the piezometer as well as the capped and installed piezometer

### *7.2.3. Catchment characteristics*

#### 7.2.3.1.Land cover

The catchment areas are mainly covered by mesic grasslands of the uKhahlamba Basalt Grassland vegetation type interspersed with Northern Afrotemperate Forest patches and wetlands (Mucina and Rutherford, 2006, Toucher et al. 2016). CP-VI is managed as a grassland, and is dominated by *Bromus speciosus*, *Pentaschistis tysoniana*, *Cymbopogon nardus* and *Themeda triandra* that are accompanied by numerous herbs and shrubs. CP-IX has been completely protected from fire since 1952 but has experienced accidental burns and wildfires in some years. As a result of the fire exclusion, the catchment is dominated by woody scrub including *Leucosidea sericea* and *Buddleia salvifolia* (Mucina and Rutherford, 2006, Toucher et al. 2016).

For this study the land cover was grouped into two separate simplified categories, depending on the location of the piezometers. These categories included terrestrial vegetation and wetland vegetation (Figure 7.2). Wetland vegetation included any hydrophytic vegetation, while terrestrial vegetation included the remaining groups of vegetation such as graminoids, forbs, shrubs, and trees. Examples of hydrophytic vegetation identified within the wetland systems include *Miscanthus ecklonii*, *Arundinella nepalensis*, *Merxmuellera macowanii* and *Cyperus congestus*, while dominant terrestrial vegetation in CP-VI and in CP-IX include poaceae such as *Themeda triandra*, *Tristachya leucothrix*, and *Harpochloa falx*, forbs such as *Acalypha punctata*, *Helichrysum sp*, *Senecio* sp., *Kohautia amatymbica* and trees including *Leucosidea sericea* and *Buddleia salvifolia* (Gordijn et al. 2018).

#### 7.2.3.2.Soils

The soils of both catchments have been classified as per the South African taxonomic classification system (Soil Classification Working Group, 2018). This classification system was then converted to the World Reference Base (WRB) for Soil Resources system utilising the tool from van Huyssteen (2020). Both catchments are dominated by deep well drained soils. Within the South African classification systems these are classified as the Inanda, Magwa, and Kranskop forms, and are categorised as the Haplic Umbrisols in the WRB system. More shallow soils occur in rocky areas or areas of steeper terrain. These are classified as the Nomanci or Mispah soil forms in the South African system and Leptic Umbrisols and Dystric Leptosol in the WRB system respectively. Hydrological flow paths are evident within the soil characteristics, with lateral flow paths displayed in the gleyic horizons of the Dartmoor, and

Highmoor soil forms of the South African system and the Stagnic Cambisols of the WRB system. More saturated gley horizons are dominated by the Champagne and Katspruit soil forms of the South African classification system and the Planosols and Luvisols of the WRB system.

Soil samples were collected from each of the piezometer locations. The samples were divided into different horizons depending on the type of soil encountered at each piezometer location. Each soil sample was analysed for total carbon percentage utilising the Leco element analyzer as well as the organic matter percentage utilising the loss-on-ignition method. This method does not have a standard protocol but rather involves three factors including the incomplete combustion of SOM at low temperatures (Ball, 1964), the removal of structural water from clay minerals (Sun et al., 2009) and the decomposition of soil carbonates at large temperatures (Kasozi et al., 2009; Hoogsteen et al. 2015).

Soils were regrouped into hydropedological soil types, namely, shallow recharge soils, deep recharge soils, interflow soils, and saturated responsive soils, based on the classifications from van Tol and Le Roux (2019). A map of the hydropedological soil groups of both catchments was created following a digital soil mapping exercise. This process is explained in detail in Harrison and van Tol (accepted in: Remote Sensing of African Mountains - Geospatial Tools Toward Sustainability), The hydropedological soil group maps are displayed in Figure 7.3, with the hydropedological soil groups utilised in this study. The piezometers were either recorded on the interflow hydropedological soil group or on the saturated responsive hydropedological soil group.

7.2.3.3.Topography and aspect

CP-VI ranges in altitude from 1845 – 2073 m.a.s.l with a north-north-east aspect, while CP-IX ranges in altitude from 1822-1982 m.a.s.l with an east-north-east aspect (Toucher et al, 2016). The topography of all the research catchments ranges from relatively flat to very steep (1–39°) (Granger and Schulze, 1977; Gordijn et al. 2018).

For this study the topography of the catchments was classified into two separate slope curvature classes, namely convex slopes, and concave slopes, depending on the location of each piezometer. Convex slopes steepen as they descend and are typically associated with low drainage resistance. Concave slopes gradually flatten as they descend and are typically

associated with receiving water from upslope, water retention and greater water infiltration into the soil profile (Job and Le Roux, 2019). A 5 m resolution Digital Elevation Model (DEM) (Ezemvelo KZN Wildlife et al., 2016) was utilised to create a curvature raster of each catchment. At the point of each piezometer the slope profile was checked to determine if the piezometer was positioned on a convex or a concave slope, with negative values from the curvature raster indicating convex, and positive values indicating concave slopes.

#### 7.2.3.4. Fire regime

The vegetation of the Cathedral Peak research catchments is largely controlled by fire. Fire regimes which were included as management treatments were established within the catchments by 1957 and included areas burnt frequently (one and three years) and infrequently (five and eight years). These burns were applied during the period winter to early spring. CP-VI is burned biennially during spring and CP-IX has been completely protected from fire since 1952 but has experienced accidental burns and wildfires in some years. Literature has shown that the species composition of the catchments is associated with the burning regimes (Gordijn et al. 2018, Gordijn and O'Conner 2021, Toucher et al. 2016). During this study CP-VI had a controlled burn on the 7$^{th}$ October 2020.

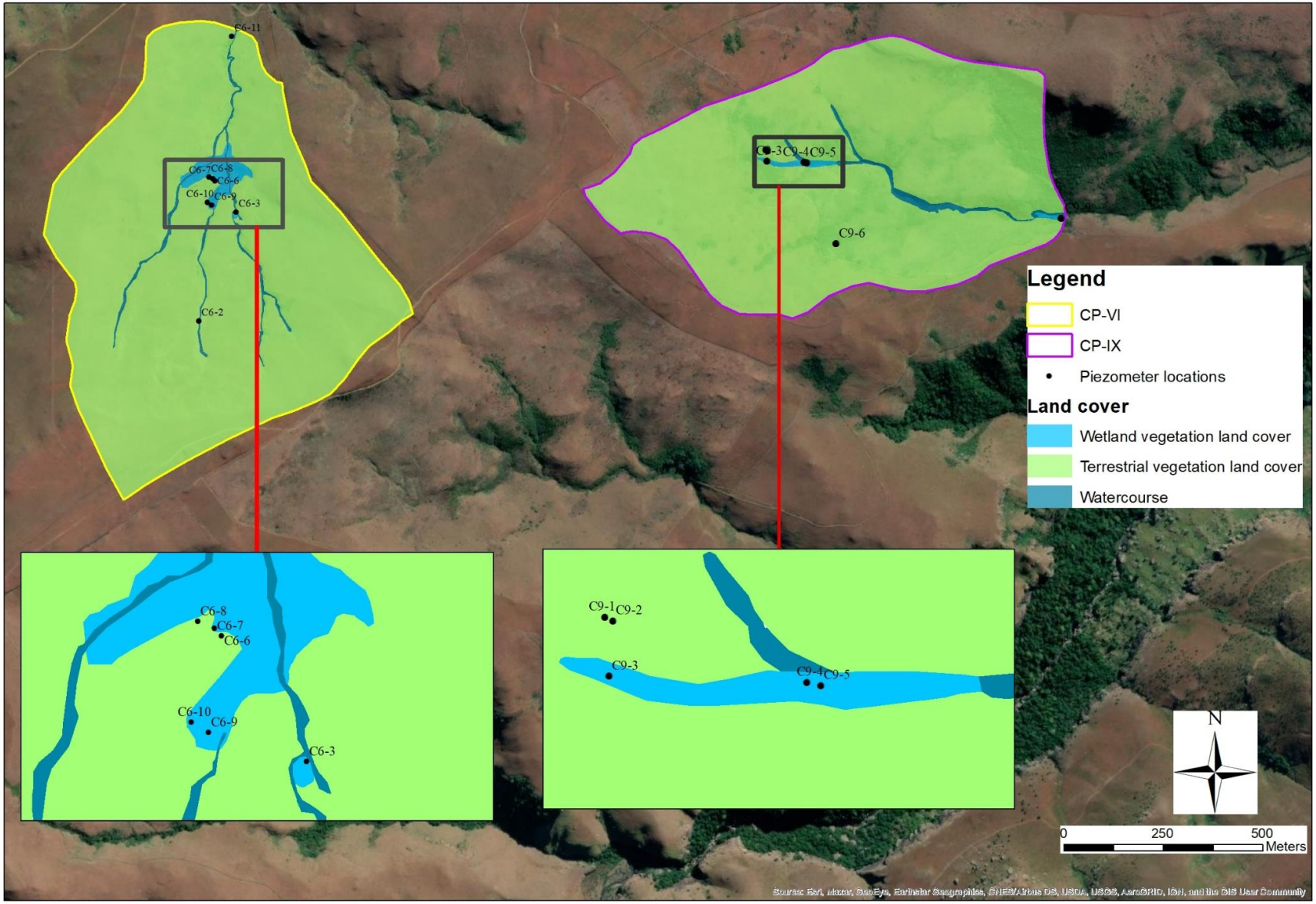


Figure 7.2: Simplified land cover maps of the two catchment areas in relation to the piezometer locations

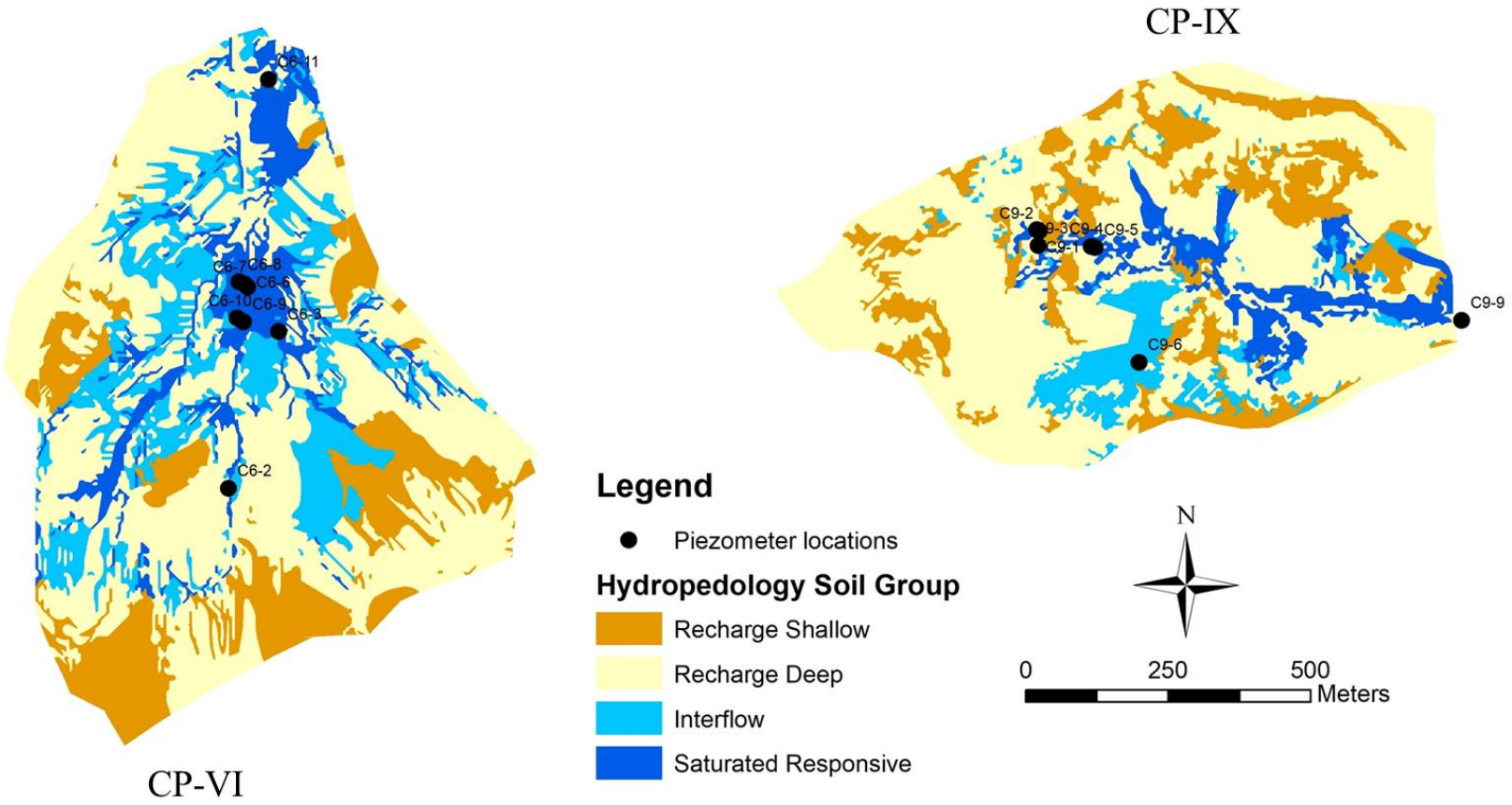


Figure 7.3: Hydropedological soil group maps for CP-VI and CP-IX in relation to the piezometer locations

### *7.2.4. Physical characteristics of the catchments utilised in this study*

In order to gain an understanding of the influence of different physical characteristics of the catchments on the DOC concentration, the catchments were classified into classes. These included classes on land cover, hydropedological soil type, the topographical position of the piezometer within the catchment and the slope profile in which the piezometer was situated.

The classes utilised in this study as well as the number of piezometers within each class is displayed in Table 7.1.

Table 7.1: Classes describing the physical characteristics of each catchment as well as the number of piezometers within each class

| **Physical characteristic of the catchment** | | **Number of piezometers** | |
|---|---|---|---|
| | | **CP-VI** | **CP-IX** |
| Land cover | Wetland vegetation | 4 | 4 |
| | Terrestrial vegetation | 3 | 3 |
| Hydropedological soil group | Saturated responsive soil group | 4 | 4 |
| | Interflow soil group | 3 | 3 |
| Topographical position of the piezometers within the catchment | Upper catchment | 2 | 3 |
| | Mid catchment | 4 | 3 |
| | Lower catchment | 1 | 1 |
| Slope profile | Convex slope | 3 | 3 |
| | Concave slope | 4 | 4 |

*7.2.5. Climate and climatic monitoring of the Cathedral Peak research catchments*

The Cathedral Peak research catchments fall within the summer rainfall region of South Africa. The mean annual precipitation (MAP) for the area is approximately 1400 mm with the south-eastern areas receiving approximately 1300 mm while the western portion receives approximately 1700 mm. Half of the rainfall events in the catchments are thunderstorms (Bosch, 1979, Everson et al. 1998, Toucher et al. 2016) during the spring and summer months (September to March) with occasional snowfall received during winter (May to August). Mean monthly temperatures range from 17.1$^{O}$C to 10$^{O}$C with frost common in autumn and winter (April to August) (Bosch, 1979, Everson et al. 1998, Gordijn et al. 2018; Toucher et al. 2016).

The collection of climatic data for the Cathedral Peak research catchments started in 1948 with a weather station located at the top of Mike's Pass. The daily variables recorded were average temperature, average relative humidity, average solar radiation, average wind direction and average wind speed. In addition to this meteorological station, precipitation was historically monitored at several sites across the catchments. Rainfall data monitoring within the catchments has been undertaken since 1950. Three tipping bucket rain gauges are currently situated within CP-IX at the top, middle and lower position of the catchment. In CP-VI one tipping bucket rain gauge is situated within the mid position of the catchment, while three tipping bucket rain gauges are situated in the adjacent catchment, CP-VII. As both catchments have a tipping bucket rain gauge in the mid position, the data from these rain gauges were utilised as they are in comparable positions.

Streamflow monitoring was initiated in both catchment areas during the late 1940's and 1950's (Toucher et al., 2016). Climatic data for this study was therefore obtained from the Mike's Pass weather station as well as from specific rain gauges located within each catchment. CP-VI has a MAP of 1340 mm, while CP-IX has a MAP of 1257 mm (Toucher et al. 2016).

At the outlet of each catchment a concrete weir and stilling hut, with 90-degree V Notches were installed. These V Notches are 45.72cm (18 inches) deep and are surmounted by 6 feet wide rectangular notches of varying depth. The stilling ponds were dug to bedrock, and rock walls for the pond were constructed. Details of how early measurements were taken, error checked and processed are given in Toucher et al. (2016). The water stage-height at each weir is currently monitored using an Orpheus Mini (Ott Hydromet GmbH, Germany) at CP-VI weir and a CS451 Stainless steel SDI-12 Pressure Transducers with CR200 loggers at CP-VI, and

CP-IX. There are two pressure transducers installed at weir CP-VI as this is the core catchment and thus the quality of streamflow records is ensured (Toucher et al. 2016).

### *7.2.6. DOC analysis*

DOC analysis of water extracted from the piezometers was conducted on a monthly basis between September 2019 and June 2021. Water was extracted from the piezometers and filtered using a 0.2 µm filter syringe. To avoid contamination from cellulose, the filter was rinsed, and this water discarded. The filtered water was acidified with 0.1M Phosphoric Acid ($H_3PO_4$) to bring the pH to 2. Water samples were brought back from the field in a coolbox and then stored in a refrigerator until analysis. This was undertaken to minimise the loss of DOC within the sample during transportation, and storage. All samples were analysed through the non-purgeable organic carbon (NPOC, referred to hereafter as DOC) concentration with a Vario TOC cube analyzer (Elementar, Germany) in the GISMO platform (UMR6282 Biogéosciences CNRS/uB), at the University of Burgundy, France.

### *7.2.7. Statistical analysis*

The data were collated from all piezometers for each catchment, with DOC values of 0 (as a result of the piezometers being dry within certain months) removed from the data set. The relationships between the climatic parameters (rainfall, streamflow, temperature, and the height to the water table within each piezometer) and the concentration of DOC within the piezometers were plotted using a combination of line and scatter plots.

Following these tests on the environmental parameters, the minimum, maximum, and mean DOC values were calculated per catchment. The data were tested for normality using the Kolmogorov–Smirnov test with an alpha value of 0.05 (Massey, 1951). As the data is not normally distributed the relationship between the different physical characteristics of the catchments (including land cover, hydropedological soil group, topographical position of the piezometer within the catchment, and the slope profile) and DOC concentrations from the piezometers were analysed using the Kruskal-Wallis non-parametric test (Kruskal & Wallis, 1952). This test was used as it assesses the differences among two or more independently sampled groups on a single, non-normally distributed continuous variable (Ostertagová et al, 2014). The Dunn's procedure, which is a nonparametric pairwise multiple comparison procedure utilised following the Kruskal-Wallis non-parametric test (Dinno, 2015, Dunn,

1964), was used during the analysis of the topographical position of the piezometers. This procedure was utilised as there are more than two parameters in this analysis.

## 7.3. RESULTS

### *7.3.1. DOC and seasonality*

Precipitation data for CP-VI and CP-IX during the study period September 2019 to June 2021 showed that precipitation largely falls within the spring-summer months (September to March), with little to no rain within the autumn and winter months (April to August) (Figure 7.4). A greater quantity of rainfall was recorded in both CP-VI and CP-IX for the spring-summer season of 2020-2021 (CP-IV = 1307 mm and CP-IX = 1045 mm) as compared to the same season within the preceding year (2019-2020) as a result of the drought conditions experienced in 2019 (CP-VI = 842 mm, and CP-IX = 771 mm). The mean monthly DOC concentrations generally followed the seasonal pattern of rainfall, with maximum values (10.92 mg/L in CP-VI and 8.59 mg/L in CP-IX) recorded in the spring-summer months and minimum values (1.91 mg/L in CP-VI and 1.24 mg/L in CP-IX) recorded in the autumn-winter months.

Correlations between the monthly streamflow discharge of the catchment areas as well as the mean monthly DOC concentrations in piezometers showed a seasonal variation with higher mean monthly DOC concentrations recorded in the spring-summer months compared to the autumn-winter months for both catchment areas (Figure 7.4 and Figure 7.5). Similar trends to the rainfall plots were noted, however interestingly there is a greater lag time for the increase in streamflow discharge within both catchments following the drought conditions experienced in 2019. As shown in Figure 7.4 and Figure 7.5 a maximum DOC concentration is obtained within the piezometers in October, November, and December 2020 with the onset of the spring-summer rains, but the maximum flow in streamflow discharge from the catchments occurs between January and March 2021 (towards the end of the summer season). This is likely due to the ‘re-wetting process’ of the wetlands that would have taken place within the catchments before these systems could contribute to the streamflow discharge, both after the initial drought conditions in 2019/2020 and following the winter drier conditions in 2020.

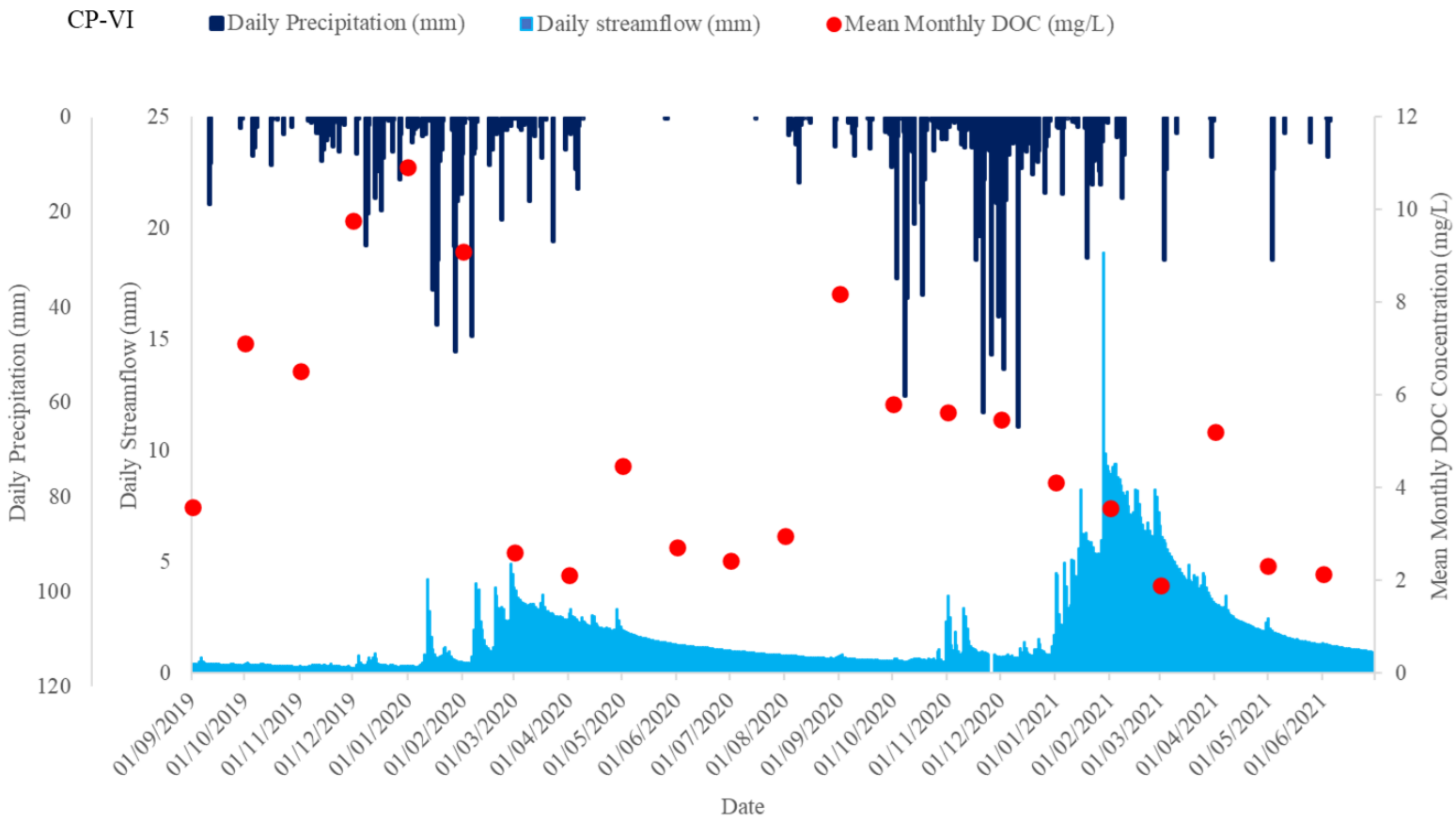


Figure 7.4: Correlations between daily rainfall (mm), daily streamflow (mm) and mean monthly DOC concentrations (mg/L) within the piezometers for CP-VI

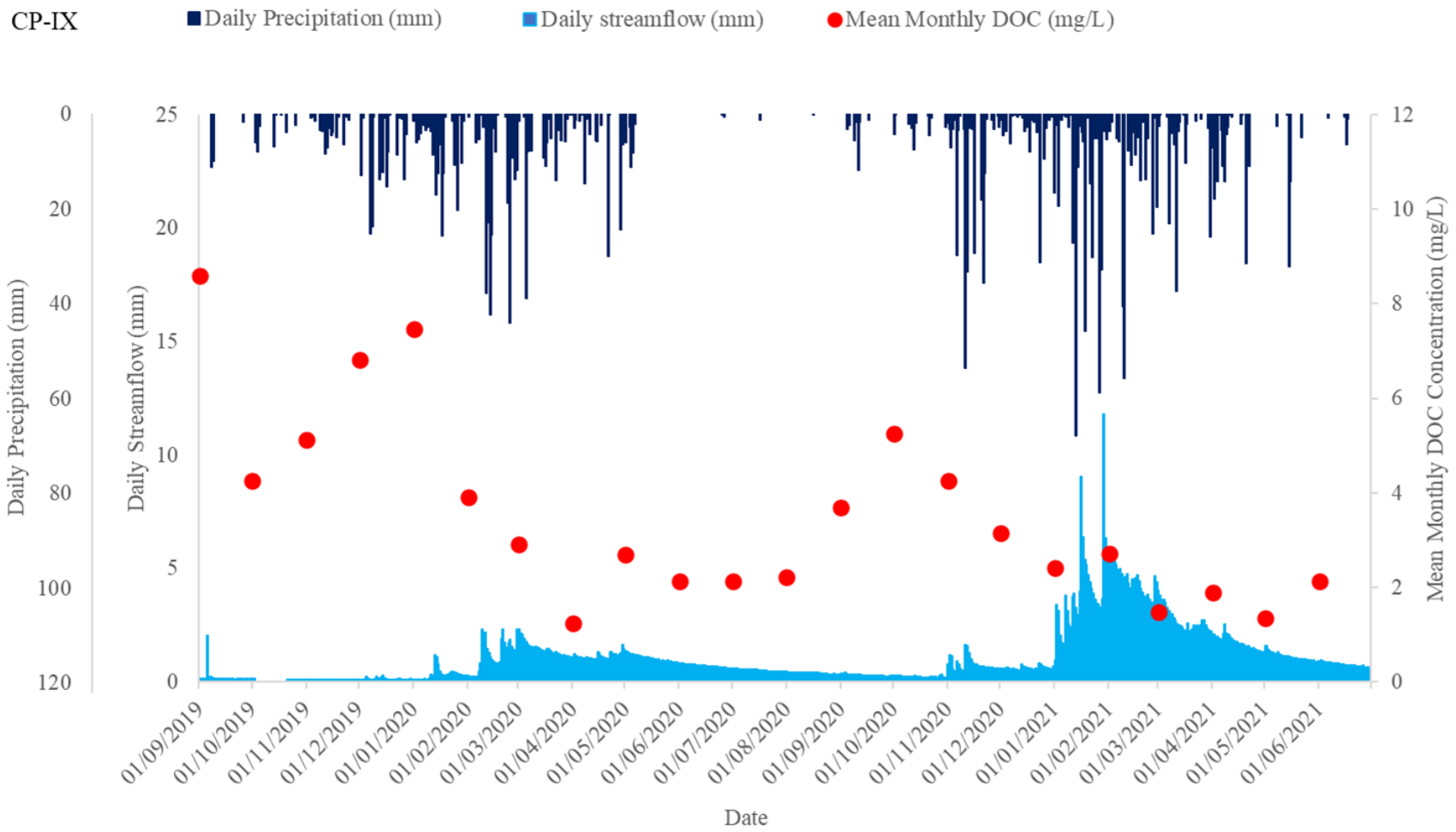


Figure 7.5: Correlations between daily rainfall (mm), daily streamflow (mm) and mean monthly DOC concentrations (mg/L) within the piezometers for CP -IX

Scatter plots of the mean monthly DOC concentrations compared to mean monthly changes in the depth to water table height within the piezometers did not show any difference between the seasons. This is most likely due to some of the piezometers becoming saturated during the sampling period and maintaining this saturation for the remainder of the sampling period. This is particularly so for the piezometers located within the wetland areas.

Figure 7.6 and Figure 7.7 provide plots of all the climatic variables measured in CP-VI and CP-IX compared against the mean monthly DOC concentrations in the piezometers. With regards to the average monthly temperature, there is an increase and decrease in the average monthly DOC concentrations with a relative increase and decrease in temperature for both catchments. Spring to summer months (September to March) have the highest mean DOC concentrations (6.55 mg/L and 5.04 mg/Lin CP-VI and CP-IX respectively) as compared to autumn and winter months (April to August) (4.41 mg/Land 2.23 mg/Lin CP-VI and CP-IX respectively).

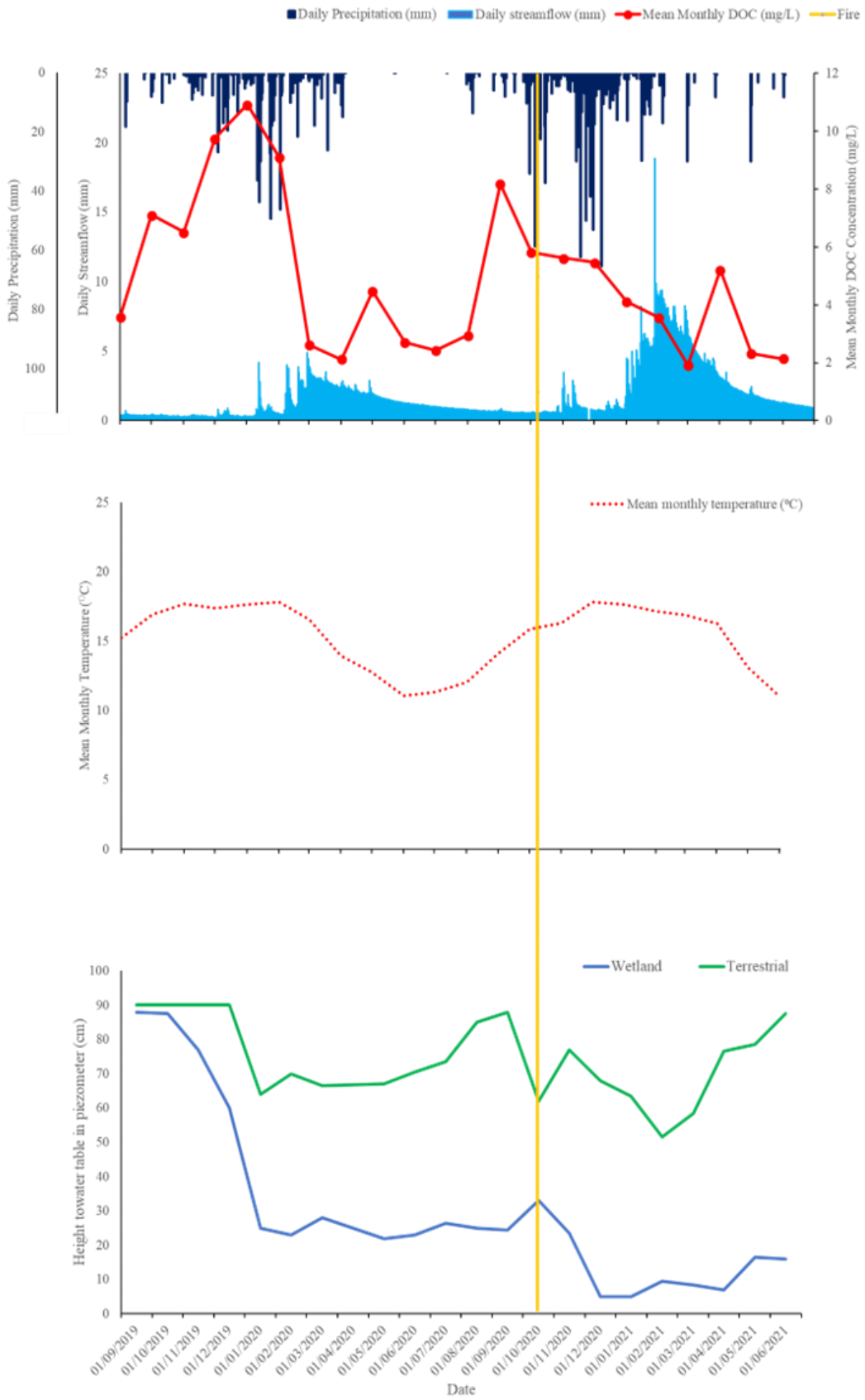


Figure 7.6: Plots of all climatic variables as well as the height to the water table in the piezometers compared against the mean monthly DOC concentrations in the piezometers for CP-VI

CP-IX

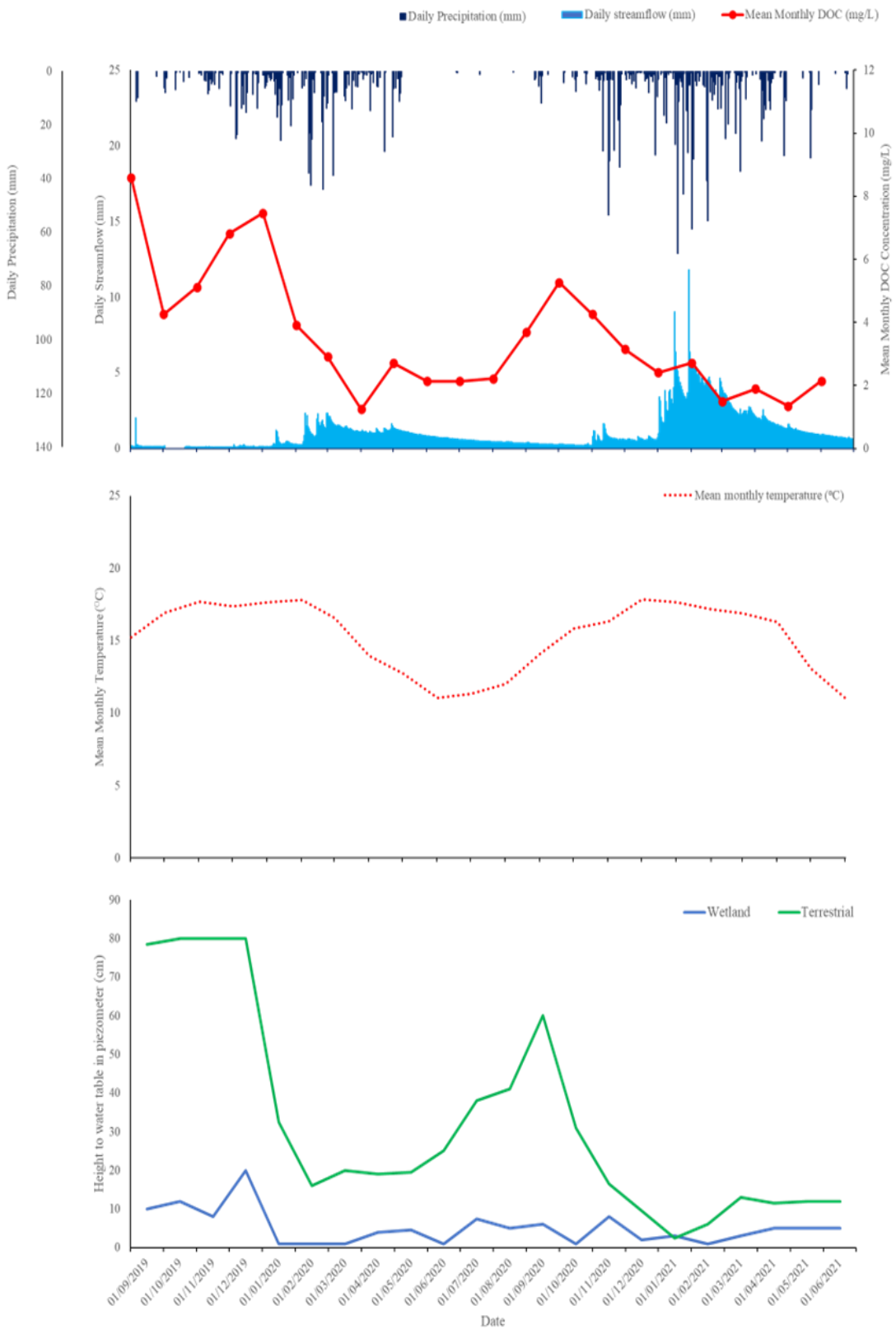


Figure 7.7: Plots of all climatic variables as well as the height to the water table in the piezometers compared against the mean monthly DOC concentrations in the piezometers for CP-IX

### *7.3.2. Physical characteristics of the catchments and DOC*

Characteristics of the soils in which the piezometers were placed are displayed in Table 7.2. Saturated responsive soils had higher organic matter content as well as carbon percentage across both catchments with mean organic matter percentages of 35.4% in the saturated responsive soils and 22.5% in the interflow soils of CP-VI and 32.4% in the saturated responsive soils and 21.4% in the interflow soils of CP-IX. Carbon percentages were higher in the saturated responsive soils (mean of 11.77% ± 5.7 in CP-VI and 7.61% ± 1.1 in CP-IX) compared to the interflow soils (mean of 5.91% ± 1.0 in CP-VI and 5.48% ± 0.81 in CP-IX).

Table 7.2: Soil characteristics associated with the piezometers

| **Piezometer Name and position in the catchment** | **Hydropedological soil group** | **Depth of Piezometer mm (to the gley or gleyic horizon)** | **Average Organic matter content (%)** | **Average Carbon %** |
|---|---|---|---|---|
| C6-3 (Upper position) | Saturated responsive | 1405 | 25.72 ±3.69 | 6.79 ±1.99 |
| C6-6 (Upper position) | Interflow | 1480 | 22.73 ±3.26 | 5.82 ±2.68 |
| C6-7 (Mid position) | Saturated responsive | 590 | 32.60 ±3.97 | 7.70 ±3.74 |
| C6-8 (Mid position) | Interflow | 1530 | 23.08 ±3.99 | 7.24 ±3.63 |
| C6-9 (Mid position) | Saturated responsive | 1340 | 43.64 ±8.09 | 11.34 ±2.38 |
| C6-10 (Mid position) | Saturated responsive | 1460 | 44.21 ±5.59 | 21.25 ±3.81 |
| C6-11 (Lower position) | Interflow | 710 | 21.80 ±4.98 | 4.69 ±3.54 |
| C9-1 (Upper position) | Interflow | 910 | 22.16 ±4.54 | 4.55 ±1.58 |
| C9-2 (Upper position) | Interflow | 930 | 18.31 ±3.92 | 5.37 ±3.20 |
| C9-3 (Upper | Saturated responsive | 280 | 22.52 ±4.00 | 9.23 ±2.25 |

| Piezometer Name and position in the catchment | Hydropedological soil group | Depth of Piezometer mm (to the gley or gleyic horizon) | Average Organic matter content (%) | Average Carbon % |
|---|---|---|---|---|
| position) | | | | |
| C9-4 (Mid position) | Saturated responsive | 685 | 55.17 ±7.93 | 6.58 ±0.25 |
| C9-5 (Mid position) | Saturated responsive | 840 | 27.02 ±5.20 | 8.57 ±2.90 |
| C9-6 (Mid position) | Interflow | 1930 | 23.74 ±4.26 | 6.54 ±4.76 |
| C9-9 (Lower position) | Saturated responsive | 730 | 25.02 ±1.85 | 6.57 ±2.44 |

Concerning DOC concentrations, the results of the Kruskal-Wallis test for CP-VI and CP-IX are displayed in Table 7.3 and the boxplots for the DOC concentrations for each category of the physical characteristic of the catchments are displayed in Figure 7.8. The categories for the physical characteristics include land cover, hydropedological soil group, topographical position of the piezometer within the catchment and the slope curvature profile.

Mean values range from 3.61 mg/L ± 2.76 to 6.29 mg/L ± 5.64 within CP-VI and 2.53 mg/L ± 1.94 to 5.01 mg/L ± 4.04 in CP-IX across all categories. There are statistical differences in the land cover ($p < 0.05$ in CP-VI; $p < 0.001$ in CP-IX) and hydropedological soil group ($p < 0.001$ in CP-VI; $p < 0.05$ in CP-IX) in both catchments. Furthermore, there is a statistical difference in the topographical position of the piezometer within the catchment in CP-VI ($p < 0.01$) but not within CP-IX ($p = 0.942$). There is no statistical difference in the slope curvature profiles in either catchment ($p = 0.306$ in CP-VI and $p = 0.907$ in CP-IX).

Thus, DOC concentrations are higher in the wetland vegetation land cover (mean = 6.29 mg/L ± 5.6 in CP-VI and 4.60 mg/L ± 4.0 in CP-IX) as compared to the terrestrial vegetation land cover (mean = 4.06 mg/L ± 3.8 in CP-VI and 2.53 mg/L ± 1.9 in CP-IX) and higher in the saturated responsive soils (mean = 6.29 mg/L ± 5.6 in CP-VI and 4.05 mg/L ± 3.7 in CP-IX) as compared to the interflow soils (mean = 3.61 mg/L ± 2.7 in CP-VI and 3.21 mg/L ± 3.09 in

CP-IX). A multiple pairwise comparison using the Dunn's procedure was undertaken on the topographical position of the piezometers within the catchments as the degree of freedom for this category is 2. Results show that within CP-VI there is a statistical difference between the upper catchment (mean = 3.05 mg/L ± 2.7) and the lower (mean = 5.60 mg/L ± 5.1) and mid catchment (mean = 5.58 mg/L ± 3.4) positions. There is no statistical difference between the mid and lower catchment positions. This is due to the majority of wetland systems within this area of the catchment. In CP-IX the lower catchment position seems to show the greatest mean value (5.01 mg/L ± 6.5) for DOC concentration compared to the mid (3.34 mg/L ± 2.1) and upper positions (3.38 mg/L ± 2.59), however these were not significantly different ($p = 0.942$). Convex slopes seem to have the highest mean DOC values (5.43 mg/L ± 5.7 in CP-VI; 4.10 mg/L ± 4.4 in CP-IX) compared to concave slopes (5.35 mg/L ± 3.9 in CP-VI; 3.40 mg/L ± 2.4 in CP-IX) in both catchments however these were not significantly different ($p = 0.360$ in CP-VI; $p = 907$ in CP-IX).

A comparison between the saturated responsive soils, the interflow soils, the wetland vegetation and terrestrial vegetation groups of CP-VI and CP-IX was also conducted using the Kruskal-Wallis test. There is a statistical difference between the saturated responsive soil group of CP-VI and CP-IX ($p = 0.00$), but no statistical difference between the interflow soil group ($p = 0.79$) as well as the wetland vegetation ($p=0.08$) and the terrestrial vegetation group ($p = 0.07$).

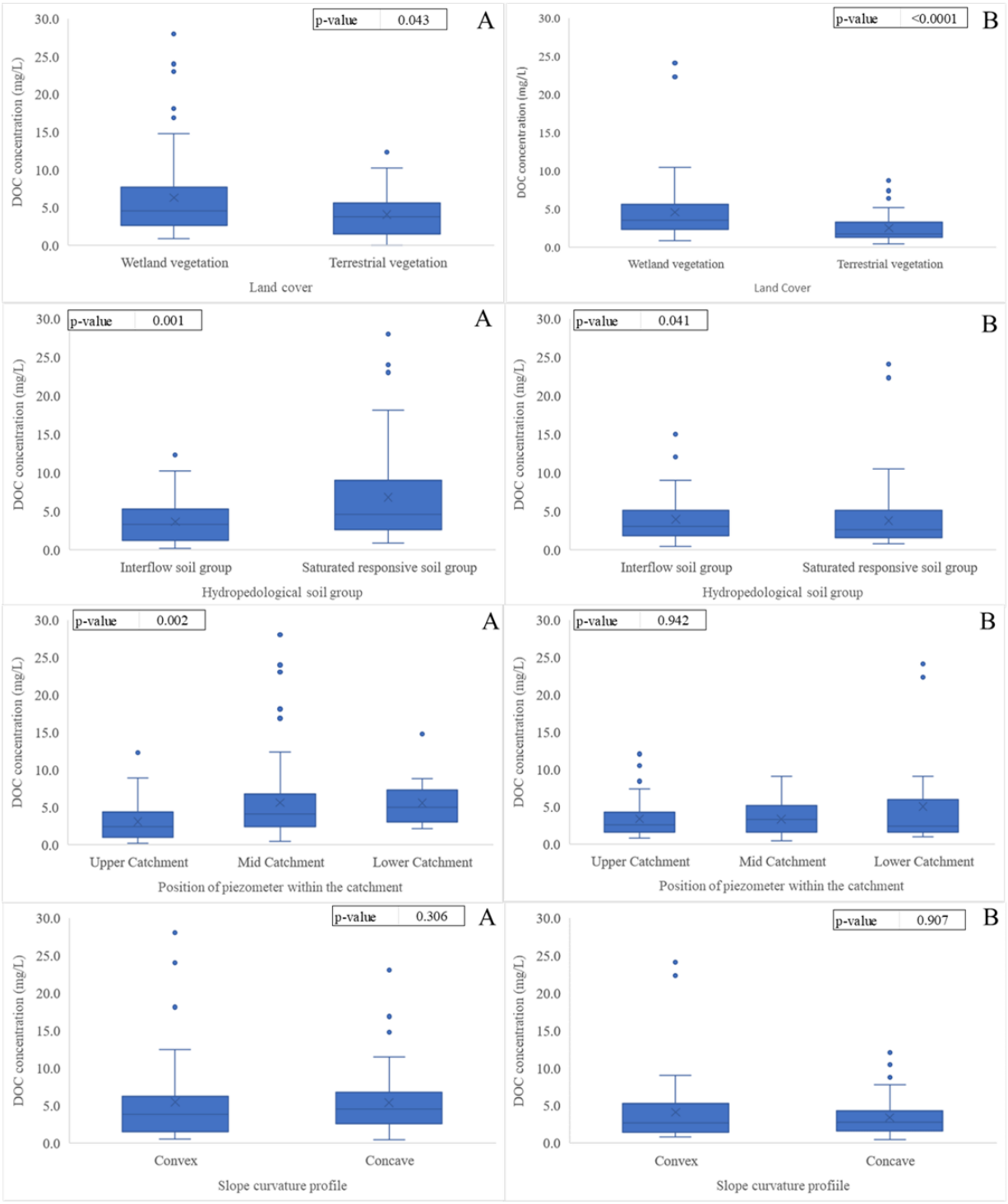


Figure 7.8: Boxplots showing the minimum, first quartile, median, third quartile, and maximum values for the range in DOC concentrations (mg/L) for the land cover, hydropedological soil groups, position of the piezometer within the catchment, and the slope curvature profile for (A) CP-VI and (B) CP-IX

Table 7.3: Statistical results for CP-VI and CP-IX

| Catchment | Physical characteristic of the catchment | | DOC Concentration ( mg/L) | | | Kruskal-Wallis test | | | | |
|---|---|---|---|---|---|---|---|---|---|---|
| | | | Minimum | Maximum | Mean | Degree of freedom | K (Observed value) | K (Critical value) | p-value (one-tailed) | Significant |
| CP-VI | Land cover | Wetland vegetation | 0.85 | 28.00 | 6.29 ±5.64 | 1 | 4.083 | 3.841 | 0.043 | Yes |
| | | Terrestrial vegetation | 0.19 | 12.31 | 4.06 ±2.83 | | | | | |
| | Hydropedological Soil Group | Saturated responsive soils | 0.85 | 28.00 | 6.29 ±5.64 | 1 | 10.128 | 3.841 | 0.001 | Yes |
| | | Interflow soils | 0.19 | 12.31 | 3.61 ±2.76 | | | | | |
| | Topographical position of the piezometer in the catchment | Upper catchment | 0.19 | 12.31 | 3.05 ±2.76 | 2 | 12.808 | 5.991 | 0.002 | Yes |
| | | Mid catchment | 0.41 | 28.00 | 5.60 ±5.17 | | | | | |
| | | Lower catchment | 2.15 | 14.78 | 5.58 ±3.42 | | | | | |
| | Slope profile | Convex slope | 0.48 | 28.00 | 5.43 ±5.71 | 1 | 1.049 | 3.841 | 0.306 | No |
| | | Concave slope | 0.41 | 23.01 | 5.35 ±3.94 | | | | | |
| CP-IX | Land cover | Wetland vegetation | 0.90 | 24.08 | 4.60 ±4.04 | 1 | 18.571 | 3.841 | <0.0001 | Yes |
| | | Terrestrial vegetation | 0.42 | 8.75 | 2.53 ±1.94 | | | | | |
| | Hydropedological Soil Group | Saturated responsive soils | 0.76 | 24.08 | 4.05 ±3.76 | 1 | 4.187 | 3.841 | 0.041 | Yes |
| | | Interflow soils | 0.42 | 15.00 | 3.21 ±3.09 | | | | | |
| | Topographical position of the piezometer in the catchment | Upper catchment | 0.81 | 12.04 | 3.38 ±2.59 | 2 | 0.121 | 5.991 | 0.942 | No |
| | | Mid catchment | 0.40 | 9.03 | 3.34 ±2.16 | | | | | |
| | | Lower catchment | 0.98 | 24.08 | 5.01 ±6.50 | | | | | |

| Catchment | Physical characteristic of the catchment | | DOC Concentration ( mg/L) | | | Kruskal-Wallis test | | | | |
|---|---|---|---|---|---|---|---|---|---|---|
| | | | Minimum | Maximum | Mean | Degree of freedom | K (Observed value) | K (Critical value) | p-value (one-tailed) | Significant |
| | Slope profile | Convex slope | 0.76 | 24.08 | 4.10 ±4.49 | 1 | 0.014 | 3.841 | 0.907 | No |
| | | Concave slope | 0.42 | 12.04 | 3.40 ±2.43 | | | | | |

## 7.4. DISCUSSION

### *7.4.1. DOC concentration in piezometers and seasonality*

The seasonal trends of rainfall as well as the temperature variations experienced in the Cathedral Peak catchments had an effect on the DOC concentrations in the piezometers. Maximum DOC concentrations were recorded in the spring-summer months and minimum DOC concentrations were recorded in the autumn-winter months. Several studies have identified similar trends in the relationship between DOC concentration and the variation in rainfall and temperature over different seasons (Hongve et al., 2004, Don and Schulze, 2008, Erlandsson et al., 2008, van den Berg et al. 2012,) with DOC concentrations often increasing significantly during storm events (Ran et al. 2013, Jung et al. 2014, Lee et al. 2019b).

In this study there was a seasonal correlation between DOC concentrations within the piezometers and the streamflow discharge, however no linear relationship was identified. This could be explained by the hydrological conditions of the catchment areas as a result of the drought experienced in 2019. It is hypothesized that a lag time effect took place in which the wetland areas were re-saturated following the onset of rain after the drought broke in early 2020. During this period the wetlands did not predominantly contribute to the streamflow. This is shown in both the rainfall events and water table height of the wetland piezometers compared to the streamflow discharge plots (Figures 7.6 and 7.7). Firstly, the piezometers in the wetland areas in both catchments reach saturation in January 2020 following the beginning of the rains after the drought, with the streamflow discharge from the catchment increasing in value in February to March of the same year. This scenario is shown again, albeit to a lesser degree in the same plots from both catchments, when, following the drier winter period, the piezometers in the wetland areas reach saturation in November/December 2020, while the streamflow discharge values increase in January/February 2021. This shows that while the wetlands were becoming saturated, they did not contribute substantially to the streamflow, but once the wetlands were saturated these could then contribute quickly to the streamflow discharge as overland flow, increasing the quantity of streamflow discharging from the catchment areas.

The DOC values within the piezometers however spiked in the preceding months before saturation was obtained in both catchment areas. Several studies have identified similar trends in DOC concentration, with increases in DOC values recorded following dry conditions (Ritson et al. 2017, Harjung et al. 2018, Coulson et al. 2022). These studies show that the desiccation

of soils may decrease the microbial biomass as well as change the composition of the microbial community as a result of some microbial communities resisting desiccation better than others. Once the rains start again, pulses of water with strongly enhanced DOC concentrations are released. This DOC and nutrient pulse originate from organic matter accumulated in the terrestrial ecosystem during drought, as well as in fluvial sediments during the dry phase (Coulson et al. 2022).

The trends in the level of saturation of the wetlands and the DOC concentration was observed in both catchments. The understanding of the dynamics of the wetlands within a catchment is therefore important. A number of studies have identified good correlations between the abundance of saturated wetland areas and the DOC concentrations within streamflow discharge of a catchment (Morel et al. 2009, van den Berg et al. 2012, Huntington and Aiken, 2013).

### *7.4.2. Effect of wetlands on DOC concentration*

Wetland vegetation and the saturated responsive soil group had the highest concentration of DOC across both catchments. This is likely due to the soils associated with the saturated responsive soil group (wetland areas) having a higher organic matter and carbon percentage as compared to the interflow soil group (terrestrial vegetation). Studies have highlighted that microbial activity degrades SOC into DOC or mineralises SOC into dissolved inorganic carbon (Bengston and Bengtsson, 2007, Chow et al. 2006, Li et al. 2019) and this may be a further study that is required in the understanding of the dynamics of the attenuation and export of DOC within these catchment areas. It has also been hypothesised that DOC can be absorbed by metal elements within the soil, such as iron and/or aluminium, but this is dependent on the organic matter dynamics in the soil (Buurman & Jongmans, 2005; Wu et al., 2012). Buurman and Jongmans, (2005) showed that in hydromorphic soils, the breakdown of organic carbon (OC) can be inhibited by complexed aluminium and iron within the soil, soil acidity, or lack of oxygen and therefore lower microbial activity, leading to an accumulation of OC within these areas. This could be a further explanation for the increase in OC in the saturated responsive soil group in this study leading to a higher concentration of DOC in the piezometers located in this group.

A statistical difference was identified between the upper and mid and lower positions of the piezometers within CP-VI, but no statistical difference was identified in the topographical position of the piezometers in CP-IX. This can be explained utilising the hydropedological soil

group maps (Figure 7.3) which show that the mid slopes of CP-VI are dominated by wetland systems with the majority of piezometers concentrated within this area. The wetland systems in CP-IX are spread out across the upper, mid, and lower positions of the catchment area, thus allowing for a more evenly distributed concentration of piezometers within this catchment area. Slope curvature did not show any significant differences between the concave and convex slopes in this study. This is most likely due to the wetlands within both catchments encompassing both convex and concave slopes within their microtopography. The presence of the wetland as a whole system was a greater indicator for higher DOC concentrations. Similar findings have been recorded by Huntington and Aiken (2013) as well as Lee et al. (2019b).

### *7.4.3. The effect of land cover on DOC concentrations in the piezometers*

A comparison of the DOC concentration from the piezometers in the wetlands in CP-VI and CP-IX shows a slightly greater concentration of DOC in CP-VI (mean of 6.29 mg/L ± 5.6 in CP-VI and a mean of 4.60mg/L ± 4.04 in CP-IX). The effect of land cover may be attributed to this difference. CP-VI is a mesic grassland catchment, interspersed with wetland systems that is burned biennially during spring. CP-IX was a grassland ecosystem, like CP-VI, but is changing to a woody dominated catchment, interspersed with wetland systems, as a result of fire exclusion. Fire is utilised as a management tool in CP-VI, and this may have an effect on the DOC concentrations. The effects of fire on DOC concentrations, have shown variation across space and time. In a study conducted by Uzan et al. (2020) wildfires had an effect on the water quality of the affected areas compared to a reference state. DOC values were significantly higher within the first year after a burn, but then returned to levels similar to the reference state within the second year.

In another study, Novora et al. (2013) experimented on the effects of using fire as a grassland management tool on the SOC stocks. Results of this study show no significant difference observed in the SOC before and after fire. In a further study conducted by Kim et al. (2016), forest fires set as a management tool did not significantly alter the organic carbon composition of the mineral soil associated with these areas. As SOC stocks have an impact on the DOC concentrations of an area, the effect of fire can induce an increase in DOC concentrations, but this does not appear to be long-lasting. In the studies the fire temperature was kept low, and this may be a determining factor in the impact of fire on DOC concentrations. González-Pérez et al. (2004) identified that the effect of fire on soil organic matter is dependent on a number of factors including the type and intensity of fire, the soil moisture at the time of the fire as well

as post recovery, the soil type, the microbial activity, and the nature of the land cover that is burned.

In a review on the effect of land use and burning on organic matter in South African soils, du Preez et al. (2011) identified that studies show that long-term burning regimes in grasslands led to a decrease in SOC up to a depth of 20 mm as a result of annual and biennial winter burning, whereas burning in spring did not affect the OC content. A recent study by Findlay et al. (2022) in the Cathedral Peak area showed an increase in SOC stocks with the use of long-term frequent fires as part of the management of these areas. This was ascribed to the acidic nature as well as the high organic matter content within these soils. This study attributed the increase in SOC stocks to an equilibria that exists between $CO_2$ and the clay mineral kaolinite that generates enough acidity to dissolve clay minerals and sustain concentrations of aluminium ($Al^{3+}$). These concentrations of $Al^{3+}$ are required for the complexation of carboxylate groups in SOM, protecting it from microbial decomposition. Similar findings, regarding the influence of $Al^{3+}$on dissolved organic matter (DOM), of which DOC forms a component, were obtained in two studies by Scheel et al. (2007 and 2008). Here it was determined that concentrations of $Al^{3+}$ reduce the bioavailability of DOM after its rainfall against microbial decay. This is particularly so at low pH values. The 2008 study went on to show that concentrations of $Al^{3+}$ do not reduce availability of DOM to microbes through toxicity but rather inhibit DOM availability through the formation of organo-Al precipitates.

In this study the effect of the management fire that was burned on the 7$^{th}$ October 2020, had no effect on the DOC concentrations in CP-VI. No elevation in DOC concentration was recorded in the piezometers between September 2020 (monthly average of 5.81 mg/L), October 2020 (monthly average of 5.61 mg/L) and November 2020 (monthly average of 5.47 mg/L). This may be explained, as is the case in the González-Pérez et al. (2004), and Kim et al. (2016) studies, by the low fire intensity used in the management of CP-VI.

Further to the discussion on the impact of land management on the DOC concentrations in CP-VI and CP-IX, a statistical difference between the saturated responsive soils ($p = 0.00$) in CP-VI and CP-IX was recorded, but no statistical difference was recorded between the interflow soil group ($p = 0.79$) as well as the wetland vegetation ($p = 0.08$) and terrestrial vegetation ($p = 0.07$) land cover groups. As the two catchment areas are managed differently, one would expect significant differences between all groups when comparing the two catchment areas. As

this was not the case, it is more likely the amount of SOC present in the wetlands, of each catchment, that has a larger effect on the recorded DOC concentrations within the piezometers.

Numerous factors are therefore influencing the concentration of DOC within both catchment areas. Studies that have focused on land cover, soil type and characteristics and fire regimes have all found variations in the contributions of these aspects to the concentration in DOC. This suggests that DOC concentrations within a particular catchment are highly variable, and no generalized trends can be recommended. It is difficult to explain impacts on DOC concentration based solely on one aspect. Despite this, the contribution of wetlands to the DOC concentrations in the Cathedral Peak catchments is evident. Wetland ecosystems are formed as a result of the surrounding landscape in which they are situated (Branton and Robinson, 2020) and can thus occur under differing land types, topographical positions, slope profiles and soil types. It is this heterogeneity of wetland systems that demonstrates that one should examine a combination of the environmental drivers of DOC concentrations within a catchment area. It is most likely that there are interactions between the different environmental drivers and the product of the impact of these drivers on the DOC concentration is greater than the effect of each individual driver alone (Clark et al. 2010).

## 7.5. CONCLUSION

DOC production and transport have been identified as being sensitive to climatic drivers including seasonal rainfall and temperature. Furthermore, this study has identified similar findings to previous studies regarding the presence of wetland systems being a major driver in DOC concentrations. The effects of the 2019 drought on the dynamics of the movement of water through the Cathedral Peak catchment areas, the streamflow discharge and how these interrelate to the DOC concentrations was observed. The connectivity of the wetlands to the streams within both catchments plays a role in the attenuation and export of DOC within these watersheds. The effects of land cover as well as the fire management regimes of the catchment areas, did not provide definitive results regarding the contribution of these factors to the DOC concentrations. The DOC concentrations are more likely affected by the SOC concentrations within the wetland systems of each catchment.

Given the sensitivity of DOC export to climatic factors, climate changes may affect the export of DOC through changes in flow rates and pathways, and changes in rates of decomposition.

This is particularly so with changes in the hydrologic conditions that would affect wetland abundance, wetland type as well as their connectivity to the stream. Effects of increasing drought as well as increasing intensity of storms could also play a role in the accumulation and transport of DOC within these Afromontane catchments. Further studies on DOC within these catchments should include incorporating stable isotopes to determine the origin of the DOC, the effect of microbial activity, as well as the effect of the fire management regimes. This will aid in understanding the contribution of DOC to the overall carbon budget of these catchment areas.

## 7.6. REFERENCES

Aufdendkampe, A., Mayorga, E., Raymond, P., Melack, J., Doney, S., Alin, S., Aalto, R., and Yoo, K. (2011). Riverine coupling of biogeochemical cycles between land, ocean and atmosphere. Frontiers in Ecology and the Environment. 9. 53-60. DOI:10.1890/100014.

Ball, D.F. (1964). Loss-on-Ignition as an estimate of organic matter and organic carbon in non-calcareous soils. Journal of Soil Science. 15. 84–92.

Battin, T.J., Luyssaert, S., Kaplan L.A., Aufdenkampe, A.K., Richter, A., and Tranvik, L.J. (2009). The boundless carbon cycle. Nature Geoscience. 2: 598–600.

Bengston, P., and Bengtsson, G. (2007). Rapid turnover of DOC in temperate forests accounts for increased CO2 production at elevated temperatures. Ecology Letters. 10. 9. 783-790. DOI: 10.1111/j.1461-0248.2007.01072.x.

Billett, M. Deacon, C., Palmer, S., Julián, J.M., and Hope, D. (2006). Connecting organic carbon in stream water and soils in a peatland catchment. Journal of Geophysical Research. 111. DOI:10.1029/2005JG000065.

Bolan, N. S., Adriano, D. C., Kunhikrishnan, A., James, T., Mc-Dowell, R., and Senesi, N. (2011). Chapter one – dissolved organic matter: Biogeochemistry, dynamics, and environmental significance in soils. Advances in Agronomy. 110. 1–75. DOI:10.1016/B978-0-12-385531-2.00001-3.

Bosch, JM. (1979). Treatment effects on annual and dry period streamflow at Cathedral Peak. South African Forestry Journal, 108(1): 29-38.

Boyer, E. W., Hornberger, G. M., Bencala, K. E., and McKnight, D. M. (1997). Response characteristics of DOC flushing in an Alpine catchment. Hydrological Processes. 11. 1635–1647.

Branton, C., and Robinson, D.T. (2020). Quantifying Topographic Characteristics of Wetlandscapes. Wetlands. 40. 433-449. DOI: 10.1007/s13157-019-01187-2.

Buurman, P., and Jongmans, A.G. (2005). Podzolisation and soil organic matter dynamics. Geoderma. 125. 71-83. DOI:10.1016/j.geoderma.2004.07.006.

Camino-Serrano, M., Guenet, B., Luyssaert, S., Ciais, P., Bastrikov, V., De Vos, B., Gielen, B., Gleixner, G., Jornet-Puig, A., Kaiser, K., Kothawala, D., Lauerwald, R., and Peñuelas, J., Schrumpf, M., Vicca, S., Vuichard, N., Walmsley, D., and Janssens, I. A. (2018).ORCHIDEE-SOM: modeling soil organic carbon (SOC) and dissolved organic carbon (DOC) dynamics along vertical soil profiles in Europe. Geoscientific Model Development. 11.3. DOI: 10.5194/gmd-11-937-2018.

Chow, A., Tanji, K., Gao, S., and Dahlgren, R. (2006). Temperature, water content and wet–dry cycle effects on DOC production and carbon mineralization in agricultural peat soils. Soil Biology and Biochemistry. 38. 477-488. DOI: 10.1016/j.soilbio.2005.06.005.

Cias, P., Chris, S., Govindasamy, B., Bopp, L., Brovkin, V., Canadell, J., Chhabra, A., Defries, R., Galloway, J., and Heimann, M. (2013). Carbon and other biogeochemical cycles. Climate Change 2013: The Physical Science Basis, 465–570.

Clair, T. A., Pollack, T.L., and Ehrman, J.M. (1994). Exports of carbon and nitrogen from river basins in Canada's Atlantic provinces, Global Biogeochemical Cycles. 8. 441–450.

Clark, J.M., Bottrell, S.H., Evans, C.D., Monteith, D.T., Bartlett, R., Rose, R., Newton, R.J., Chapman, P.J. (2010). The importance of the relationship between scale and process in understanding long-term DOC dynamics. Science of The Total Environment. 408. 13. doi.org/10.1016/j.scitotenv.2010.02.046.

Cole JJ and Caraco NF. 2001. Carbon in catchments: connecting terrestrial carbon losses with aquatic metabolism. Marine and Freshwater Research. 52. 101–10.

Coulson, L.E., Weigelhofer, G., Gill, S., Hein, T., Griebler, C., and Schelker, J. (2022). Small rain events during drought alter sediment dissolved organic carbon leaching and respiration in

intermittent stream sediments. Biogeochemistry. 159. 159–178. DOI:10.1007/s10533-022-00919-7.

Dawson, J. J. C., Billett, M. F., Neal, C., and Hill, S. (2002), A comparison of particulate, dissolved and gaseous carbon in two contrasting upland streams in the UK, Journal of Hydrology. 257. 226– 246.

de Menezes, M.D., Silva, S.H.G., Owens, P.R., and Curi, N. (2014). Solum depth spatial prediction comparing conventional with knowledge-based digital soil mapping approaches. Scientia Agricola. Vol. 71. No. 4. doi.org/10.1590/0103-9016-2013-0416.

Dixon, R.K., Solomon, A.M., Brown, S., Houghton, R.A., Trexier, M.C., and Wisniewski, J. (1994). Carbon Pools and Flux of Global Forest Ecosystems. Science. 263. 185–190.

Don, A., and Schulze, E.D. (2008). Controls on fluxes and export of dissolved organic carbon (DOC) in grasslands with contrasting soil types. Biogeochemistry. 91. 117-131. DOI: 10.1007/s10533-008-9263-y.

du Preez, C.C., van Huyssteen, C., and Pearson, M. (2011). Land use and soil organic matter in South Africa: 1. A review of spatial variability and the influence of rangeland stock production. Land use and soil organic matter in South Africa: 1. A review of spatial variability and the influence of rangeland stock production. South African Journal of Science. 107. 27-34. DOI: 10.4102/sajs.v107i5/6.354.

Eckhardt, B., and Moore T. R. (1990). Controls on dissolved organic carbon concentrations in streams, southern Quebec, Canada. Journal of Fisheries and Aquatic Sciences. 47. 1537–1544.

Erlandsson, M., Buffam, I., Fölster, J., Laudon, H., Temnerud, J., Weyhenmeyer, G.A., and Bishop. K. (2008). Thirty-five years of synchrony in the organic matter concentrations of Swedish rivers explained by variation in flow and sulphate. Global Change Biology 14. 1191–1198. DOI:10.1111/j.1365-2486.2008. 01551.x.

Everson, C.E., Molefe, G.L., and Everson, T.M. (1998). Monitoring and modelling components of the water balance in a grassland catchment in the summer rainfall area of South Africa. Water Research Commission. RSA. Report 493/1/98.

Fernández, I., Cabaneiro, A., and Carballas, T. (1997). Organic matter changes immediately after a wildfire in an Atlantic forest soil and comparison with laboratory soil heating. Soil Biology & Biochemistry. 29. 1–11.

Findlay, N., Manson, A., Cromsigt, J., Gordijn, P., Nixon, C., Rietkerk, M, Thibaud, G., Wassen, M.J., and te Beest, M. (2022). Long-term frequent fires do not decrease topsoil carbon and nitrogen in an Afromontane grassland. African Journal of Range & Forage Science. 39.1. 44-55. DOI: 10.2989/10220119.2021.2016966.

Fu, J., Gasche, R., Wang, N., Lu, H., Butterbach-Bahl, K., and Kiese, R. (2019). Dissolved organic carbon leaching from montane grasslands under contrasting climate, soil and management conditions. Biogeochemistry. 145. 1-15. DOI: 10.1007/s10533-019-00589-y.

Galy, V., Peucker-Ehrenbrink, B., and Eglinton, T. (2015). Global carbon export from the terrestrial biosphere controlled by erosion: Nature. 521. 204-207. DOI: 10.1038/nature14400.

Garcia-Pausas, J., Casals, P., Camarero, L., Huguet, C., Sebastia, M. Thompson, R., and Romanyà, J. (2007). Soil organic carbon storage in mountain grasslands of the Pyrenees: Effects of climate and topography. Biogeochemistry. 82. 279-289. DOI:10.1007/s10533-007-9071-9.

Garcia-Pausas, J., Romanyà, J., Montané, F., Rios, A., Taull, M., Rovira, P., and Casals, P. (2017). Are Soil Carbon Stocks in Mountain Grasslands Compromised by Land-Use Changes?. DOI:10.1007/978-3-319-55982-7_9.

González-Pérez, J., González-Vila, F.J., Almendros, G., and Heike, K. (2004). The effect of fire on soil organic matter—a review. Environment International. 30. 855-70. DOI: 10.1016/j.envint.2004.02.003.

Gordijn, P.J., Everson, T.M., and O'Connor, T.G. (2018). Resistance of Drakensberg grasslands to compositional change depends on the influence of fire-return interval and grassland structure on richness and spatial turnover. Perspectives in Plant Ecology, Evolution and Systematics. 34. 26-36. https://doi.org/10.1016/j.ppees.2018.07.005.

Gordijn, P.J., and O'Connor, T.G. (2021). Multidecadal effects of fire in a grassland biodiversity hotspot: Does pyrodiversity enhance plant diversity? Ecological Applications. 00(00): e02391. 10.1002/eap.2391.

Granger, J.E., and Schulze, R.E. (1977). Incoming solar radiation patterns and vegetation response: examples from the Natal Drakensberg. Vegetatio. 35. 47–54.

Grieve, I. C. (1990). Seasonal, hydrological and land management factors controlling dissolved organic carbon concentrations in the Loch Fleet catchments, southwest Scotland, Hydrological Processes. 4. 231–239.

Harjung, A., Ejarque, E., Battin, T., Butturini, A., Sabater, F., Stadler, M., and Schelker, J. (2018). Experimental evidence reveals impact of drought periods on dissolved organic matter quality and ecosystem metabolism in subalpine streams: DOM and metabolism under drought. Limnology and Oceanography. 64. DOI:10.1002/lno.11018.

Hibbard, K.A., Schimel, D.S., Archer, S., Ojima, D.S., and Parton, W. (2003). Grassland to woodland transitions: integrating changes in landscape structure and biogeochemistry. Ecological Applications 13. 911–926.

Hilton, R.G., Galy, A., Hovius, N., Kao, S.J., Horng, M.J., and Chen, H. (2012), Climatic and geomorphic controls on the erosion of terrestrial biomass from subtropical mountain forest. Global Biogeochemical Cycles. 26. 3. GB3014, DOI: 10.1029/2012GB004314.

Hinton, M. J., Schiff, S. L., and English, M. C. (1998), Sources and flowpaths of dissolved organic carbon during storms in two forested watersheds of the Precambrian Shield, Biogeochemistry. 41. 175–197.

Hood, E., McKnight, D.M., and Williams, M.W. (2003). Sources and chemical character of dissolved organic carbon across an alpine/subalpine ecotone, Green Lakes Valley, Colorado Front Range, United States. Water Resources Research. 39. 7. DOI: 10.1029/2002WR001738.

Hongve, D., Riise, G. and Kristiansen, J.F. (2004) Increased colour and organic acid concentrations in Norwegian forest lakes and drinking water – a result of increased precipitation? Aquatic Sciences. 66. 231–238.

Hoogsteen, M.J.J., Lantinga, E.A., Bakker, E.J., Groot, C.J., and Tittonell, P.A. (2015). Estimating soil organic carbon through loss on ignition: Effects of ignition conditions and structural water loss. European Journal of Soil Science. 66. DOI:10.1111/ejss.12224.

Huang, W., McDowell, W.H., Zou, X., Ruan, H., Wang, J., and Li, L. (2013). Dissolved Organic Carbon in Headwater Streams and Riparian Soil Organic Carbon along an Altitudinal Gradient in the Wuyi Mountains, China. PLOS One. 8. 11. https://doi.org/10.1371/journal.pone.0078973.

Huntington, T.G., and Aiken, G.R. (2013). Export of dissolved organic carbon from the Penobscot River basin in north-central Maine. Journal of Hydrology. 476. 244-256. https://doi.org/10.1016/j.jhydrol.2012.10.039.

Job, N.M. and Le Roux, P.A.L. (2019). Developing Wetland Distribution and Transfer Functions from Land Type Data as a basis for the Critical Evaluation of Wetland Delineation Guidelines by inclusion of Soil Water Flow Dynamics in Catchment Areas. Volume 2. Preliminary Guidelines to Apply Hydropedology in Support of Wetland Assessment and Reserve Determination. WRC Project No. K5/2461.

Jung, B.J., Lee, J.K., Kim, H., and Park, J. H. (2014). Export, biodegradation, and disinfection byproduct formation of dissolved and particulate organic carbon in a forested headwater stream during extreme rainfall events. Biogeosciences. 11. 6119-6129. DOI:10.5194/bg-11-6119-2014.

Kalbitz, K., Solinger, St., Park, J., Michalzik, B., and Matzner, E. (2000). Controls on the Dynamics of Dissolved Organic Matter in Soils: A Review. Soil Science. 165. 277-304. 10.1097/00010694-200004000-00001.

Kasozi, G.N., Nkedi-Kizza, P. and Harris, W.G. (2009). Varied carbon content of organic matter in Histosols, spodosols, and carbonatic soils. Soil Science Society of America Journal. 73. 1313–1318. DOI: 10.2136/sssaj2008.0070.

Kim, D.G., Taddese, H., Belay, A., and Kolka, R. (2016). The impact of traditional fire management on soil carbon and nitrogen pools in a montane forest, southern Ethiopia. International Journal of Wildland Fire. 25. 1110-1116. http://dx.doi.org/10.1071/WF16022.

Knorr, K-H. (2013). DOC-dynamics in a small headwater catchment as driven by redox fluctuations and hydrological flow paths - Are DOC exports mediated by iron reduction/oxidation cycles?. Biogeosciences. 10. 891-904. DOI:10.5194/bg-10-891-2013.

Kruskal, W. H., and Wallis, W. A. (1952). Use of ranks in one-criterion variance analysis. Journal of the American Statistical Association, 47, 583–621.

Laudon, H., Berggren, M., Ågren, A., Buffam, I., Bishop, K., Grabs, T., Jansson, M., and Köhler, S. (2011). Patterns and Dynamics of Dissolved Organic Carbon (DOC) in Boreal Streams: The Role of Processes, Connectivity, and Scaling. Ecosystems. 14. 880-893. 10.1007/s10021-011-9452-8.

Le Quéré, C., Moriarty, R., Andrew, R. M., Peters, G. P., Ciais, P., Friedlingstein, P., Jones, S. D., Sitch, S., Tans, P., Arneth, A., Boden, T. A., Bopp, L., Bozec, Y., Canadell, J. G., Chini, L. P., Chevallier, F., Cosca, C. E., Harris, I., Hoppema, M., Houghton, R. A., House, J. I., Jain, A. K., Johannessen, T., Kato, E., Keeling, R. F., Kitidis, V., Klein Goldewijk, K., Koven, C., Landa, C. S., Landschützer, P., Lenton, A., Lima, I. D., Marland, G., Mathis, J. T., Metzl, N., Nojiri, Y., Olsen, A., Ono, T., Peng, S., Peters,W., Pfeil, B., Poulter, B., Raupach, M. R., Regnier, P., Rödenbeck, C., Saito, S., Salisbury, J. E., Schuster, U., Schwinger, J., Séférian, R., Segschneider, J., Steinhoff, T., Stocker, B. D., Sutton, A. J., Takahashi, T., Tilbrook, B., van der Werf, G. R., Viovy, N.,Wang, Y.-P.,Wanninkhof, R.,Wiltshire, A., and Zeng, N. (2015). Global carbon budget 2014, Earth System Science Data. 7. https://doi.org/10.5194/essd-7-47-2015.

Lee (a), L-C., Hsu, T-C., Lee, T-Y., Shih, Y., Lin, C-Y., Jien, S-H., Hein, T., Zehetner, F., Shiah, F-K., and Huang, J-C. (2019). Unusual Roles of Discharge, Slope and SOC in DOC Transport in Small Mountainous Rivers, Taiwan. Scientific Reports. 9. 1574. DOI:10.1038/s41598-018-38276-x.

Lee (b), M.H., Lee, Y.K., Derrien, M., Choi, K., Shin, K.H., Jang, K.S., and Hur, J. (2019). Evaluating the contributions of different organic matter sources to urban river water during a storm event via optical indices and molecular composition. Water Research.165. 115006. DOI: 10.1016/j.watres.2019.115006.

Lennon, J. T., Hamilton, S.K., Muscarella, M.E., Grandy, A.S., Wickings, K., and Jones, S. E. (2013). A Source of Terrestrial Organic Carbon to Investigate the Browning of Aquatic Ecosystems. PLOS ONE 8. 10. https://doi.org/10.1371/journal.pone.0075771.

Li, X., Xu, J., Shi, Z., and Li, R. (2019). Response of Bacterial Metabolic Activity to the River Discharge in the Pearl River Estuary: Implication for CO2 Degassing Fluxes. Frontiers in Microbiology. 10. 1026. https://doi.org/10.3389/fmicb.2019.01026.

Liu, W., Jiang, Y., Yang, Q., Yang, H., Li, Y., Li, Z., Mao, W., Luo, Y., Wang, X., and Tan, Z., (2021). Spatial distribution and stability mechanisms of soil organic carbon in a tropical montane rainforest. Ecological Indicators. 129. https://doi.org/10.1016/j.ecolind.2021.107965.

Mann, C.J., Wetzel, R.G. Dissolved organic carbon and its utilization in a riverine wetland ecosystem. Biogeochemistry 31, 99–120 (1995). https://doi.org/10.1007/BF00000941.

Massey, F. J. (1951). The Kolmogorov-Smirnov Test for Goodness of Fit. Journal of the American Statistical Association, 46(253), 68–78. https://doi.org/10.2307/2280095.

Mbaye, M.L., Gaye, A.T., Spitzy, A., Dähnke, K., Afouda, A., and Gaye, B. (2016). Seasonal and spatial variation in suspended matter, organic carbon, nitrogen, and nutrient concentrations of the Senegal River in West Africa. Limnologica. 57. 1-13. doi.org/10.1016/j.limno.2015.12.003.

Montané, F., Rovira, P., and Casals, P. (2007). Shrub encroachment into mesic mountain grasslands in the Iberian Peninsula: Effects of plant quality and temperature on soil C and N stocks. Global Biogeochemical Cycles. 21. GB4016. DOI:10.1029/2006GB002853.

Montané, F., Romanyà, J., Rovira, P., and Casals, P. (2010). Aboveground litter quality changes may drive soil organic carbon increase after shrub encroachment into mountain grasslands. Plant and Soil. 337. 151-165. DOI:10.1007/s11104-010-0512-1.

Morel, B., P. Durand, A. Jaffrezic, G. Gruau, and J. Molenat. 2009. Sources of dissolved organic carbon during stormflow in a headwater agricultural catchment. Hydrological Processes. 23. 20. 2888–2901. DOI:10.1002/hyp.7379.

Mucina, L., Rutherford, M.C. & Powrie, L.W. (eds). (2006). Vegetation Map of South Africa, Lesotho and Swaziland. Edn. 2. South African National Biodiversity Institute, Pretoria. ISBN 978-1-919976-42-6.

Nänni, U.W. (1956). Forest Hydrological Research at the Cathedral Peak Research Station. Journal of the South African Forestry Association 27(1). 2-35.

Novara, A., Gristina, L., Rühl, J., Pasta, S., D'Angelo, G., La Mantia, T., Pereira, P. (2013). Grassland fire effect on soil organic carbon reservoirs in a semiarid environment. Solid Earth. 4. 381-385. DOI:10.5194/se-4-381-2013.

Ostertagová, E., Ostertag, O., & Kováč, J. (2014). Methodology and Application of the Kruskal-Wallis Test. Applied Mechanics and Materials, 611, 115–120. https://doi.org/10.4028/www.scientific.net/amm.611.115.

Pagano, T., Bida, M., Kenny, J. (2014). Trends in Levels of Allochthonous Dissolved Organic Carbon in Natural Water: A Review of Potential Mechanisms under a Changing Climate. Water. 6. 2862-2897. DOI:10.3390/w6102862.

Scheel, T., Doerfler, C., Kalbitz, K. (2007). Precipitation of Dissolved Organic Matter by Aluminum Stabilizes Carbon in Acidic Forest Soils. Soil Science Society of America Journal. 71. 64-74. DOI:10.2136/sssaj2006.0111.

Scheel, T., Jansen, B., Wijk, A., Verstraten, J., Kalbitz, K. (2008). Stabilization of dissolved organic matter by aluminium: A toxic effect or stabilization through precipitation? European Journal of Soil Science. 59. 1122 - 1132. DOI:10.1111/j.1365-2389.2008.01074.x.

Schindler, D. W. and P. J. Curtis, P.J. (1997). Dissolved Organic Carbon as an Integration of Global Stresses on Freshwater. Biogeochemistry. Vol. 36. Springer.

Soil Classification Working Group. (2018). Soil Classification: A Natural and Anthropogenic System for South Africa. ARC-Institute for Soil, Climate and Water. Pretoria.

Strohmeier, S., Knorr, K. H., Reichert, M., Frei, S., Fleckenstein, J., Peiffer, S., and Matzner, E. (2013). Concentrations and fluxes of dissolved organic carbon in runoff from a forested catchment: Insights from high frequency measurements. Biogeosciences. 10. 10.5194/bg-10-905-2013.

Smith, D.L., and Johnson, L.C. (2003). Expansion of Juniperus virginiana L. in the Great Plains: changes in soil organic carbon dynamics. Global Biogeochemical Cycles. 17.1062. DOI:10.1029/2002GB001990.

Snyman, H.A. (2003). Short-term response of a rangeland following an unplanned fire in terms of soil characteristics in a semiarid climate of South Africa. Journal of Arid Environments. 55. 160-180. DOI: 10.1016/S0140-1963(02)00252-5.

Ran, L., Lu, X.X., Sun, H., Han, J., Li, R. and Zhang, J. (2013). Spatial and seasonal variability of organic carbon transport in the Yellow River, China. Journal of Hydrology. 498. 76-88. https://doi.org/10.1016/j.jhydrol.2013.06.018.

Regnier, P., Lauerwald, R., Ciais, P. (2014). Carbon Leakage through the Terrestrial-aquatic Interface: Implications for the Anthropogenic CO2 Budget. Procedia Earth and Planetary Science. 10. 319-324. 10.1016/j.proeps.2014.08.025.

Reyna-Bowen, L., Jarosław , J., Lenin, V., Baly, V., and Ewa, B. (2019). Distribution and Factors Influencing Organic Carbon Stock in Mountain Soils in Babia Góra National Park, Poland. Applied Sciences. 9. 14. DOI:10.3390/app9153070.

Ritson, J., Brazier, R., Graham, N., Freeman, C., Templeton, M., and Clark, J. (2017). The effect of drought on dissolved organic carbon (DOC) release from peatland soil and vegetation sources. Biogeosciences. 14. 2891-2902. DOI:10.5194/bg-14-2891-2017.

Roig-Planasdemunt, M., Llorens, P., and Latron, J. (2017) Seasonal and storm flow dynamics of dissolved organic carbon in a Mediterranean mountain catchment (Vallcebre, eastern Pyrenees). Hydrological Sciences Journal. 62. 1. 50-63. DOI: 10.1080/02626667.2016.1170942.

Rutherford, J.E., and Hynes, H.B.N. (1987). Dissolved organic carbon in streams and groundwater. Hydrobiologia . 154. 33–48. https://doi.org/10.1007/BF00026829.

Ryder, E., Eyto, E., Dillane, M., Poole, R., and Jennings, E. (2014). Identifying the role of environmental drivers in organic carbon export from a forested peat catchment. The Science of the Total Environment. 490C. 28-36. DOI:10.1016/j.scitotenv.2014.04.091.

Tao, F., Zhou, Z., Huang, Y., Li, Q., Lu, X., Ma, S., Huang, X., Liang, Y., Hugelius, G., Jiang, L., Doughty, R., Ren, Z., and Luo, Y. (2020). Deep learning optimizes data-driven representation of soil organic carbon in earth system model over the conterminous United States. Front. Big Data 3. https://doi.org/10.3389/fdata.2020.00017.

Toucher, M.L., Clulow, A., van Rensburg, S., Morris, F., Gray, B., Majozi, S., Everson, C.E., Jewitt, G.P.W., Taylor, M.A., Mfeka, S., and Lawrence, K. (2016). Establishment of a more robust observation network to improve understanding of global change in the sensitive and critical water supply area of the Drakensberg. 2236/1/16. Water Research Commission, Pretoria, South Africa.

Tranvik, L.J., Downing, J.A., Cotner, J.B., Loiselle, S.A., Striegl, R.G., Ballatore, T.J., Dillon, P., Finlay, K., Fortino, K., Knoll, L.B., Kortelainene, P.L., Kutser, T., Larsen, S., Laurion, I., Leech, D.M., McCallister, S.L., McKnight, D.M., Melack, J.M., Overholt, E., Porter, J.A., Prairie, Y., Renwick, W.H., Roland, F., Sherman, B.S., Schindler, D.W., Sobek, S., Tremblay, A., Vanni, M.J., Verschoor, A.M., von Wachenfeldt, E., Weyhenmeyer, G.A. (2009). Lakes and reservoirs as regulators of carbon cycling and climate. Limnology and Oceanography. 54 (6), 2298–2314. https://doi.org/10.4319/lo.2009.54.6_part_2.2298.

Turowski, J.M., Hilton, R.G., and Sparkes, R. (2016). Decadal carbon discharge by a mountain stream is dominated by coarse organic matter. Geology. 44. 27-30. doi:10.1130/G37192.1.

Sainepo, B., Gachene, C., and Karuma, A. (2018). Assessment of soil organic carbon fractions and carbon management index under different land use types in Olesharo Catchment, Narok County, Kenya. Carbon Balance and Management. 13. DOI: 10.1186/s13021-018-0091-7.

Sheikh, M.A., Kumar, M. and Bussmann, R.W. (2009). Altitudinal variation in soil organic carbon stock in coniferous subtropical and broadleaf temperate forests in Garhwal Himalaya. Carbon Balance and Management. 4. 6. https://doi.org/10.1186/1750-0680-4-6.

Six, J., Callewaert, P., Lenders, S., De Gryze, S., Morris, S.J., Gregorich, E.G., Paul, A., and Paustian, K. (2002). Measuring and Understanding Carbon Storage in Afforested Soils by Physical Fractionation. Soil Science Society of America. 66. 1981–1987.

Uzan, H., Dahlgren, R.A., Olivares, C., Erdem, C.U., Karanfil, T., and Chow, A.T. (2020). Two years of post-wildfire impacts on dissolved organic matter, nitrogen, and precursors of disinfection by-products in California stream waters. Water Research. 181. doi.org/10.1016/j.watres.2020.115891.

van den Berg, L., Shotbolt, L., and Ashmore, M. (2012). Dissolved organic carbon (DOC) concentrations in UK soils and the influence of soil, vegetation type and seasonality. The Science of the Total Environment. 427-428. 269-76. DOI: 10.1016/j.scitotenv.2012.03.069.

van Huyssteen, C.W. (2020). Relating the South African soil taxonomy to the World Reference Base for soil resources. DOI: 10.18820/9781928424666.

van Tol, J.J., and Le Roux, P.A.L. (2019). Hydropedological grouping of South African soil forms. South African Journal of Plant and Soil. 36(3). 233-235. DOI:10.1080/02571862.2018.1537012.

Wan, M., Su, Y., Yang, X. (2014). Spatial Distribution of Soil Organic Carbon and its Influencing Factors in Desert Grasslands of the Hexi Corridor, Northwest China. PLOS ONE. DOI:10.1371/journal.pone.0094652.

Warner, K.A., Fowler, R.A., and Saros, J.E. (2020). Differences in the Effects of Storms on Dissolved Organic Carbon (DOC) in Boreal Lakes during an Early Summer Storm and an Autumn Storm. Water. 12. DOI:10.3390/w12051452.

Wei, X., Hayes, D. J., Fernandez, I., Zhao, J., Fraver, S., Chan, C., and Diao, J. (2021). Identifying Key Environmental Factors Explaining Temporal Patterns of DOC Export from

Watersheds in the Conterminous United States. Journal of Geophysical Research: Biogeosciences. https://doi.org/10.1029/2020JG005813.

Wiesmeier, M., Urbanski, L., Hobley, E., Lang, B., von Lützow, M., Marin-Spiotta, E., van Wesemael, B., Rabot, E., Ließ, M., Garcia-Franco, N., Wollschläger, U., Vogel, H-J., Kögel-Knabner, I. (2019). Soil organic carbon storage as a key function of soils - A review of drivers and indicators at various scales. Geoderma. 333. 149-162. doi.org/10.1016/j.geoderma.2018.07.026.

Wu, J., Zhang, H., Yao, Q.-S., Shao, L.-M., and He, P.-J. (2012). Toward understanding the role of individual fluorescent components in DOM-metal binding. Journal of Hazardous Materials. 215. 294-301.

Yan, J., Zhu, X., and Zhao, J. (2009). Effects of grassland conversion to cropland and forest on soil organic carbon and dissolved organic carbon in the farming-pastoral ecotone of Inner Mongolia. Acta Ecologica Sinica. 29. 3. doi.org/10.1016/j.chnaes.2009.07.001.

Zhu, A.X., Band, L., Vertessy, R., and Dutton, B. (1997). Derivation of soil properties using a soil land inference model (SoLIM). Soil Science Society of American Journal. 61. 523-533.

# CHAPTER 8 – THE USE OF HIGH FREQUENCY MEASUREMENTS TO DETERMINE THE INFLUENCE OF HYDROPEDOLOGY ON DOC EXPORT IN AFROMONTANE CATCHMENTS

**Abstract**

Carbon is one of the most important elements in the biosphere, and the ability to trace its path and residence time enhances our ability to study biogeochemical cycles. The use of high frequency optical sensors enables a deeper understanding of the importance of the influence of the hydropedological connectivity of catchment areas, and in particular the wetland systems, on dissolved organic carbon export. This study aimed to determine the factors which control fluxes of DOC from two Afromontane catchments. Data was collected every 15 minutes for a three-year study period. The average DOC concentration per day was calculated from this data set. We used this data to compare DOC concentrations against the daily rainfall, daily average water temperature, daily average turbidity, daily average conductivity, daily average total organic carbon and daily streamflow discharge for the study period. Furthermore, the daily flux rate was calculated utilising the average daily DOC concentration and the daily streamflow measurements recorded at each catchment's individual weir. We identified seasonal variability of DOC concentrations and flux rates with these being generally lower in dryer seasons and higher in wetter seasons. We furthermore identified the importance of the connectivity of flow paths and how these influence the fluxes of DOC. Connected flow paths between upslope wetland areas and the stream network increase DOC export from the catchment areas. The hydropedological influence of the soil groups and how these interact with each other at various timescales including seasonal flow paths as well as event flow paths affects the flow of DOC within the stream networks. Given the importance of these mountainous watersheds to the ecohydrological services of downstream ecosystems, the data gathered by the optical sensors has allowed for an explanation in determining the drivers of DOC export both at the seasonal scale as well as during event driven periods.

## 8.1. INTRODUCTION

Carbon is one of the most important elements in the biosphere, and the ability to trace its path and residence time enhances our ability to study biogeochemical cycles (McNichol and Aluwihare, 2007). One of the crucial linkages between the land and ocean within the global carbon cycle is the transport of dissolved organic carbon (DOC) along streams and rivers (Jeong et al. 2012). The understanding of the dynamics of how DOC is processed and transported through stream networks is of importance as this organic carbon element is not only a master water quality variable in aquatic ecosystems (Ruhala and Zarnetske, 2017) but is also a major contributor to the carbon budget of a catchment area (Rüegg et al. 2015).

The input of allochthonous material in the form of DOC to streams and rivers is dominated by the direct inputs of organic matter associated with the transport of surface water or groundwater, which passes through or over soil before entering surface water. The majority of organic matter enters a stream this way, as only a small fraction of water typically enters a stream directly as rainfall (Aitkenhead-Peterson et al. 2003). The river itself is therefore not the source of the majority of DOC but is instead the conduit of DOC (Worrall et al. 2012). The importance of soils in the fluxes of DOC in streams and rivers has therefore gained considerable interest, with many studies identifying that the fluxes of DOC relate to soil characteristics as well as the size of the soil carbon pool (Aitkenhead et al. 2007, Worrall et al. 2012).

Fluxes of DOC have also been found to be highly variable in time and have been attributed to climatic factors, such as rainfall, temperature, and storm events, as well as stream discharge, soil type, the slope of a catchment and the chemical attributes of the stream water including the pH, the carbon : nitrogen ratio, and the electrical conductivity (Aitkenhead et al. 2007, Worrall et al. 2012). Further to these factors, understanding changes in hydrological flow paths through catchment areas is fundamental in understanding the temporal dynamics of DOC (Tunaley et al. 2016).

This variability in both the concentration and controls of DOC often leads to a rapid shift in DOC concentrations. This is due to DOC concentrations being dependant on varying hydrological conditions and how these relate to the flow paths of a catchment area. For example, DOC concentrations can be controlled by the hydrological conditions during a storm event as well as the preconditions of the catchment before the storm event occurs (Werner et

al. 2019). During drought years, or a dry season, the lack of connectivity of hydrological flow paths to the stream reduces the export of DOC, while in wetter years, or wetter seasons, connected flow paths allow for the movement of DOC out of the catchment at much quicker time scales (Chaplot and Ribolzi, 2014). These conditions result in highly dynamic systems with processes interacting at timescales ranging from the event scale of hours to days to the timescales of seasons (Werner et al. 2019).

The importance of high frequency sampling in capturing these rapid shifts is emerging as a critical tool for understanding DOC transport and processing from hillslopes to streams and from streams to downgradient ecosystems (Ruhala and Zarnetske, 2017). The use of high frequency sensors allows one to capture DOC variations at time scales corresponding to the hydrological and biogeochemical dynamics of a stream system (Tunaley et al. 2016). High frequency optical sensors have become major tools in understanding the fluxes of DOC from catchment areas. By combining DOC concentration measurements taken every 15 minutes by the optical sensor and stream discharge measurement we can improve our understanding of solute transport pathways as well as active source areas within a catchment (Vaughan et al. 2017).

Many studies have established the importance of understanding DOC dynamics within aquatic ecosystems (Pagano et al. 2014, Kharbush et al. 2020). However, in South Africa, little work has been completed on the dynamics of DOC (Chaplot and Ribolzi, 2014, Kieft et al. 2018, Nkambule et al. 2020). Furthermore, mountainous watersheds have received little attention as sources of DOC (Milliman and Syvitski, 1992) across the globe and this is particularly so in the Afromontane regions of South Africa. Small mountainous streams are of importance as, they are vital sources of freshwater for both local and national economies and provide several ecohydrological services to downstream locations (Brooks and Vivoni, 2015).

Mountainous streams are also located in areas of heterogenous climatic conditions and topography, and these generate fluctuating scales of the impact of the various factors that control DOC export across both seasonal and event (storms) scales (Rosset et al. 2020). In South Africa, the uKhahlamba-Drakensberg Mountain range is one such area in which varying climatic, land cover and topographical conditions allow for the study of the contributing factors which control DOC export. By combining the use of high frequency optical probe data with

the collection of environmental data, we can improve our understanding of the key controls of the DOC dynamics of this area.

This study aimed to determine the factors which control fluxes of DOC from two Afromontane catchments in the Cathedral Peak area of the uKhahlamba-Drakensberg Mountain range, with the use of high frequency optical sensors installed at the outlets of each catchment. Three years of data were used to couple DOC concentrations with (i) the climatic conditions experienced in the catchment areas, (ii) the streamflow dynamics of the stream systems and (iii) the temporal variability in the hydrological connectivity of the catchment areas. Furthermore, the DOC flux patterns are compared against two similar catchment areas, but with different land management regimes.

## 8.2. MATERIALS AND METHODS

### *8.2.1. Study site*

Details of the study area are given in Chapter 3. Two of the research catchments were selected for this study, namely, CP-VI and CP-IX.

### *8.2.2. UV-Vis high frequency optical probe measurements*

Two submersible, portable multi-parameter UV–Vis probes (spectro::lyser, s::can Messtechnik GmbH, Austria) were installed in the weirs of CP-VI and CP-IX. The sensors were housed in PVC tubing installed within the weirs for protection from debris and deep enough to be submerged all along the year. Solar and battery power were utilised for the operations of the data logger and the data downloaded on a monthly basis (Figure 8.1). These spectrometer probes work according to the principle of the UV-Vis spectrometry and thus measure light absorbance at wavelengths ranging from 220 nm to 750 nm at 2.5 nm increments along an optical length of 35 mm suitable for natural surface water. A xenon light beam is therefore emitted by a lamp within the probe and this light will weaken after coming into contact with various dissolved substances within the water being measured. The intensity of the light is measured by a detector over a range of wavelengths, as each molecule of a dissolved substance absorbs radiation at a certain and known wavelength. The concentration of the dissolved substances is then determined by the intensity of the absorption of the sample. For example, the higher the concentration of a certain substance, the more it will weaken the light beam (Langergraber et al. 2003).

The UV–Vis probes calculates dissolved organic carbon concentration (DOC), total organic carbon concentration (TOC) and turbidity every 15 minutes using a global calibration proposed by the manufacturer which is based on partial least square analysis (PLSR) of hundreds of datasets containing UV-vis spectra and laboratory measurements of these parameters in different surface water (Van den Broeke, 2007). Even if this global calibration gives correct estimates of these parameters (Vallet et al., 2020), a lot of studies generally proposed their own calibration approach in order to adapt it to the specificity of the studied sites (Brandstetter et al. 1996; Werner et al. 2019 among others). In this study, the sampling sites were unreachable during or near rainfall events (because of security issues), and thus it was not possible to establish our own calibrations. We therefore used the global calibration. In the rest of the chapter, the DOC and TOC concentration as well as the turbidity will be called DOC probe, TOC probe and turbidity probe respectively. DOC and TOC concentrations are given a with a 2.3% precision.

A separate probe (condu::lyser, s::can Messtechnik GmbH, Austria) measured the conductivity (the ability of an aqueous solution to carry an electric current) and the water temperature with the same time step (Roosmini et al. 2018).


Figure 8.1: The different components of the UV–Vis probes installed at the weir in CP-VI and CP-IX, including the data logger installed in the weir hut

### *8.2.3. Climate and climatic monitoring of the Cathedral Peak research catchments*

The Cathedral Peak research catchments fall within the summer rainfall region of South Africa. The mean annual precipitation (MAP) for the area is approximately 1400 mm with a gradient of increasing rain between the south-eastern areas (which receive approximately 1300 mm) to the western areas (which receive approximately 1700 mm). CP-III has a MAP of 1564 mm, CP-VI has a MAP of 1340 mm, and CP-IX has a MAP of 1257 mm (Toucher et al. 2016). Rainfall is measured with tipping bucket rain gauges installed in the mid position of each of the catchments. Half of the rainfall events in the catchments are brought about by localised thunderstorms which fall during the spring and summer months (September to March), with occasional snowfall received during winter (May to August). The clouds forming these thunderstorms come from the west of the catchment areas. Orographic rainfall, produced from clouds forming in the east of the catchments, also create longer periods of softer rainfall which can fall for several days (Bosch, 1979, Nänni, 1956, Everson et al. 1998, Toucher et al. 2016). Mean monthly temperatures range from 17.1$^{O}$C to 10$^{O}$C with frost common in autumn and winter (April to August) (Bosch, 1979, Everson et al. 1998, Gordijn et al. 2018; Toucher et al. 2016).

Streamflow monitoring was initiated in the two catchment areas during the late 1940's and 1950's (Toucher et al., 2016). At the outlet of each catchment a concrete weir and stilling hut, with 90-degree V Notches were installed. These V Notches are 18 inches deep and are surmounted by 6 feet wide rectangular notches of varying depth. Details of how early measurements were taken, error checked and processed are given in Toucher et al. (2016). The water stage-height at each weir is currently monitored using an Orpheus Mini (Ott Hydromet GmbH, Germany) at CP-VI weir and CS451 Stainless steel SDI-12 Pressure Transducers with CR200 loggers at the CP-VI and CP-IX weirs. There are two pressure transducers installed at weir CP-VI as this is the core catchment and thus the quality of streamflow records is ensured (Toucher et al. 2016).

Catchment specific rainfall and streamflow data were therefore utilised for this study. However, in CP-IX equipment problems led to periods of missing streamflow discharge data in October 2019 as well as between August and November 2020. These periods of missing data were removed from the database.

*8.2.4. Hydropedological characteristics of the research catchments*

A detailed description of the hydropedological flow paths of the two research catchments is provided in Chapter 5 and is briefly described here. Utilising the hydropedological soil group maps created for the catchment areas as described in Harrison and van Tol (2022) (Figure 8.2) as well as site specific measurements of the precipitation, streamflow discharge data and water table depth measurements, an understanding of the hydropedological flow paths of the catchment areas was achieved.

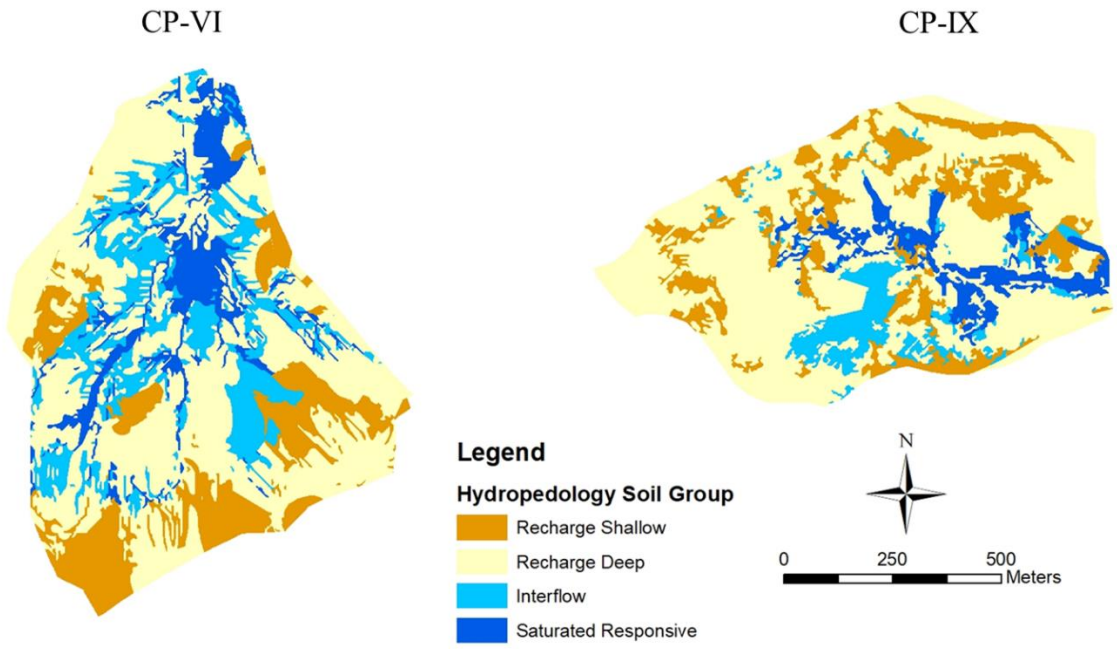


Figure 8.2: Hydropedological soil group maps for CP-VI and CP-IX (from Harrison and van Tol, 2022)

Soils of the catchment areas were grouped into hydropedological soil types, namely, shallow recharge soils, deep recharge soils, interflow soils, and saturated responsive soils, based on the classifications from van Tol and Le Roux (2019).

Utilising these classifications, the following hydropedological flow paths have been determined. When rainfall falls in the upper reaches of the two catchment areas it will enter into the hydropedological recharge soil group. The dominant flow direction in recharge soils is the vertical flow of water through and out of the profile into the underlying bedrock. In the catchment areas this hydropedological soil group is separated into the recharge shallow soils

and the recharge deep soils. Recharge shallow soils occur in the steeper areas of the catchments, and this forms their shallow nature (<500 mm). Here the freely drained B horizon merges with fractured rock or a lithic horizon. The recharge deep soils are similar to the recharge shallow soils, but the thickness of the profile is far greater (>500 mm). This is largely due to their position within gentler topographical areas of the catchments. Water that moves through these soils would recharge the deeper aquifers associated with the catchment areas, or if it encounters more impermeable rock such as sandstone or basaltic outcrops, it will flow laterally, and recharge shallow aquifers associated with seasonal hillslope seepage areas.

Interflow soils located downgradient of the recharge soils are associated with two dominant flow paths. Rainfall would first flow vertically through the free-draining upper profile of these soils before it encounters relatively impermeable bedrock. Hydromorphic properties have developed at this point in the soil profile, signifying periodic saturation associated with a water table. At this soil bedrock interface water will move laterally into the stream network or downgradient. The contribution of the flow dynamics of the interflow soils to the streamflow network is dependent on the climatic conditions of the catchment areas. The saturation levels of these soils increase during the wetter years as well as the wetter seasons. However, they do not become saturated and thus contribute to the baseflow of the streams year-round through lateral flow.

The recharge saturated soils are located in the wetland areas. These soils show morphological evidence of long periods of saturation such as a gleyed matrix as well as mottling. Based on site specific measurements of the catchments areas, these soils have drying and wetting cycles which follow seasonal trends. During drier years as well as drier seasons these soils attenuate water, and do not contribute substantially to the streamflow discharge of the catchment. During wetter years as well as wetter seasons the saturated responsive soils become saturated and will remain saturated until climatic conditions change. Once saturated, they cannot attenuate any further water, and will generate shallow subsurface as well overland flow to the stream network. Diagrams of the flow paths identified in CP-VI and CP-IX are displayed in Figure 8.3 and Figure 8.4.

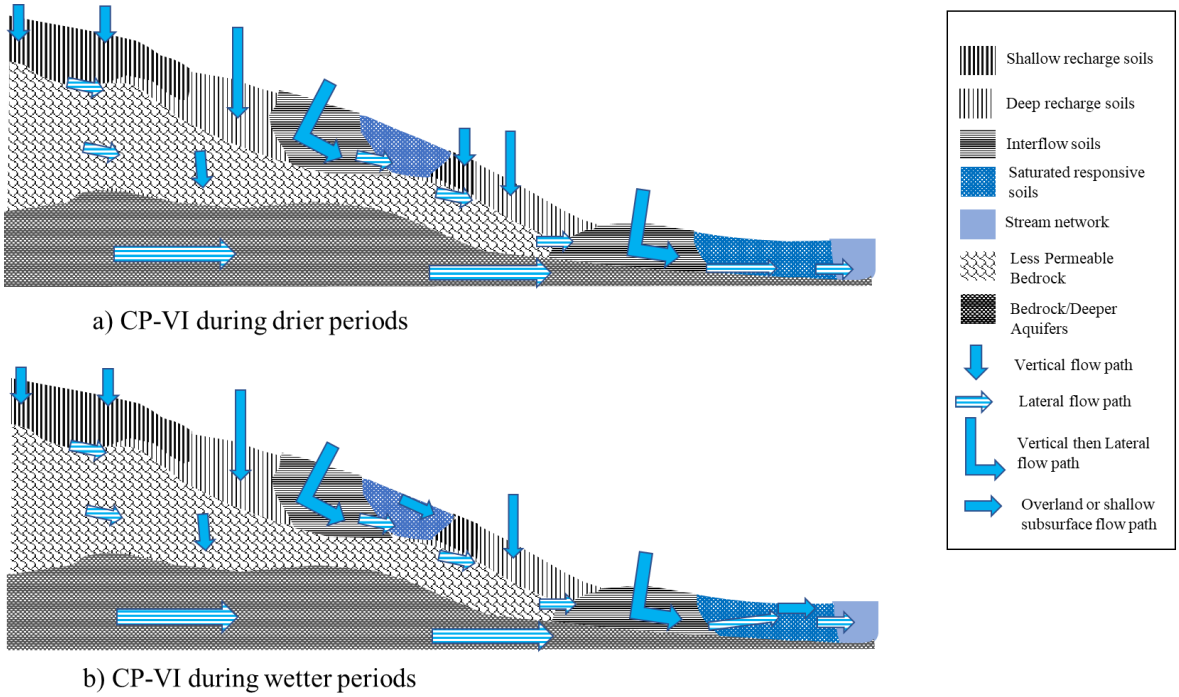


Figure 8.3: Flow path diagrams for a) the drier periods and b) wetter periods for CP-VI

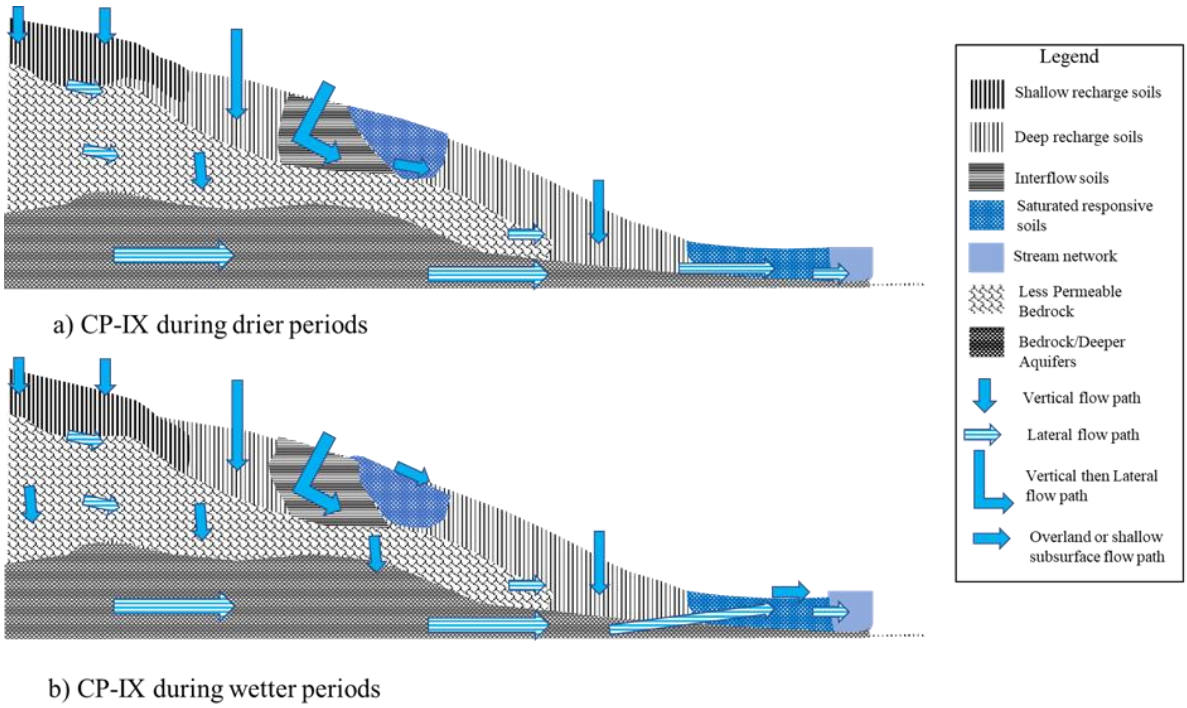


Figure 8.4: Flow path diagrams for a) the drier periods and b) wetter periods for CP-IX

### *8.2.5. Data Analysis*

The UV–Vis probes measured data every 15 minutes for a three-year study period from the 1st of July 2019 to the 28th of June 2022 for both CP-VI and CP-IX. The average DOC probe

concentration per day was calculated from this data set. The data set for CP-VI however had a number of gaps as a result of power failures during particular times of the study period. The gaps in the data ranged from particular times within a day as well as multiple days within a month. As no formal rule could be identified in how to deal with missing data (Anderson and Gough, 2018), we took into account the World Meteorological Organisation (WMO) guidelines on the calculation of climate normals (World Meteorological Organization, 2017). These guidelines recommend that if there is greater than 11 days of consecutive data missing in a month, the month should be excluded. Further, we choose to exclude a day within a month if more than 30% of the daily record was missing. For CP-VI, we therefore excluded 01/2020, 12/2020, 01/2021, 02/2021 and 08/2021 from the data set. We did not exclude any optical probe data from CP-IX, however as already stated streamflow data from CP-IX was excluded for 10/2019 and 08/2020 to 11/2020.

The minimum, maximum, and weighted mean DOC probe values were calculated per catchment from the data set. The weighted mean was calculated according to Equation 1.

$$C_m = \frac{\sum_{i=1}^{n}[C_i.Q_i]}{\sum_{i=1}^{n}[Q_i]} \qquad (1)$$

Cm is the discharge weighted mean concentration of the given time period

Ci is the instantaneous concentration measured n times during the period

Qi is the instantaneous discharge corresponding to the measured instantaneous concentration Ci

The daily average DOC probe concentrations were compared against the daily rainfall, daily average water temperature, daily average turbidity probe concentration, daily average conductivity, daily average total organic carbon (TOC) and daily streamflow discharge for the study period. Plots of the comparisons were created, and linear regression analysis was undertaken.

### *8.2.6. DOC flux rates*

The daily flux rate was calculated utilising the average daily DOC probe concentration and the daily streamflow measurements recorded at each catchment's individual weir as per Equation 2.

$$Flux = \frac{\sum_{i=1}^{n}[C_i.Q_i]}{\sum_{i=1}^{n}[Q_i]} * Qm \qquad (2)$$

Flux is the daily DOC probe flux rate

Ci is the instantaneous concentration measured n times during the period

Qi is the instantaneous discharge corresponding to the measured instantaneous concentration Ci

Qm is the average discharge of the considered period

The relationships between streamflow discharge, rainfall, and the monthly average DOC fluxes were plotted using line plots to identify potential controlling variables on the DOC fluxes.

### *8.2.7. Rainfall events data collection*

Three typical rainfall events were selected during the study period to identify relationships between rainfall, streamflow discharge and DOC probe concentrations. Five minute rainfall data was correlated to thirty minute height changes in the streamflow discharge at the weirs as well as fifteen minute DOC probe concentration data as recorded by the optical sensors. The following rainfall events were selected; (i) a short rainfall event of 3 hours and 40 mins (7.62 mm in CP-VI and 19.30 mm in CP-IX) which occurred on the 28$^{th\ of}$ November 2019 during the drought period, (ii) a longer rainfall event of 79 hours (146.81 mm in CP-VI and 139.70 mm in CP-IX) which occurred between 6$^{th}$ February to the 10th February 2020, as the drought period was ending, and (iii) a shorter but larger rainfall event of 23 hours (52.59 mm in CP-VI and 50.04 mm in CP-IX) which occurred on the 4$^{th}$ February 2022 during the wettest season within the study period.

## 8.3. RESULTS

### *8.3.1. General trends in DOC concentration*

Daily rainfall data compared against daily streamflow discharge and average daily DOC probes concentration data are shown in Figure 8.5 for CP-VI and Figure 8.6 for CP-IX during the study period July 2019 to June 2022. Rainfall largely falls within the spring-summer months (September to March), with little to no rain within the autumn and winter months (April to August). Drought conditions were experienced within both catchment areas during 2019 and thus the yearly total for the July 2019 to June 2020 period (CP-VI = 802.6 mm; CP-IX = 927.4 mm) was lower than the July 2020 to June 2021 (CP-VI = 1129.8 mm; CP-IX = 1331.0 mm) period. The July 2021 to June 2022 period was wetter still (CP-VI = 1603.5 mm; CP-IX = 1458.7 mm) with this shift in climatic conditions likely to have been brought about by the La

Niña conditions experienced during this time. La Niña conditions are associated with a substantial increase in the occurrences of cut-off lows over subtropical southern Africa, and this influences rainfall events (Singleton and Reason, 2007). Comparisons of the rainfall data obtained during the study period with rainfall data collected since 2014, shows that 2019 was a typically dry year, with 2020 and 2021 being a typically wetter year (Table 8.1).

Table 8.1: Rainfall data for CP-VI and CP-IX from 2014

| **Year** | **Rainfall (mm)** | |
|---|---|---|
| | **CP-VI** | **CP-IX** |
| 2014 | 893.6 | 1167.2 |
| 2015 | 607.3 | 771.8 |
| 2016 | 1180.1 | 1285.2 |
| 2017 | 1263.9 | 1146.1 |
| 2018 | 770.1 | 977.9 |
| 2019 | 829.6 | 884.9 |
| 2020 | 1261.1 | 1274.1 |
| 2021 | 1472.7 | 1378.7 |

The streamflow discharge data generally followed a similar trend to the rainfall data, with higher streamflow conditions experienced in the wetter seasons (spring-summer) as well as the wetter years (2021, 2022) (Figure 8.5 and Figure 8.6). There was furthermore a general increase in the DOC probes concentration with an increase in stream discharge. However, this relationship was not linear, with the highest values for stream discharge not always corresponding to the highest values for DOC probes concentration in either season, or in the wetter versus drier years.

The weighted mean average daily DOC probes concentration over the study period was 0.7 mg/L in CP-VI and 0.8 mg/L in CP-IX. During summer the concentrations of DOC were generally higher, with the maximum value of 3.7 mg/L (7$^{th}$ February 2020) in CP-VI and 3.0 mg/L (1$^{st}$ November 2020) in CP-IX recorded in the summer season and following the onset of rains after dry conditions. The minimum value of 0.4 mg/L (26$^{th}$ July 2020) in CP-VI and 0.4 mg/L (27$^{th}$ July 2020) in CP-IX were recorded in the winter season, coupled with low flow conditions in both catchments.

A summary of the values recorded is provided in Table 8.2.

Table 8.2: Summary of recorded data for the study period in CP-VI and CP-IX

| | | | **Mean** | **Max** | **Min** | **Std Dev** |
|---|---|---|---|---|---|---|
| CP-VI | Rainfall (mm) | July 2019 - June 2020 | 2.7 | 49.5 | 0.0 | 7.1 |
| | | July 2020 - June 2021 | 3.9 | 65.3 | 0.0 | 9.8 |
| | | July 2021 - June 2022 | 4.5 | 61.7 | 0.0 | 9.4 |
| | | Whole Study Period | 3.7 | 65.3 | 0.0 | 8.8 |
| | Streamflow Discharge (mm) | July 2019 - June 2020 | 1.1 | 4.9 | 0.2 | 1.0 |
| | | July 2020 - June 2021 | 2.3 | 18.9 | 0.5 | 2.4 |
| | | July 2021 - June 2022 | 2.6 | 11.0 | 0.4 | 2.2 |
| | | Whole Study Period | 2.0 | 18.9 | 0.2 | 2.1 |
| | DOC probe concentration (mg/L) | July 2019 - June 2020 | 0.7 | 3.7 | 0.4 | 0.4 |
| | | July 2020 - June 2021 | 0.6 | 2.9 | 0.4 | 0.3 |
| | | July 2021 - June 2022 | 0.7 | 2.5 | 0.5 | 0.3 |
| | | Whole Study Period | 0.7 | 3.7 | 0.4 | 0.4 |
| | Discharged Weighted Mean (mg/L) | July 2019 - June 2020 | 0.7 | | | |
| | | July 2020 - June 2021 | 0.7 | | | |
| | | July 2021 - June 2022 | 0.7 | | | |
| | | Whole Study Period | 0.7 | | | |
| | Daily Average Water Temperature ($^{O}$C) | July 2019 - June 2020 | 14.3 | 19.6 | 9.1 | 2.5 |
| | | July 2020 - June 2021 | 13.7 | 18.3 | 8.8 | 2.5 |
| | | July 2021 - June 2022 | 14.7 | 18.2 | 8.2 | 2.1 |
| | | Whole Study Period | 14.3 | 19.6 | 8.2 | 2.4 |
| | Daily Average Turbidity (FTU) | July 2019 - June 2020 | 1.8 | 8.7 | 0.5 | 1.2 |
| | | July 2020 - June 2021 | 2.6 | 13.2 | 0.9 | 1.6 |
| | | July 2021 - June 2022 | 3.4 | 14.5 | 1.2 | 1.6 |
| | | Whole Study Period | 2.6 | 14.5 | 0.5 | 1.6 |
| | Daily Average Conductivity (uS/cm) | July 2019 - June 2020 | 95.1 | 102.2 | 60.4 | 6.3 |
| | | July 2020 - June 2021 | 94.1 | 114.6 | 70.9 | 5.8 |
| | | July 2021 - June 2022 | 88.0 | 98.1 | 65.2 | 5.6 |
| | | Whole Study Period | 92.3 | 114.6 | 60.4 | 6.8 |
| CP-IX | Rainfall (mm) | July 2019 - June 2020 | 2.9 | 51.1 | 0.0 | 7.2 |
| | | July 2020 - June 2021 | 3.9 | 68.3 | 0.0 | 9.7 |
| | | July 2021 - June 2022 | 4.0 | 57.9 | 0.0 | 8.8 |
| | | Whole Study Period | 3.6 | 68.3 | 0.0 | 8.7 |
| | Streamflow Discharge (mm) | July 2019 - June 2020 | 0.6 | 2.3 | 0.1 | 0.6 |
| | | July 2020 - June 2021 | 1.9 | 11.8 | 0.5 | 1.6 |
| | | July 2021 - June 2022 | 1.5 | 6.6 | 0.2 | 1.3 |
| | | Whole Study Period | 1.3 | 11.8 | 0.1 | 1.3 |
| | DOC probe concentration (mg/L) | July 2019 - June 2020 | 0.6 | 2.7 | 0.4 | 0.3 |
| | | July 2020 - June 2021 | 0.6 | 3.1 | 0.4 | 0.3 |
| | | July 2021 - June 2022 | 0.8 | 2.5 | 0.5 | 0.3 |
| | | Whole Study Period | 0.7 | 3.1 | 0.4 | 0.3 |

| | | | Mean | Max | Min | Std Dev |
|---|---|---|---|---|---|---|
| | Discharged Weighted Mean (mg/L) | July 2019 - June 2020 | 0.7 | | | |
| | | July 2020 - June 2021 | 0.7 | | | |
| | | July 2021 - June 2022 | 0.9 | | | |
| | | Whole Study Period | 0.8 | | | |
| | Daily Average Water Temperature ($^{O}$C) | July 2019 - June 2020 | 14.0 | 19.2 | 8.2 | 2.8 |
| | | July 2020 - June 2021 | 13.3 | 17.2 | 7.6 | 2.4 |
| | | July 2021 - June 2022 | 13.6 | 18.5 | 6.7 | 2.6 |
| | | Whole Study Period | 13.7 | 19.2 | 6.7 | 2.6 |
| | Daily Average Turbidity (FTU) | July 2019 - June 2020 | 1.1 | 8.8 | 0.2 | 0.9 |
| | | July 2020 - June 2021 | 1.8 | 10.8 | 0.7 | 1.3 |
| | | July 2021 - June 2022 | 2.3 | 11.2 | 0.7 | 1.4 |
| | | Whole Study Period | 1.7 | 11.2 | 0.2 | 1.3 |
| | Daily Average Conductivity (uS/cm) | July 2019 - June 2020 | 76.1 | 86.1 | 53.5 | 6.1 |
| | | July 2020 - June 2021 | 71.1 | 83.1 | 47.9 | 6.8 |
| | | July 2021 - June 2022 | 70.0 | 85.4 | 53.8 | 5.8 |
| | | Whole Study Period | 72.4 | 86.1 | 47.9 | 6.8 |

Average daily and monthly water temperatures recorded by the probes exhibited strong seasonal patterns with an increase and decrease in water temperature for the summer and winter months respectively. When compared against DOC probes concentrations results show that increase and decrease trends in the average monthly DOC probes concentrations are correlated with trends in water temperature for both catchments (Figure 8.7 and Figure 8.8).

Daily average turbidity probes patterns ranged from 0.5 FTU (in CP-VI) and 0.2 FTU (in CP-IX) both recorded in the winter dry period, to 14.5 FTU (in CP-VI) and 11.2 FTU (in CP-IX) both recorded in the wetter summer season. The average turbidity probes values are 2.6 FTU (for CP-VI) and 1.7 FTU (for CP-IX) with increases and decreases in the values following the hydrological cycle of the catchment areas. There is an increase in turbidity during the wetter seasons and a decrease in the drier seasons. Higher values for turbidity were captured by the probe in the weir of CP-VI as compared to the probe in the weir of CP-IX (Figure 8.9).

Daily average conductivity values range from 60.5 µs/cm to 114.6 µs/cm for CP-IV and 47.9 µs/cm to 86.1 µs/cm for CP-IX. Conductivity values gives an index of the total solute concentration within the stream waters. Conductivity values decreased during wetter periods and increased during drier periods. Correlations between the daily average DOC probes

concentrations show an inverse relationship, with an increase in DOC correlated to a decrease in conductivity during the same time periods for both catchment areas (Figure 8.10).

Correlations between the TOC probes values and the DOC probes values show a linear relationship in both catchments. The majority of TOC within the streams of CP-VI and CP-IX can therefore be linked to DOC (Figure 8.11).

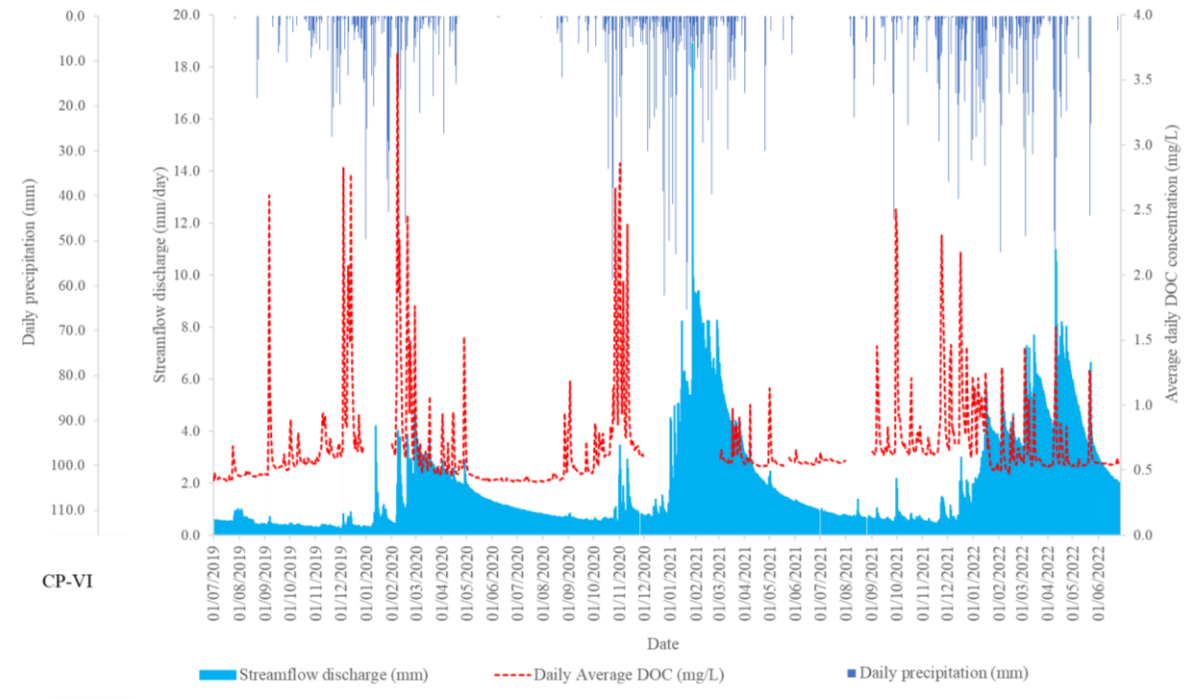


Figure 8.5: Graphical depictions of the daily rainfall and streamflow compared against the average daily DOC probe concentration as measured by the probes in CP-VI

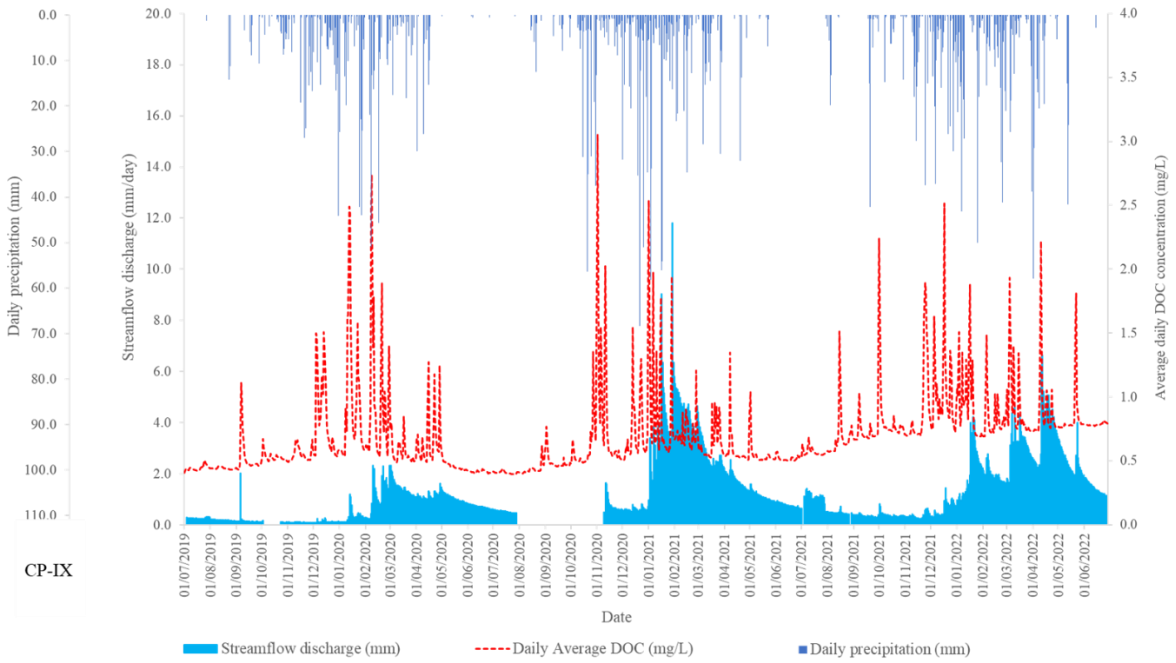


Figure 8.6: Graphical depictions of the daily rainfall and streamflow compared against the average daily DOC probe concentration as measured by the probes in CP-IX

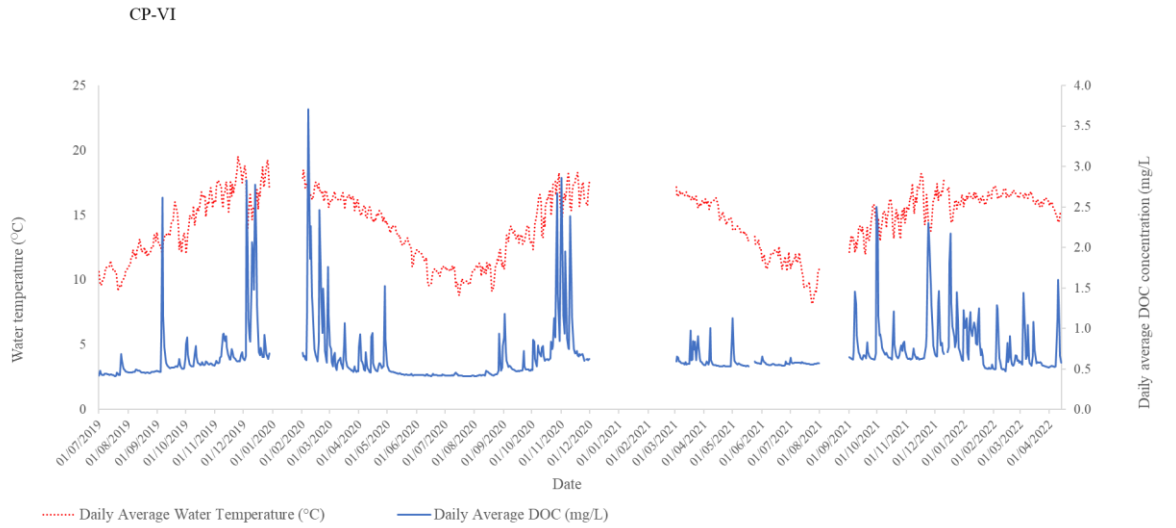


Figure 8.7: Correlations between daily water temperature and the average daily DOC probe concentration as measured by the probes in CP-VI

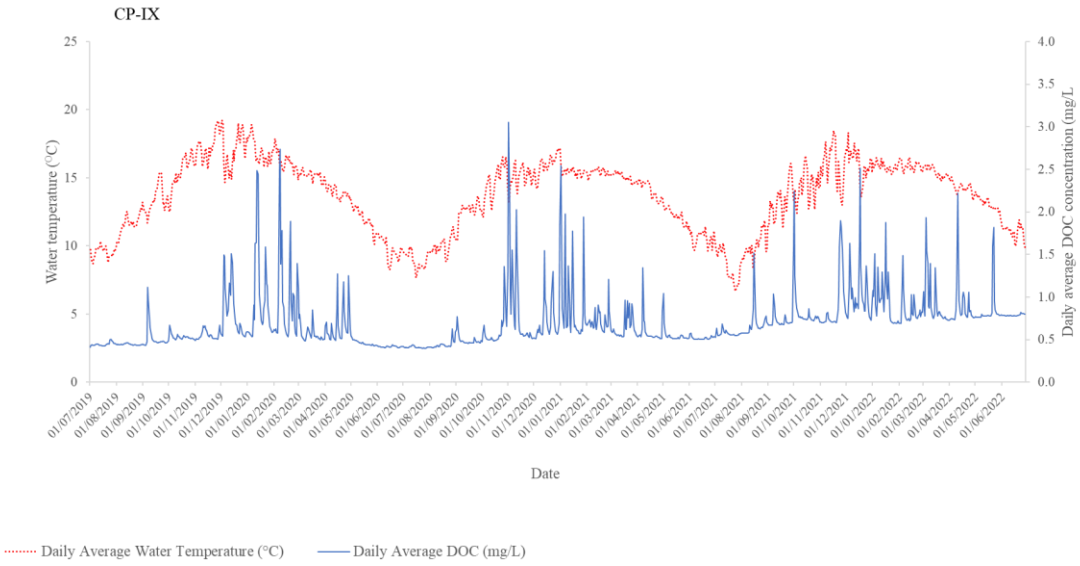


Figure 8.8: Correlations between daily water temperature and the average daily DOC probe concentration as measured by the probes in CP-IX

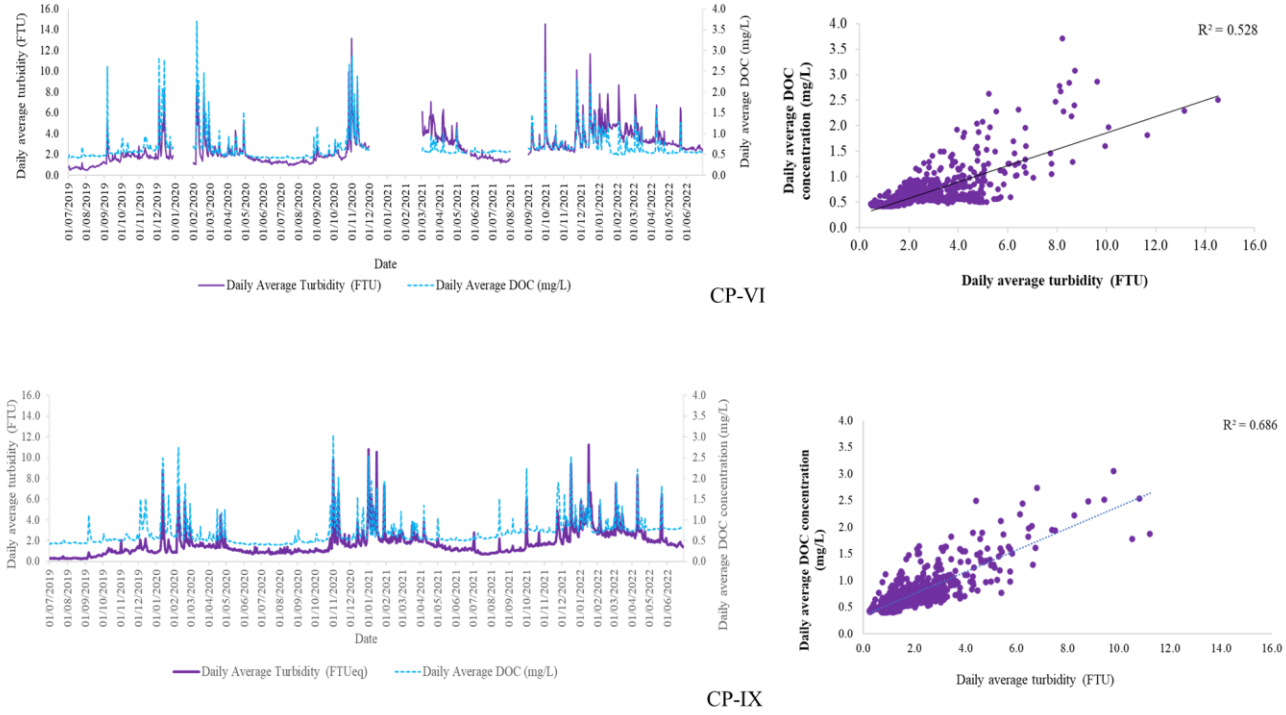


Figure 8.9: Correlations between the daily average DOC probe concentrations and the daily average turbidity for CP-VI and CP-IX

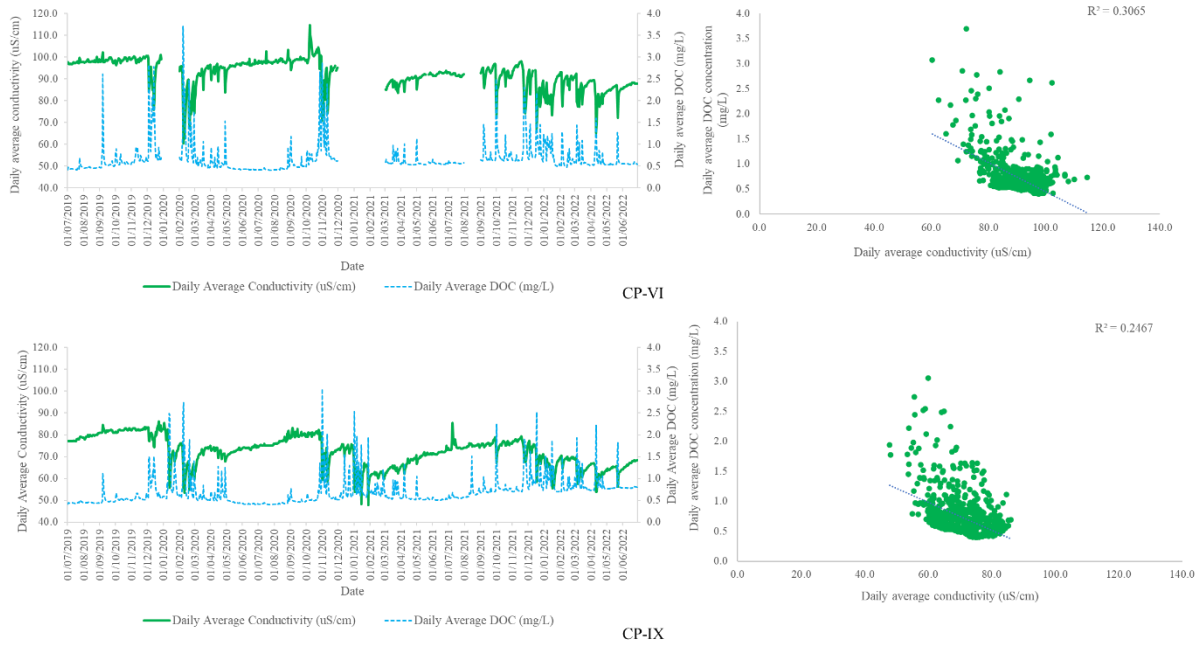


Figure 8.10: Correlations between the daily average DOC probe concentrations and the daily average conductivity for CP-VI and CP-IX

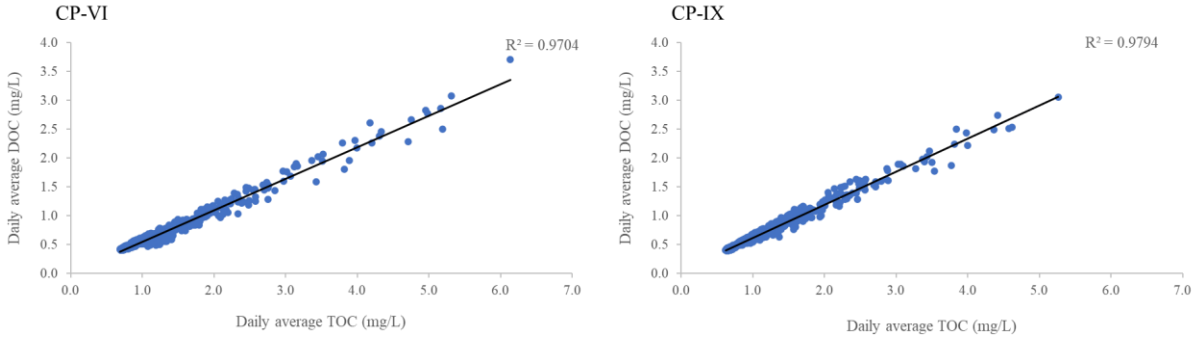


Figure 8.11: Correlations between the DOC and TOC values as measured by the probes in CP-VI and CP-IX

### *8.3.2. Monthly DOC fluxes*

Monthly DOC flux calculations (kg/month) ranged from 4.54 kg/month to 98.70 kg/month in CP-VI and 1.16 kg/month to 69.49 kg/month in CP-IX (Figure 8.12, and Figure 8.13).

Comparisons of the monthly DOC probe fluxes against rainfall and monthly streamflow show that the lower fluxes occurred in the drier months, both seasonally (autumn-winter period) as well as during the drought period in 2019 (October 2019 to January 2020), while the higher values occurred in the wetter seasons (spring-summer period), when streamflow discharge levels were higher.

These general trends were however not linear, with the highest concentration of DOC not corresponding with the highest discharge for the study period in either catchment. Higher flux rates were recorded in the initial re-wetting of the catchment areas following dry periods. For example, in CP-VI the highest recorded flux rate of 98.70 kg/month of DOC occurred in February 2020 following the onset of rains after the drought period. The streamflow discharge values during this month (61.47 mm/month) were however not the highest recorded values for the study period. In fact, the streamflow discharge values continue to increase in March 2020 (91.13 mm/month), despite the decline in DOC probe flux rates. In CP-IX, there is an increase and decrease in DOC flux rates during the same time period (8.25 kg/month in January, 40.45 kg/month in February, 16.96 kg/month in March), however the streamflow discharge values continue to increase despite the decrease in DOC flux rates (streamflow values increase from 10.80 mm/month in January to 45.45 mm/month in March).

As detailed in Chapter 5, and briefly described here, flow paths between the catchment and the streamflow network became more connected in February 2020 after the end of the drought period. Wetland systems started contributing more to the streamflow as overland and shallow subsurface flow from this time. Furthermore, individual wetland systems differed in their saturation levels throughout the study period with some wetlands contributing more to overland and subsurface flow for longer periods as compared to others, with these contributions also dependant on seasonal climatic changes. The connection of the flow paths to the stream network as a result of the saturation levels of the wetland systems follows the general trends seen in the DOC flux rates, with larger fluxes of DOC within the wetter seasons (spring-summer) and lower flux rates in the dryer seasons (autumn to winter) and dryer years (i.e., 2019) corresponding with the various connectivity of the flow paths.

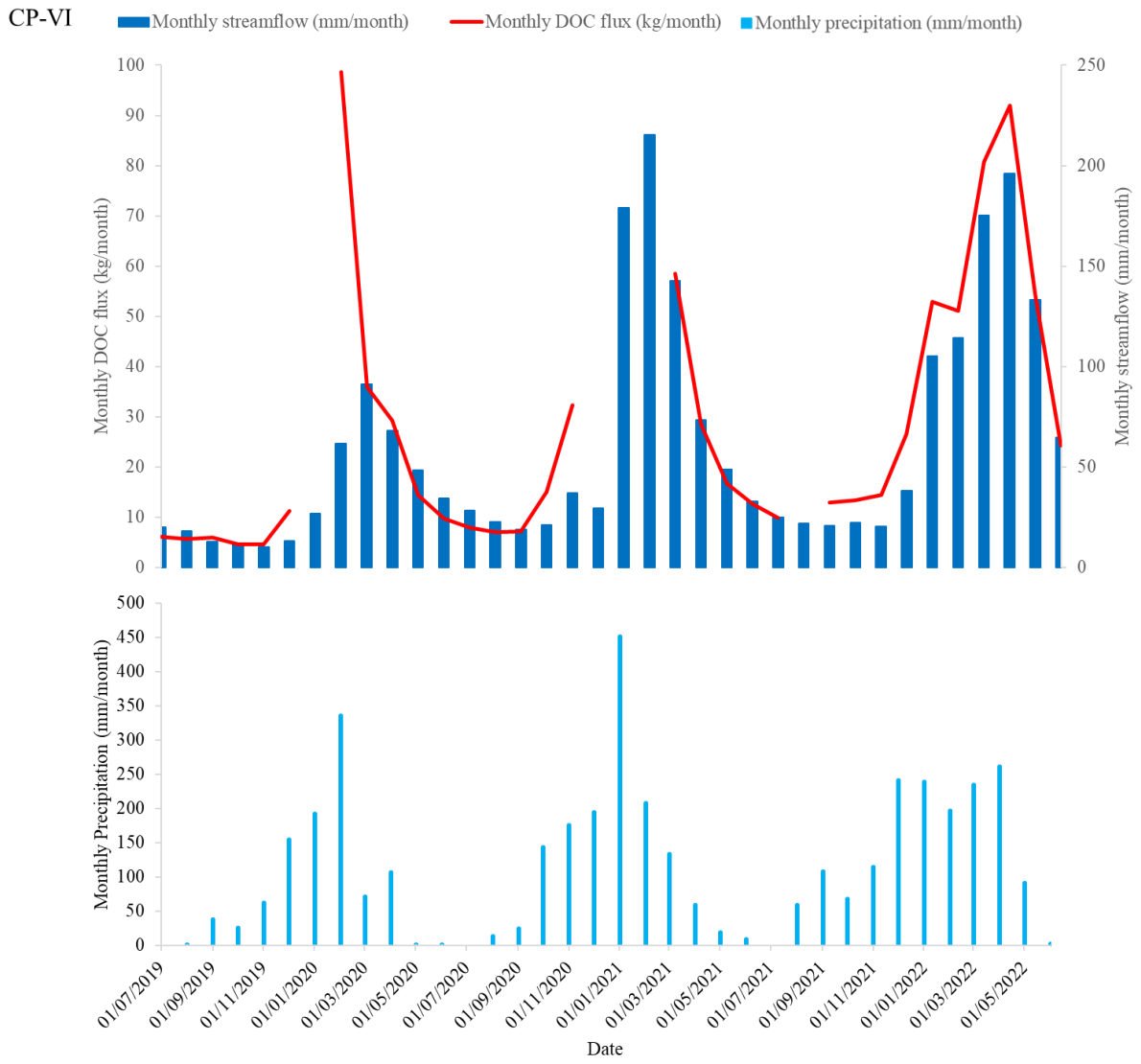


Figure 8.12: Correlations between monthly streamflow discharge, monthly rainfall, and monthly DOC fluxes (kg/month) and average monthly DOC fluxes in CP-VI

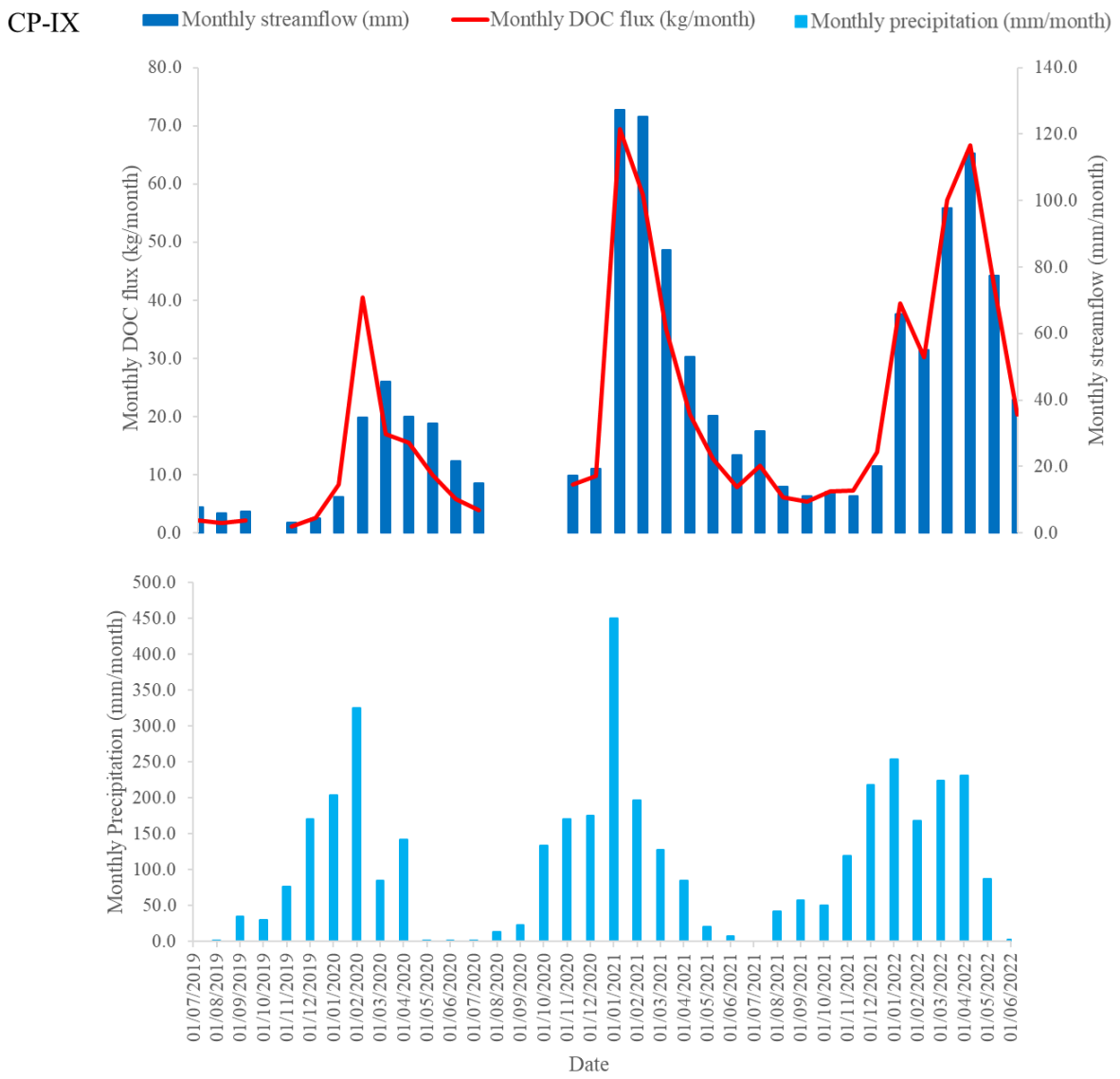


Figure 8.13: Correlations between monthly streamflow discharge, monthly rainfall, and monthly DOC fluxes (kg/month) in CP-IX

### *8.3.3. DOC concentrations at the scale of the rainfall event*

Correlations between DOC probe concentration and the rainfall events differed depending on the timing of the event as shown in Figures 8.13, 8.14 and 8.15. On the 28$^{th}$ of November 2019, rainfall fell between the times of 13:20 and 14:25 in both catchments. The height of the streamflow discharge increased during the rainfall event, reached a maximum 2 hours after the beginning of the event and remained at a higher level for one to two hours after the end of the event before decreasing to pre-event levels. The DOC probe concentrations in CP-VI started increasing at the same time than the height of the streamflow, reached a maximum value of 0.9 mg/L 4 h after the beginning of the event before decreasing slightly to an average of 0.75 mg/L

over the next 24 hours. In CP-IX, an increase in DOC probe concentrations of 0.5 to 0.7 mg/l beginning toward the end of the rainfall event is recorded, with the maximum level being kept for 10 hours after the event before decreasing slightly to an average of 0.67 mg/L for the next 24 hours.

During the longer rainfall event on the 6th of February 2020, rainfall started falling at 14:50 in CP-VI and CP-IX and continued falling intermittently until the 10th of February 2020. During rainfall there is a corresponding increase in both streamflow discharge and DOC probe concentration. More intense rainfall produces higher concentrations of DOC within the stream water, with these higher concentration values declining more rapidly as the rainfall event continues into the 4th and 5th day in both catchment areas. During this event, maximum DOC probe concentrations occur about 2 hours after the peak discharge in both catchments, but this lag seems to decrease as the peak discharge increased.

On the 4th of February 2022, rainfall fell in both catchment areas from 05:15 to 06:30 and then there was a larger rainfall event from 15:00. There is a corresponding increase in DOC probe concentration toward the end of both events in both concentrations, with the larger rainfall event occurring later in the day having a correlating larger increase in DOC probe concentration, particularly toward the end of the event. Again, there is a lag between the peak discharge and the maximum DOC probe concentration. Given the wetter season in which this event took place the streamflow discharge values do not decline to pre-event levels but remain at an elevated level after the event.

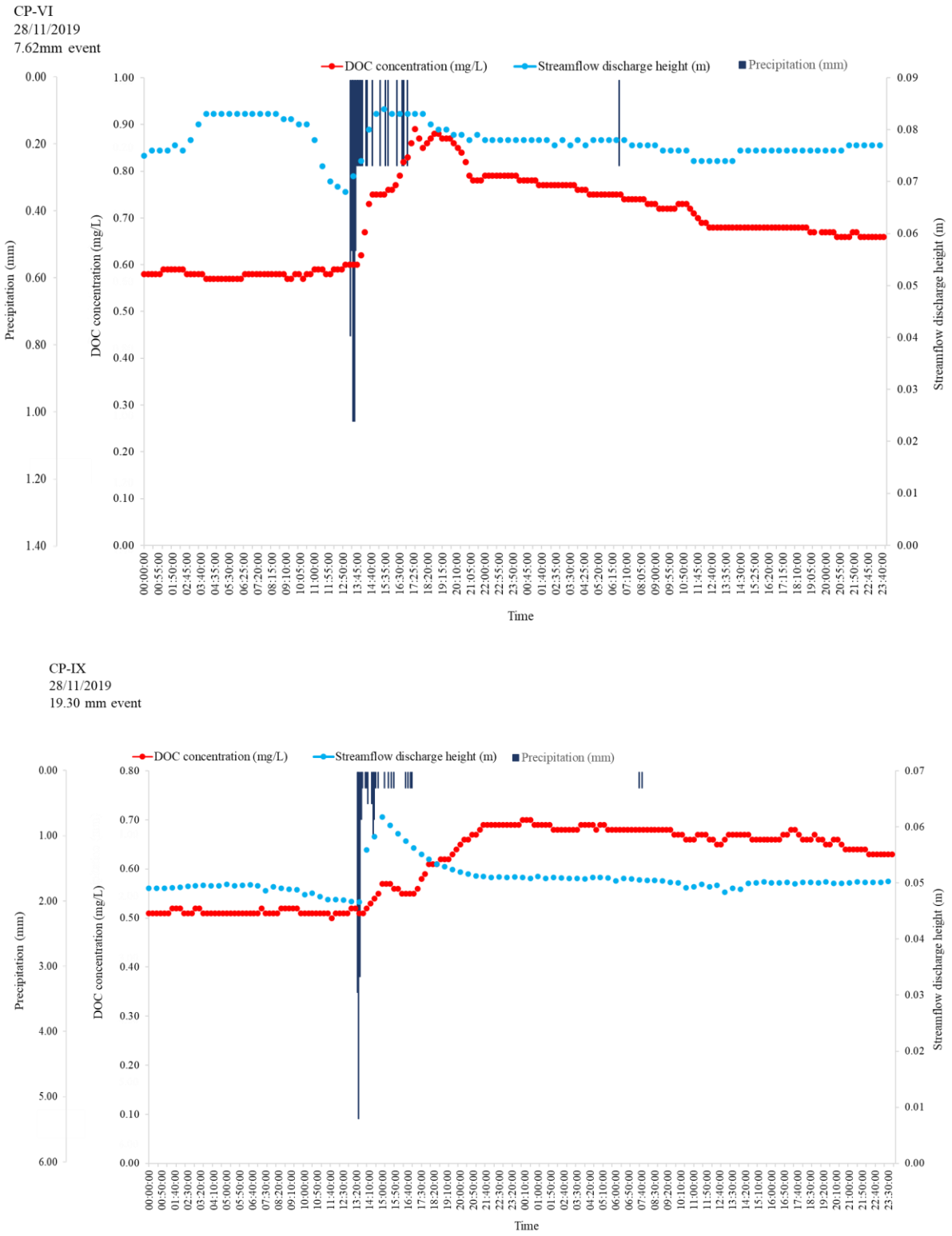


Figure 8.14: Correlations between rainfall, streamflow discharge and DOC probe concentrations during a rainfall event on the 28th of November 2019 for CP-VI and CP-IX

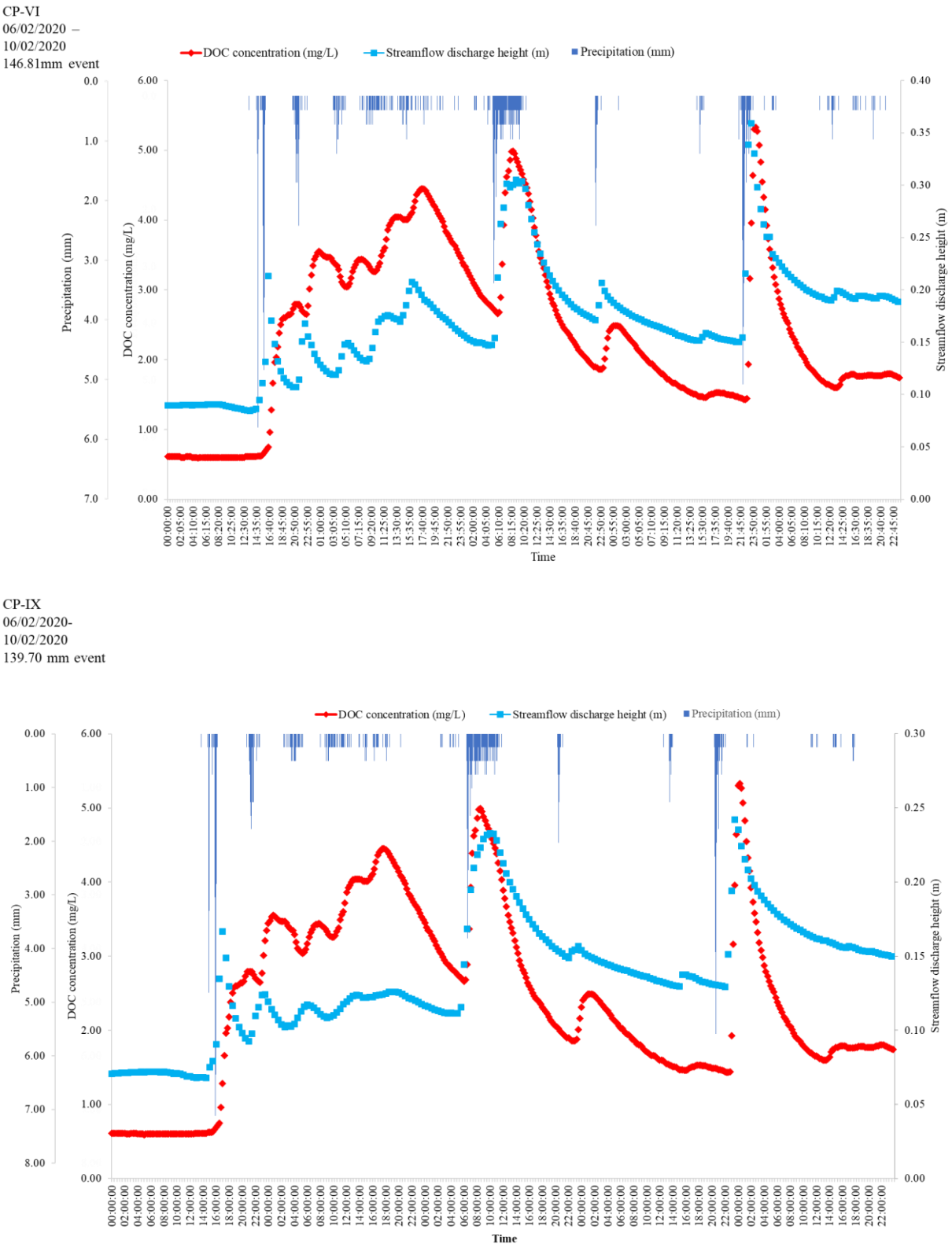


Figure 8.15: Correlations between rainfall, streamflow discharge and DOC probe concentrations during a rainfall event from the 6th of February to the 10th of February 2020 for CP-VI and CP-IX

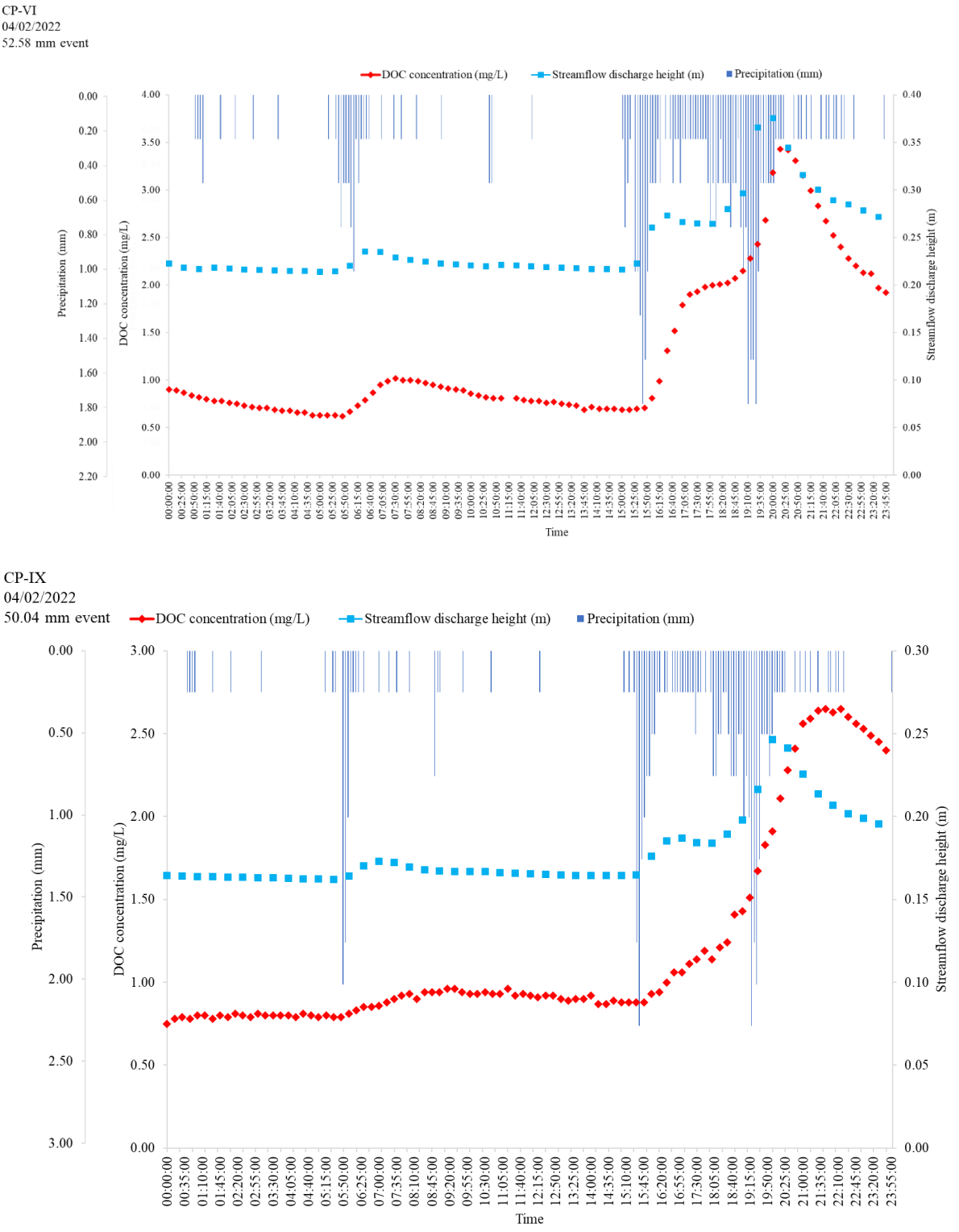


Figure 8.16: Correlations between rainfall, streamflow discharge and DOC probe concentrations during a rainfall event on the 4th of February 2022 for CP-VI and CP-IX

## 8.4. DISCUSSION

### *8.4.1. Factors affecting general trends of DOC probe concentration*

The high frequency data collected by the optical probes in CP-VI and CP-IX highlighted the variable DOC export dynamics of these catchment areas over the three-year study period. The seasonal variability of DOC concentration and flux rates showed that these were generally lower in dryer seasons (autumn and winter) and higher in wetter seasons (spring and summer). This seasonal variability is noted in a number of studies, with differences in DOC concentrations following the seasonal patterns of rainfall (Jeong et al. 2012, Tunaley et al. 2016, Werner et al. 2019). The effects of seasonal patterns of temperature, turbidity, and conductivity on the concentrations of DOC have furthermore been highlighted, with increases in temperature leading to increases in DOC concentration, and colder temperatures as experienced in the winter months, being more unfavourable for the net production of DOC within the soils of the catchment areas (Clark et al. 2009, Sawicka et al. 2016, Werner et al. 2019). These studies however highlight that the effects of temperature alone on the overall DOC flow dynamics of catchment areas is negligible with other climatic factors such as rainfall as well as the hydrology of these areas taking precedence over this factor. Turbidity increases correlated to increases in DOC concentration, with these occurring generally following rainfall events. This is most likely due to rainfall generating more surface runoff, carrying more sediment, and increasing the turbidity in the stream network. An inverse relationship was identified between conductivity and DOC concentration. Dryer periods (both the 2019 drought year as well as seasonally) recorded higher conductivity but lower DOC concentration values, while wetter periods recorded lower conductivities and higher DOC concentrations. This relationship has been attributed to the different contributions of both baseflow and overland flow to the streamflow discharge (Monteiro et al. 2014, Tunaley et al. 2016) with these studies showing that baseflow during drier conditions is mostly made up of more mineralised groundwater, while during wetter periods shallower subsurface or overland flow, composed of more diluted water, contributes more to the stream network, affecting the conductivity values.

The importance of carbon storage within soils in DOC cycling is well recognised, with carbon losses from the soils increasing DOC concentrations within stream networks. The influence of land management on carbon storage within soils has been highlighted by a number of studies with the effect of land management practices on the decomposition of soil organic matter and the resultant release of DOC being well documented (Grieve, 1990, Amiotte Suchet et al., 2007,

Sanderman and Amundson, 2008; Yallop and Clutterbuck, 2009, Lepistö et al. 2014, Hosen et al. 2018). In this study, CP-VI is a mesic grassland catchment, interspersed with wetland systems that is burned biennially during spring. CP-IX was a grassland ecosystem, like CP-VI, but is changing to a woody dominated catchment, interspersed with wetland systems, as a result of fire exclusion. Discharge weighted mean DOC probe concentrations from these two catchments were recorded as being very similar (0.7 mg/L in CP-VI and 0.8 mg/L in CP-IX), over the study period with general trends in DOC export the same for both catchment areas. Several studies have shown that vegetation is not a major contributor to DOC export but that this is more controlled by climatic parameters as well as the hydrological conditions of the catchment areas (Don and Shulze, 2008, Sanderman and Amundson, 2008, Yallop and Clutterbuck, 2009), and given the similarities in the results obtained for these two catchment areas, this is likely to be the case in this study. Furthermore, the effects of fire on DOC export have been studied (Klimas et al. 2020, Wei et al. 2021), with these studies showing both a minimal impact of fire as well as a decrease in DOC export following a fire event. Ranalli (2004), however showed, following an extensive literature review, that the effect of fire is dependent on the fire intensity, the climatic conditions such as wind and storm events, as well as the topography of the catchment in which the fire occurs.

Comparisons of the average DOC flux between CP-VI and CP-IX, shows that more DOC is exported from CP-VI (27.3 kg/month) on average than from CP-IX (19.9 kg/month).We did not have enough data during fire events to accurately address the effects of fire on DOC export. However, we have shown the definitive impact of climatic conditions on DOC export. The differences between the two catchments could also be related to the greater area of wetland systems within CP-VI as compared to CP-IX. As shown in Figure 8.2, there are more and larger wetland systems in CP-VI as compared to CP-IX, allowing for the export of greater quantities of SOC as DOC during rainfall events

### *8.4.2. Hydrologic connectivity of the catchments and DOC probe dynamics*

The connectivity of flow paths and how these influence the fluxes of DOC have been investigated in this study, with the findings showing that connected flow paths between upslope wetland areas and the stream network increase DOC export from the catchment areas. The hydropedological influence of the soil groups and how these interact with each other at various timescales including seasonal flow paths as well as event flow paths affects the flow of DOC within the stream networks.

Several studies have identified similar findings, showing that the hydrologic conditions, and in particular, the antecedent soil moisture conditions, to be a prime determinant in the movement of DOC (McCarthy, 2005, Lepistö et al. 2014, Broder and Biester, 2015, Tunaley et al. 2016). In this study, as shown by the piezometer data, the soil information, as well as the climatic data, the flow paths of the wetland systems dried out considerably during the 2019 drought period and this limited the DOC flux rates recorded by the optical sensors during this time. With the onset of rains, particularly in February 2020, many of the wetland systems became saturated once more. This allowed for the flushing of available DOC within the wetlands to the stream networks. This period is correlated to a substantial increase in DOC flux rates in both catchments (Figure 8.16 and Figure 8.17).

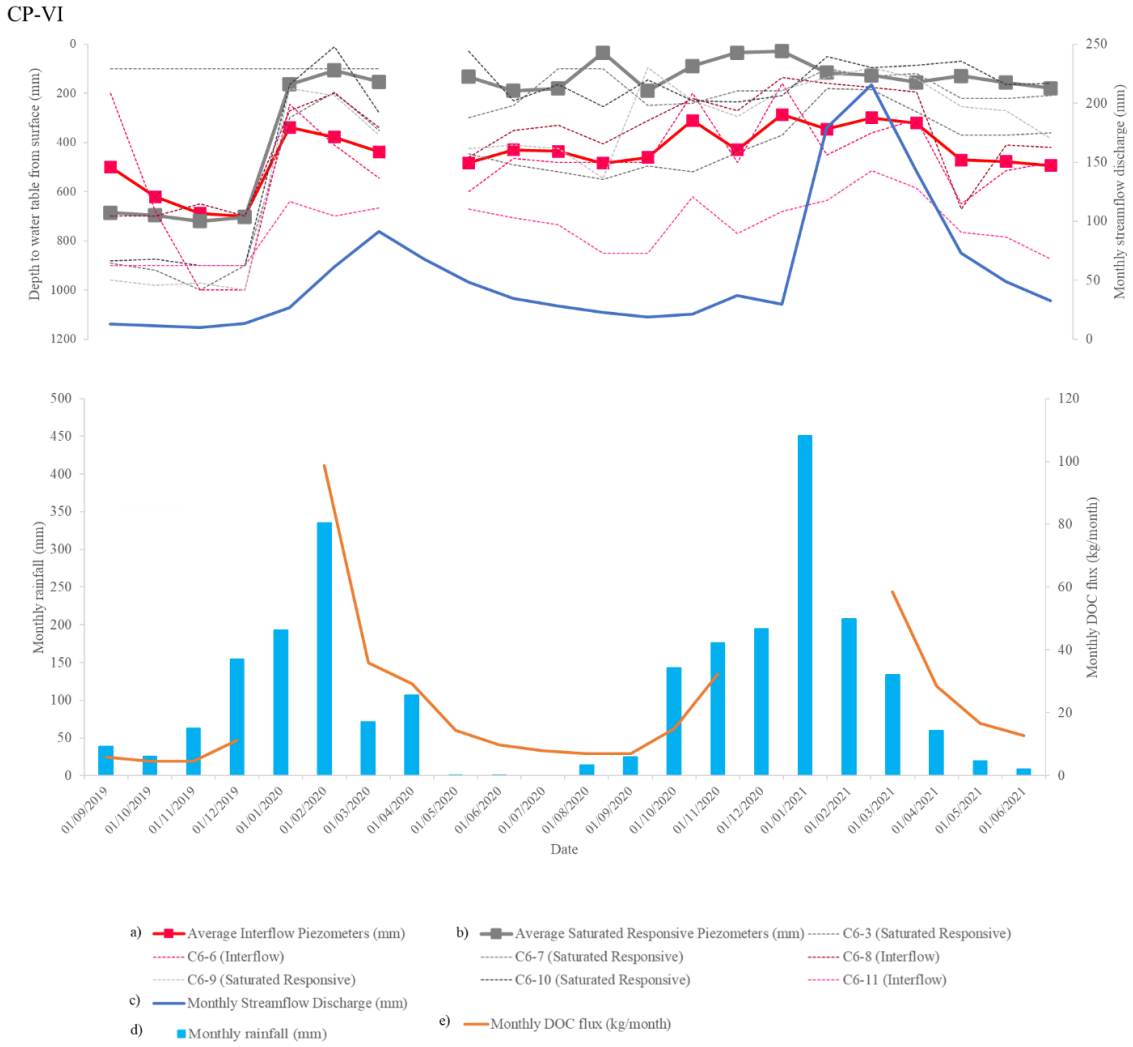


Figure 8.17: Comparisons of average and individual depths to the water table within a) interflow soils, b) saturated responsive soils utilising piezometer data, c) monthly streamflow, d) monthly rainfall and e) monthly DOC flux in CP-VI (adapted from Harrison et al. 2022)

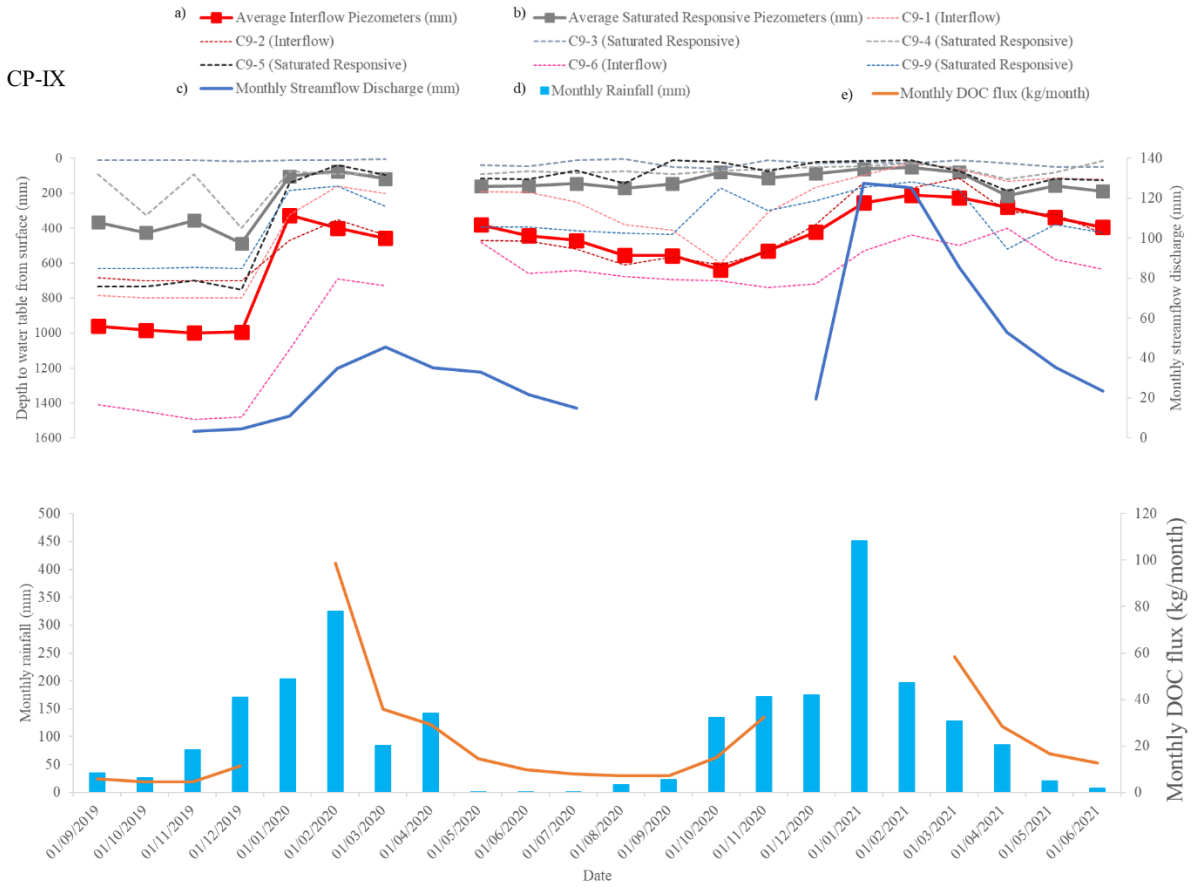


Figure 8.18: Comparisons of average and individual depths to the water table within a) interflow soils, b) saturated responsive soils utilising piezometer data, c) monthly streamflow, d) monthly rainfall and e) monthly DOC flux in CP-IX (adapted from Harrison et al. 2022)

The impact of rainfall events on the export of DOC has also been highlighted in this study. During the small rainfall event which occurred in November 2019, only a small increase in the quantity of DOC was exported from both catchments during the event.

A far greater export of DOC was noted in rainfall events, such as the one which occurred between the 6th to the 10th of February 2020, which took place during the initial onset of rains following the drought. In the initial phases of this event, maximum DOC export was recorded approximately 6 hours after the streamflow reached its maximum. This could be linked to the accumulated soil organic carbon being flushed by runoff in the early rainfall period, while the streamflow discharge is attributed to surface runoff (Wang et al. 2019). However, as the rainfall event progressed, the lag time between the maximum streamflow discharge and the maximum DOC values decreases, so that from the third day of the rainfall event the maximum of these

two variable occurs around the same time. This could be linked to the flow paths of the catchments becoming more connected as rainfall progresses, allowing for the increased transport of DOC reservoirs which have been stored, more rapidly toward the stream. Lambert et al. (2014), identified similar trends in a study conducted on linking $^{13}C$ isotopes to the flow paths of a catchment area. With increased connectivity of flow paths, as well as the activation of the various flow paths (i.e. baseflow, shallow subsurface flow, and overland flow) there is a corresponding rise in DOC export from the catchment areas.

During wetter years and wetter seasons, rainfall events, such as the one on the 4th of February 2022, produced an increase in DOC export, but not at the same level as rainfall events which occurred after dry conditions. Shanley et al. (2002) showed that when a rainfall event occurs during dry periods there is greater infiltration into the more desiccated wetland systems and this causes a greater displacement of 'old' water, which had been stored in the wetland to the stream. This 'older' stored water is typically not as rich in DOC as compared to overland and shallow subsurface flow, which move where the majority of soil organic carbon is stored. Rainfall events which then occur once the wetlands are saturated, following a dry period, flow more as overland flow or shallow subsurface flow and can therefore access available DOC and export this to the stream network. Longer rainfall events, as well as events which take place in very wet conditions, however, have a decrease in DOC concentration, with time, following the initial increase, and this may be attributed to a dilution effect of DOC in the soil water that is exported from the catchments (Tunaley et al. 2016).

DOC concentration variability is closely linked to distinct DOC source zones in catchments and their hydrologic connectivity to the stream network (Werner et al. 2019). In particular, the drying and wetting cycles of individual wetland systems as well as specific saturation zones of these wetlands influenced both the baseflow connectivity as well as the overland flow during wetter periods and during rainfall events. As highlighted in Chapter 5, particular wetlands within the catchments provided more overland flow during rainfall events as compared to others. These wetland systems include the large wetland system located in the central region of CP-VI, as well as the wetland system located in the upper reaches of CP-IX. These wetland systems could therefore be correlated to having a greater contribution to DOC export. Seepage areas that do not become saturated provide little DOC export and contribute mainly to baseflows and base DOC fluxes from the catchment areas.

## 8.5. CONCLUSION

The findings of this study provide an explanation on the drivers of DOC export from the two catchment areas. The use of the optical sensors enabled a deeper understanding of the importance of the influence of the hydropedological connectivity of catchment areas, and in particular the wetland systems, on DOC export. The event-scale export of DOC is a major contributor to the overall flux of carbon from the catchment; however, this is dependent on the antecedent connectivity of flow paths and how these affect baseflow as well as shallow subsurface and overland flow of water through the catchment and into the stream networks.

Despite the challenges faced in obtaining consistent data throughout the study period as a result of the Covid-19 pandemic as well as the remote location of the study site, the significance of the data gathered by this study has been highlighted. It has allowed for an explanation in determining the drivers of DOC export both at the seasonal scale as well as during event driven periods. Historic long term data records as well as the continual gathering of data, particularly by the optical sensors, are vital to ensuring that we can gain a deeper understanding of the importance of these mountainous watersheds to the ecohydrological services of downstream ecosystems. The knowledge we have gained on the importance of healthy functioning wetland systems, which have natural wetting and drying cycles, and how these influence the entire catchment area is of importance. These cycles create a balance within the ecosystem, both with regards to hydrological flow, as well as the carbon budget. Future studies to determine the impact of the ever-changing climatic influence, and how this will affect flow paths as well as the DOC export are needed.

## 8.6. REFERENCES

Aitkenhead, M., Aitkenhead-Peterson, J., McDowell, W., Smart, P., and Cresser, M. (2007). Modelling DOC export from watersheds in Scotland using neural networks. Computers & Geosciences. 33. 423-436. DOI:10.1016/j.cageo.2006.08.002.

Aitkenhead-Peterson, J., McDowell, W., and Neff, J. (2003). Sources, Production, and Regulation of Allochthonous Dissolved Organic Matter Inputs to Surface Waters. DOI:10.1016/B978-012256371-3/50003-2.

Anderson, C., and Gough, W. (2018). Accounting for missing data in monthly temperature series: Testing rule-of-thumb omission of months with missing values. International Journal of Climatology. DOI: 10.1002/joc.5801.

Amiotte-suchet, P., Linglois, N., Leveque, J., Andreux, F. (2007). 13C composition of dissolved organic carbon in upland forested catchments of the Morvan Mountains (France): Influence of coniferous and deciduous vegetation. Journal of Hydrology 335, 354–363.

Bosch, JM. (1979). Treatment effects on annual and dry period streamflow at Cathedral Peak. South African Forestry Journal, 108(1): 29-38.

Brandstetter A., Sletten R. S., Mentler A. and Wenzel W. (1996). Estimating dissolved organic carbon in natural waters by UV absorbance (254 nm). Journal of Plant Nutrition and Soil Science. 159, 605–607.

Broder, T. and Biester, H. (2015). Hydrologic controls on DOC, As and Pb export from a polluted peatland – the importance of heavy rain events, antecedent moisture conditions and hydrological connectivity, Biogeosciences. 12. 4651–4664. https://doi.org/10.5194/bg-12-4651-2015.

Brooks, P.D., and Vivoni, E.R. (2015). Editorial. Mountain ecohydrology: quantifying the role of vegetation in the water balance of montane catchments. Ecohydrology. 1. 187-192. DOI: 10.1002/eco.27.

Clark, J.M., Ashley, D., Wagner, M., Chapman, P.J., Lane, S.N., Evans, C.D. and Heathwaite, A.L. (2009), Increased temperature sensitivity of net DOC production from ombrotrophic peat due to water table draw-down. Global Change Biology. 15. 794-807. https://doi.org/10.1111/j.1365-2486.2008.01683.x.

Don, A., and Schulze, E.D. (2008). Controls on fluxes and export of dissolved organic carbon in grasslands with contrasting soil types. Biogeochemistry. 91. 117–131. https://doi.org/10.1007/s10533-008-9263-y.

Everson, C.E., Molefe, G.L., and Everson, T.M. (1998). Monitoring and modelling components of the water balance in a grassland catchment in the summer rainfall area of South Africa. Water Research Commission. RSA. Report 493/1/98.

Gordijn, P.J., Everson, T.M., and O'Connor, T.G. (2018). Resistance of Drakensberg grasslands to compositional change depends on the influence of fire-return interval and

grassland structure on richness and spatial turnover. Perspectives in Plant Ecology, Evolution and Systematics. 34. 26-36. https://doi.org/10.1016/j.ppees.2018.07.005.

Grieve, I. (1990). Seasonal, Hydrological, and Land Management Factors controlling Dissolved Organic Carbon Concentrations in the Loch Fleet Catchments, Southwest Scotland. Hydrological Processes. 4. 231-239.

Harrison, R., van Tol, J. (2022). Digital Soil Mapping for Hydropedological Purposes of the Cathedral Peak Research Catchments, South Africa. In: Adelabu, S., Ramoelo, A., Olusola, A., Adagbasa, E. (eds) Remote Sensing of African Mountains. Springer, Cham. https://doi.org/10.1007/978-3-031-04855-5_10.

Harrison, R., van Tol, J., and Amiotte Suchet, P. (2022). Hydropedological characteristics of the Cathedral Peak research catchments. Hydrology. 9. 11. 189. https://doi.org/10.3390/hydrology9110189.

Hosen, J., Armstrong, A., and Palmer, M. (2017). Dissolved organic matter variations in Coastal Plain wetland watersheds: the integrated role of hydrological connectivity, land use, and seasonality. Hydrological Processes. 32. DOI:10.1002/hyp.11519.

Kharbush, J. J., Close, H. G., Van Mooy, B. A. S., Arnosti, C., Smittenberg, R. H., Le Moigne, F. A. C., Mollenhauer, G., Scholz-Böttcher, B., Obreht, I., Koch, B. P., Becker, K. W., Iversen, M. H., and Mohr, W. (2020). Particulate Organic Carbon Deconstructed: Molecular and Chemical Composition of Particulate Organic Carbon in the Ocean. Frontiers in Marine Science. 7. DOI=10.3389/fmars.2020.00518.

Kieft, T., Walters, C., Higgins, M., Mennito, A., Clewett, C., Heuer, V., Pullin, M., Hendrickson, S., Heerden, E., Lollar, B., Lau, M., and Onstott, T. (2018). Dissolved Organic Matter Compositions in 0.6–3.4 km Deep Fracture Waters, Kaapvaal Craton, South Africa. Organic Geochemistry. 118. DOI:10.1016/j.orggeochem.2018.02.003.

Klimas, K., Hiesl, P., Hagan, D., and Park, D. (2020). Prescribed fire effects on sediment and nutrient exports in forested environments: A review. Journal of Environmental Quality. 49. 793– 811. https://doi.org/10.1002/jeq2.20108.

Jeong, J.-J., Bartsch, S., Fleckenstein, J.H., Matzner, E., Tenhunen, J.D., Lee, S.D., Park, S.K., Park, J.-H., 2012. Differential storm responses of dissolved and particulate organic carbon in a

mountainous headwater stream, investigated by high-frequency, in situ optical measurements. Journal of Geophysical Research 117, 1-13.

Langergraber, G., Fleischmann, N., and Hofstädter, F. (2003). A multivariate calibration procedure for UV/VIS spectrometric quantification of organic matter and nitrate in wastewater. Water Science and Technology 47, 63-71. DOI:10.2166/wst.2003.0086.

Lepistö, A., Futter, M., and Kortelainen, P. (2014). Almost 50 Years of Monitoring Shows that Climate, not Forestry, Controls Long-Term Organic Carbon Fluxes in a Large Boreal Watershed. Global Change Biology. 20. 1225-1237. DOI:10.1111/gcb.12491.

McCarthy, J. F. (2005). Carbon fluxes in soil. Journal of Geographical Sciences. 15. 149–154. (2005). https://doi.org/10.1007/BF02872680.

McnNichol, A., and Aluwihare, L. (2007). The Power of Radiocarbon in Biogeochemical Studies of the Marine Carbon Cycle: Insights from Studies of Dissolved and Particulate Organic Carbon (DOC and POC). Chemical reviews. 107. 443-66. DOI:10.1021/cr050374g.

Milliman, J.D. and Syvitski, J.P.M. (1992) Geomorphic/Tectonic Control of Sediment Discharge to the Ocean: The Importance of Small Mountainous Rivers. The Journal of Geology, 100. 525-544.http://dx.doi.org/10.1086/629606.

Monteiro, M. T. F., Oliveira, S. M., Luizão, F. J., Cândido, L. A., Ishida, F. Y., and Tomasella, J. (2014). Dissolved organic carbon concentration and its relationship to electrical conductivity in the waters of a stream in a forested Amazonian blackwater catchment. Plant Ecology and Diversity. 7. 1-2. 205-213. DOI: 10.1080/17550874.2013.820223.

Mucina, L., Rutherford, M.C. & Powrie, L.W. (eds). (2006). Vegetation Map of South Africa, Lesotho and Swaziland. Edn. 2. South African National Biodiversity Institute, Pretoria. ISBN 978-1-919976-42-6.

Nänni, U.W. (1956). Forest Hydrological Research at the Cathedral Peak Research Station. Journal of the South African Forestry Association 27(1). 2-35.

Nkambule, T.I. Krause, R.W.M., Haarhoff, J., and Mamba, B. (2011). Natural organic matter (NOM) in South African waters: NOM characterisation using combined assessment techniques. Water SA. 38. 697-706. DOI:10.4314/wsa.v38i5.7.

Pagano, T., Bida, M., and Kenny, J. (2014). Trends in Levels of Allochthonous Dissolved Organic Carbon in Natural Water: A Review of Potential Mechanisms under a Changing Climate. Water. 6. 2862-2897. DOI:10.3390/w6102862.

Ranalli, A.J. (2004). A Summary of the Scientific Literature on the Effects of Fire on the Concentration of Nutrients in Surface Waters in Surface Waters: U.S. Geological Survey Open-File Report 2004-1296.23.

Roosmini, D., Notodarmojo, S., and Sururi, M. (2018). The characteristic of Natural Organic Matter (NOM) of water from Cikapundung River Pond. IOP Conference Series: Earth and Environmental Science. 160. 012021. DOI:10.1088/1755-1315/160/1/012021.

Rüegg, J., Eichmiller, J., Mladenov, N., Walter, K., and Dodds, W. (2015). Dissolved organic carbon concentration and flux in a grassland stream: spatial and temporal patterns and processes from long-term data. Biogeochemistry. 125. 393. DOI:10.1007/s10533-015-0134-z.

Ruhala, S., and Zarnetske, J. (2016). Using in-situ optical sensors to study dissolved organic carbon dynamics of streams and watersheds: A review. Science of The Total Environment. 575. DOI:10.1016/j.scitotenv.2016.09.113.

Sanderman, J., Amundson, R. (2008). A comparative study of dissolved organic carbon transport and stabilization in California forest and grassland soils. Biogeochemistry. 89. 309–327. https://doi.org/10.1007/s10533-008-9221-8.

Sawicka, K., Rowe, E., Evans, C., Monteith, D., Vanguelova, E., Wade, A., and Clark, J. (2016). Modelling impacts of atmospheric deposition and temperature on long-term DOC trends. Science of The Total Environment. 578. DOI:10.1016/j.scitotenv.2016.10.164.

Singleton, A. and Reason, C. (2007). Variability in the characteristics of cut-off low pressure systems over subtropical southern Africa. International Journal of Climatology. 27. 295 - 310. DOI: 10.1002/joc.1399.

Toucher, M.L., Clulow, A., van Rensburg, S., Morris, F., Gray, B., Majozi, S., Everson, C.E., Jewitt, G.P.W., Taylor, M.A., Mfeka, S., and Lawrence, K. (2016). Establishment of a more robust observation network to improve understanding of global change in the sensitive and critical water supply area of the Drakensberg. 2236/1/16. Water Research Commission, Pretoria, South Africa.

Tunaley, C., Tetzlaff, D., Lessels, J. (2016). Linking high-frequency DOC dynamics to the age of connected water sources. Water Resources Research. 52. DOI:10.1002/2015WR018419. Chaplot, V., and Ribolzi, O. (2014). Hydrograph separation to improve understanding of Dissolved Organic Carbon Dynamics in Headwater catchments. Hydrological Processes. 28. DOI:10.1002/hyp.10010.

Rosset, T., Binet, S., Antoine, J-M., Lerigoleur, É., Rigal, F., and Gandois, L. (2020). Drivers of seasonal- and event-scale DOC dynamics at the outlet of mountainous peatlands revealed by high-frequency monitoring. Biogeosciences. 17. 3705-3722. DOI:10.5194/bg-17-3705-2020.

Vallet, A., Moiroux, F., Charlier, J.-B. (2020). Optimization of High-Resolution Monitoring of Nutrients and TOC in Karst Waters Using a Partial Least-Squares Regression Model of a UV–Visible Spectrometer, in: Bertrand, C., Denimal, S., Steinmann, M., Renard, P. (Eds.), Eurokarst 2018, Besançon, Advances in Karst Science. Springer International Publishing, Cham, pp. 109–115. https://doi.org/10.1007/978-3-030-14015-1_13.

Van den Broeke, J. (2007). On-line and In-situ UV/Vis Spectroscopy - AWE Magazine [WWW Document]. URL https://www.aweimagazine.com/article/on-line-and-in-situ-uv-vis-spectroscopy/ (accessed 10.24.22).

van Tol, J.J., and Le Roux, P.A.L. (2019). Hydropedological grouping of South African soil forms. South African Journal of Plant and Soil. 36(3). 233-235. DOI: 10.1080/02571862.2018.1537012.

Vaughan, M., Bowden, W., Shanley, J., Vermilyea, A., Sleeper, R., Gold, A., Pradhanang, S., Inamdar, S., Levia, D., Andres, A., Birgand, F., and Schroth, A. (2017). High-frequency dissolved organic carbon and nitrate measurements reveal differences in storm hysteresis and loading in relation to land cover and seasonality. Water Resources Research. 53. DOI: 10.1002/2017WR020491.

Wang, L., Yen, H., Chen, L-D., and Wang, Y. (2019). Dissolved Organic Carbon Driven by Rainfall Events from a Semi-arid Catchment during Concentrated Rainfall Season in the Loess Plateau, China. Hydrology and Earth System Sciences. 23. DOI:10.5194/hess-23-3141-2019.

Warner, K., Fowler, R., and Saros, J. (2020). Differences in the Effects of Storms on Dissolved Organic Carbon (DOC) in Boreal Lakes during an Early Summer Storm and an Autumn Storm. Water. 12. 1452. DOI:10.3390/w12051452.

Wei, X., Hayes, D., and Fernandez, I. (2021). Fire reduces riverine DOC concentration draining a watershed and alters post-fire DOC recovery patterns. Environmental Research Letters. 16. 024022. DOI:10.1088/1748-9326/abd7ae.

Werner, B., Musolff, A., Lechtenfeld, O., de Rooij, G., Oosterwoud, M., and Fleckenstein, J., (2019). High-frequency measurements explain quantity and quality of dissolved organic carbon mobilization in a headwater catchment. Biogeosciences. 16. 4497-4516. DOI:10.5194/bg-16-4497-2019.

World Meteorological Organization (WMO) (2017). Guidelines on the Calculation of Climate Normals (WMO No. 1203). World Meteorological Organization.

Worrall, F., Davies, H., Bhogal, A., Lilly, A., Evans, M., Turner, K., Burt, T., Barraclough, D., Smith, P., and Merrington, G. (2012). The flux of DOC from the UK – Predicting the role of soils, land use and net watershed losses. Journal of Hydrology. 448-449. 149-160. https://doi.org/10.1016/j.jhydrol.2012.04.053.

Yallop, A.R. and Clutterbuck, B. (2009). Land management as a factor controlling dissolved organic carbon release from upland peat soils 1: Spatial variation in DOC productivity, Science of The Total Environment. Volume 407. Issue 12. 3803 – 3813. https://doi.org/10.1016/j.scitotenv.2009.03.012.

# CHAPTER 9 – CONCLUSIONS

Globally there has been an increase in the rise of DOC within stream waters, affecting the food webs of stream networks, the acid-based chemistry of soils and surface waters, as well as carbon budgets within catchment areas (Laudon et al. 2011). Several factors have been attributed to explaining this increase including biochemical factors, changes to land management as well as factors associated with climate change such as climate extremes in the form of flooding and droughts as well as the increase in the intensity of storm events (Laudon et al. 2011, Jung et al. 2014, Lawrence and Roy, 2021). In order to understand why these increases are occurring, it is first imperative to understand the basic dynamics associated with the storage and export of DOC from catchment areas.

Despite the numerous research on the dynamics of DOC from watersheds, which has particularly taken place within the northern hemisphere, little work has been conducted on the influence of the hydrological connectivity of catchment flow paths and how these impact the storage and export of DOC. In particular montane grassland dominated catchments, as well as areas in South Africa, have often been overlooked within research associated with the sources of DOC (Milliman and Syvitski, 1992, Chaplot and Ribolzi, 2014). We therefore utilised three research catchments within the uKhahlamba-Drakensberg Mountain range of South Africa to conduct this study in order to enhance our knowledge of these important headwater catchment areas and how they influence downstream locations.

The main aims of this study were to determine how the hydropedological characteristics interact with the DOC dynamics of these catchment ecosystems. The first aim of the thesis was to gain a general understanding of the hydropedological characteristics of the catchments through the use of a digital soil mapping exercise (Chapter 4). Both a rules-based approach as well as a validation exercise were utilised within the ArcSIE (Soil Inference Engine) software to create hydropedological maps of the catchments. The hydropedological soil maps, classified the three catchment areas into four different hydropedological soil groups based on the South African hydropedology classifications (van Tol and Le Roux, 2019). These included the shallow recharge soils, deep recharge soils, interflow soils, and saturated responsive soils. It was identified however through the use of the Kappa coefficient (CP-III is 0.57, for CP-VI is 0.59, and for CP-IX is 0.74) that there are some discrepancies between the hydropedological

soil maps created and the site-specific soils identified within the catchment areas but that the maps provide a general understanding of the flow paths and storage areas of these watersheds. Of importance is that the accuracies and inaccuracies within the maps can be quantified, allowing for a confidence rating in the use of these maps. These maps can therefore be used in further applications in water and land management for the area, highlighting the importance of digital soil mapping in remote areas. The use of digital soil mapping could allow for more integration of soil knowledge into land management policies (Mora-Vallejo et al., 2008, van Zijl, 2019).

Utilising the hydropedological soil maps coupled with catchment specific climate and streamflow data, water table depth measurements as well as an understanding of how historic and current land management practices have influenced the soil properties, this study was able to gain a more accurate interpretation of the response of each hydropedological soil group following a rainfall event (Chapter 5). A number of factors which are interrelated play a key role in determining the flow paths and the connection between flow paths in these areas. These factors are dominated by antecedent soil moisture, rainfall intensity, the duration of dry and wet periods as well as the depth of soil profiles. Furthermore, the dominant role of wetland systems and how these have drying, and wetting cycles are the key focus in understanding the connectivity between the hydropedological flow paths (Tetzlaff et al. 2014, Furlan et al. 2020), and the contribution of soil water to the stream networks of the three catchments.

The study was then expanded to gain a deeper understanding of the hydropedological flow paths of the catchments and their influence on the streamflow dynamics through the use of a SWAT modelling approach (Chapter 6). Specific lateral time inputs, for each hydropedological soil group were utilised. These lateral time inputs were calculated from the formation of a hydrograph for CP-VI showing the time it takes for water to flow through the catchment and contribute to streamflow (Kunene et al. (2011). This study identified that the input of site-specific lateral time inputs showed a definitive improvement in modelling accuracy. Numerous research studies have highlighted the importance of detailed soil information on improving SWAT model accuracy (Adem et al. 2020; Chen et al. 2016, Krepec et al. 2020). Soil information should therefore be coupled with ecological information such as the effects of fire, vegetation as well as rates of evapotranspiration on hydrological modelling accuracy. These aspects have been shown to all be interrelated.

Through these studies we gained a deeper understanding of the hydropedological characteristics and how these have an impact on the flow dynamics of the catchments. This knowledge was then transferred to studying the effect of different environmental factors on the dynamics of DOC. The principle environmental factors that influence DOC concentrations in two of the selected catchments (CP-VI and CP-IX) were investigated in Chapter 7. These environmental factors included land cover, soils, topography and aspect, and land management regimes. It was identified that DOC production is sensitive to climatic drivers including seasonal rainfall and temperature, but that the presence of wetland systems is the major driver in DOC concentrations. Similar findings have been recorded by Huntington and Aiken (2013) as well as Lee et al. (2019), with the connectivity of the wetlands to the streams within both catchments playing a role in the attenuation and export of DOC within these watersheds.

DOC concentration variability is closely linked to distinct DOC source zones in catchments and their hydrologic connectivity to the stream network (Werner et al. 2019). The use of high frequency optical sensors placed in the weirs of CP-VI and CP-IX enabled a deeper understanding of the importance of the influence of the hydropedological connectivity of catchment areas, and in particular the wetland systems, on DOC export (Chapter 8). The DOC export is dependent on the antecedent connectivity of flow paths and how these affect baseflow as well as shallow subsurface and overland flow of water through the catchment and into the stream networks. SOC is largely attenuated within the upper reaches of the soil profile, so when dry conditions prevail, baseflow from the lower reaches of the soil profile does not contribute significantly to DOC export. However, during wetter conditions, wetland systems become saturated, and this reconnects hydrologic flow paths within the catchment. When this occurs, water moves more freely as overland flow or shallow subsurface flow, carrying with it larger quantities of stored SOC in the form of DOC. Storm events furthermore move large quantities of DOC, however this is dependent on the antecedent soil moisture conditions before the event and the connection of soil water flow paths.

Given the importance of these mountainous watersheds to the ecohydrological services of downstream ecosystems, long term data gathered within the catchments on the hydrologic pathways and DOC concentrations has the potential to allow for future studies to determine the impact of the ever-changing climatic influence on the dynamics within these catchment areas. These climatic changes will affect flow paths as well as the DOC export, and this has implications on downstream ecosystems. Further studies on DOC within these catchments

should include incorporating stable isotopes to determine the origin of the DOC, the effect of microbial activity, as well as the effect of the fire management regimes. This will aid in understanding the contribution of DOC to the overall carbon budget of these catchment areas.

This thesis provides valuable insight into the interactions of DOC and hydropedology in these Afromontane areas. It identifies a variety of factors that influence DOC storage and export on a catchment scale. The results highlight the importance of understanding the hydropedological characteristics of a watershed for both improving our knowledge on the streamflow aspects as well as understanding the DOC dynamics and how these affect the overall carbon budget of a system.

## 9.1. REFERENCES

Adem, A.A., Dile, Y.T., Worqlul, A.W., Ayana, E.K., Tilahun, S.A., and Steenhuis, T.S. (2020). Assessing digital soil inventories for predicting streamflow in the headwaters of the Blue Nile. Hydrology. 7.1. doi.org/10.3390/hydrology7010008.

Chaplot, V., and Ribolzi, O. (2014). Hydrograph separation to improve understanding of Dissolved Organic Carbon Dynamics in Headwater catchments. Hydrological Processes. 28. DOI:10.1002/hyp.10010.

Chen, L., Wang, G., Zhong, Y., Zhao, X., and Shen, Z. (2016). Using site-specific soil samples as a substitution for improved hydrological and nonpoint source predictions. Environmental Science and Pollution Research. 23. 16037–16046. DOI:10.1007/s11356-016-6789-8.

Huntington, T.G., and Aiken, G.R. (2013). Export of dissolved organic carbon from the Penobscot River basin in north-central Maine. Journal of Hydrology. 476. 244-256. https://doi.org/10.1016/j.jhydrol.2012.10.039.

Jung, B.J., Lee, J.K., Kim, H., and Park, J. H. (2014). Export, biodegradation, and disinfection byproduct formation of dissolved and particulate organic carbon in a forested headwater stream during extreme rainfall events. Biogeosciences. 11. 6119-6129. DOI:10.5194/bg-11-6119-2014.

Krpec, P., Horáček, M., and Šarapatka, B. (2020). A comparison of the use of local legacy soil data and global datasets for hydrological modelling a small-scale watersheds: Implications for nitrate loading estimation. Geoderma. 377. 114575. doi.org/10.1016/j.geoderma.2020.114575.

Laudon, H., Berggren, M., Ågren, A., Buffam, I., Bishop, K., Grabs, T., Jansson, M., and Köhler, S. (2011). Patterns and Dynamics of Dissolved Organic Carbon (DOC) in Boreal Streams: The Role of Processes, Connectivity, and Scaling. Ecosystems. 14. 880-893. 10.1007/s10021-011-9452-8.

Lawrence, G.B., and Roy, K.M. (2021). Ongoing increases in dissolved organic carbon are sustained by decreases in ionic strength rather than decreased acidity in waters recovering from acidic deposition. Science of The Total Environment. 766. 142529. https://doi.org/10.1016/j.scitotenv.2020.142529.

Lee, M.H., Lee, Y.K., Derrien, M., Choi, K., Shin, K.H., Jang, K.S., and Hur, J. (2019). Evaluating the contributions of different organic matter sources to urban river water during a storm event via optical indices and molecular composition. Water Research.165. 115006. DOI: 10.1016/j.watres.2019.115006.

Milliman, J.D. and Syvitski, J.P.M. (1992). Geomorphic/Tectonic Control of Sediment Discharge to the Ocean: The Importance of Small Mountainous Rivers. The Journal of Geology, 100. 525-544. http://dx.doi.org/10.1086/629606.

Mora-Vallejo, A., Claessens, L., Stoorvogel, J., and Heuvelink, G. (2008). Small scale digital soil mapping in Southeastern Kenya. Catena. 76. 44-53. DOI:10.1016/j.catena.2008.09.008.

Mucina, L., Rutherford, M.C. & Powrie, L.W. (eds). (2006). Vegetation Map of South Africa, Lesotho and Swaziland. Edn. 2. South African National Biodiversity Institute, Pretoria. ISBN 978-1-919976-42-6.

van Tol, J.J., and Le Roux, P.A.L. (2019). Hydropedological grouping of South African soil forms. South African Journal of Plant and Soil. 36(3). 233-235. DOI: 10.1080/02571862.2018.1537012.

van Zijl, G. (2019). Digital soil mapping approaches to address real world problems in southern Africa. Geoderma. 337. 1301-1308. https://doi.org/10.1016/ j.geoderma.2018.07.052.

Werner, B., Musolff, A., Lechtenfeld, O., de Rooij, G., Oosterwoud, M., and Fleckenstein, J., (2019). High-frequency measurements explain quantity and quality of dissolved organic carbon mobilization in a headwater catchment. Biogeosciences. 16. 4497-4516. DOI:10.5194/bg-16-4497-2019.